
The University Of Sheffield.

# Elucidating the role of the AP-2 endocytic adaptor complex in *Candida albicans* morphology and virulence

Harriet Knafler

A thesis submitted in partial fulfilment of the requirements for the degree of Doctor of Philosophy

The University of Sheffield
Faculty of Science
Department of Biomedical Science

September 2019

# Abstract

Despite being a critical player in mammalian endocytosis, the AP-2 endocytic adaptor complex was long thought to be unimportant or redundant in yeast. It has since been shown that, despite being dispensable for the endocytic process in general, AP-2 has several important roles in polarised growth and cell wall maintenance in yeast and fungi. In this study, we investigate the role of the AP-2 complex in the important human fungal pathogen *Candida albicans*. By characterising the phenotype of mutants lacking functional AP-2, we show that AP-2 is critical to *C. albicans* cell wall composition and organisation; plasma membrane lipid distribution; and to the maintenance of polarised hyphal growth. We demonstrate that this is partially due to its requirement for the endocytic recycling of chitin synthase 3 (Chs3), the absence of which leads to mis-localised Chs3; defective cell wall deposition; and morphological defects. We further show that AP-2-mediated endocytic recycling is crucial for correct polarisation of the secretory pathway during hyphal growth. The findings of this study have demonstrated that AP-2 has critical roles in the endocytosis of particular cargo proteins in *C. albicans*. These findings have underlined the importance of endocytic recycling of specific cargoes in the maintenance of polarised growth and correct cell wall organisation in filamentous fungi. In *C. albicans* both its cell wall and its ability to form hyphae are key virulence factors, so we hope that insights into their mechanisms of regulation may be valuable for future antifungal drugs studies.

# Acknowledgements

Firstly, my supervisor Kathryn, for reminding me every Monday morning to look at the bigger picture. Thanks for telling me so many things and putting up with my terrible early attempts at science. Also my second supervisor Simon, for his positivity and optimism.

Everyone in the KA/SW/ER lab – past and present – for all the coffees, advice and laughs. It would have been really boring without you! Special mention to Iwona – without you I would definitely still be stuck on my first bit of cloning.

Thank you to everyone who took time to help me with my experiments – there's too many to list but especially: Chris Hill in EM; Darren Robinson in the LMF; Spyros Sovatzoglou and Jamie Hobbs in AFM; David Caballero-Lima for teaching me 2D gels; Craig Murdoch for teaching me biofilm assays; Michael Goldberg and Christine Richardson for having me in Durham; everyone at the Aberdeen Fungal Group for teaching me loads and making me welcome, especially Louise Walker, Kathy Lee, Gillian Milne, Maria Spyrou, Katja Schaefer and Neil Gow.

Thanks to all the great BMS friends I have made over the four years, for lunches and moans and countless Interval pints, I'm really lucky to have met such a nice bunch.

Special thanks to my lovely housemates Emma, Sarah, Dave, and Alex, and of course Josh, and honorary members Studd and Fay. I genuinely couldn't have done it without you. You've made my time in Sheffield the best time of my life. Thanks for being all round good eggs!

And thank you to my family for always being supportive. Please don't feel like you have to read this :P

# Contents

# List of figures

# List of tables

# List of abbreviations

| | |
|---|---|
| % | percentage |
| °C | degrees Celsius |
| 2D | two dimensional |
| *A. nidulans* | *Aspergillus nidulans* |
| ADP | adenosine diphosphate |
| AFM | atomic force microscopy |
| AFS | automated freeze substitution |
| AIDS | acquired immune deficiency syndrome |
| Alexa-488 | Alexa Fluor 488 dye |
| Alexa-594 | Alexa Fluor 594 dye |
| ANOVA | analysis of variance |
| AP-1 | adaptor protein complex 1 |
| AP-2 | adaptor protein complex 2 |
| AP-3 | adaptor protein complex 3 |
| AP-4 | adaptor protein complex 4 |
| AP-5 | adaptor protein complex 5 |
| *apm4*$^{1\text{-}454}$ | *APM4* gene truncated after the first 454 nucleotides |
| APS | ammonium persulfate |
| ARF | ADP ribosylation factor |
| ATG | adenine thymine guanine (start codon) |
| BLAST | basic local alignment search tool |
| bp | base pair |
| BSA | bovine serum albumin |
| *C. albicans* | *Candida albicans* |
| C’ | carboxy terminal |
| $CaCl_2$ | calcium chloride |
| CALM | clathrin assembly lymphoid myeloid leukemia protein |
| CCD | charge-coupled device |

| | |
|---|---|
| CCP | clathrin-coated pit |
| cER | cortical endoplasmic reticulum |
| CFW | calcofluor white |
| Chs | chitin synthase |
| CIE | clathrin-independent endocytosis |
| CIP | calf intestinal phosphatase |
| CME | clathrin-mediated endocytosis |
| $CO_2$ | carbon dioxide |
| ConA | concanavalin-A |
| CR | congo red |
| CR | complement receptor |
| CWI | cell wall integrity |
| CWP | cell wall protein |
| D/ExxxLL/I | di-Leucine motif |
| $dH_2O$ | distilled water |
| DMSO | dimethylsulfoxide |
| DNA | deoxyribose nucleic acid |
| dNTP | deoxyribonucleotide triphosphate |
| DTT | dithiothreitol |
| E | Elastic modulus / Young's modulus |
| *E. coli* | *Escherichia coli* |
| ECL | enhanced chemiluminescence |
| EDTA | ethylenediaminetetraacetic acid |
| EGF | epidermal growth factor |
| EGTA | ethylene glycol-bis(β-aminoethyl ether)-N,N,N',N'-tetraacetic acid |
| ER | endoplasmic reticulum |
| ERD | ergosterol-rich domain |
| F-actin | filamentous actin |
| FBS | fetal bovine serun |
| FCHo | FER / CIP4 homology domain only proteins |

| | |
|---|---|
| FIJI | FIJI Is Just ImageJ |
| fL | femtolitre |
| Flc | fluconazole |
| *g* | gravity |
| g | grams |
| G1 | gap1 cell cycle phase |
| GDI | guanine dissociation inhibitor |
| GEF | guanine nucleotide exchange factor |
| GFP | green fluorescent protein |
| GGA | Golgi-localised γ-ear-containing ARF-binding proteins |
| GOI | gene of interest |
| GOLD | Golgi dynamics domain |
| GPI | glycosylphosphatidylinositol |
| GTP | guanosine triphosphate |
| HA | human influenza haemagglutinin |
| HCl | hydrochloric acid |
| HPAEC-PAD | high-performance anion-exchange chromatography with pulsed amperometric detection |
| HPF | high pressure freezing |
| HPLC | high performance liquid chromatography |
| HRP | horseradish peroxidase |
| IgG | immunoglobulin G |
| IP | immunoprecipitate |
| IPG | immobilised pH gradient |
| kDa | kilodalton |
| kV | kilovolt |
| LiOAc | lithium acetate |
| LUT | look up table |
| LY | Lucifer Yellow |
| M | molar |

| | |
|---|---|
| MAPK | mitogen-activated protein kinase |
| MCS | membrane contact sites |
| MeOH | methanol |
| mg | milligrams |
| $MgCl_2$ | magnesium chloride |
| mins | minutes |
| mL | millilitre |
| mM | millimolar |
| MMD | myosin motor domain |
| MPa | megapascals |
| MR | mannose receptor |
| *N. crassa* | *Neurospora crassa* |
| N' | amino terminal |
| NaCl | sodium chloride |
| NaOH | sodium hydroxide |
| NECAP | adaptin ear-binding coat-associated protein |
| ng | nanograms |
| nm | nanometres |
| ns | nanoseconds |
| $O_2$ | oxygen |
| OD | optical density |
| ORD | OSBP-related domain |
| ORP | OSBP-related protein |
| OSBP | oxysterol-binding protein |
| $OsO_4$ | osmium tetroxide |
| PAGE | polyacrylamide gel electrophoresis |
| PAMP | pathogen associated molecular pattern |
| PB | polybasic region |
| PBS | phosphate buffered saline |
| PCR | polymerase chain reaction |

| | |
|---|---|
| PEG | polyethylene glycol |
| pg | picograms |
| pI | isoelectric point |
| PI(4)P | phosphatidylinositol 4-phosphate |
| $PI(4,5)P_2$ | phosphatidylinositol 4,5-bisphosphate |
| Pir | protein with internal repeats |
| PM | plasma membrane |
| pmol | picomoles |
| PMT | protein O-mannosyltransferase |
| PRR | pathogen recognition receptor |
| PVDF | polyvinylidene difluoride |
| RFP | red fluorescent protein |
| ROI | region of interest |
| *S. cerevisiae* | *Saccharomyces cerevisiae* |
| *S. pombe* | *Schizosaccharomyces pombe* |
| SD | standard deviation |
| SDM | site directed mutagenesis |
| SDS | sodium dodecyl sulphate |
| SEM | scanning electron microscopy |
| Ser | serine |
| SNARE | soluble NSF attachment protein receptor |
| SPR | surface plasmon resonance |
| SRD | sterol-rich domain |
| ssDNA | single stranded deoxyribose nucleic acid |
| TAE | Tris, acetic acid and EDTA |
| TBST | Tris-buffered saline with Tween |
| TE | Tris-EDTA |
| TEM | transmission electron microscopy |
| TEMED | tetramethylethylenediamine |
| TGN | trans-Golgi network |

| | |
|---|---|
| Thr | threonine |
| TIFF | tagged image file format |
| TIRF | total internal reflection fluorescence |
| TLR | Toll-like receptor |
| UDP | uridine diphosphate |
| UV | ultraviolet |
| V | Volts |
| v/v | volume / volume |
| VSC | vesicle supply centre |
| w/v | weight / volume |
| WGA | wheat germ-agglutinin |
| WT | wild type |
| XTT | 2,3-bis(2-methoxy-4-nitro-5-sulfophenyl)-2H-tetrazolium-5-carbonxanilide inner salt |
| YPA | yeast extract peptone agar |
| YPD | yeast extract peptone dextrose |
| YPS | yeast extract peptone sucrose |
| YxxΦ | tyrosine motif |
| α2 | AP-2 alpha subunit |
| β2 | AP-2 beta subunit |
| Δ | delta; deletion |
| Δ/Δ | homozygous / double deletion |
| μ2 | AP-2 mu subunit |
| μg | micrograms |
| μL | microlitres |
| σ2 | AP-2 sigma subunit |

Please note: various abbreviations have been used to describe the major *C. albicans* strains used in this thesis.

WT; SN148 WT and *APM4* WT all refer to the *C. albicans* strain SN148 which has not been further modified (wild-type strain).

*apm4*; *apm4Δ/Δ*; *apm4Δ / apm4Δ* and *apm4* deletion all refer to the above strain in which both copies of *apm4* have been deleted (homozygous *apm4* deletion).

# Chapter 1: Introduction

## 1.1. *Candida albicans* is a fungal pathogen

*Candida albicans* is an ascomycete fungus and member of the *Candida* genus. This genus comprises over 200 species, 17 of which are known to cause disease to humans, *with C. albicans* being the most common pathogen (Sardi et al. 2013). *Candida glabrata*, *Candida parapsilosis*, *Candida tropicalis* and *Candida krusei* are other notable pathogens; together these five species cause 90% of invasive *Candida* infections (Pfaller 2012). The relative prevalence of the non-*albicans* species is increasing and differs in different parts of the world (Sardi et al. 2013). For example, a study in Brazil in 2011 found *C. albicans* accounted for 40.9% of cases of candidemia and *C. tropicalis* was responsible for 20.9% of cases (Colombo et al. 2007) whereas analysis of European countries showed that >50% of infections were caused by *C. albicans*, followed by 14% each by *C. glabrata* and *C. parapsilosis* (Tortorano et al. 2006).

*C. albicans* is rarely found in environmental niches and is not thought to proliferate outside of a host animal (Hube 2004). Instead, it is highly specialised to live in a variety of niches within the environment of a human host. Here it forms part of the 'microbiome' – the commensal microorganisms which live upon and within us. The bacterial microbiota has been known for some time to play an important role in shaping healthy tissues and the immune system. However, the importance of the 'mycobiota' – the yeast and fungi which colonise our skin, digestive system and mucosal membranes – has been far less well studied. The prevalence of commensal fungi may have been underestimated, due to their more complex culture conditions, and lower availability of genomic information, compared with bacterial species. It is becoming clear however that commensal fungi are key players in human health and disease; they can become agents of opportunistic infection and influence the progression of other infections, as well as being critical to normal health and immune function (Underhill and Iliev 2014).

*Candida* species reside within many of us without causing harm. They are the most prevalent group of fungi in the human colon and vagina, and are also found in the oral

cavity; toe web space and heel of healthy humans (Underhill and Iliev 2014). *C. albicans* is present in faecal samples of 65% of healthy adults (Cohen et al. 1969), and on the mucus membranes of 30 – 60% (Lim et al. 2012). This close association and dynamic interplay between humans and *C. albicans* has shaped the evolution of both species. Our colonisation by *Candida* species can be altered by changes in diet; infection with bacteria; and treatment with antibiotics (David et al. 2014). Increases in *Candida* growth can in turn affect our commensal microflora (Erb Downward et al. 2013).

Under certain circumstances however, commensal *C. albicans* can become opportunistic agents of infection. Changes in the host immune system or microflora can tip the balance, allowing *C. albicans* to proliferate and become pathogenic (Hube 2004, Calderone and Fonzi 2001). Superficial mucosal infections, in which *C. albicans* colonises mucosal surfaces for example in the oral or vaginal cavity, are extremely common. Vulvovaginal candidiasis (thrush) will affect 50 – 75% of women worldwide (Sobel 2007); and 70% of AIDS patients will experience oropharyngeal candidiasis (Fidel, Vazquez and Sobel 1999). Humans have evolved myriad receptors to detect and respond to fungal colonisers and must be able to distinguish between passive commensals and problematic fungal invasions. The immune system must continuously control commensal fungi, and mutations in various immune receptors leads to increased susceptibility to fungal infections (Romani 2011).

In some cases, *C. albicans* can invade deeper tissue and enter the blood stream. Here it can be carried around the body and, unusually for a pathogen, infect almost any tissue (Kullberg and Arendrup 2015). This systemic or invasive infection is much less common than mucosal infection, and far more dangerous. Candidemia is the fourth most common bloodstream infection in intensive care units (Wisplinghoff et al. 2004) with an associated mortality rate as high as 46% - 75% (Brown et al. 2012). Invasive candidiasis occurs in immunocompromised individuals, including transplant recipients; AIDS patients; cancer patients; patients on broad-spectrum antibiotics; and the elderly (Cleveland et al. 2015, Kullberg and Arendrup 2015). As such it is a common nosocomial infection; *Candida* species cause around 10% of all hospital-acquired infections in the US (Lim et al. 2012); and *C. albicans* is responsible for 40 – 70% of these (Falagas, Roussos and Vardakas 2010). The prevalence of such infections is increasing, due to the growing immunocompromised population caused by medical advances and improved life expectancy (Harpaz, Dahl and Dooling 2016). Resistance of *C. albicans* to antifungal

drugs is also a growing problem, and many current treatments have negative side effects (Toenjes et al. 2005).

*Candida* species must be highly dynamic and adaptable in order to survive in different niches within the host and respond to the constantly changing conditions. The gut; oral cavity and vaginal mucosa are physiologically very different environments, each presenting challenges such as pH, nutrient availability and competition with other microflora. *C. albicans* is unusual in its ability to reside and cause disease in such diverse environments (Calderone and Fonzi 2001). Both commensal and pathogenic states require adaptation to environmental conditions. *C. albicans* must also continuously sense and respond to the strategies of the host immune system to evade detection and elimination. *C. albicans* has evolved myriad virulence factors, which can be rapidly turned on and off, to enable both its survival as a commensal, and its colonisation as a pathogen (Calderone and Fonzi 2001, Mayer, Wilson and Hube 2013).

## 1.2. Hyphal growth is key to its virulence

One of the most important virulence factors of *C. albicans* is its ability to switch its morphology between budding yeast cells; pseudohyphal cells; and hyphal (filamentous) cells (see figure 1.1). Yeast are oval cells which divide by budding in a similar manner to the baker's yeast *Saccharomyces cerevisiae*. Pseudohyphae appear similar to chains of elongated yeast cells which have not divided after septation. True hyphae, in contrast, are narrow filaments with parallel sides which do not show constrictions at septa (Sudbery, Gow and Berman 2004). *C. albicans* is fairly unique in this ability; most other *Candida* species are only able to grow as yeast and pseudohyphae, though the more closely related *C. dubliensis*, *C. tropicalis* and *C. auris* do also form true hyphae, albeit under a more limited range of conditions (Lackey et al. 2013, Yue et al. 2018).

The exact roles of yeast, pseudohyphae and hyphae in virulence has been the subject of some debate. Hyphae are associated with tissue invasion and damage. Hyphal cells have increased adhesion and can infiltrate epithelia via induced endocytosis or active penetration (Wächtler et al. 2011, Dalle et al. 2010). Hyphae can also escape from macrophages after phagocytosis (Lorenz, Bender and Fink 2004). This led some to propose that hyphae are the morphology associated with pathogenesis and yeast cells are commensal. However, yeast cells have been shown to be able to cross the mouse

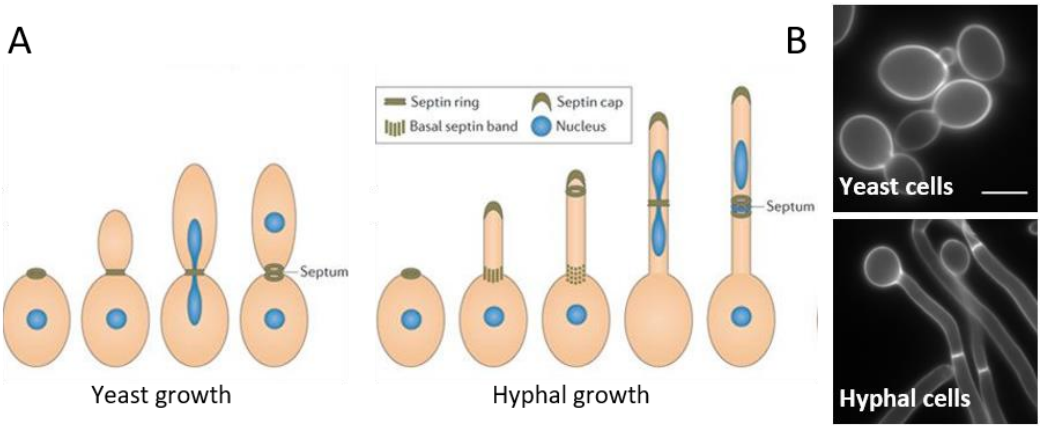


1.1. Yeast and hyphal cells of Ca*ndida albicans*

(A) Cartoons showing modes of yeast and hyphal growth of *C. albicans* cells. Each shows its progression through the cell cycle. Nuclei are shown in blue and septins in brown. Reproduced with permission from Sudbery, 2011. (B) Microscopy images of yeast (above) and hyphal (below) *C. albicans* cells, stained with Calcofluor White for visualisation.

gut wall (Pope and Cole 1982) and secrete proteinases (Ray and Payne 1988). The yeast form has also been associated with dissemination in the bloodstream, which is important in systemic infection (Mavor, Thewes and Hube 2005). It is now thought that, although hyphae are more invasive, both morphologies have important roles in infection. The ability to switch between them is essential to virulence; mutants 'locked' in either morphology are avirulent (Lo et al. 1997, Murad et al. 2001) and cells of both morphologies are found in infected organs (Lionakis et al. 2011). It is still unclear whether hyphae are ever formed during commensal growth. Hypha-specific gene expression has been detected during asymptomatic colonisation (Naglik et al. 2006), however yeast cells have been shown to express hyphal-specific genes under certain conditions (Fradin et al. 2005).

Yeast and hyphae are also known to interact with the immune system in different ways. Sensing of the different morphologies could help the host immune system to distinguish between commensal colonisation and invasive fungal growth. However the mechanisms behind this remain unclear. Cell wall organisation differs between the different morphologies, leading to differential recognition by immune receptors. For example, the Toll-like receptor TLR4 recognises *C. albicans* yeast cells but not hyphae, so hyphae do not activate interferon-γ (van der Graaf et al. 2005). Differential glucan exposure in hyphae compared to yeast leads to different cytokine induction (Gantner, Simmons and Underhill 2005). Moyes et al (2010) demonstrated a mechanism by which oral epithelial cells can distinguish between *C. albicans* yeast and hyphal cells. The epithelial cells

activated one signalling pathway in response to fungal cell wall in general; and a second signalling pathway dependent on the detection of hyphae. This was subsequently shown to be due to the ability of hyphae to secrete the cytolytic toxin Candidalysin. Discovered in 2016 (Moyes et al.), Candidalysin is the first known peptide toxin of a pathogenic fungus. It is encoded by a cleaved fragment of the *ECE1* gene, and induces epithelial damage and immune activation (Swidergall et al. 2019). Candidalysin is a classical virulence factor, directly damaging host cells. Its discovery also demonstrated a mechanism by which the host can distinguish between commensal and invasive *C. albicans*.

Switching between the forms is induced by changing environmental conditions. The switch from yeast to hyphal morphology has been an area of particularly active research due to its importance in infection. In research and diagnostic labs, culture at 30°C in rich medium is used to study yeast growth, and culture at 37°C with the addition of serum is used to reliably induce hyphal growth. However there are myriad different signals which induce hyphal formation *in vivo*. Environmental signals known to induce hyphal growth include low pH; low $O_2$; high $CO_2$; carbon or nitrogen starvation; cells density (via quorum sensing molecules) and *N*-acetylglucosamine (Hall, Cottier and Mühlschlegel 2009, Sudbery 2011). Hyphal formation can also be induced by endogenous cellular signals such as cell cycle progression (Kornitzer 2019). Once sensed, these signals activate intracellular signalling cascades which target specific transcription factors, leading to activation of a set of hypha-specific genes (Sudbery 2011).

Once hyphal formation is induced in the lab, a germ tube can be seen after around 15 minutes of growth. This germ tube evagination depends on many of the same proteins which control yeast budding, but does not follow the same cell cycle cues (Hazan, Sepulveda-Becerra and Liu 2002). As in yeast budding, the actin cytoskeleton and therefore secretion is targeted to the tip of the new germ tube via the master regulator Cdc42 (Ushinsky et al. 2002). However instead of then being re-directed to isotropic growth, this machinery is maintained at the hyphal tip, allowing polarised growth to continue (Anderson and Soll 1986). In hyphae, the first septum is formed within the germ tube rather at the mother-bud neck (Sudbery 2001). The nucleus then divides across this septum, along with much of the mother cell's cytoplasm ((Gow 1997), see figure 1.1). After the first cell cycle, the mother cell becomes highly vacuolated and remains in G1 phase, leaving the apical compartment to continue to grow. Subapical

compartments however can re-enter the cell cycle in order form new germ tube branches (Gow and Gooday 1982).

## 1.3. The fungal cell wall structure and function

Another important virulence factor is the *C. albicans* cell wall. The cell wall is a dynamic network of polysaccharides and proteins which surrounds the cell and protects it from osmotic shock, chemical and temperature stress, and the host immune system. Similarly to the *S. cerevisiae* cell wall it is composed of three major polysaccharides and various proteins (see figure 1.2). Chitin and glucan carbohydrates form the structural basis of the cell wall. Glucan is a polymer of glucose; and chitin a polymer of *N*-acetylglucosamine. The inner cell wall is composed of glucan and chitin fibres, forming a structural meshwork to which other cell wall components are covalently attached (Kapteyn et al. 2000, Klis, de Groot and Hellingwerf 2001). The outer cell wall is predominantly glycoproteins; specifically mannoproteins, in which proteins have been modified by *N*- or *O*-linked fibrillar mannans (Shibata et al. 1995). These glycoproteins are mostly attached to glucans via glycophosphatidylinositol (GPI) anchor remnants. Mannan can also be attached to lipids, as phospholipomannan. For overviews of the cell fungal cell wall, see (Klis et al. 2001, Bowman and Free 2006, Gow, Latge and Munro 2017).

New fungal cell wall must be constantly synthesised as the cell grows, to allow cell expansion. Chitin and glucan are both synthesised by transmembrane enzymes which use nucleotide diphosphate sugars from within the cell and extrude polymer out to the extracellular space (vectorial synthesis). Chitin is polymerised from *N*-acetylglucosamine, joined by linear β-1,4-linkages, by four enzymes in *C. albicans*: chitin synthases 1, 2, 3 and 8 (Chs1, 2, 3, 8) (Lenardon, Munro and Gow 2010). Hydrogen bonds between these chains generate microfibrils. Chitin comprises just 1 – 2% of the yeast cell wall (dry weight), but contributes significantly to the strength and integrity of the wall due to its very high tensile strength (Klis et al. 2001). Glucan is polymerised from glucose by the glucan synthase enzyme Fks1 (Douglas et al. 1997). Monomers are joined by β-1,3-linkages; β-1,6-glucans can be added in the cell wall to generate branched filaments (Cabib et al. 1988). Glucan is the most abundant polysaccharide, making up 50 – 60% of the dry cell wall weight (Klis et al. 2001). Mannose, in contrast, is added to proteins as

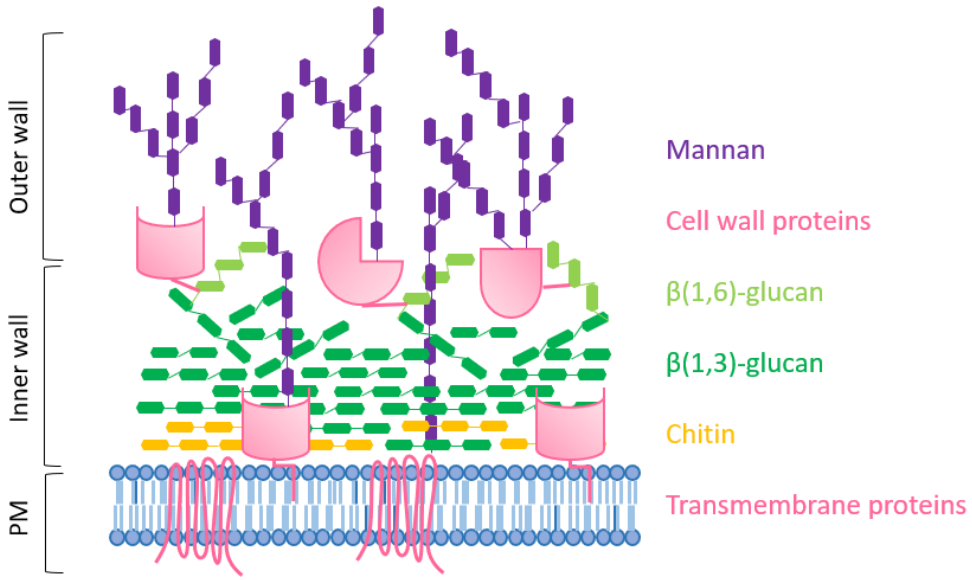


1.2. Structure of the *Candida albicans* cell wall

Cartoon representation of the different components making up the *C. albicans* cell wall. The cell membrane is at the bottom; chitin is shown in orange; glucans are shown in green (β, 1-3 darker and β, 1-6 lighter green); mannans are shown in purple and proteins in pink. Protein classes depicted are transmembrane proteins; plasma membrane GPI-anchored proteins; and cell wall GPI proteins which are bound to β, 1-6 glucans via a GPI remnant (Caro et al, 2007). Figure based on information from: Richard and Plaine, 2007; Erwig and Gow, 2016; Bowman and Free, 2006.

they are being translated in the ER and is modified in the ER and Golgi. The mannosylated proteins then enter the cell wall via the secretory pathway (Hall and Gow 2013).

Proteins in the *C. albicans* cell wall play important structural and functional roles. Some are adhesins, allowing the cell to adhere to host tissues (Sundstrom 2002). Some are enzymes, which may lyse host tissue during invasion, or remodel the cell wall itself. There are two main classes of proteins in the *C. albicans* cell wall (Chaffin 2008). The first are covalently attached to the cell wall via a GPI remnant (GPI-CWPs) or an alkali-labile linkage (Pir (proteins with internal repeats)) (Kapteyn et al. 2000, Alberti-Segui et al. 2004). The second group are secreted into the extracellular space (via the classic secretory pathway or an alternative route) and do not have an attachment sequence (Monteoliva et al. 2002). Some of these remain associated with the cell (see figure 1.2), and some are released into the environment. *C. albicans* has twice as many GPI-anchored proteins as *S. cerevisiae*, and these are known to play many key roles in cell wall maintenance and virulence (Richard and Plaine 2007, Plaine et al. 2008).

The fungal cell wall is not only a static protective structure. It is constantly regulated and remodelled in response to changing environmental conditions. The cell must maintain a cell wall which is both strong enough to resist turgor pressure and other stresses; and elastic enough to allow expansion and growth of the cell (Latgé 2007, Gow et al. 2017). A complex network of sensing and signalling pathways allow the cell to maintain this fine balance. After a stress is sensed, the cell wall can be regulated on a number of different levels. The expression or activity of biosynthetic enzymes can be up or down regulated. The availability of substrate can be controlled. The existing wall can also be modified. For example, linear glucan and chitin polymers can be cross-linked or branched by enzymes outside the cell, altering the tensile strength of the wall. Transglycosidase enzymes within the cell wall mediate cross-linking (Mouyna et al. 2000). The cell wall also contains hydrolases which break down chitin and glucan. Hydrolases are known to be required for cell division during cytokinesis (Cabib, Silverman and Shaw 1992, Martín-Cuadrado et al. 2003). The *C. albicans* cell wall has been shown to have a dramatically different ultrastructure depending on growth conditions (Ene et al. 2012) and in response to stress (Ene et al. 2015, Heilmann et al. 2013).

If the fungal cell wall is removed altogether, the cell (termed spheroplast) becomes spherical. The fungal cell wall therefore determines the shape of the cell which, as described above, is key to *C. albicans* virulence. Yeast and hyphal cells are known to have differences in cell wall composition and organisation, for example hyphae have more chitin than yeast cells (Braun and Calderone 1978) and less exposed β-glucan (Gantner et al. 2005). Universal links between wall composition and cell morphology however have not been defined. Better understood is how the cell controls its morphology by restricting the location of cell wall synthesis. Cell growth requires addition of both membrane and cell wall, however lipid membrane can flow and deform, whereas the cell wall is cross-linked and less deformable and thus governs the cell shape (Klis, Boorsma and De Groot 2006). Therefore, cell wall biosynthesis enzymes are maintained at sites of active growth at the hyphal tip or yeast bud (Bartnicki-Garcia and Lippman 1969, Smits, van den Ende and Klis 2001). Bartnicki-Garcia (1989) has modelled cell wall biosynthesis at the hyphal tip (via directed delivery of vesicles containing cell wall enzymes and materials) and has shown that it predicts the distinctive shape of fungal hyphae. Another mathematical model by Caballero-Lima and colleagues (2013) used Rho1 as a marker for cell wall deposition (Rho1 activates Fks1 for

β(1,3)-glucan biosynthesis) and showed that its polarised secretion to the hyphal tip, and subsequent removal by endocytosis, was sufficient to drive hyphal growth. This model assumes that the presence of active cell wall biosynthetic enzyme is the key factor driving wall biogenesis. A *S. cerevisiae* mutant with 50% less UDP-glucose, the substrate of glucan synthase, did not have reduced growth rate, suggesting that the supply of substrate is not rate limiting in cell wall biosynthesis (Daran et al. 1995).

As the barrier between the cell and its environment, the *C. albicans* cell wall is also the interface between the fungus and its host. The fungal cell wall contains many components which are not found in human cells, so serves as a key mechanism by which the human immune system recognises fungal cells. The immune system has evolved numerous pathogen recognition receptors (PRRs) which recognise specific PAMPs (pathogen-associated molecular patterns). For example, Toll-like receptor 4 (TLR4) recognises mannan; dectin-1 (a C-type lectin) recognises glucan; and Toll-like receptor 9 (TLR9) recognises chitin (Netea et al. 2008, van de Veerdonk et al. 2008). Recognition of these fungal structures by immune cells can lead to phagocytosis of the fungus and activation of an immune response. *C. albicans* meanwhile has various adaptations enabling it to evade the host immune system (Erwig and Gow 2016). Cells can rapidly alter their cell wall composition (Ene et al. 2013), and shield the most immunogenic components (Wheeler et al. 2008), to avoid immune detection.

## 1.4. The role of endocytosis in yeast and hyphal growth

The endocytic process, by which cells internalise cell membrane, associated proteins and extracellular fluid, has been described in detail in the model yeast *S. cerevisiae* (figure 1.3). Clathrin-mediated endocytosis (CME) is the most common and well characterised pathway in both yeast and mammalian cells. Patches of actin at the cell periphery were first observed in yeast in the 1980s (Adams and Pringle 1984), and were later shown to be sites of endocytic internalisation (Kübler and Riezman 1993, Kaksonen, Sun and Drubin 2003). Since then, the highly ordered arrival of ~60 proteins, culminating in membrane invagination and scission to form an intracellular vesicle, has been described in great detail (Weinberg and Drubin 2012, Riezman et al. 1997, Kaksonen 2008, Goode, Eskin and Wendland 2015).

Briefly, early proteins such as Ede1, Syp1 and Pal1 arrive at the membrane and mark the start of an endocytic site, which begins with an 'immobile' phase (Stimpson et al. 2009). We still do not know how this site is selected; though binding to specific plasma membrane (PM) lipids has been implicated (Aguilar, Watson and Wendland 2003, Henne et al. 2010). Transmembrane cargo proteins are then clustered at this site (Toshima et al. 2006), along with coat proteins such as adaptors and clathrin. The adaptors bind to peptide motifs on cargo proteins, or covalently attached ubiquitin signals, and help to cluster cargo and to recruit other coat proteins (Reider and Wendland 2011). There is a hypothesised transition point here, when sufficient cargo is found to be concentrated at the endocytic site, and from this point proteins are recruited at very consistent timepoints (Loerke et al. 2009). Middle and late coat proteins are likely to mediate the transition into the 'mobile' phase of endocytosis. Sla2 and epsins Ent1 and Ent2, followed by Sla1 and Pan1 are all recruited to the endocytic patch (Goode et al. 2015).

Nucleation promoting factors (Las17, Myo3/5 and Abp1) and the actin nucleator Arp2/3 then arrive and produce the branched F-actin network required to generate the force needed for invagination of the yeast membrane, beginning the 'mobile' phase (Sun, Martin and Drubin 2006, Aghamohammadzadeh and Ayscough 2009). Sla2, in binding the actin network, coat proteins and plasma membrane, is critical in transducing the force produced via actin polymerisation to membrane invagination (Engqvist-Goldstein et al. 2004). In the later stages, BAR family proteins Rvs161/167 and the yeast dynamin like protein Vps1 help to constrict the 'neck' of the invagination (Liu et al. 2006, Smaczynska-de Rooij et al. 2010), allowing pinching-off of a vesicle, which is then uncoated in cytoplasm (see figure 1.3 for schematic). Uncoating is mostly mediated by phosphorylation of coat proteins which disrupts their interactions and leads to disassembly (Sekiya-Kawasaki et al. 2003); this allows coat proteins to be re-used and allows the vesicle to fuse with other membrane compartments.

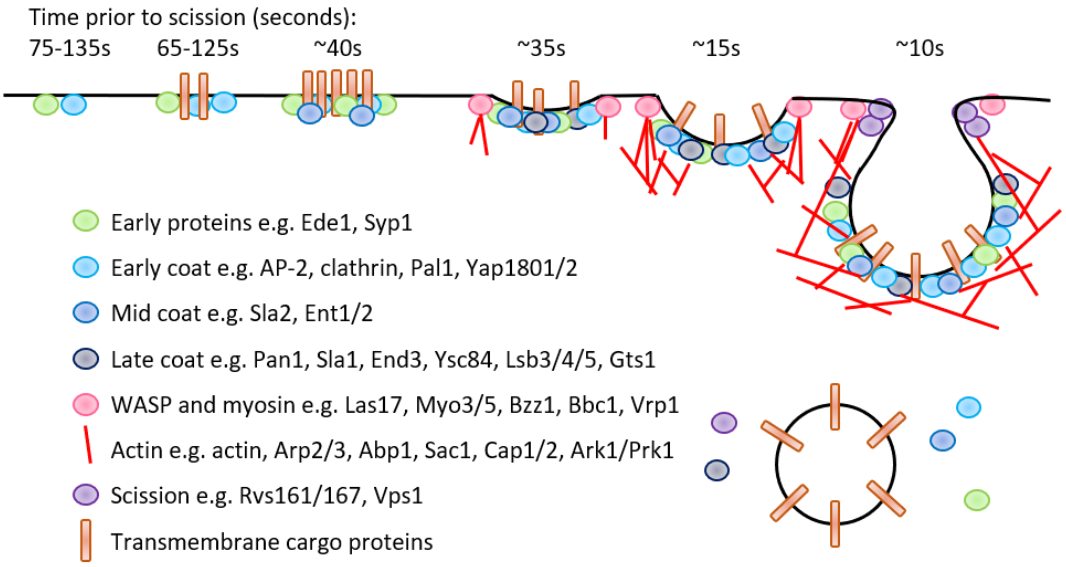


**1.3. Schematic of the process of clathrin-mediated endocytosis in *S. cerevisiae***

Schematic showing the process of yeast clathrin-mediated endocytosis over time from left to right, and the proteins which are recruited at each stage. The plasma membrane is shown in black, with invagination to form an intracellular vesicle at the end. The various protein depictions are explained in the key. Each coloured circle represents a group of proteins, and some of these proteins are listed in the key; the list is not exhaustive though. Above the schematic are the average times prior to scission that each module is recruited to the endocytic site. Figure based on information from: Weinberg and Drubin, 2012; Lu et al, 2016; Boettner et al, 2012; Goode et al, 2015.

Much of this sequence of events was discovered through work on *S. cerevisiae*, but the process is highly conserved through to mammalian cells (Smythe and Ayscough 2006). There are however a few differences between yeast and mammalian endocytosis. Firstly, clathrin is proposed to be more important in mammalian CME compared to yeast. In mammalian cells, clathrin triskelia form a latticed cage around the endocytic pit, and are essential for CME (Royle 2006). In yeast, though clathrin is recruited to endocytic sites, its deletion does not completely abrogate endocytosis (Payne et al. 1988, Kaksonen, Toret and Drubin 2005), and there seem to be fewer clathrin molecules present at sites of endocytosis (Sirotkin et al. 2010). Secondly, actin polymerisation is absolutely required for yeast endocytosis whereas endocytosis can sometimes proceed without it in mammalian cells. Aghamohammadzadeh and Ayscough (2009) showed that this apparent difference is due to the higher turgor pressure of yeast cells; F-actin is required to generate the force for invagination into the cell against turgor pressure. When turgor pressure was artificially reduced, the requirement for F-actin was decreased. Work from Boulant and colleagues (2011) confirmed that clathrin assembly is

sufficient to drive invagination of membranes under low tension, however actin polymerisation is required when the membrane is under tension due to osmosis or mechanical stretching. Finally, the differential roles of the AP-2 adaptor complex in yeast and mammalian CME will be discussed later on.

Despite its well established role in *S. cerevisiae* however, as recently as the early 2000s it was not known whether endocytosis occurred in fungal hyphae (Read and Kalkman 2003). In 2002, (Torralba and Heath) studied the markers Lucifer Yellow and Lanthanum and concluded that they were not endocytosed in *Neurospora crassa* hyphae. They argued that the uptake of FM4-64 observed by others (Fischer-Parton et al. 2000) could be a consequence of PM lipid flippases, and that as growing hyphae are continuously expanding they would not require endocytic retrieval of PM. However, genome sequencing showed that filamentous fungi have homologues of most proteins involved in yeast endocytosis, and it is now well accepted that endocytosis is actually critical to hyphal growth (Peñalva 2010, Shaw et al. 2011).

Polarised hyphal growth requires a fine balance of secretion and endocytosis (see figure 1.4). The actin cytoskeleton is polarised towards the hyphal tip, mediated by core polarity machinery such as the Rho GTPase Cdc42 and its downstream effectors (Hazan and Liu 2002). This ensures that the secretory pathway is directed towards the hyphal tip, providing a continuous stream of secretory vesicles to deliver the new membrane and cell wall components required for growth. The vesicle supply centre (VSC) model of hyphal growth proposes that the fungal Spitzenkörper accumulates secretory vesicles at the hyphal tip, before they fuse with the PM at the hyphal apex (Bartnicki-Garcia et al. 1989, Bartnicki-Garcia et al. 2000). Targeted delivery alone however may not maintain the polarised localisation of proteins at the hyphal tip in the face of continuous new membrane addition. Endocytic recycling is proposed to capture cargo sub-apically, so they can be recycled back to the hyphal tip and thus maintain their polarised localisation (Taheri-Talesh et al. 2008, Araujo-Bazán, Peñalva and Espeso 2008, Hernández-González et al. 2018).

This apical recycling model is supported by the fact that sites of endocytosis are indeed found in a 'collar' just behind the hyphal tip (Araujo-Bazán et al. 2008, Anderson and Soll 1986) and the fact that the endocytic marker FM4-64 rapidly stains the hyphal Spitzenkörper, suggesting endocytic vesicles are recycled here and contribute to apical extension (Fischer-Parton et al. 2000). Accordingly, the deletion of many key endocytic proteins leads to defects in hyphal growth. In *C. albicans*, deletions of Sla1 (Reijnst, Walther and Wendland 2010); Sla2 (Asleson et al. 2001); Pan1 (Martin et al. 2007); Wal1 (WASP homologue (Walther and Wendland 2004)); Vrp1 (Borth et al. 2010) and Myo5 (Oberholzer et al. 2002) all caused defective endocytosis and aberrant hyphal growth.

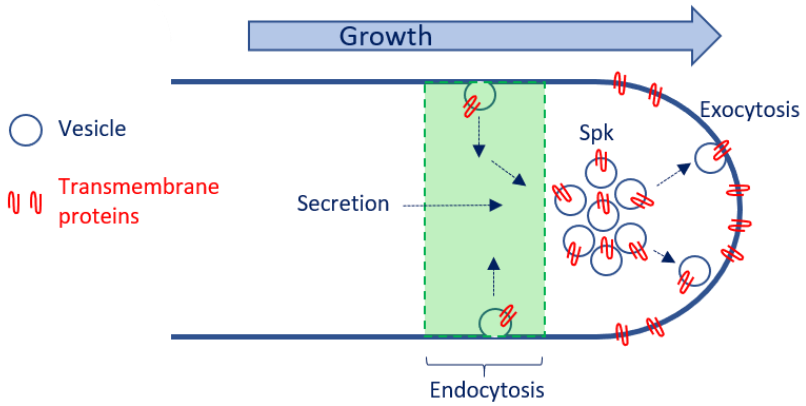


1.4. The apical recycling model of hyphal growth

Cartoon of a *C. albicans* hyphal tip. Membrane, including the plasma membrane and membrane vesicles shown in blue. Transmembrane cargo proteins shown in red. Secretion is directed towards the hyphal tip; secretory vesicles accumulate in a Spitzenkörper just behind the hyphal tip, prior to exocytosis at the tip. Endocytosis occurs in a sub-apical 'collar' region (highlighted in green) and serves to capture cargo which is then recycled back to the Spitzenkörper and thus re-polarised. This is a highly simplified diagram meant to describe the basic principle of the apical recycling model.

The role of this apical recycling in hyphal growth could be to re-absorb excess membrane inserted via secretory vesicles, and / or to recycle and thus re-polarise specific membrane proteins. Valdez-Taubas and Pelham (2003) showed that slow diffusion rates within the yeast plasma membrane enable polarisation to be maintained by endocytic recycling. In *S. cerevisiae*, the polarity landmark Cdc42 is maintained in a polarised localisation via endocytic recycling (Wedlich-Soldner et al. 2003). A combination of classical endocytosis via actin patches, and fast recycling mediated by the GDI (guanine nucleotide dissociation inhibitor) Rdi1, have been shown to maintain Cdc42 at the site of active bud or shmoo growth (Slaughter et al. 2009). Rdi1 mediates

extraction of Cdc42 from the membrane, by binding its C-terminal prenyl group and thus maintaining Cdc42 in the cytoplasm and enabling its recycling (Masuda et al. 1994, Slaughter et al. 2009). However whether this is how polarity markers are maintained in filamentous fungi is not yet known. Very few specific cargoes have been shown to be recycled during hyphal growth. Among these are the synaptobrevin SynA (Taheri-Talesh et al. 2008) and the phospholipid flippase DnfA (Schultzhaus, Yan and Shaw 2015) in *A. nidulans*. The endocytic mutants mentioned above, in which the endocytic process is defective, do not allow us to distinguish between the need to re-absorb membrane or the need to recycle certain proteins. Work presented here and in Knafler et al (2019) uses a mutant lacking the AP-2 endocytic adaptor complex, which is impaired in the uptake of some protein cargoes but does not have a reduction in endocytosis overall. The hyphal growth defect observed in this strain has underscored the importance of recycling specific protein cargoes in hyphal growth.

## 1.5. The role of endocytosis in cell wall regulation

As described above, *C. albicans* can rapidly remodel its cell surface, and this is key to its survival within different host niches and evasion of the host immune system. Transmembrane proteins such as receptors, transporters and enzymes are dynamically regulated to ensure continuous adaptation to changing conditions. Cell wall biosynthesis enzymes are controlled by membrane trafficking, to ensure that new cell wall deposition occurs when and where it is needed for growth and repair. During hyphal growth cell wall synthases must be maintained at the hyphal tip, to ensure that new cell wall deposition and hence cell growth occurs from the apex. The trafficking of chitin synthase enzymes has been studied in both yeast and filamentous fungi.

Chitin synthases are proposed to reside within the cell in vesicles termed chitosomes (Bracker, Ruiz-Herrera and Bartnicki-Garcia 1976). These can be isolated via subcellular fractionation, and have chitin biosynthetic activity in vitro (Ruiz-Herrera and Bartnicki-Garcia 1974). A great deal is now known about trafficking of Chs3 to the *S. cerevisiae* plasma membrane. *Sc*Chs3 is bound, via its acidic di-Leucine motif, by the adaptor complex AP-1, which mediates its traffic between the trans-Golgi network (TGN) and endosomes (Starr et al. 2012, Valdivia et al. 2002). Its transport to the plasma membrane is mediated by a protein complex named exomer (Sanchatjate and Schekman 2006, Wang et al. 2006), though it can still reach the plasma membrane via an

alternative route in the absence of exomer (Valdivia et al. 2002). AP-3 has also been shown to be important in Chs3 trafficking, possibly between the TGN and endosomes (Starr et al., 2012), although this pathway has not been defined. Interestingly, the exomer is not required for Chs3 trafficking in *C. albicans* (Anton, Taubas and Roncero 2018). Although these Chs3 homologues share over 50% sequence identity, their C' and N' regions are quite different, which could correspond to interactions with different trafficking adaptors (Anton et al. 2018).

There has been some dispute over whether chitosomes represent a stage in the endocytic pathway or not. Bartnicki-Garcia considers chitosomes to be involved in secretion of chitin synthase to the cell surface, but not in recycling. This is supported by the fact that the chitosome membrane is thinner than the plasma membrane (Bartnicki-Garcia 2006), suggesting a different lipid composition and therefore that chitosomes are not derived from the PM. Studies in *S. cerevisiae* however support the notion that chitosomes are also used for endocytic recycling. Ziman et al (1996) showed that intracellular chitosomes were decreased in an *end4* mutant defective in the internalisation step of endocytosis; suggesting that chitosomes are at least partially of endocytic origin.

Class V and VII chitin synthases, present in many filamentous fungi, are fused to myosin motor domains (MMDs) (Fujiwara et al. 1997). These MMD-Chss are critical to chitin deposition at the hyphal tip, though they are absent in *C. albicans* and *S. cerevisiae* (Lenardon et al. 2010). Work on the plant pathogen *Ustilago maydis* by the Steinberg lab has suggested that the MMD is required not for the cytoplasmic trafficking of chitosomes, but in tethering the vesicles to cortical actin at the hyphal apex and thus promoting exocytosis at the hyphal tip (Steinberg 2011).

It has been assumed that cell wall biosynthesis enzymes, including chitin synthase, would be regulated via endocytic recycling in filamentous fungi (Caballero-Lima et al. 2013, Steinberg 2007). As mentioned previously, cell wall deposition is restricted to the hyphal tip, to ensure growth occurs from the apex, and this has been shown in modelling to be achieved through targeted secretion and sub-apical endocytosis (Caballero-Lima et al. 2013). Actual evidence for recycling of those enzymes though has been lacking until recently. In 2018, the *A. nidulans* chitin synthase ChsB was shown to be polarised via endocytic recycling (Hernández-González et al.). Furthermore, work presented here and in Knafler et al (2019) demonstrates that Chs3 is also polarised via

endocytic recycling in *C. albicans*. We also demonstrate the physiological importance of this, as cells which cannot recycle Chs3 have dysregulated cell wall composition and hence defective morphology and virulence.

## 1.6. The AP-2 endocytic adaptor complex

Adaptors are proteins or complexes which select cargo proteins for inclusion in membrane vesicles, throughout the secretory and endocytic trafficking pathways. They provide a mechanism of selectivity, enabling the cell to enrich certain cargoes to certain destinations in a dynamic way (Robinson 2004, Robinson and Bonifacino 2001, Pawson and Scott 1997)). The existence of protein adaptors was first hypothesised in the 1980s, when scientists observed proteins of roughly 100,000 Mw size which co-purified with clathrin coated vesicles (Unanue, Ungewickell and Branton 1981, Vigers, Crowther and Pearse 1986, Pearse 1985, Robinson 1987). Observing that these proteins were positioned between the clathrin lattice and the membrane vesicle, and that they could bind certain cargo proteins, led to speculation that these components could explain how cells sort proteins into specific vesicles, and therefore send cargo to the right place in the cell at the right time (Robinson 1987).

This was soon proven to be the case, with heterotetrameric adaptor proteins 1 and 2 (AP-1 and AP-2) the first to be described (Pearse and Robinson 1984, Ahle et al. 1988). AP-1 is found at the trans-Golgi network (TGN) and endosomes, whilst AP-2 is found at the plasma membrane (PM). There is now known to be a host of other cargo adaptors: AP-3, AP-4 and AP-5; the monomeric adaptor family; the GGAs (Golgi-localized, γ-ear-containing, ARF-binding proteins); and a range of cargo-specific adaptors (reviewed in (Robinson 2004)). These adaptors each enrich a subset of cargoes to a particular membrane trafficking pathway.

The AP-2 adaptor complex was the first endocytic adaptor to be characterised, and has since been much studied in mammalian systems, and plays a key role in CME (Robinson 1987). Endocytic adaptor proteins bind to the cell membrane; to specific motifs on cargo proteins; and to clathrin. Their role in selecting specific cargo to be internalised, linking these to the forming endocytic pit, and recruiting other regulatory components, is critical to selection and stabilisation of the early endocytic site. The binding of cargo and clathrin by an adaptor complex is crucial for progression of endocytosis and may be a

limiting step in CME (Ehrlich et al. 2004). AP-2 is known to enable the endocytic uptake of many important transmembrane cargoes (see (Kirchhausen 1999, Collins et al. 2002).

Like the other AP complexes, AP-2 has larger (~100 kD) α and β subunits which bind the plasma membrane, allowing the smaller μ (~50 kD) or δ (~18 kD) subunits (see figure 1.5) to bind specific internalisation motifs on transmembrane cargo (Conner and Schmid 2003b). Detailed structural information of the complex has been elucidated by the lab of David Owen (Collins et al. 2002). On the μ subunit is a site which binds YxxΦ internalisation motifs; where Y is a tyrosine, x is any amino acid and Φ is a bulky, hydrophobic amino acid (Ohno et al. 1995, Owen and Evans 1998). On the α / σ

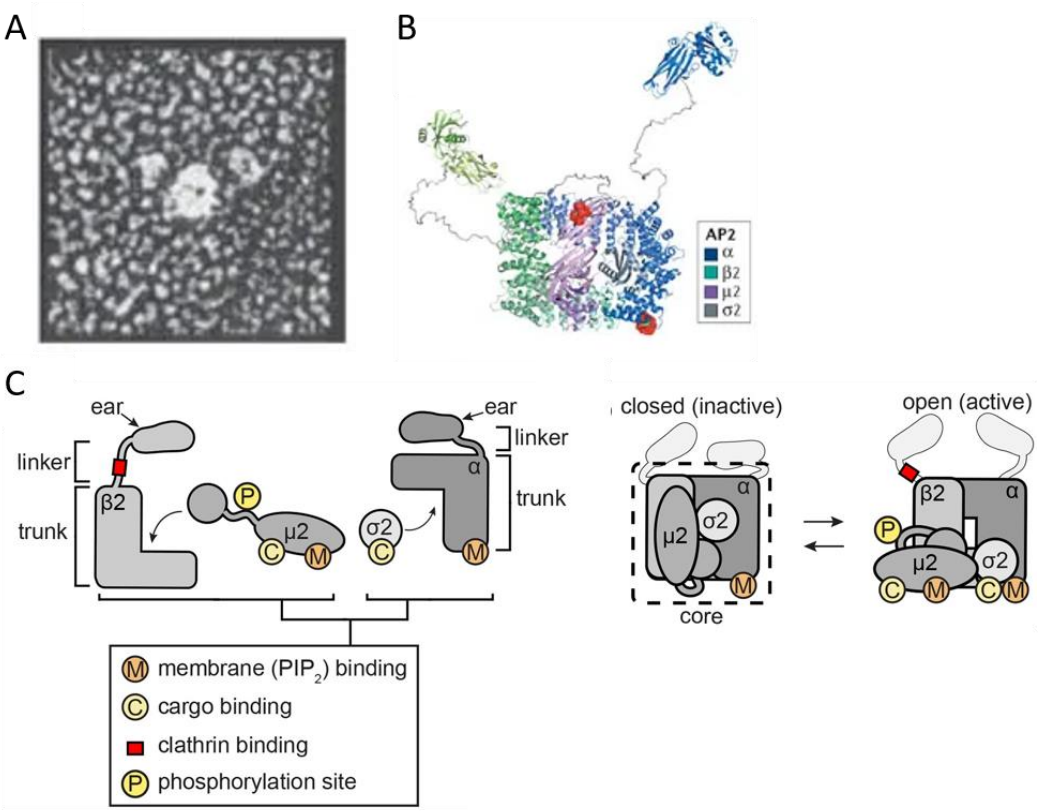


1.5. Structure of the mammalian AP-2 endocytic adaptor complex

(A) An early electron microscopy image of an adaptor protein complex from 1988; the central trunk and two 'ears' or appendages are visible. Reproduced with permission from Heuser and Keen, 1988. (B) Model of AP-2 structure from x-ray crystallography data from Collins et al. 2002. The four subunits (α, β, μ and δ) are shown in different colours, and in red are phosphoinositide head group mimics which were co-crystallised with the complex. Reproduced with permission from Edeling, Smith and Owen, 2006. (C) Left: cartoon representation of the four subunits of AP-2 and the locations of various binding sites; the subunits are shown separately for clarity. Right: the AP-2 complex in its closed then open conformations; note that most of the binding sites are inaccessible in the closed conformation but accessible in the open conformation. Reproduced with permission from Beacham et al. 2018.

subcomplex is a site which binds D/ExxxLL/I (a dileucine motif; D is aspartate, E is glutamate, L is leucine and I is isoleucine (Doray et al. 2007)). The α and β subunit core 'trunk' domains are connected via flexible linkers to small appendage or 'ear' domains, which are proposed to bind and recruit many other accessory proteins (Slepnev and De Camilli 2000, Traub et al. 1999). The α appendage domain binds Eps15, epsin, amphiphysin, AP180 and dynamin, suggesting that it is a central hub for interactions between endocytic proteins (Traub et al. 1999). AP-2 interacts with clathrin via a clathrin box motif on the β linker (ter Haar, Harrison and Kirchhausen 2000) and via its β appendage domain (Owen et al. 2000) thus recruiting clathrin to endocytic sites (clathrin cannot bind membrane itself). Finally, both the μ subunit and the α subunit trunk domain bind $PI(4,5)P_2$ headgroups, positioning AP-2 at the plasma membrane (Collins et al. 2002, Gaidarov and Keen 1999).

AP-2 is known to exist in different conformational states which allow its spatial and temporal regulation (figure 1.5C). In the first crystal structure of AP-2, both the cargo and clathrin binding sites were inaccessible (Collins et al. 2002). Only one membrane binding site, on the α subunit, was available for binding (Gaidarov et al. 1996). This conformation, known as the closed or inactive confirmation, is hypothesised to prevent AP-2 from binding cargo or clathrin when it is soluble in the cytoplasm. Co-crystallisation of AP-2 with a tyrosine motif peptide enabled elucidation of the open conformation (Jackson et al. 2010). In this state, the cargo and membrane binding sites are exposed and in one plane (figure 1.5C). This conformational switch provides a mechanism for the cell to regulate AP-2 activity, however it is unclear how this conformational change is induced at precisely the right time and place. The presence of cargo motifs was shown to generate an open conformation (Jackson et al. 2010), but how the motif might initiate interaction with inactive 'closed' AP-2 in which its binding site is inaccessible is unclear. Inactive 'closed' AP-2 can bind $PI(4,5)P_2$ (Collins et al. 2002) which has been shown to enhance cargo binding (Höning et al. 2005) but whether membrane binding is sufficient to activate AP-2 is unknown. One study has suggested that two AP-2 complexes must bind the membrane before endocytosis can be initiated (Cocucci et al. 2012) possibly adding another layer of regulation.

Cargo and clathrin binding are thought to stabilise the open form of AP-2, perhaps providing a checkpoint to ensure a productive endocytic event (Ehrlich et al. 2004). FCHo (Fer/CIP4 homology domain only) proteins, which are recruited to endocytic sites at a similar time to AP-2, are proposed to increase the affinity of AP-2 for the membrane,

thereby stabilising endocytic sites (Cocucci et al. 2012). Phosphorylation of the µ subunit at a conserved residue in its linker region increases the affinity of AP-2 for membrane and cargo (Ricotta et al. 2002, Fingerhut, von Figura and Honing 2001). It is unclear whether phosphorylation induces, or stabilises the AP-2 open confirmation, see chapter 3 for further discussion.

There are also unanswered questions as to how AP-2 is inactivated after endocytosis has occurred. The endocytic coat must disassemble after the vesicle is pinched into the cell, to allow the vesicle to bind other factors on target membranes. A protein family called adaptiN Ear-binding Coat-Associated Proteins (NECAPs) have been suggested to be negative regulators of AP-2, as loss of NECAP in *C. elegans* leads to accumulation of active AP-2 (Beacham et al. 2018). NECAPs bind phosphorylated, open AP-2, and are recruited to endocytic sites after clathrin, therefore could bind active AP-2 here and mediate its inactivation (Beacham, Partlow and Hollopeter 2019).

## 1.7. The role of AP-2 in yeast and fungi

The bakers' yeast, *S. cerevisiae*, has been a model organism for many years due to its relative biological simplicity, amenability to genetic manipulation and overall similarity to mammalian cells. It has a range of resources which, along with its genetic tractability, facilitate relatively simple study of key biological processes. One such example is the process of endocytosis, which studies in *S. cerevisiae* have been central to describing. As mentioned previously, clathrin mediated endocytosis (CME) is broadly similar in yeast and mammalian cells, but with a few important distinctions (see earlier).

One such difference appears to be the role of the AP-2 complex. AP-2 is critical for clathrin recruitment in mammalian cells and, although CME can occur in its absence, its disruption via RNA interference leads to dramatically fewer CCPs forming (Hinrichsen et al. 2003, Boucrot et al. 2010, Motley et al. 2003). AP-2 is required for endocytosis of the mammalian transferrin receptor, but not of the EGF (epidermal growth factor) receptor (Motley et al. 2003). *S. cerevisiae* is known to encode homologues to AP-1, AP-2 and AP-3 subunits (Yeung, Phan and Payne 1999). In yeast however, AP-2 depletion gives a very mild phenotype, so AP-2 was long thought to be unimportant or redundant. Research in yeast has historically focussed on endocytosis of marker dyes rather than of specific proteins, and AP-2 disrupted yeast cells are not defective in Lucifer Yellow dye uptake.

Moreover, yeast AP-2 has been shown not to interact genetically or physically with clathrin (Yeung et al. 1999).

More recent research has pointed to a cargo-specific role for yeast AP-2. The first role for yeast AP-2 came to light in 2009 when the Drubin lab showed its requirement for the response of cells to K28 killer toxin (Carroll et al. 2009). K28 is an A/B toxin whose uptake requires interaction with a cell wall mannoprotein, then with the transmembrane receptor Erd2, which triggers its uptake via CME. It is trafficked to the ER, from where it translocates into the cytoplasm (Becker and Schmitt 2017). A screen of mutants with altered sensitivity to K28 showed that deletion of any of the AP-2 subunits led to strong K28 resistance. Mutants lacking AP-2 did not accumulate K28 in their cytoplasm, suggesting that AP-2 mediates the endocytic uptake of this receptor-toxin complex. Further light was shone on its importance in 2014 by the Ayscough lab (Chapa-Y-Lazo and Ayscough 2014, Chapa-y-Lazo et al. 2014). Here, AP-2 was shown to play a role in the formation of pseudohyphae (filamentous growth of yeast upon nutrient starvation) and mating projections. This was suggested to be in part due to its role in re-localisation of the Mid2 cell wall stress sensor, implicating AP-2 in both polarised growth and the cell wall integrity pathway in yeast.

It is therefore intriguing that deletion of the AP-2 complex has a much stronger phenotype in *C. albicans*. The Ayscough lab showed by deleting the µ subunit (*apm4*) that AP-2 is required for the maintenance of polarised hyphal growth in *C. albicans*. Mutants had short and misshapen hyphae (Chapa-y-Lazo et al. 2014), supporting the idea that the complex is involved in polarised cell growth. A role for AP-2 in polarised growth was also shown in a more recent paper by Martzoukou and colleagues (2017) who studied the complex in *Aspergillus nidulans* and observed it to have a role in polarised lipid and cell wall deposition. This paper suggested a role for AP-2 in the recycling of lipid flippases *An*DnfA and *An*DnfB as AP-2 depletion caused loss of their polarised localisation. Two recent studies carried out similar experiments but in the plant pathogen *Fusarium graminearum* and showed that here also AP-2 is critical to hyphal growth and cell wall integrity. They showed that in this species, AP-2 is responsible for the localisation of a different CWI sensor *Fg*Wsc2B (Xu et al. 2019), and the lipid flippases *Fg*DnfA and *Fg*DnfB (Zhang et al. 2019).

Interestingly, though evolutionary genetics has shown that all fungi contain AP-2 subunits (Barlow, Dacks and Wideman 2014), more detailed analysis from Martzoukou

et al (2017) showed that dikarya (higher fungi) have lost the C-terminal appendage of their β subunits and thus lost the conserved clathrin binding domains. The authors observed that in *A. nidulans* clathrin was required for the endocytosis of transporters but dispensable for apical recycling of polarised cargoes; and the converse was true of AP-2. This led Martzoukou and colleagues to hypothesise that fungal AP-2 has evolved a specialised, clathrin independent function, perhaps to enable their highly polarised manner of growth. It is not yet clear whether this is the complete story. The absence of a canonical clathrin binding motif does not necessarily mean fungal AP-2 cannot bind clathrin; some known clathrin interactors such as CALM and Synaptojanin 1 do not contain known clathrin binding motifs (Dell'Angelica 2001). The observation that clathrin and AP-2 do not co-localise at endocytic sites could be due to weak fluorescence signals; quantitative analysis in *S. pombe* showed as few as 30 clathrin molecules present at each endocytic site (Sirotkin et al. 2010). If fungal AP-2 complexes have indeed lost their clathrin binding ability, there are many other endocytic coat proteins which bind clathrin and could fulfil this function (Dell'Angelica 2001). It does seem likely however that AP-2 has a specialised role in fungi, involving endocytosis of specific cargoes for the maintenance of polarised growth and cell wall integrity.

## 1.8. Aims and objectives

The overall aim of this study has been to elucidate the role of the AP-2 endocytic adaptor complex in the fungal pathogen *C. albicans*. The main objectives of this work were to:

- Characterise *C. albicans* mutants which are deleted in *apm4* and hence do not have functional AP-2 complexes
- Identify endocytic cargoes of AP-2 and therefore gain insight into the mechanisms underlying the observed defects
- Determine whether the regulation via phosphorylation described for mammalian AP-2 occurs in *C. albicans* AP-2

Some of the key findings from this study are summarised below:

- Microscopic analysis showed that *C. albicans* cells without AP-2 had severe defects, particularly in hyphal morphology, demonstrating the importance of the AP-2 complex in polarised growth in *C. albicans*

- Staining of *C. albicans* cells with various dyes and markers, and HPLC analysis of purified cell wall material, revealed that AP-2 is critical for the correct composition and organisation of both the *C. albicans* cell wall and plasma membrane
- Labelling of proteins with fluorescent tags, in strains both with and without Apm4, enabled identification of several proteins whose correct localisation requires the AP-2 complex. These included Chs3; and members of the polarisome and exocyst complexes
- Further genetic manipulation revealed that excess chitin production via surface-localised Chs3 was partially responsible for the morphological defects of the *apm4* mutant; and that Chs3 localisation was dependent on the YxxΦ motif binding domain of Apm4
- Immunoprecipitation of Apm4 and analysis via gel electrophoresis indicated that *C. albicans* Apm4 may have multiple phosphorylation sites and was more phosphorylated during yeast growth compared to hyphal growth
- Atomic force microscopy analysis revealed that cell wall defects may lead to altered mechanical properties in hyphae lacking AP-2

The work presented in this thesis includes the paper: Knafler, H. C., Smaczynska-de Rooij, I. I., Walker, L. A., Lee, K. K., Gow, N. A. R., Ayscough, K. R (2019) AP-2-Dependent Endocytic Recycling of the Chitin Synthase Chs3 Regulates Polarized Growth in *Candida albicans*. *mBio*, 10:e02421-18. Additional unpublished work is presented in three results chapters. Taken together, this work establishes the crucial role of endocytosis of specific membrane cargoes, via the AP-2 complex, in the maintenance of polarity and cell wall integrity of this important fungal pathogen.

# Chapter 2: Materials and Methods

Please note, all buffers and media mentioned in the methods are described in more detail in tables at the end of the section. Antibodies and *C. albicans* strains used are also listed at the end of this section.

## 2.1. Bacterial methods

### 2.1.1. Preparation of competent bacteria

*Escherichia coli* DH5α or XL 10-Gold cells were made chemically competent for transformation. Cells from a frozen glycerol stock were grown on 2xYT agar plates at 37°C overnight. A single colony was inoculated into 5 mL liquid 2xYT and grown at 37°C overnight, then 500 µL was added to 50 mL 2xYT and grown at 37°C until the $OD_{600}$ reached 0.5. From this point, cells were kept chilled at all times. Cells were harvested by centrifugation at 4000 x *g* for 5 minutes and resuspended in 10 mL ice cold 0.1 M $CaCl_2$. Cells were incubated on ice for 2 hours then spun as before and resuspended in 2 mL ice cold 0.1 M $CaCl_2$. Glycerol was added to a final concentration of 15% (v/v) prior to flash freezing in liquid nitrogen and storage at -80°C.

### 2.1.2. Bacterial transformation

20 - 40 µL of competent bacterial cells were thawed on ice, then 100 – 500 ng plasmid DNA added, and incubated on ice for 20 minutes. Cells were heat shocked at 42°C for 45 seconds then returned to ice for 3 minutes (without mixing). 750 µL warm 2xYT was added and tube incubated in 37°C shaking incubator for 1 hour. Cells were spun at 18,000 x *g* in a microcentrifuge for 30 seconds, most of supernatant removed, then cells resuspended in remaining medium and spread onto 2xYT plates containing selection agent (100 µg / mL ampicillin or 30 µg / mL kanamycin). Plates incubated at 37°C overnight. Stocks of transformed bacteria (overnight cultures) were stored 1:1 in 50% glycerol at -80°C.

### 2.1.3. Bacterial plasmid isolation

A single colony of *E. coli* expressing the required plasmid was inoculated to 5 mL 2xYT with selection agent (100 µg / mL ampicillin or 30 µg / mL kanamycin) and grown in 37°C

shaking incubator overnight. Then the Qiagen miniprep or midiprep kits were used, as per manufacturers' instructions. Purified plasmid DNA was resuspended in either $dH_2O$ or TE buffer and stored at 4°C (<2 weeks) or -20°C (longer term). DNA concentration and purity were measured using a NanoDrop spectrophotometer.

## 2.2. DNA methods

### 2.2.1. Integration cassettes via PCR

For PCR-based gene targeting in *C. albicans*, cassettes were made by PCR amplification of the appropriate deletion or tagging module from a plasmid, with primers incorporating long regions of homology to the target gene. Primers were designed with 20 bp homology to the appropriate regions on the plasmid, then 100 bp homology to the target gene (before ATG and after stop codon if gene was to be deleted; or immediately before and after stop codon if gene was to be tagged on C'). Primers were synthesised by Eurofins. Plasmids used were pFA modules (Gola et al., 2003 and Schaub et al., 2006) kindly shared by the Wendland lab: pFA-HIS1, pFA-ARG4, pFA-URA3, pFA-SAT1, pFA-LEU2-GFP.

For PCR amplification, 4 x 100 µL reactions were prepared each with: 1 pmol/µL each primer; 0.8 mM dNTPs (Bioline); 20 – 200 ng plasmid template (0.2 µL miniprep); 2 mM $MgCl_2$ (Bioline); 2 Units Taq polymerase (Bioline); 1x Taq buffer (Bioline).

The PCR reaction was run on the following schedule:

1. 95°C – 3 minutes
2. 92°C – 1 minute
3. 53°C – 1 minute
4. 72°C – 4 minutes – cycle to step 2 x30
5. 72°C – 10 minutes
6. 4°C – 10 minutes

PCR product was precipitated in ethanol at -20°C and resuspended in TE buffer ready for transformation to *C. albicans* (see section 2.3).

### 2.2.2. Agarose gel electrophoresis

Agarose gels were prepared with 1% agarose in TAE buffer (melted to dissolve) plus ~ 10 µg/mL Ethidium Bromide. DNA samples were mixed with Orange G 10x loading dye (30%

glycerol; 2 mg/mL Orange G) and loaded into wells of the set gels. Gels were run at 100 V until the dye front had migrated down 2/3rds of the gel. Gels were visualised on a UV transilluminator.

### 2.2.3. Integration plasmids

For integration of constructs into the *RPS1* (ribosomal protein 1 coding region) locus in the *C. albicans* genome, pExpArg plasmids were kindly provided by the Arkowitz lab (Bassilana et al., 2003).

Plasmids were transformed to DH5α *E. coli* cells and isolated via miniprep as described above. 5 – 10 µg of plasmid DNA was linearized with *Stu1* restriction enzyme (New England Biolabs) at 37°C for 3 hours. This was run on an agarose gel to confirm linearization then cleaned via ethanol precipitation. This was transformed to *C. albicans* cells as described below, where the construct integrates into the *RPS1* locus. Correct integration was confirmed by colony PCR and sequencing (see below).

To re-introduce the *APM4* gene into *C. albicans*, this gene was cloned into the empty pExpArg plasmid. First, *APM4* was amplified from genomic DNA with primers designed to add *Sph1* restriction sites to both ends of the gene. The gene and vector were then both digested with *Sph1* (New England Biolabs; 1 hour at 37°C) then cleaned via the Quiagen PCR Purification Kit or Gel Extraction Kit (as per manufacturer's instructions). The gene was then ligated into the vector with the T4 DNA ligase kit (New England Biolabs) as per manufacturer's instructions and at an insert : vector ration of 7:1. After ligation for 2 hours at 25°C, the ligated plasmid was transformed to competent DH5α cells. Correct gene insertion was confirmed via digestion with *Sph1* (insert and vector bands should be visible on an agarose gel) and sequencing. This new plasmid could then be linearized and transformed to *C. albicans* for integration as described above.

### 2.2.4. Site directed mutagenesis

For site directed mutagenesis, the QuikChange Lightning Site-Directed Mutagenesis Kit (Agilent) was used as per manufacturer's instructions. Plasmids were sequenced to confirm correct mutation.

### 2.2.5. Colony PCR

Colony PCR was used on *C. albicans* colonies after transformation, to confirm that the construct had integrated in the desired location. Transformants were lysed in 0.02M NaOH at 100°C for 20 minutes. 2.5 µL of this material was added to a 20 µL PCR reaction, containing Phusion High-Fidelity PCR Master Mix with HF Buffer (New England Biolabs) and appropriate diagnostic primers. Primers were designed to anneal to the flanking sequence of the target gene, and to the auxotrophic marker gene in the cassette. Therefore, if PCR products were observed via agarose gel electrophoresis, this indicated that the cassette was integrated into the target gene. Correct integration was confirmed by sequencing.

### 2.2.6. Genomic DNA extraction (*C. albicans*)

Genomic DNA was extracted from transformed *C. albicans* strains for sequencing. Cells were grown overnight as described in section 2.3, then harvested by centrifugation. 200 µL lysis buffer; 200 µL of glass beads; and 200 µL phenol chloroform (phenol : chloroform : isoamyl alcohol 24:24:1; Merck) were added to each pellet. These were vortexed for 3 minutes. 200 µL TE was added and tubes centrifuged for 5 minutes at 18,000 x *g*. The supernatant was added to 1 mL ice cold ethanol, then centrifuged for 2 minutes. This supernatant was discarded, and the pellet dried at 37°C. This was then re-suspended in TE and incubated with 10 µg/mL ribonuclease A (from bovine pancreas; Merck) for 30 minutes at 37°C. Then 100 mM ammonium acetate was added, and the ethanol precipitation and wash step repeated. The pellet was finally resuspended in TE and 1 µL used in PCR.

## 2.3. Yeast methods

### 2.3.1. *C. albicans* culture

For long term storage, *C. albicans* cells were grown to stationary phase and stored in cryovials with 25% glycerol at -80°C. When needed, frozen cells were struck onto YPD agar plates and incubated at 30°C. For experiments, one colony was taken from an agar plate with a sterile toothpick and inoculated to 5 mL liquid YPD and grown at 30°C with shaking (180 rpm) for 16 – 18 hours to reach stationary phase. For yeast cells, this overnight culture was diluted 1:10 into fresh YPD and incubated for a further 3 – 4 hours at 30°C with shaking to attain logarithmic growth phase ($OD_{600}$ ~ 0.5). For hyphal cells,

the stationary phase culture was diluted 1:10 into fresh YPD with 10% fetal bovine serum (FBS; Gibco) and grown at 37°C with shaking for 90 minutes, unless otherwise stated.

### 2.3.2. Growth curves

For analysis of growth rate, *C. albicans* cells were grown overnight and the $OD_{600}$ measured on a spectrophotometer. They were then diluted into 50 mL fresh YPD such that the $OD_{600}$ would be 0.1. The $OD_{600}$ was measured after dilution, and cells then incubated at 30°C with shaking, with the $OD_{600}$ of a 1 mL sample measured each hour.

### 2.3.3. Plate spotting assays

Plate spotting assays were used to assess growth of *C. albicans* strains when exposed to various chemicals. YPD agar plates were made, containing either 150 µg/mL Congo Red; 80 µg/mL Calcofluor White; 10 mM caffeine; 0.01% SDS; 2 – 4 µg/mL Fluconazole (in DMSO); 180 µM Edelfosine; 1 - 2 µg/mL Myriocin (in methanol) or 2% lactate (on lactate plates glucose was omitted). Chemicals were added to molten agar after it had cooled to room temperature, prior to pouring plates. A haemocytometer was used to count *C. albicans* cell numbers (from overnight cultures) then serial dilutions were made; starting at $10^7$ cells / mL (then $10^6$, $10^5$, $10^4$, $10^3$ cells / mL). These were spotted onto the agar plates using a 'hedgehog' tool sterilised with ethanol and flame. Plates were incubated at 30°C or 37°C then photographed after 48 hours and growth observed. Spotting onto YPD plates without additional chemicals, or with DMSO or methanol where this was the solvent used, was used as a control for even loading between strains. Each assay was repeated three times and a representative photograph selected.

### 2.3.4. *C. albicans* strain generation

*C. albicans* strains used are listed in Table 2.4. Background strains used were SN76 (which has *ura3*; *his1* and *arg4* auxotrophies enabling selection of mutants) and SN148 (*ura3*, *his1*, *arg4* and *leu2* auxotrophies), both from (Noble and Johnson 2005).

Gene tagging and deletion was performed as described in (Longtine et al. 1998). An overview of the process is show in figure 2.1. DNA constructs or 'cassettes' were

designed which would integrate to the target gene within the *C. albicans* genome and thereby either delete or add a tag (such as GFP) to the gene of interest. These integrative cassettes were synthesised via PCR as described in section 2.2.1. Their 100 bp regions of homology with the target gene meant that, upon transformation to *C. albicans* as described in below, the cassettes integrated into the target gene via homologous recombination – see figure 2.1 for an overview. For gene deletion, the presence of the cassette within the target gene lead to that gene not being expressed. For gene tagging, the presence of the tagging cassette lead to expression of the gene of interest fused to a tag protein such as GFP.

For transformation, 500 µL of overnight culture was inoculated into 50 mL YPD in a flask and incubated in 37°C shaking incubator for 4 hours. Cells were harvested by centrifugation at 3000 *x g* for 3 minutes, then resuspended in 1 mL TE buffer. Cells were spun as before and resuspended in 1 mL lithium acetate solution. Cells were then spun again and re-suspended in 150 µL LiOAc solution. 100 µL of this was added to 10 µL salmon sperm ssDNA (10 mg/mL; Merck) and 1 – 8 µg DNA (~ 40 µL PCR product) and mixed gently. Then 600 µL 50 % $PEG_{400}$ (v/v in LiOAc solution) was added and mixed gently again. Cells were incubated overnight at 30°C without shaking, then heat-shocked at 44°C for 15 minutes. Cells were briefly spun in a microcentrifuge, then resuspended in 100 µL $dH_2O$ and spread on agar plates with the appropriate selective agent (either dropout Uridine, Leucine, Arginine or Histidine; or 100 µg / mL Nourseothricin). Plates were incubated at 30°C for 2 – 5 days.

After growth, single colonies were struck out on fresh selection plates, and correct integration confirmed by checking PCR and / or sequencing (see above).

### .3.5. Preparation of *C. albicans* cell extracts

*C. albicans* cells were grown as described. Cells were harvested by centrifugation at 3000 *x g* for 3 minutes, washed in cold sterile $dH_2O$ and kept chilled from this point. Cells were harvested again and resuspended in lysis buffer. Either:

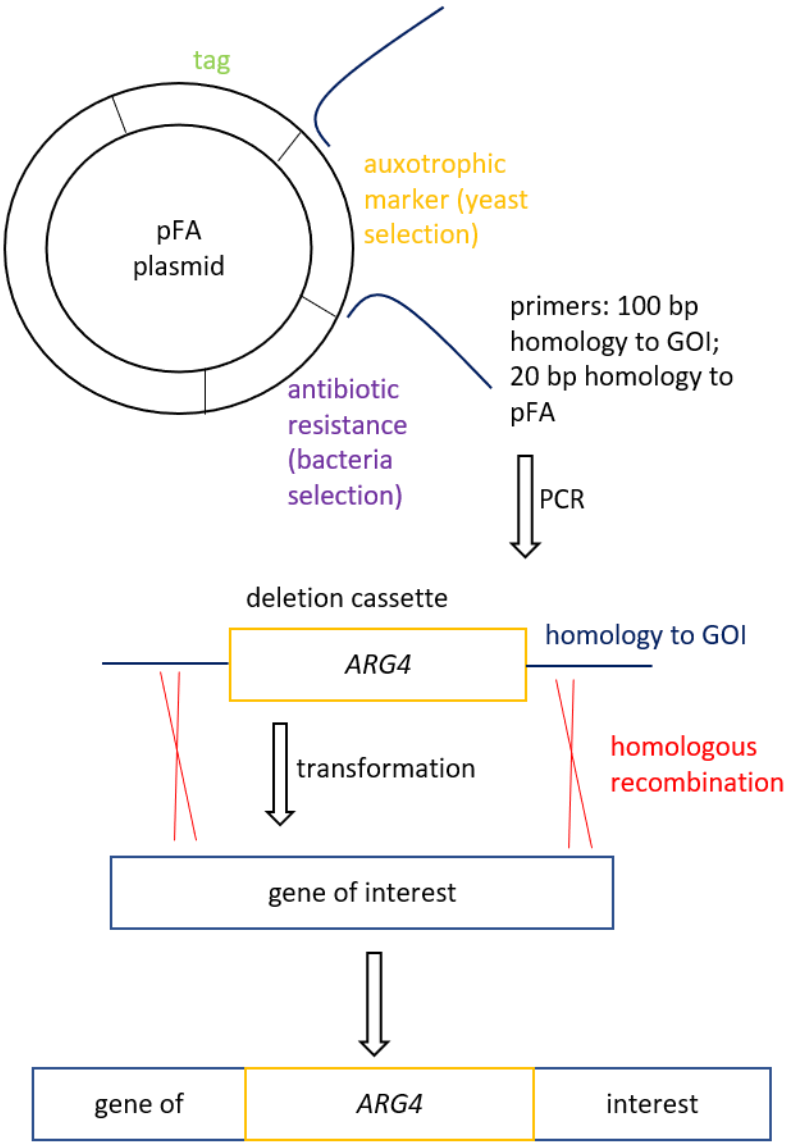


By altering the primers, tagging rather than deleting is achieved:


2.1. Overview of approach used to tag or delete genes in *C. albicans*

Cartoon representation of PCR-based amplification of deletion or tagging cassettes, then transformation into *C. albicans* such that the cassette is integrated into the gene of interest within the genome. This is described in more detail in the text.

(A) Cell mix was added to an equal volume of glass beads, and 1x Laemmli sample buffer. Vortexed for 3 minutes then boiled for 3 minutes, then cooled on ice. Sample was spun down at 18,000 x *g* then supernatant removed to fresh tube. Samples run on SDS-PAGE gel or stored at -20°C.

(B) Cell mix was dripped into liquid nitrogen then ground in a pestle and mortar under liquid nitrogen to break cells. This powder was slightly thawed then thawed on ice for 10 minutes. Powder was then mixed with lysis buffer + 2% (v/v) glycerol. Lysate spun at 18, 000 *x g* for 5 minutes to remove cell debris and lysate removed to a fresh tube. Samples were then ready for immunoprecipitation (see below) or 1x Laemlli sample buffer was added, boiled, and ran on an SDS-PAGE gel.

### 2.3.6. Biofilm assay

The biofilm assay was used to assess biofilm formation of different strains on plastic substrate. $10^5$ *C. albicans* cells, resuspended from an overnight culture into fresh YPD with 10% FBS, were added per well to 96-well plates. Each strain to be analysed had at least 10 wells, and 'blank' wells were filled with medium alone. Plates were incubated at 37°C for 48 hours and $OD_{600}$ measured using a plate reading spectrophotometer, to assess overall cell growth. Then, wells were washed 3 times with sterile PBS to remove non-adhered cells and examined via light microscopy. Then, 20 µL XTT reagent (Merck) was added per well, incubated for 2 hours at 37°C, the supernatant from each well was removed and its absorbance at 450nm was measured, using a fluorimeter, as an assay of metabolic activity. Background absorbance at 690nm was subtracted from values.

### 2.3.7. Agar penetration assays

Overnight cultures of *C. albicans* were mixed 1:6000 with YPS agar which had been melted then cooled to room temperature. YPS with either 1%, 2% or 4% agar was used. This was poured into petri dishes and left to set then incubated at room temperature for 48 hours. Cells were imaged via light microscopy either directly through bottom of agar plate, or by cutting sections of agar and placing on glass slides.

### 2.3.8. Lucifer Yellow uptake assay

Fluid phase endocytosis was assessed using an assay adapted from Bar-Yosef et al.(2017). Yeast cells were refreshed to log phase, as described above, then incubated with 2 mg/mL Lucifer Yellow (LY) dye for 1 hour at room temperature with rotating. Cells were harvested by centrifugation at 3000 *x g* for 3 minutes, then washed in sterile PBS 5 times to remove external LY dye. Cells were then lysed using Zymolyase-20T (mpBio) at 2000 Units / mL and fluorescence measured at 426 nm excitation / 550 nm emission.

Concurrently, an aliquot of sample was taken after lysis and the protein concentration measured via Bradford assay (see below). The fluorescence intensity measured was then normalised to the protein concentration of each sample, to correct for differential growth rates.

### 2.3.9. Zymolyase sensitivity assay

Yeast cells were refreshed to log phase as described, harvested by centrifugation, washed in $dH_2O$ and resuspended in 50mM potassium phosphate buffer (pH 7.5). 10 µg/mL Zymolyase-20T (mpBio; made up in phosphate buffer) was added and incubated at 30°C with gentle shaking. A sample was taken every 10 minutes for 90 minutes and the $OD_{600}$ measured to assess cell lysis.

### 2.3.10. Alcian blue binding assay

This assay was used to compare levels of phospho-mannan between strains. Yeast and hyphal cells were counted on a haemocytometer and diluted to $10^8$ cells / mL. 1 mL was centrifuged then resuspended in 1 mL Alcian blue solution (30 µg/mL in 0.02M HCl) and incubated for 10 minutes at room temperature. Then cells were centrifuged again, and the supernatant removed and $OD_{620}$ measured. This was calibrated to a standard curve of $OD_{620}$ measurements of a range of Alcian blue concentrations. The difference between the starting concentration (30 µg/mL) and the end concentration of the supernatant is equivalent to the amount of Alcian blue bound by cells; which is proportional to the cells' phospho-mannan levels.

### 2.3.11. Rhodamine-phalloidin staining

For visualisation of actin patches and cables, *C. albicans* cells were stained with Rhodamine-conjugated phalloidin. Yeast or hyphal cells were fixed in 3.7% formaldehyde for 30 minutes, then washed x2 in PBS + 1 mg/mL BSA + 0.1% Triton-100. They were then incubated with 5% (v/v) Rhodamine-phalloidin (Invitrogen, Thermo Fisher) for 30 minutes at room temperature. They were then washed 3 times in PBS with 1 mg/mL BSA and imaged.

### 2.3.12. Lucifer Yellow staining

Yeast or hyphal cells were incubated with 10 mg/mL Lucifer Yellow dilithium salt (LY; Merck) solution for 1 hour at 30°C. Cells were then washed 3 times with cold succinate-azide buffer then imaged.

### 2.3.13. FM4-64 staining

Yeast or hyphal cells were washed into PBS, then added 0.1% (v/v) FM4-64-FX (Invitrogen; stock 16mM in DMSO). Cells were incubated for 5 to 30 minutes, depending on the structure to be visualised, then imaged. Plasma membrane staining and peripheral puncta could be seen after 5 minutes; the Spitzenkörper (in hyphae) could be visualised after 5 – 10 minutes; vacuoles could be seen after 15 -20 minutes.

### 2.3.14. Calcofluor White staining

To visualise chitin in the *C. albicans* cell walls, Calcofluor White (Fluorescent Brightener 28; Merck) was incubated with live cells at a concentration of 2 µg/mL for 5 minutes. Cells were then washed with PBS and imaged.

### 2.3.15. Concanavalin-A staining

Concanavalin-A (ConA) conjugated with Alexafluor-488 or Alexafluor-594 (Thermo Fisher) was used to stain mannose residues in the outer cell wall. Stationary phase yeast were stained with 50 µg/mL ConA-Alexa-594 for 10 minutes at room temperature, then washed in PBS and induced to form hyphae for 90 minutes. These were then stained with 5 µg/mL ConA-Alexa-488 for 10 minutes at room temperature. Cells were washed 3 times in PBS and imaged.

### 2.3.16. Wheat germ agglutinin-fluorescein staining

Wheat germ agglutinin (WGA) conjugated to fluorescein (Thermo Fisher) was used to visualise exposed chitin in the *C. albicans* cell wall. 100 µg/mL WGA was incubated with live cells for 30 minutes at room temperature with rotation. Cells were then washed 3 times in PBS and imaged.

### 2.3.17. Filipin staining

To visualise ergosterol in the *C. albicans* plasma membrane, filipin complex from *Streptomyces* (Merck) was used at 9 µg/mL from a 10 mg/mL stock made fresh each experiment in DMSO. Cells were fixed in 3.7% formaldehyde immediately prior to staining and were incubated with both the formaldehyde and filipin for 15 minutes at room temperature with rotation. Cells were then washed 3 times in PBS and imaged.

For the low-level Fluconazole experiments, cells were induced to form hyphae as described, but with 2 or 8 µg/mL fluconazole (Merck; in DMSO) or DMSO only in the media. After growth for 90 mins, hyphae were fixed and filipin stained as above to assess ergosterol localisation.

### 2.3.18. Aniline Blue staining

To visualise cell wall glucan, cells were harvested via centrifugation and washed in PBS. Then 1:400 dilution of Aniline Blue solution (2.5% in 2% acetic acid; Merck) was added and incubated for 10 minutes. Cells were washed 3 times in PBS then imaged.

### 2.3.19. High pressure liquid chromatography cell wall analysis

High pressure liquid chromatography (HPLC) analysis was used to measure the relative amounts of the three major polysaccharide components in the *C. albicans* cell wall. This experiment was performed at the University of Aberdeen in collaboration with Dr Kathy Lee. *C. albicans* cells were grown as yeast or hyphae as previously described then lysed by adding glass beads to samples and disrupted using a FastPrep machine (Qbiogene). Samples were washed 5 times with 1 M NaCl. Cell walls were extracted by boiling samples for 10 minutes in extraction buffer. Wall pellets were spun down then resuspended in sterile $dH_2O$ and freeze dried, then the dry weight measured and recorded.

Cell walls were acid hydrolysed using 2M trifluoroacetic acid for 3 hours at 100°C. Acid was evaporated at 65°C and samples resuspended in $dH_2O$. Hydrolysed samples were analysed via high-performance anion-exchange chromatography with pulsed amperometric detection (HPAEC-PAD) in a carbohydrate analyser system (CarboPac PA10, guard and analytical columns from Thermo Scientific). The concentration of each cell wall component was stated in µg per mg of dry cell wall, as calibrated by a standard curve of monomeric sugars, and expressed as a % of total wall material.

## 2.4. Protein methods

### 2.4.1. Immunoprecipitation

*C. albicans* cell extracts were prepared as described above from an Apm4-HA tagged strain. All steps performed at 4°C. 1 mL of roughly 3 mg/mL cell extract was added to 60 µL EZview red anti-HA affinity beads (Merck; 1:1 in glycerol; pre-washed x3 in cold lysis buffer). This was incubated at 4°C with rotation for 2 hours. Then beads were spun down at 100 x *g* for 5 minutes and incubated with fresh lysis buffer for 10 minutes. This wash was repeated 3 times. To elute protein, beads were incubated in Laemmli sample buffer at 50°C for 10 minutes (eluent A) then boiled for 5 minutes (eluent B). This could then be run on gel or stored at -20°C.

### 2.4.2. Bradford assay

Where protein quantification was required, concentrations were determined via Bradford assay. 30 µL of sample was mixed with 1.5 µL Bradford Reagent (Merck), incubated for 5 minutes then the absorbance at 595 nm measured on a spectrophotometer. This was compared to a standard curve of absorbances prepared from 5 – 100 µg bovine serum albumin (BSA; Merck). Protein sample was diluted and re-measured if it did not fall within the linear range.

### 2.4.3. SDS-PAGE protein separation

Sodium dodecyl sulphate polyacrylamide gel electrophoresis (SDS-PAGE) was carried out in Bio-Rad mini protean tetra systems. Gels of 10 – 15% acrylamide were used, prepared to the following recipe:

| | 10% resolving (10 mL) | 15% resolving (10 mL) | Stacking gel (5 mL) |
|---|---|---|---|
| 30% acrylamide 0.8% bis-acrylamide (37.5:1) | 3.35 mL | 5 mL | 0.8 mL |
| Resolving / stacking buffer | 3.75 mL | 3.75 mL | 0.6 mL |
| $dH_2O$ | 2.85 mL | 1.2 mL | 3.5 mL |
| 10% ammonium persulphate (APS) | 100 µL | 100 µL | 50 µL |
| TEMED | 5 µL | 5 µL | 15 µL |

5 mL of resolving gel was poured into each glass plate sandwich and allowed to set with a layer of isopropanol on top to prevent bubbles. The isopropanol was then poured away, and 2 mL of stacking gel poured on top and allowed to set around a 1 mm comb. Gels were placed in the Bio-Rad tanks and immersed in SDS-PAGE running buffer.

Samples to be analysed were diluted in Laemmli sample buffer, boiled for 5 minutes and vortexed for 5 minutes, before being loaded into wells, alongside PageRuler Plus protein ladder (Thermo Fisher). Gels were run at 100 Volts, increased to 150 V as sample ran into resolving layer, until the dye front ran off the gel. For protein visualisation, gels were immersed in Coomassie stain solution for 1 hour then immersed in de-stain solution until bands were clearly visible. These were imaged on a gel documentation system (Bio-Rad).

### 2.4.4. Phos-tag SDS-PAGE

For increased separation of phosphorylated species, proteins were run on 10% SDS-PAGE gels made as above, but with the addition of 20 µM Phos-tag$^{TM}$ $Mn^{2+}$ (Alpha Laboratories) as per manufacturer's instructions. Samples were run on gels as for normal SDS-PAGE, then gels washed in 1 mM EDTA for 2 x 10 minutes to eliminate $Mn^{2+}$ ions prior to transfer to PVDF membrane for Western blotting (see below).

### 2.4.5. Low bis-acrylamide SDS-PAGE

For increased protein separation SDS-PAGE gels with varying ratios of acrylamide : bis-

acrylamide were used. Gels were made and run exactly as described above, except the resolving gel was modified to the following recipe:

| | 12% total acrylamide resolving (10mL) | | |
|---|---|---|---|
| | 0.1% bis-acrylamide | 0.5% bis-acrylamide | 1% bis-acrylamide |
| Acrylamide (40%) | 3 mL | 3 mL | 3 mL |
| Bis-acrylamide (2%) | 60 µL | 300 µL | 600 µL |
| Resolving buffer | 3.75 mL | 3.75 mL | 3.75 mL |
| $dH_2O$ | 3.1 mL | 2.85 mL | 2.55 mL |
| 10% ammonium persulphate (APS) | 100 µL | 100 µL | 100 µL |
| TEMED | 5 µL | 5 µL | 5 µL |

### 2.4.6. 2-dimensional SDS-PAGE

For 2D gel analysis, immunoprecipitation (IP) of Apm4-HA was performed as described above. The sample to be phosphatase treated was IP'd in the absence of phosphatase inhibitors including EDTA. After washing beads, this sample was incubated with 3 µL Lambda phosphatase (Merck; in buffer supplied) for 60 minutes at 37°C. All samples were then eluted from beads in 97 µL hydration buffer for 30 minutes with gentle shaking. Beads were spun down at 12,000 x *g* for 1 minute and eluent taken into fresh tubes. This was reduced with 1 mM DTT for 20 minutes. 1.2 µL de-streak and 0.5 µL ampholytes pH3 – 10 (both GE Healthcare) were added to each sample. Samples were spun again to remove all beads.

7 cm IPG strips, pH3 – 10 (GE Healthcare) were rehydrated overnight in 125 µL hydration buffer in a plastic tray. They were then placed in a Bio-Rad Protean IEF (isoelectric focusing) system. Samples and strips were set up as per manufacturer's instructions and run at the following protocol:

300 V, 30 minutes

1000 V, gradient, 30 minutes

5000 V, gradient, 80 minutes

5000 V, step + hold, 20 minutes

500 V, step + hold, 120 minutes

After running, strips were dipped into $dH_2O$ x 4 then into balancing buffer x 4. Strips were reduced in 2% (w/v in balancing buffer) DTT for 30 minutes. Washing in water and balancing buffer was repeated, then strips were alquilated in 2.5% (w/v in balancing buffer) iodoacetamide for 30 minutes. Strips were washed in $dH_2O$ x 4 then in SDS-PAGE buffer.

Strips were placed on top of a 12% pre-cast gel without a comb (Bio-Rad) and secured with melted 0.5% agarose (made with running buffer, with bromophenol blue) ensuring no bubbles were present. A rectangle of filter paper was soaked with PageRuler Plus protein ladder and placed at the same point along each strip. Gels were then run normally and blotted for HA as described below.

### 2.4.7. Western blotting

After running an SDS-PAGE gel as described above, Western blotting was used to probe for specific proteins of interest. After the gel had run, it was equilibrated in Towbin transfer buffer for 15 minutes. Then the gel was sandwiched with a piece of PDVF membrane (0.45 µm pore size, Immobilon-P, Merck; pre-activated with methanol and equilibrated in Towbin buffer) between layers of filter paper and sponges. The proteins were transferred from gel to membrane in a Bio-Rad gel tank, in Towbin buffer kept cool with an ice pack, for 90 minutes at 100 Volts.

Transfer of proteins was confirmed via Ponceau Red staining: the membrane was incubated with ~15 mL Ponceau S solution for 10 minutes. It was then washed with $dH_2O$ until bands became clear and photographed if necessary. Further washing in $dH_2O$ removed remaining stain.

The membrane was blocked in either 5% skimmed milk powder or 2% BSA (w/v in TBST) for at least 1 hour at room temperature. The membrane was washed in fresh TBST 3 times for 5 minutes each.

Primary antibody was diluted 1:1000 in milk / BSA : TBST and incubated with the membrane overnight at 4°C. This was then washed three times in TBST for 5 minutes each. Secondary antibody was diluted 1:10,000 in milk / BSA : TBST and incubated with the membrane for 1 hour at room temperature. The membrane was washed a final three times in TBST (5 minutes each). See Table 2.3 for antibodies used.

HRP (horseradish peroxidase) - conjugated secondary antibodies were visualised by addition of ECL reagent (enhanced chemiluminescence; GE Healthcare). Stable peroxide solution and enhanced luminol solution were mixed together 1:1 then applied to the membrane for 2 minutes. Excess liquid was shaken off before visualisation using a gel documentation system (Bio-Rad).

When required, blots were stripped for re-probing by incubation in mild stripping buffer for 10 minutes; fresh stripping buffer for another 10 minutes; 2 x 10 minutes washes in PBS then 2 x 5 minutes washes in TBST. Membranes were then re-blocked and re-probed.

## 2.5. Microscopy methods

### 2.5.1. Fluorescence microscopy

For imaging in liquid medium cells were grown as described, harvested via centrifugation at 3000 x *g* for 3 minutes, washed in sterile PBS x 3 and re-suspended in 30 – 300 µL PBS. 2.7 µL of this was spotted onto a glass slide (1.0 – 1.2 mm; Fisher) and covered with a glass coverslip (Deckgläser) which was sealed with nail varnish.

For imaging on solid media, 'agar pads' were made in cavity slides. 1% agar (melted); 10% fetal bovine serum (FBS); 2% glucose and 80 µg/mL uridine were mixed. 100 µL was pipetted into the cavity of each glass cavity slide (15-18 mm, depth 0.6-0.8 mm; BRAND, Merck) and a glass slide placed on top to ensure the agar pad would dry flat. Once the agar had solidified, 5 µL of stationary phase *C. albicans* culture was spotted onto the agar pad, then a glass coverslip placed over it and sealed with nail varnish. Slide was incubated at 37°C for 90 minutes then hyphae imaged.

Fluorescence microscopy was performed on the following microscopes:
(A) Nikon IX-81 inverted microscope with a Retiga R3 CCD camera (QImaging) and Micromanager software

(B) Nikon eclipse Ti inverted microscope with TIRF3 on which oblique illumination was used, with an iXon Du-897 EM-CCD camera (Andor) and NIS-elements software

### 2.5.2. Transmission electron microscopy

High pressure freezing (HPF) and freeze substitution were performed at the Microscopy and Histology Facility at the University of Aberdeen, in collaboration with Gillian Milne and Dr Louise Walker. Cells were grown as yeast and hyphae as described, then washed x 3 in distilled water, spotted onto a flat specimen carrier and frozen in a Leica EM PACT 2 (Leica Microsystems).

Freeze substitution was performed by Gillian Milne using the following protocol: The Leica AFS 2 machine and 1% $OsO_4$ in acetone solution were pre-cooled with liquid nitrogen. Samples from HPF were transferred to the AFS under liquid nitrogen. The following programme was used:

| T start (°C) | T end (°C) | Slope (°C/h) | Time (h:m) | Reagent |
|---|---|---|---|---|
| -95 | -90 | 10.1 | 00:30 | Acetone $OsO_4$ |
| -90 | -90 | 0 | 10:00 | Acetone $OsO_4$ |
| -90 | -30 | 7.5 | 08:00 | Acetone $OsO_4$ |
| -30 | -10 | 20 | 01:00 | Acetone |
| -10 | 4 | 14 | 01:00 | Acetone |
| 4 | 20 | 16 | 01:00 | Acetone |
| 20 | 20 | 0 | 01:00 | Ac/Epoxy 10% |
| 20 | 20 | 0 | 01:00 | Ac/Epoxy 30% |
| 20 | 20 | 0 | 02:00 | Ac/Epoxy 60% |
| 20 | 20 | 0 | 19:00 | Ac/Epoxy 90% |
| 20 | 20 | 0 | 01:00 | Epoxy |

Samples in epoxy resin were then set in a 60°C oven, then ultrathin 100 nm sections cut, and stained with 2% uranyl acetate and lead citrate (REYNOLDS 1963).

Samples were imaged (by me, with the help of Dr Chris Hill) at the University of Sheffield EM facility with a FEI Tecnai T12 Spirit TEM with Gatan camera. Cell walls were measured on FIJI with 5 measurements averaged per cell (n>20 cells per condition).

### 2.5.3. Scanning electron microscopy

Scanning electron microscopy (SEM) was carried out at the University of Sheffield EM facility; with sample preparation carried out by Dr Chris Hill.

Cells were grown as described then fixed in 3% glutaraldehyde in PBS overnight. Cells were washed in 0.1 M PBS for 2 x 10 minutes, then fixed again in 1% aqueous osmium tetroxide for 1 hour at room temperature. Cells were washed again as before, then dehydrated in an ethanol gradient at room temperature: 75% ethanol for 15 mins; 95% ethanol for 15 mins; 100% ethanol for 15 mins; 100% ethanol for 15 mins; then 100% ethanol dried over anhydrous copper sulphate for 15 mins. Cells were then placed in 50:50 100% ethanol : 100% hexamethyldisilazane for 30 mins followed by 100% hexamethyldisilazane for 30 mins. Specimens were air dried overnight. Dried specimens were mounted on aluminium stubs, attached with Carbon Sticky Tabs and coated with gold in an Edwards S150B sputter coater.

Specimens imaged (by me, with the help of Dr Chris Hill, University of Sheffield) in a TESCAN Vega 3 LMU Scanning Electron Microscope at an accelerating voltage of 10.0 kV.

### 2.5.4. Atomic force microscopy

For atomic force microscopy (AFM), *C. albicans* cultures were induced to form hyphae as described. Hyphal cells were harvested by centrifugation at 3000 x *g* and washed three times with acetate buffer which had been passed through an 0.2 µm filter.

The hyphal cell pellet was resuspended 1:10 in acetate buffer, and 2 µL of this pipetted onto a glass slide. A glass coverslip was placed on top of the cells and left for two minutes to allow cells to adhere. Then the coverslip was removed with forceps and washed three times with acetate buffer to remove excess cells.

AFM was performed by Spyridon Sovatzoglou using an MFP-3D-BIO Atomic Force microscope (Asylum Research) in Force mode, and PPP-CONTSC-20 cantilevers (Nanosensors; k: 0.2 N/m, freq: 25 kHz). Imaging was performed in liquid (acetate buffer) aiming to obtain the variation of modulus over the cell wall's surface. Data analysis was performed by Spyridon Sovatzoglou using Hertz parabolic contact mechanics model.

## 2.6. Analysis of data

### 2.6.1. Image processing

Images were exported as TIFFs and analysed on ImageJ (FIJI). Unless otherwise stated, ROIs of 400 $\mu m^2$ were taken, and a 5 µm scale bar added.

### 2.6.2. Line profiles (cell periphery)

To analyse the extent to which fluorescent signal was concentrated at the cell periphery, line profile analysis was performed in FIJI. Lines of equal length were drawn such that the lines started outside the cell and finished inside the cell, with the centre of the line at the cell periphery (as judged by a brightfield image of the cell). The Analyse > Plot Profile function was used on the fluorescence image. These numbers were exported to Excel then line graphs plotted in GraphPad Prism. Data from at least 20 cells was averaged to give one line with error bars showing SD for each point.

### 2.6.3. Line profiles (hyphal tip)

Line profile analysis was also used to analyse how concentrated a fluorescent signal was at the hyphal tip, and how tight a 'cap' it formed. For this, curved lines were drawn on FIJI which followed the hyphal cell periphery around the tip with the centre of the line at the centre of the hyphal tip. Line profiles were generated as described above. For this analysis, line profiles were plotted individually, and three representative lines shown, instead of an average.

### 2.6.4. Mean fluorescence intensity

To quantify the amount of fluorescent staining in cells, the mean grey values were determined on FIJI. An ROI was selected on FIJI – either the whole yeast cell was drawn around, or a box of a set size was placed over the region of interest on the cell. The Analyse > Measure function was used to record the 'mean grey value' of that area. The background fluorescence (taken from an average of 3 measurements per image) was subtracted from each measurement. Alternatively, for measuring peripheral signal, 3 lines profiles across each cell periphery were taken, and the lowest value (background fluorescence) was subtracted from the highest value (peak fluorescence staining) and these 3 values averaged. These values were then exported and plotted on GraphPad

Prism.

### 2.6.5. Endocytic patch timing

For endocytic patch timing, time-lapse movies were taken on the Nikon Ti microscope typically at 1 frame / second for 5 or 10 minutes. The frame at which an individual punctum first appeared and disappeared was recorded, to calculate an approximate lifetime for that punctum.

### 2.6.6. Statistical analysis

Statistical tests, unless otherwise stated, were either T-tests or one-way ANOVAs with Tukey's post hoc tests for multiple comparisons. These tests were performed using GraphPad Prism. Confidence interval was set to 95%. P value style: 0.1234 (ns), 0.0332 (*), 0.0021 (**), 0.0002 (***), <0.0001 (****).

## Table 2.1: Buffers used in this study

| Name | Recipe | Use |
|---|---|---|
| PBS (phosphate buffered saline) | 0.8% (w/v) NaCl; 0.02% (w/v) KCl; 0.144% (w/v) $Na_2HPO_4$; 0.024% (w/v) $KH_2PO_4$; pH 7.4 | Buffer for *C. albicans* cells, often used for washing or suspending cells for visualisation via microscopy |
| Succinate-azide buffer | 50 mM succinate; 20 mM sodium azide; pH 5.0 with NaOH | Blocks cellular metabolism, used to halt endocytosis prior to visualising Lucifer Yellow uptake |
| Acetate buffer | 18mM sodium acetate, 1 mM $CaCl_2$, 1 mM $MnCl_2$, pH 5.2 (with acetic acid) | Used in AFM experiments to buffer *C. albicans* cells |
| TE buffer (Tris-EDTA) | 10 mM Tris-HCl; 1 mM EDTA; pH 8.0 | Buffer for solubilising and storing DNA, the EDTA is protective against degradative enzymes |
| TAE buffer (Tris acetate EDTA) | 40 mM Tris; 20 mM acetic acid; 1 mM EDTA; pH 8.3 | Buffer when making and running agarose DNA gels |
| Stacking gel buffer | 0.5 M Tris-HCl pH 6.8; 0.4% (w/v) SDS | Buffering the stacking part of an SDS-PAGE gel |
| Resolving gel buffer | 1.5 M Tris-HCl pH 8.8; 0.4% (w/v) SDS | Buffering the resolving part of an SDS-PAGE gel |
| 1 x SDS-PAGE running buffer | 25 mM Tris-HCl pH 8.6; 250 mM glycine; 0.1% (w/v) SDS | Buffer when running SDS-PAGE gels |
| 2 x Laemmli sample buffer | 100 mM Tris-HCl pH 6.8; 4% (w/v) SDS; 20% (v/v) glycerol; 25 mM EDTA; 0.04% (w/v) Bromophenol Blue; 2% (v/v) 2- | Mix with protein samples prior to loading on SDS-PAGE gel. Denatures and negatively charges proteins |

| | | |
|---|---|---|
| | mercaptoethanol added prior to use | |
| Coomassie stain solution | 0.05% (w/v) Coomassie R250; 45% (v/v) methanol; 10% (v/v) acetic acid | Visualising proteins on an SDS-PAGE gel |
| De-stain solution | 40% (v/v) methanol; 10% (v/v) acetic acid | Removing Coomassie stain from the protein gel, so protein bands can be better visualised |
| TBST (Tris-buffered saline with Tween) | 20 mM Tris; 150 mM NaCl; 0.1% Tween 20; pH 7.6 with HCl | Buffer used when probing a western blot; used to wash the membrane and during blocking and antibody incubations |
| Towbin transfer buffer | 25 mM Tris, 192 mM glycine, pH 8.3, 20% methanol added before use | Buffer used when transferring proteins from SDS-PAGE gel to PVDF membrane for western blotting |
| Mild stripping buffer | 25 mM glycine; 2% (w/v) SDS; 1% (v/v) Tween 20; pH 2.2 | Removal of antibodies from western blot membranes, whilst leaving sample protein for re-probing |
| Ponceau S stain solution | 0.1% (w/v) Ponceau S; 1% (v/v) glacial acetic acid | Reversibly staining proteins on a western blot membrane |
| Lysis buffer | 50 mM Tris-HCl pH 7.5; 100 mM NaCl; 1 mM EGTA; 0.1% Triton X-100; 2.5 mM EDTA. 1x Roche PIC; 1 mM PMSF; 10 µM Leupeptin; 1 µM Pepstatin-A; 1 mM NaF; 0.5 mM $Na_3VO_4$ | Buffer *C. albicans* cells when preparing cell extracts. Inhibitors added just prior to use. Phosphatase inhibitors omitted when phosphatase treatment required. |
| Extraction buffer | 50 mM Tris-HCl, 2% SDS, 0.3 M 2-mercaptoethanol, 1 mM EDTA; pH 8.0 | Buffer *C. albicans* cells when preparing cell extracts to isolate cell wall material from |
| Hydration buffer | 8 M urea; 2 M thiourea; 4% (v/v) CHAPS; 0.5% ampholytes (pH3 – 10); 1.2% de-streak; bit of bromophenol blue. 50 mM DTT added just before use. | To reduce and denature proteins, used to elute sample from beads prior to 2D-gel electrophoresis |
| Balancing buffer | 6 M urea; 50 mM Tris pH 8.8; 2% (w/v) SDS; 30% (v/v) glycerol | Maintains proteins in solution during 2D-gel electrophoresis without altering the pI of proteins. |
| Lithium acetate solution | 100 mM LiOAc; 10 mM Tris-HCl; 1mM EDTA; pH 7.5 | Used to permeabilise *C. albicans* cell wall prior to transformation |

Table 2.2: Media used in this study

| Name | Recipe | Use |
|---|---|---|
| 2 x YT | 1% (w/v) yeast extract (Difco); 1.6% (w/v) tryptone (Difco); 0.5% (w/v) NaCl | Rich medium for liquid growth of *E. coli* |

| | | |
|---|---|---|
| 2 x YT agar | As above with 2% (w/v) agar | Rich medium for *E. coli* growth on plates |
| YPD | 1% (w/v) yeast extract; 2% (w/v) peptone; 2% (w/v) glucose; plus 40 µg/mL adenine and 80 µg/mL uridine | Rich medium for liquid growth of *C. albicans* |
| YPA | As above with 2% (w/v) agar | Rich medium for *C. albicans* growth on plates |
| YPS | 1% (w/v) yeast extract; 1% (w/v) peptone; 1% (w/v) sucrose; 1/2/4% (w/v) agar | Solid medium used for substrate penetration assays |
| SC | 0.675 (w/v) yeast Nitrogen base without amino acids; 2% (w/v) glucose<br>Add the following supplements as required: 80 µg/mL uridine; 30 µg/mL L-leucine; 128 µg/mL arginine; 80 µg/mL histidine | Synthetic complete medium for *C. albicans* growth, amino acids removed as required to make 'drop out' media for auxotrophic marker selection |

Table 2.3: Antibodies used in this study

| Antibody | Clonality | Host (from) | Use | Working concentration |
|---|---|---|---|---|
| anti-HA high affinity (Merck) | Monoclonal | Rat | Primary antibody for Western blotting | 1:1000 (100 ng / mL) |
| anti-Rat IgG – peroxidase (Merck) | Polyclonal | Goat | Secondary antibody for Western blotting | 1:10,000 |
| anti-GFP (Merck) | Monoclonal | Mouse | Primary antibody for Western blotting | 1:1000 (400 ng / mL) |
| anti-Mouse IgG – peroxidase (Merck) | Polyclonal | Goat | Secondary antibody for Western blotting | 1: 10,000 |

Table 2.4: *C. albicans* strains used in this study

| Strain name | Genotype | Origin |
|---|---|---|
| SN76 | *ura3Δ::imm$^{434}$ / ura3Δ::imm$^{434}$, iro1Δ::imm$^{434}$ / iro1Δ::imm$^{434}$, his1Δ / his1Δ, arg4Δ / arg4Δ* | Noble and Johnson, 2005 |

| | | |
|---|---|---|
| SN148 | *ura3Δ::imm$^{434}$ / ura3Δ::imm$^{434}$, iro1Δ::imm$^{434}$ / iro1Δ::imm$^{434}$, his1Δ / his1Δ, arg4Δ / arg4Δ, leu2Δ / leu2Δ* | Noble and Johnson, 2005 |
| KAF33 | SN76 *APM4 / apm4Δ::HIS1* | Smaczynska de-Rooij (Ayscough lab) |
| KAF37 | SN76 *apm4Δ::HIS1 / apm4Δ::ARG4* | Smaczynska de-Rooij (Ayscough lab) |
| KAF39 | SN148 *APM4 / APM4-HA::ARG4* | Smaczynska de-Rooij (Ayscough lab) |
| KAF44 | SN148 *SLA1 / SLA1-GFP::LEU2* | Smaczynska de-Rooij (Ayscough lab) |
| KAF45 | SN148 *CHS3 / CHS3-GFP::LEU2* | Smaczynska de-Rooij (Ayscough lab) |
| KAF47 | SN148 *APL1 / APL1-GFP::LEU2* | Smaczynska de-Rooij (Ayscough lab) |
| KAF49 | SN148 *CHS3 / CHS3-GFP::LEU2, apm4Δ*::HIS1 / *apm4Δ*::ARG4 | Smaczynska de-Rooij (Ayscough lab) |
| KAF50 | SN148 *APL1 / APL1-GFP::LEU2, apm4Δ::HIS1 / apm4Δ::ARG4* | Smaczynska de-Rooij (Ayscough lab) |
| KAF51 | SN148 *SLA1 / SLA1-GFP::LEU2, APL1 / APL1-RFP::ARG4* | This study (me) |
| KAF52 | SN76 *apm4Δ::HIS1 / apm4Δ::ARG4, CHS3 / chs3Δ::SAT1* | This study (me) |
| KAF53 | SN76 *CHS8 / CHS8-GFP::URA3* | This study (me) |
| KAF54 | SN76 *CHS8 / CHS8-GFP::URA3, apm4Δ::HIS1 / apm4Δ::ARG4* | This study (me) |
| KAF55 | SN148 *APL1 / APL1-GFP::LEU2, apm4Δ::ARG4 / apm4$^{1-454}$::HIS1* | This study (me) |
| KAF56 | SN76 *apm4Δ::ARG4 / apm4$^{1-454}$::HIS1* | This study (me) |
| KAF57 | SN148 CHS3 / *CHS3-GFP::LEU2, apm4Δ::ARG4 / apm4$^{1-454}$::HIS1* | This study (me) |
| KAF59 | SN148 *apm4Δ::HIS1 / apm4Δ::ARG4* | Stella Christou (Ayscough lab) |
| KAF61 | SN148 *apm4Δ::HIS1 / apm4Δ::URA3* | This study (me) |
| KAF64 | *SN148 SPA2 / SPA2-GFP::LEU2, apm4Δ::HIS1 / apm4Δ::ARG4* | This study (me) |
| KAF65 | *SN148 MLC1 / MLC1-GFP::LEU2* | This study (me) |
| KAF66 | *SN148 SEC3 / SEC3-GFP::LEU2, apm4Δ::HIS1 / apm4Δ::ARG4* | This study (me) |
| KAF68 | *SN148 SEC8 / SEC8-GFP::LEU2* | This study (me) |
| KAF69 | *SN148 SEC8 / SEC8-GFP::LEU2, apm4Δ::HIS1 / apm4Δ::ARG4* | This study (me) |
| KAF70 | *SN148 SEC3 / SEC3-GFP::LEU2* | This study (me) |

| | | |
|---|---|---|
| KAF71 | *SN148 MLC1 / MLC1-GFP::LEU2, apm4Δ::HIS1 / apm4Δ::ARG4* | This study (me) |
| KAF72 | SN148 *SPA2 / SPA2-GFP::LEU2* | This study (me) |
| KAF73 | *SN148 pADH1-GFP-PH(CaOsh2H340R)-PH(CaOsh2H340R)-GFP::ARG4* (integrated to RPS1 locus) | Plasmid from Arkowitz lab (Ghugtyal et al., 2015) integrated to SN148 by me |
| KAF74 | *SN148 pADH1-GFP-PH(CaOsh2H340R)-PH(CaOsh2H340R)-GFP::ARG4, apm4Δ::HIS1 / apm4Δ::URA3* (integrated to RPS1 locus) | Plasmid from Arkowitz lab (Ghugtyal et al., 2015) integrated to SN148 by me |
| KAF75 | *SN148 pADH1-GFP-PH$^{Plcδ}$-PH$^{Plcδ}$-GFP.SDM1a3::ARG4* (integrated to RPS1 locus) | Plasmid from Arkowitz lab (Vernay et al., 2012) integrated to SN148 by me |
| KAF76 | *SN148 pADH1-GFP-PH$^{Plcδ}$-PH$^{Plcδ}$-GFP.SDM1a3::ARG4, apm4Δ::HIS1 / apm4Δ::URA3* (integrated to RPS1 locus) | Plasmid from Arkowitz lab (Vernay et al., 2012) integrated to SN148 by me |
| KAF79 | *SN148 CHS3 / chs3Δ::HIS1* | This study (me) |
| KAF80 | SN148 *CHS3 / CHS3-GFP::LEU2, APL1 / APL1-RFP::ARG4* | This study (me) |
| KAF81 | SN148 *chs3Δ::HIS1 / chs3$^{1-564}$-GFP::LEU2* | This study (me) |
| KAF82 | SN148 *chs3Δ::HIS1 / chs3$^{1-752}$-GFP::LEU2* | This study (me) |
| KAF83 | SN148 *chs3Δ::HIS1 / chs3$^{1-820}$-GFP::LEU2* | This study (me) |
| KAF84 | SN148 *APL1 / APL1-GFP::LEU2, CHS3 / CHS3-yEmRFP::ARG4* | This study (me) |
| KAF85 | SN148 *CHS3 / chs3$^{1-820}$-GFP::LEU2* | This study (me) |
| KAF86 | SN148 *chs3Δ::HIS1 / CHS3-GFP::LEU2* | This study (me) |
| KAF87 | SN76 *CHS3 / chs3Δ::HIS1* | This study (me) |
| KAF89 | SN148 *chs3Δ::HIS1 / chs3$^{1-850}$-GFP::LEU2* | This study (me) |
| KAF90 | SN148 *chs3Δ::HIS1 / chs3$^{1-850}$-GFP::LEU2* | This study (me) |
| KAF91 | SN148 *OSH3 / OSH3-GFP::LEU2* | This study (me) |
| KAF92 | SN148 *OSH3 / OSH3-GFP::LEU2, apm4Δ::HIS1 / apm4Δ::ARG4* | This study (me) |
| KAF93 | SN148 *OSH4 / OSH4-GFP::LEU2* | This study (me) |
| KAF94 | SN148 *OSH4 / OSH4-GFP::LEU2, apm4Δ::HIS1 / apm4Δ::ARG4* | This study (me) |
| KAF95 | SN148 *apm4Δ::HIS1 / apm4Δ::URA3 + APM4::ARG4* (integrated to RPS1 locus) | This study (me) |
| KAF98 | SN148 *SAC1 / SAC1-GFP::LEU2* | This study (me) |
| KAF99 | SN148 *SAC1 / SAC1-GFP::LEU2, apm4Δ::HIS1 / apm4Δ::URA3* | This study (me) |
| KAF100 | SN148 *IST2 / IST2-GFP::LEU2* | This study (me) |
| KAF101 | SN148 *IST2 / IST2-GFP::LEU2, apm4Δ::HIS1 / apm4Δ::URA3* | This study (me) |

| | | |
|---|---|---|
| KAF107 | SN148 *apm4Δ::HIS1 / apm4Δ::URA3* + *APM4$^{S/T-A}$::ARG4* (integrated to RPS1 locus)<br>S/T-A = 4 Ser / Thr residues mutated to Ala: S165A, T166A, S174A, S193A | This study (me) |
| KAF108 | SN148 *apm4Δ::HIS1 / apm4Δ::URA3* + *APM4$^{S/T-A}$::ARG4* (integrated to RPS1 locus), *APL1 / APL1-GFP::LEU2* | This study (me) |

# Chapter 3: Introducing Apm4 and its possible regulation in *Candida albicans*

## 3.1. Introduction to chapter 3

This chapter contains data which provide some background to the work published in Knafler et al (2019), chapter 4. It also includes data which are related to the published findings, but which were not sufficiently expanded to be included for publication.

### 3.1.1. *C. albicans* lab strains

The most commonly used *C. albicans* laboratory strains are derived from strain SC5314 (see figure 3.1), which was originally isolated from a patient, and engineered by Fonzi and Irwin (1993) to produce a uridine auxotrophic mutant. This was a breakthrough in the study of this diploid fungus, as the *URA3* gene could then be re-introduced to rapidly identify positive transformants in a gene of interest.

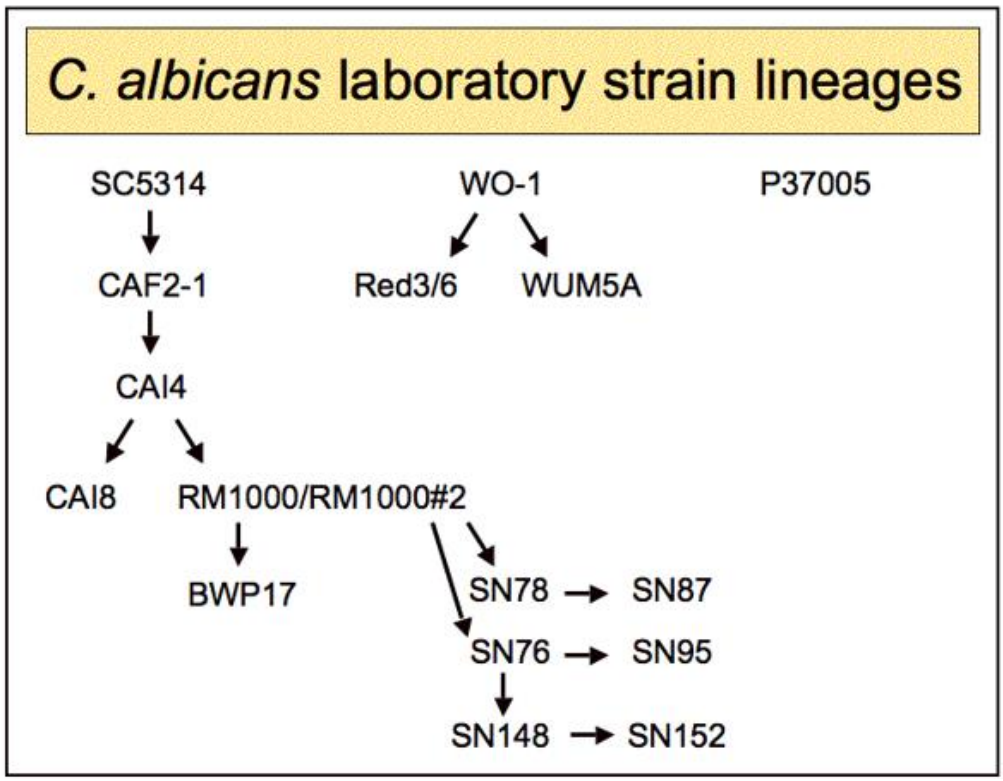


3.1. Commonly used *Candida albicans* laboratory strains
Figure taken from the Candida Genome Database (candidagenome.org), which outlines the most common laboratory strains of *C. albicans* and their lineages.

It was later discovered however, that expression levels of the *URA3* gene can affect *C. albicans* virulence in a mouse model, therefore the use of *URA3* as a selectable marker

has been called into question (Brand et al. 2004). It was also found that the commonly used lab strain BWP17 (via its parental strain RM1000) had undergone a deletion of a portion of chromosome 5 (Forche et al. 2004). This could have unknown effects on any genetic studies in this background.

Noble and Johnson (2005) later constructed strains which were auxotrophic for *HIS1*, *ARG1* and *LEU2* (the SN strains, see figure 3.1). These strains allow multiple mutations to be made and selected for in a single strain, enabling more complex genetic experiments. These nutritional markers were tested extensively and their expression in different genomic locations did not affect *C. albicans* virulence. The SN strains are derived from strain RM1000#2 which did not undergo the partial loss of chromosome 5.

### 3.1.2. Apm4 regulation via phosphorylation

Phosphorylation and dephosphorylation of proteins by various cellular kinases and phosphatases is a ubiquitous regulatory mechanism. Addition of a phosphate group to a serine, threonine or tyrosine amino acid adds negative charge to the protein which can alter its conformation and therefore its activity. Phosphorylation can also alter the ability of the protein to form bonds, thus directly affecting its interactions. This reversible modulation of protein activity occurs in response to internal and external stimuli and allows cellular processes to be precisely regulated in space and time. Protein phosphorylation has been shown to be critical to many aspects of *C. albicans* growth and virulence (Sudbery 2011, Willger et al. 2015).

Wilde and Brodsky (1996) first showed that mammalian AP-2 µ2 was *phosphorylated in vivo*, and Olusanya et al (2001) demonstrated that phosphorylation of a key residue – threonine 156 – is required for AP-2 mediated uptake of transferrin receptor. This phosphorylation has been reported to occur via the adaptor associated kinase AAK1 (Ricotta et al. 2002) and via the cyclin-G-associated kinase GAK (Korolchuk and Banting 2002).

This phosphorylation has been shown to modulate AP-2 binding affinity to YxxΦ motifs on endocytic cargo (Fingerhut et al. 2001, Ricotta et al. 2002). Collins et al (2002) proposed a model in which this phosphorylation event, which occurs on the central disordered linker region of µ2, drives a conformational change from the closed to open form, which exposes the buried YxxΦ binding site and enables AP-2 to bind YxxΦ motifs

on cargoes. This mechanism of activating adaptor - cargo binding could help to regulate the precise temporal sequence of endocytic vesicle formation and disassembly. Consistent with this, inhibiting T156 phosphorylation via mutagenesis or via kinase inhibitors, led to defects in cargo internalisation (Kadlecova et al. 2017, Olusanya et al. 2001).

There is also evidence however, that suggests it is the open conformation of AP-2 which is phosphorylated. In *C. elegans*, AP-2 was mutated to promote its open / active conformation, and the μ hinge region became hyper-phosphorylated. The constitutively inactive form was less phosphorylated (Hollopeter et al. 2014). Additionally, GAK and AAK1 recruitment and activity occur after clathrin recruitment to endocytic sites (Taylor, Perrais and Merrifield 2011, Conner, Schröter and Schmid 2003), therefore presumably after AP-2 has bound to cargo and clathrin. A recent paper used surface plasmon resonance (SPR) to show that phosphorylation of T156 did not in fact increase the affinity of AP-2 for plasma membrane or transmembrane cargoes (Wrobel et al. 2019). These data suggest phosphorylation may occur during endocytic coat formation, stabilising rather than inducing AP-2's open conformation.

There is even some evidence to suggest that phosphorylation may de-activate AP-2. AAK1 overexpression has been shown to inhibit endocytosis in an in vitro assay (Conner and Schmid 2002) and in tissue culture (Conner et al. 2003). Wrobel and colleagues (2019) have proposed that, rather than playing a role in AP-2 activation, μ2 phosphorylation is important for endocytic progression. They showed that μ2 phosphorylation, which increases over a CCP's lifetime, recruits NECAP, which in turn recruits late-stage effectors for membrane remodelling and scission.

Yeast AP-2 is less well characterised than the mammalian protein, with no protein structure available. It is not known whether yeast μ subunit (Apm4) is regulated via phosphorylation in a similar way. However phosphoproteome screens in both *S. cerevisiae* and *C. albicans* have identified regions of phosphorylation in the Apm4 central hinge region (Willger et al. 2015, Amoutzias et al. 2012), suggesting that this mechanism of regulation could be conserved. Additionally, *S. cerevisiae* Apm4 has been shown to interact with the protein kinase C Pkc1, and mutagenesis of a predicted Pkc1 phosphorylation site in the Apm4 hinge region – threonine 176 – impaired AP-2 recruitment to sites of endocytosis (Chapa-Y-Lazo and Ayscough 2014).

## 3.2. Characterising hyphal growth in our *C. albicans* strains

Throughout this study, the wild-type *C. albicans* strains SN76 and SN148 were used (Noble and Johnson 2005). Many methods of inducing *C. albicans* cells to form hyphae in the lab have been described. In order to establish the best conditions to use for the rest of the study, three different inducing conditions were trialled. These were: growth at 37°C; growth at 37°C in medium adjusted to pH7 via NaOH; and growth at 37°C with 10% fetal bovine serum (FBS). Each condition used rich medium (YPD). As shown in figure 3.2A, 37°C with 10% FBS most reliably induced hyphal formation in WT strain SN148. Under this condition, around 80% of cells formed a hypha, and 30% of these had at least one septum after 2 hours. Therefore this condition was used as the standard method of inducing hyphal growth throughout the study. Figure 3.2B shows representative images of SN148 cells at 15 minute intervals post hyphal induction. Hyphae were stained using Calcofluor White (CFW) to enable easy visualisation.

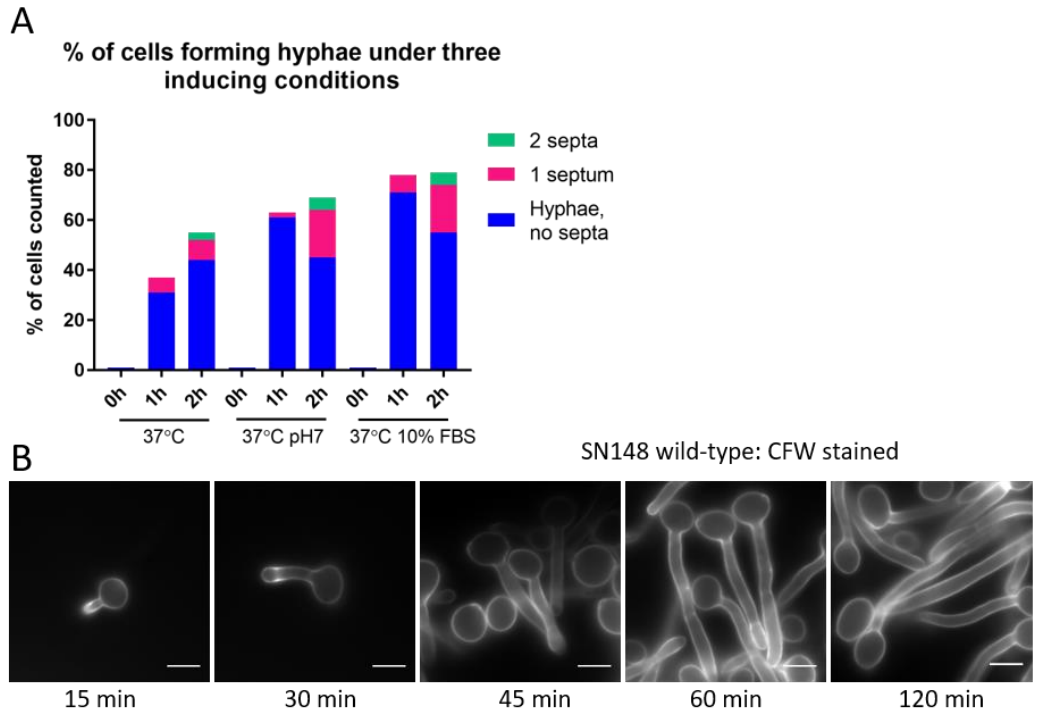


**3.2. Growth at 37°C with FBS reliably induces hyphal formation**

(A) SN148 cells were induced to form hyphae under 3 different conditions. Samples were Calcofluor White (CFW) stained and imaged at 0 hour; 1 hour and 2 hours post induction and the % of cells which had formed hyphae were counted, and number of septa recorded. Graph shows data from >50 cells / condition; 1 representative experiment. (B) SN148 cells induced to form hyphae at 37°C with 10% FBS, then samples taken every 15 minutes, CFW stained and imaged. Representative images shown, all scale bars 5 µm.

## 3.3. Cells without AP-2 are larger and slower to divide

Homozygous deletions of *apm4* (*apm4 Δ/Δ*), the mu (μ) subunit of AP-2, were generated in an otherwise WT strain. This deletion prevents AP-2 complex formation (see Knafler et al., 2019; figure S1). As shown in Knafler et al (2019; figure 2), the *apm4* deletion mutant does not show a significantly reduced growth rate within the first 5 hours of growth, as measured by optical density ($OD_{600}$) over time. However when cells were grown for longer (figure 3.3A) greater differences were observed. When the *apm4* mutant was refreshed into rich media, it had a lag phase and initial growth rate similar to WT cells, however after growth for around 10 hours, the *apm4* mutant growth rate

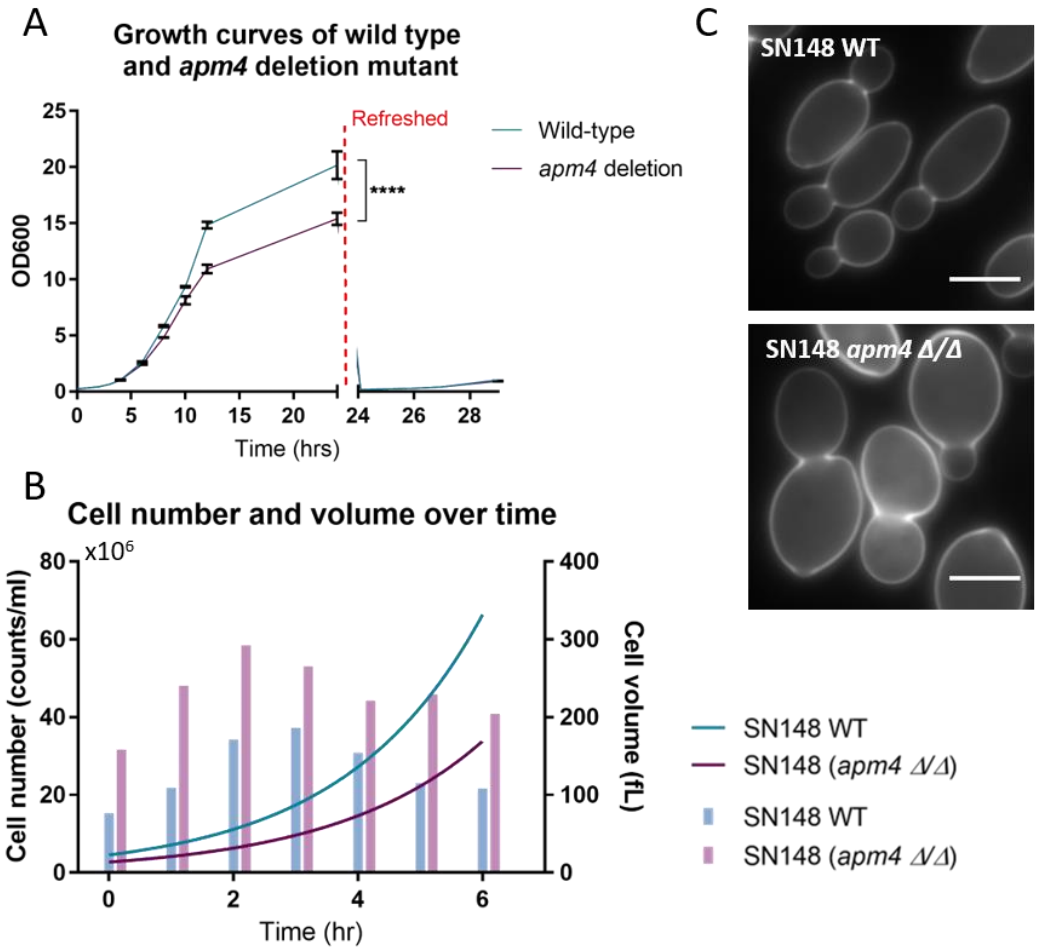


**3.3. Cells without AP-2 are larger and slower to divide than WT cells**

(A) WT and *apm4* deletion strains were grown as yeast and the $OD_{600}$ measured at intervals for 20 hours. After 24 hours, cells were refreshed to $OD_{600}$ = 0.1 in fresh media, then readings started again. 2-way ANOVA was performed and shown here is the comparison between strains at the 24 hour timepoint, showing that the $OD_{600}$ of the two strains was significantly different at this timepoint. (B) Yeast cells of both strains grown for 6 hours; sample taken each hour and cell number and volume measured on a CASY counter. Lines show cell number (counts x $10^6$ / mL) and bars show cell volume (fL). Each point is the mean of 3 replica; from 1

began to slow and reached a significantly lower final $OD_{600}$ than the WT culture. After being diluted into fresh media, the *apm4* deletion strain began to grow again at a similar rate to WT (figure 3.3A).

Growth rate was also assessed using a CASY$^{TM}$ Counter to measure the cell number and cell volume every hour over 6 hours (figure 3.3B). The lines on the graph represent cell number, and the bars represent cell size. This experiment showed that over 6 hours of growth the *apm4* mutant grew larger cells (with a mean volume of 292 fL at their largest timepoint, compared with 186 fL for WT cells), which were slower to divide. These two factors could combine to give the culture a similar optical density reading to WT. As shown in figure 3.3C, the much larger size of *apm4* mutant yeast cells can also be seen via microscopy (cells stained with CFW).

## 3.4. Cells without AP-2 show gross morphological differences via SEM

Both WT and *apm4* deletion cells were imaged via scanning electron microscopy (SEM) to visualise any changes at the cell surface. This was performed in collaboration with Dr Chris Hill at the University of Sheffield Electron Microscopy facility. It was observed that *apm4* deletion cells were much more likely to appear 'rough' or 'indented' at the surface (39% of mutant yeast cells were classified as such, compared to 11% of WT cells; see figure 3.4A, B). Whilst WT yeast generally had just one bud per cell, *apm4* deletion cells often had multiple protrusions (see figure 3.4C) though it is unclear whether these are multiple budding sites, or bud scars from previous budding events.

When looking at hyphal cells via SEM, the morphological differences between WT and *apm4* deletion cells were clear (figure 3.4C). WT hyphae were long and narrow, whereas *apm4* mutant hyphae were clearly much wider and shorter. In the mutant sample, more hyphae appeared to have broken from their mother cells during processing, which could indicate some weakness in the hypha or 'neck' region.

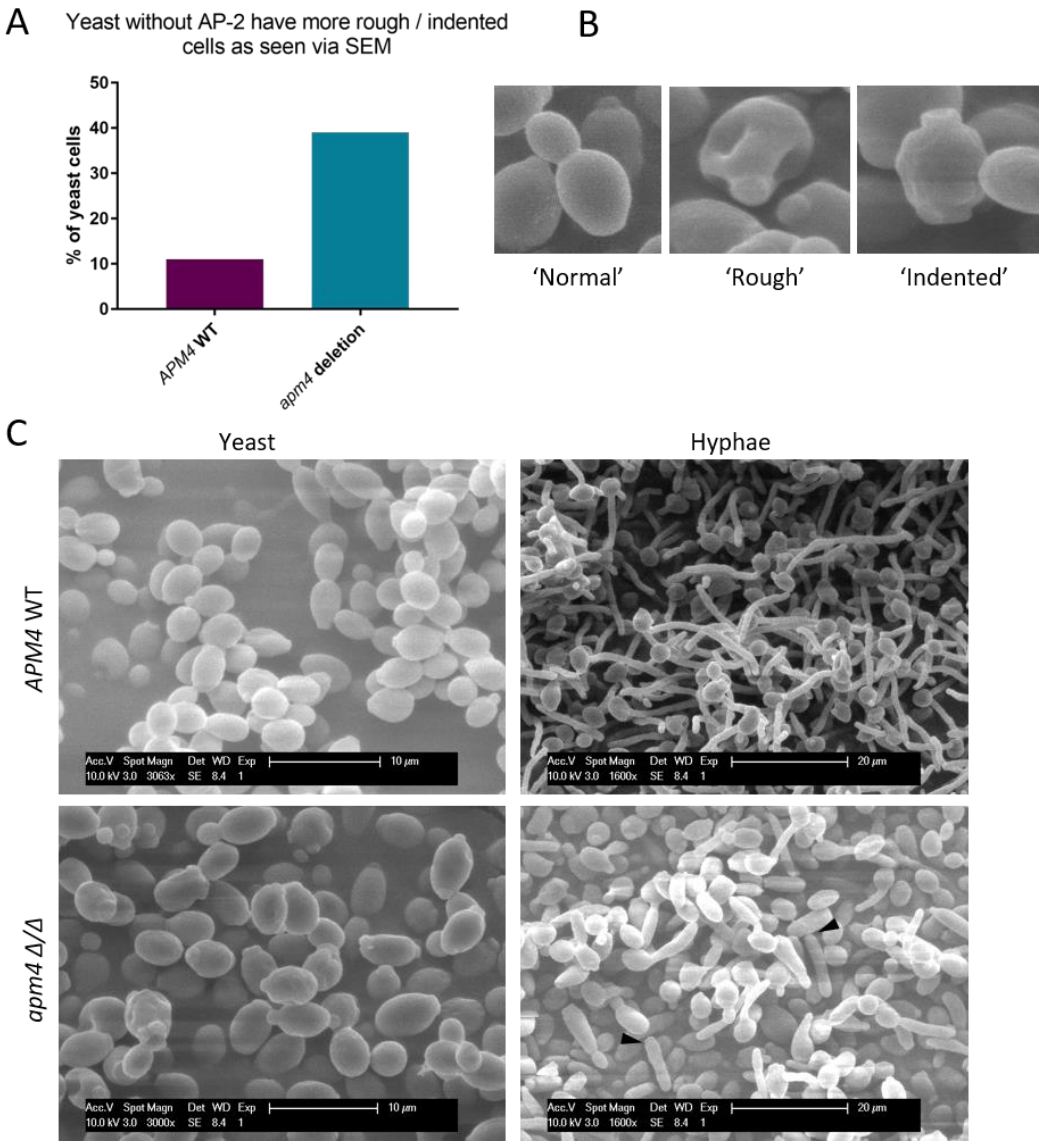


**3.4. Cells without AP-2 show gross morphological defects via SEM**

(A) Yeast cells from SEM images were counted and the number of cells which looked rough or indented were recorded. Graph shows data from >80 cells / strain; 1 experiment. (B) Shows example SEM images of cells which would be classified as 'rough' or 'indented'. (C) Representative SEM images of yeast and hyphal cells from both WT and *apm4* deletion strains. SEM sample preparation was carried out by Dr Chris Hill; images were taken by me with help from Dr Chris Hill.

## 3.5. The morphological defects observed are reversed upon complementation with *APM4*

The morphological defects of the *apm4* deletion mutant are extensively characterised in Knafler et al, 2019 (chapter 4). To confirm that these defects were indeed caused by loss

of the *apm4* gene (and therefore of the AP-2 complex), a copy of WT *APM4* was integrated into the RPS1 locus in the *apm4 Δ/Δ* strain. As shown in figure 3.5A – C, this rescued the morphology defects (shorter and wider hyphae; larger yeast cells) back to WT levels. The elevated CFW staining (figure 3.5D, E) was also rescued, as was the increased sensitivity to cell wall disrupting agents Congo Red (CR) and CFW (figure 3.5F). Taken together, this confirms that the *apm4* mutant defects are caused by loss of the *APM4* gene, and re-introduction of just one WT copy is sufficient to rescue these defects.

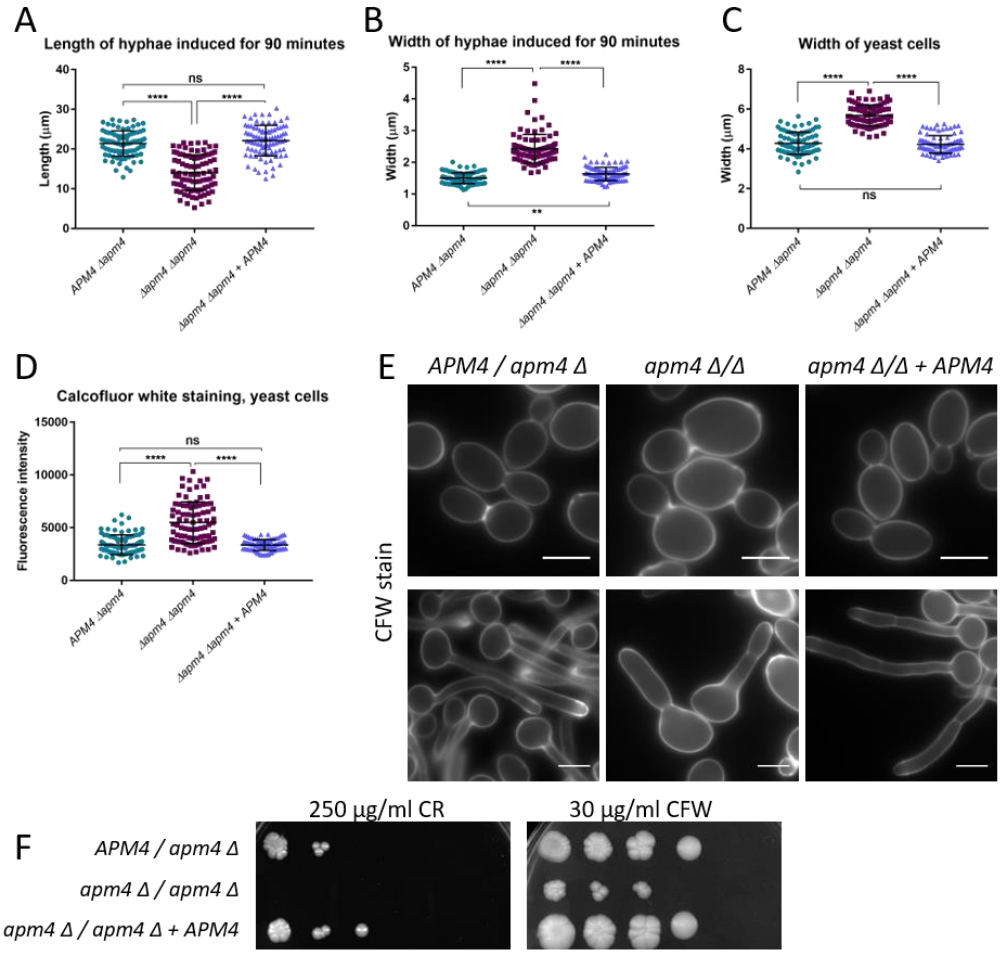


### 3.5. Morphological defects of the *apm4* deletion mutant are rescued by integration of wild-type *APM4*

(A) Cells of each strain were induced to form hyphae for 90 minutes then stained with CFW and imaged. Hyphal length was measured on FIJI. (B) Width of these same hyphae was measured on FIJI. (C) Yeast cells stained with CFW and imaged. Width and (D) mean grey value measured on FIJI. (A-D) Data from 90 cells / strain from 3 independent experiments. Stats are 1-way ANOVAs with Tukey's multiple comparisons. Error bars show SD. (E) Representative images of yeast and hyphal cells from each strain, stained with CFW. Scale bars 5 μm. (F) Serial dilutions of each strain spotted onto YPD plates containing Congo Red or Calcofluor White (as labelled). Photographs of plates after incubation at 30°C for 48 hours.

## 3.6. Apm4 may be phosphorylated in vivo

The mammalian Apm4 protein is known to be phosphorylated in vivo (Wilde and Brodsky 1996), and specifically phosphorylation at residue threonine 156 is critical to the endocytic process (Olusanya et al. 2001). We considered therefore whether *C. albicans* Apm4 undergoes similar regulation via phosphorylation. Apm4 was tagged with HA (human influenza hemagglutinin) to facilitate its immunoprecipitation and analysis via immunoblotting. Phosphorylated proteins often migrate slower on an SDS-PAGE gel, due to their additional negative charge(s). However a 'band-shift' was never observed on standard SDS-PAGE gels (data not shown).

Instead, variations of the SDS-PAGE method were used to see if a band-shift could be observed. Low bis-acrylamide gels can be used to enhance a band shift. Decreasing the ratio of bis-acrylamide (the crosslinker) to acrylamide results in a more open pore structure, which can enhance separation of proteins. A range of bis-acrylamide concentrations were tested, but a clear band shift was never observed. The best separation appeared to be on a 12% total acrylamide; 1% bis-acrylamide gel (see figure 3.6A). Apm4-HA was immunoprecipitated (IP'd) from yeast and hyphal cell extracts and run on these 1% bis-acrylamide gels, which were blotted for HA, and possible double bands can be seen (figure 3.6A). However these are not clearly separated.

Similar Apm4-HA samples from yeast and hyphal cells were also run on Phos-tag™ gels (figure 3.6B). Phos-tag™ gels utilise metal cations contained in the gel which bind to phosphate groups and therefore further slow the migration of phosphorylated proteins. As shown in figure 3.6B, both samples had one bright Apm4-HA band, with some bands higher up the gel (perhaps 4 bands were visible for the yeast sample; perhaps 2 or 3 for the hyphal sample). These may represent phosphorylated species.

Finally, IP'd Apm4-HA from yeast and hyphal extracts was run on two-dimensional (2D) gels, which separate the protein first by isoelectric point (pI) along an immobilised pH gradient (IPG) strip, and then by size on a conventional SDS-PAGE gel. These gels were then blotted and probed for HA. As phosphate groups alter the charge (and therefore pI) of a protein, this allows differently phosphorylated species of a protein to be separated (Zhu et al. 2005). The predicted pI of Apm4 is 8.19 (estimated via isoelectric.org), therefore IPG strips of pH3 – 10 were selected.

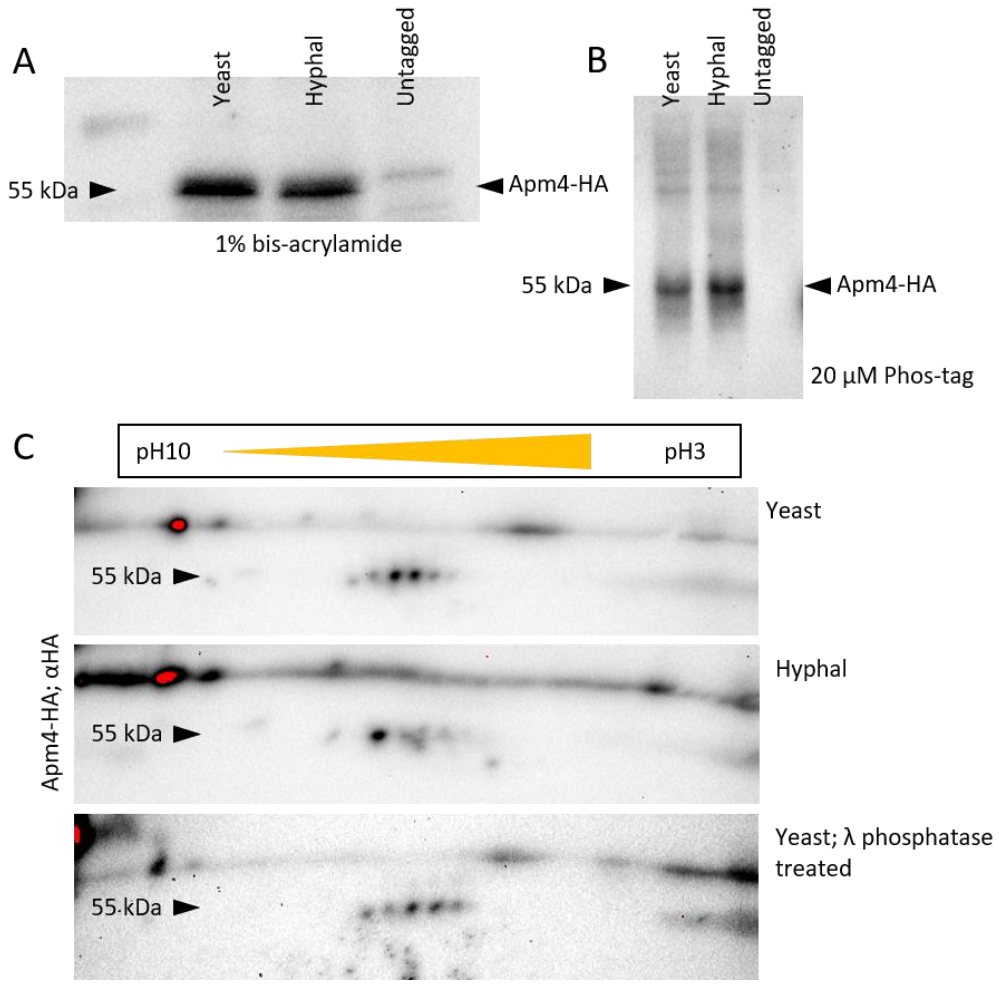


3.6. Apm4 may be phosphorylated in *C. albicans*

(A) Apm4-HA was immunoprecipitated (IP'd) from cells grown as yeast or hyphae, then run on a 12% total acrylamide; 1% bis-acrylamide gel, blotted and probed for HA. A non-HA-tagged strain is included for negative control. (B) As in (A), but samples run on a 10% 20 µM Phos-tag gel. (A and B) are representative images from 2 experiments. (C) Apm4-HA was IP'd from yeast and hyphal cells and 2-dimensional SDS-PAGE gels run, blotted and probed for HA. Images are aligned, with the strip pH decreasing from left to right. This image is representative from 3 experiments. All gels show protein size as determined by PageRuler Plus protein ladder.

As shown in figure 3.6C, 2D electrophoresis of Apm4 from yeast cells separated into 5 spots, indicating the presence of 5 differently phosphorylated species, with an enrichment to spots '3' and '4'. The further to the right the spots are (towards the lower pH), the lower their pI is, meaning the more negatively charged they are. Therefore, the spots represent increasingly phosphorylated species from left to right. Apm4 IP'd from hyphal extracts separates into just 2 or 3 spots (this was consistent across 3 repeats), with the darkest spot to the left of that of yeast Apm4, indicating a less phosphorylated species.

In this analysis, one sample was treated with phosphatase to see where the de-phosphorylated protein would run. Different protocols of treatment with either lambda (λ) or calf intestinal phosphatase (CIP) were tried, but these never led to a change in the pattern of spots. Therefore it cannot be concluded that the species observed via 2D electrophoresis are definitely phosphorylated protein species. If time allowed, different phosphatase treatments could be tried, or a modified non-phosphorylatable mutant used as a negative control.

## 3.7. Mutating phosphorylatable residues on Apm4 abrogates correct AP-2 complex localisation

A screen was carried out by Willger et al (2015), to identify phosphorylated proteins in the *C. albicans* proteome. This identified four phosphorylated residues (three serines and one threonine) in *Ca*Apm4 (figure 3.7). These residues are in a similar region to the mammalian residue threonine 156 which is known to be critical to AP-2 regulation


3.7. *C. albicans* and *H. sapiens* Apm4 are phosphorylated in a similar region

Sequence alignment of the Apm4 amino acid sequences from *Candida albicans* (top line) and *Homo sapiens* (bottom line) made using UniProt.org. Highlighted in red is the amino acid threonine 156 which is known to be phosphorylated in mammalian Apm4 (Olusanya et al., 2001). Highlighted in blue are the residues in *C. albicans* Apm4 which were shown to be phosphorylated via a phosphoproteome screen (Willger et al., 2015).

(Olusanya et al. 2001). Therefore a mutant was made to test whether these residues carry out a similar regulatory role in *C. albicans* AP-2.

*APM4* was cloned from *C. albicans* DNA then four rounds of site-directed mutagenesis (SDM) mutagenized the four serine / threonine residues to alanine, which is non-phosphorylatable. This non-phosphorylatable gene was then integrated into an *apm4 Δ/Δ* strain at the RPS1 locus, to give the strain *apm4 Δ/Δ* + *apm4*$^{S/T\text{-}A}$. Each step was confirmed via sequencing.

In contrast to the rescues observed upon integration of WT *APM4*, integration of *apm4*$^{S/T\text{-}A}$ resulted in similar morphological defects to the full *apm4* deletion (figure 3.8A – D), indicating that the non-phosphorylatable protein was essentially non-functional. Apl1 was then tagged with GFP in this strain, to see whether the AP-2 complex was able to form and localise correctly. Surprisingly, in the *apm4 Δ/Δ* + *apm4*$^{S/T\text{-}A}$ mutant, Apl1-GFP was not observed in bright puncta, but rather evenly dispersed around the cell periphery (see figure 3.8E). There was also an accumulation in vacuoles. This indicates that after mutagenesis of these four phosphorylated residues, the AP-2 complex was defective in its formation and / or localisation to sites of endocytosis. More work is needed to say whether this defect is due to loss of Apm4 phosphorylation.

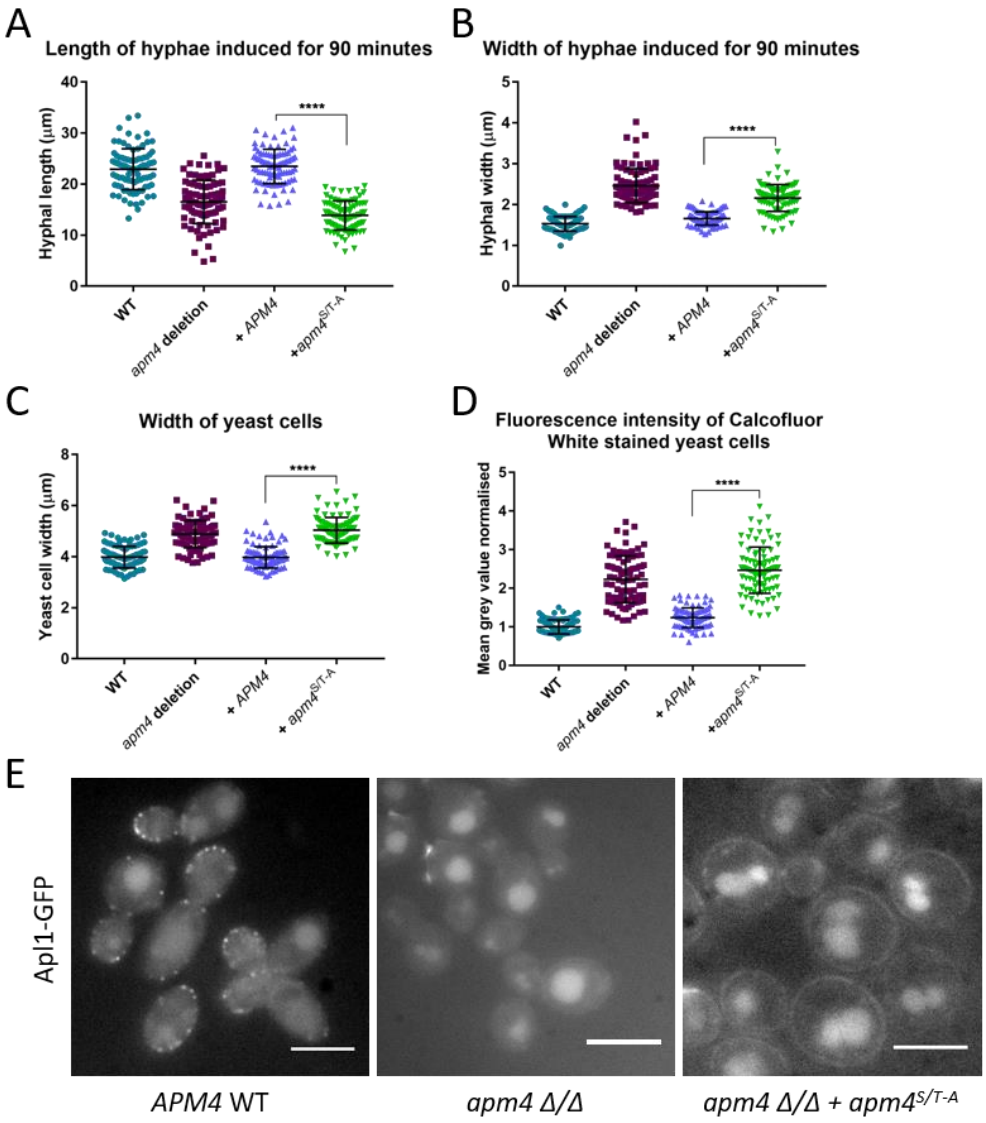


### 3.8. Mutating phosphorylatable residues on *Ca*Apm4 abrogates correct AP-2 complex localisation

(A) Four strains were grown as hyphae for 90 mins: WT; *apm4* deletion; *apm4* deletion complemented with WT *APM4*; and *apm4* deletion complemented with a copy of *apm4* which has four Ser / Thr residues mutated to Ala. Hyphae were stained with CFW and imaged, and the length and (B) width measured using FIJI. (C) The same four strains were grown as yeast, stained with CFW and imaged, and the width and (D) mean grey value measured using FIJI. (A – D) Graphs show data from 90 cells / strain; 3 independent experiments. Stats are one-way ANOVAs; error bars show SD. (E) Apl1 tagged with GFP in 3 different strains as indicated, and imaged; representative images of yeast cells shown. Scale bars 5 µm.

## 3.8. Chapter 3 discussion

### 3.8.1. Discussion of yeast cell size and surface

One of the first phenotypes observed in the *apm4* deletion mutant was the notably larger size of its yeast cells (figure 3.3B, C). It makes sense that if endocytosis is disrupted and material is being added but not removed from the cell membrane, this will lead to expansion of the cell. However, as shown in Knafler et al (2019), the *apm4* deletion mutant does not have a defect in overall fluid phase endocytosis (of Lucifer Yellow dye), nor in number of endocytic sites (actin patches). Therefore it appears these cells are still internalising as much membrane as WT cells, so this is not the cause of the enlarged cell phenotype.

The enlarged yeast cells could be caused by reduced endocytic recycling of components which are normally localised to the bud during bud growth. This could lead to the de-polarisation of the secretory machinery, leading to continued growth of yeast mother cells when growth would normally be exclusively in the bud. This could also explain the slower growth of this strain as measured by cell number. However when investigating polarity factors such as polarisome and exocyst (see chapter 6), this de-polarisation of secretion in cells without AP-2 was observed in hyphae but not in yeast cells.

Alternatively, the enlarged yeast cells could be caused by a loss of recycling of Chs3 (and possibly other cell wall biosynthesis enzymes); in *apm4* mutant yeast cells Chs3 is spread all around the cell surface, rather than focussed to growing buds (Knafler et al., 2019). This could lead to new cell wall deposition in mother cells which would normally occur only in growing buds, leading to enlargement of yeast mother cells.

The enlarged size of yeast cells without *apm4* could be the cause of their slower doubling time (figure 3.3B). If the cells are putting more material into their mother cells, it may take longer for the buds to grow and divide. Conversely, delayed cell division could be leading to larger cell size in the mutant. The larger cell volume and lower cell number over time in the *apm4* mutant could combine to give the similar OD (absorbance) measurements to WT seen in the first 7 hours of growth.

The cell surface defects observed via SEM could be caused by the *apm4* mutant's disrupted cell wall (see Knafler et al, 2019 and chapter 5). Alterations in the levels and distribution of the various cell wall polysaccharides could cause the surface to appear rougher. One study has found that mutants exhibiting cell wall defects including glucan

'unmasking' have increased surface roughness as measured by AFM (Hasim et al. 2017). Alternatively, the *apm4* mutant's weakened cell wall may leave it more susceptible to damage during the processing required for SEM.

### 3.8.2. Discussion of Apm4 phosphorylation

The work presented in this chapter on Apm4 phosphorylation is very preliminary and requires further study to draw any real conclusions. However it does offer some interesting hints that *Ca*Apm4 may be regulated by phosphorylation of its hinge region, in a similar mechanism to mammalian μ2. The fact that a 'band-shift' was not observed when Apm4-HA was run on SDS-PAGE gels could mean that *Ca*Apm4 is very transiently phosphorylated, or that its phosphorylation does not alter its electrophoretic mobility sufficiently to be visualised. 2D gel electrophoresis has given the most convincing evidence of phosphorylation – five 'spots' were reproducibly observed from yeast Apm4-HA (figure 3.6C). This very nicely matches the four phosphorylation sites reported in *Ca*Apm4 (figure 3.7) – with one spot being the non-phosphorylated form.

Perhaps surprisingly, Apm4 from hyphal samples always appeared less phosphorylated than that from yeast cells. Hyphal Apm4-HA consistently separated into 2 or 3 spots, enriched at the left (high pH) side of the strip – indicating less phosphorylated species. This was surprising to us because loss of AP-2 seems to produce more severe defects in hyphal *C. albicans* cells, therefore we reasoned that AP-2 would be more active – and more phosphorylated - in hyphal cells.

One explanation for this could be that Apm4 phosphorylation is not directly coupled to activation. As mentioned, the role of μ phosphorylation is not clear, and some evidence suggests that phosphorylation of mammalian μ2 actually inhibits endocytic uptake. Another could be that only a subset of hyphal AP-2 requires activation (at the hyphal 'collar region') so a smaller fraction of Apm4 is phosphorylated in hyphal compared to yeast cells. Alternatively, the more rapid endocytic recycling required for hyphal growth may require faster AP-2 turnover leading to more Apm4 appearing in a de-phosphorylated state. The 'hyphal' sample was made from cell extracts after 90 minutes of hyphal growth; perhaps looking at hyphal cells directly after hyphal induction would give a different result, as endocytic recycling could be more important at the hyphal 'switch'.

A major caveat to this experiment is that treatment with phosphatase did not shift the pattern of spots observed. Several protocols using lambda and calf intestinal phosphatase after Apm4-HA immunoprecipitation (prior to elution) were trialled, but a shift towards less phosphorylated species upon phosphatase treatment was never observed. This may be due to these particular phosphorylation sites being inaccessible to these enzymes; if more time were available then different phosphatases could be trialled. Alternatively, a non-phosphorylatable or kinase-dead mutant could be used as a negative control. Without this proper negative control, we cannot conclusively say that the spots observed are due to phosphorylation. Various other post-translational modifications such as acetylation and deamination can also induce shifts in the pI of a protein (Mayer, Albrecht and Schaller 2015). The presence of phosphorylation in *Ca*Apm4 could be further confirmed via mass spectrometry, and this could also offer insight into whether phosphorylation levels vary at different times during yeast or hyphal growth.

To try to examine the importance of these reported phosphorylation sites, four serines and threonines (see figure 3.7) in *Ca*Apm4 were mutated to alanines, then this 'non-phosphorylatable' version of the protein was integrated into the *apm4 Δ/Δ* strain. In contrast to integration of WT *APM4*, this *apm4 Δ/Δ* + *apm4*$^{S/T\text{-}A}$ strain had morphological defects similar to *apm4* deletion alone (figure 3.8). When Apl1 (AP-2 β subunit) was tagged with GFP in this strain, it clearly showed that the AP-2 complex was unable to form and / or localise correctly. Instead of bright puncta at the cell periphery, the Apl1-GFP signal was evenly dispersed around the cell periphery, and also accumulated in vacuoles. These dramatic phenotypes were quite unexpected and show the importance of these residues in the disordered hinge region of *Ca*Apm4.

The dramatic phenotype of the non-phosphorylatable mutant could mean that the AP-2 complex cannot form without Apm4 phosphorylation – perhaps because it is unstable or subject to degradation in its non-phosphorylated state. This would lead to morphological defects as severe as the full deletion mutant. Alternatively, the AP-2 complex may form but be unable to bind cargo and / or lipids correctly in the absence of Apm4 phosphorylation. This may lead to loss of AP-2 recruitment to endocytic sites, and therefore its diffuse localisation around the cell periphery and in the vacuole. However the *apm4*$^{S/T\text{-}A}$ mutant may prevent AP-2 complex formation for other reasons aside from loss of phosphorylation. For example the change in amino acid sequence may preclude correct Apm4 folding, leading to non-formation or breakdown of AP-2.

To further investigate the role of these phosphorylation sites, they could be mutagenized one at a time, or changed to phospho-mimetic residues, to see whether a different phenotype is observed. As an alternative approach, if the kinase responsible for Apm4 phosphorylation was identified, it could be blocked, or its recognition site mutagenized to study the effects of blocking phosphorylation. A good starting point in finding the kinase responsible would be the *C. albicans* homologue of *Sc*Pkc1, which is thought to phosphorylate Apm4 in *S. cerevisiae*.

### 3.8.3. Concluding remarks

This chapter has shown that depletion of AP-2 leads to larger yeast cells which are slower growing and have gross morphological defects compared to WT. We demonstrate that the defects observed in the *apm4* mutant are rescued by integration of wild-type *APM4*, showing that the phenotypes are indeed caused by loss of *apm4*. We also provide preliminary evidence that *C. albicans* Apm4 is phosphorylated in vivo; and that when its putative phosphorylation sites are mutagenized this abrogates AP-2 complex formation and / or localisation. More work is needed to conclusively prove Apm4 phosphorylation and determine its functional role in *C. albicans*.

# Chapter 4: AP-2-dependent endocytic recycling of the chitin synthase Chs3 regulates polarized growth in *Candida albicans*

The major results of this phD project were published in this 2019 mBio paper. The accepted and peer reviewed paper is presented here in full. This paper demonstrates that AP-2 is present at sites of endocytosis in *C. albicans* but that its depletion does not affect overall endocytic flux. It characterises the defects in morphology; biofilm forming ability; and cell wall organisation caused by loss of AP-2. The paper shows that AP-2 is required for endocytic recycling of Chs3, and that loss of this causes excess cell wall chitin leading to morphological defects. Chs3 recycling is shown to depend on the YxxΦ motif binding domain of Apm4. The paper also shows that loss of AP-2 leads to loss of polarised ergosterol and mannose deposition, and that these defects are independent of chitin biosynthesis.

All of the experiments, unless stated below, were carried out by me (Harriet Knafler). All analysis, unless stated below, was carried out by me. The experiments were designed, and the manuscript written, by me and Kathryn Ayscough.

The following pieces of data are not my own work:

Dr Iwona Smaczynska-de Rooij constructed some of the *C. albicans* mutant strains. Table 2.4 (p55 – 57) details all *C. albicans* strains used in this study (both in the paper and the rest of the thesis) and states who made each strain.

HPLC analysis in figure 6A was carried out by Dr Kathy Lee; both the experiment and the analysis were done by Kathy, with me assisting / observing.

TEM images in figure 6C: grids were made by Gillian Milne and Dr Louise Walker at the University of Aberdeen Microscopy and Histology core facility. Images were taken by me.

Harriet Knafler

Kathryn Ayscough

AMERICAN SOCIETY FOR MICROBIOLOGY | mBio®

RESEARCH ARTICLE
Molecular Biology and Physiology

# AP-2-Dependent Endocytic Recycling of the Chitin Synthase Chs3 Regulates Polarized Growth in *Candida albicans*

H. C. Knafler,[a] I. I. Smaczynska-de Rooij,[a] L. A. Walker,[b] K. K. Lee,[b] N. A. R. Gow,[b]* K. R. Ayscough[a]

[a]Department of Biomedical Science, University of Sheffield, Sheffield, United Kingdom
[b]Aberdeen Fungal Group, Institute of Medical Sciences, Foresterhill, University of Aberdeen, Aberdeen, United Kingdom

**ABSTRACT** The human fungal pathogen *Candida albicans* is known to require endocytosis to enable its adaptation to diverse niches and to maintain its highly polarized hyphal growth phase. While studies have identified changes in transcription leading to the synthesis and secretion of new proteins to facilitate hyphal growth, effective maintenance of hyphae also requires concomitant removal or relocalization of other cell surface molecules. The key molecules which must be removed from the cell surface, and the mechanisms behind this, have, however, remained elusive. In this study, we show that the AP-2 endocytic adaptor complex is required for the internalization of the major cell wall biosynthesis enzyme Chs3. We demonstrate that this interaction is mediated by the AP-2 mu subunit (Apm4) YXXΦ binding domain. We also show that in the absence of Chs3 recycling via AP-2, cells have abnormal cell wall composition, defective polarized cell wall deposition, and morphological defects. The study also highlights key distinctions between endocytic requirements of growth at yeast buds compared to that at hyphal tips and different requirements of AP-2 in maintaining the polarity of mannosylated proteins and ergosterol at hyphal tips. Together, our findings highlight the importance of correct cell wall deposition in cell shape maintenance and polarized growth and the key regulatory role of endocytic recycling via the AP-2 complex.

**IMPORTANCE** *Candida albicans* is a human commensal yeast that can cause significant morbidity and mortality in immunocompromised individuals. Within humans, *C. albicans* can adopt different morphologies as yeast or filamentous hyphae and can occupy different niches with distinct temperatures, pHs, $CO_2$ levels, and nutrient availability. Both morphological switching and growth in different environments require cell surface remodelling, which involves both the addition of newly synthesized proteins as well as the removal of other proteins. In our study, we demonstrate the importance of an adaptor complex AP-2 in internalizing and recycling a specific cell surface enzyme to maintain effective polarized hyphal growth. Defects in formation of the complex or in its ability to interact directly with cargo inhibit enzyme uptake and lead to defective cell walls and aberrant hyphal morphology. Our data indicate that the AP-2 adaptor plays a central role in regulating cell surface composition in *Candida*.

**KEYWORDS** *Candida albicans*, cell polarity, cell wall, endocytosis, membrane trafficking, yeasts

*Candida albicans* occupies many niches within humans which are distinct in terms of temperature, pH, $CO_2$ level, and nutrient availability. Pathogens such as *C. albicans* must adapt to these changes to maintain growth and survival. Central to *C. albicans* virulence is the ability of cells to switch morphologies between rounded (yeast) and filamentous (hyphal) forms. This capacity is proposed to allow the organism to disseminate effectively in blood (as yeast) and invade tissues (with hyphae) (1). While the

**Citation** Knafler HC, Smaczynska-de Rooij II, Walker LA, Lee KK, Gow NAR, Ayscough KR. 2019. AP-2-dependent endocytic recycling of the chitin synthase Chs3 regulates polarized growth in *Candida albicans*. mBio 10:e02421-18. https://doi.org/10.1128/mBio.02421-18.

**Editor** Judith Berman, Tel Aviv University



Address correspondence to K. R. Ayscough, k.ayscough@sheffield.ac.uk.

* Present address: N. A. R. Gow, Office of the Vice-Chancellor and Senior Executive, University of Exeter, Exeter, United Kingdom.

**Received** 25 January 2019
**Accepted** 8 February 2019
**Published** 19 March 2019

yeast-to-hyphal transition has been extensively studied, with many sensing and signaling pathways described, how membrane trafficking pathways are integrated to regulate surface composition and facilitate morphological changes is still not well understood. A major change that occurs in each niche is surface remodelling. Proteins required for nutrient uptake or cell wall biosynthesis in the new environment are incorporated into the plasma membrane via the secretory pathway. Critically, however, the removal of certain proteins is also required to achieve appropriate surface composition. The downregulation of transporters, cell wall synthesis enzymes, and signaling molecules from the *C. albicans* cell surface is achieved by endocytosis. A functional endocytic pathway is known to be required for the morphological switch from yeast to filamentous hyphal growth and in the maintenance of polarized growth in hyphae (2–4). While the detailed analysis of endocytosis in *C. albicans* is not as extensive as for the model organism *Saccharomyces cerevisiae*, the evidence for the importance of endocytic proteins in morphogenesis and virulence is robust. (2–6). However, deletion of a number of genes encoding proteins involved in endocytosis has mostly led to a general inhibition of the endocytic process itself and has not facilitated broader understanding of the key molecules that must be removed from the surface to ensure fitness in distinct niches.

One of the best-understood endocytic processes in eukaryotes is clathrin-mediated endocytosis. While studies in *S. cerevisiae* have led the way in understanding the spatiotemporal molecular interactions leading up to membrane invagination and scission to release endocytic vesicles, work in mammalian cells has been key in determining how specific endocytic cargoes are recruited to sites of internalization. These latter studies have demonstrated the importance of a key heterotetrameric adaptor protein complex, AP-2, in recognizing peptide motifs on transmembrane proteins that are required for their internalization (7). As with the other AP-adaptor complexes involved in different membrane trafficking steps, AP-2 contains two large subunits of approximately 100 kDa, referred to as $\alpha$ and $\beta$ adaptins (encoded by *APL3* and *APL1* in *Candida*, respectively), a medium subunit mu (*APM4*), and a small subunit sigma (*APS2*). Elegant structural analysis has mapped key interaction surfaces required for cargo recognition to the mu and sigma subunits as well as plasma membrane and clathrin coat protein binding (8–10). However, despite AP-2 localizing to endocytic sites in *S. cerevisiae*, deletion of genes encoding its subunits had almost no detectable effect on endocytosis, though this deletion mutant showed an intriguing, but yet to be explained, resistance to killer toxin (11). Further studies suggested defects in polarized cell responses to pheromone and heat shock, though again, robust evidence for a strong, mechanistic, endocytic link has remained elusive (12). Most recently, a role for fungal AP-2 in polarized growth has been demonstrated in the fungal pathogen *Aspergillus nidulans* (13). In that study, AP-2 was proposed to play a clathrin-independent role in polarized lipid and cell wall deposition. To date, however, the focus of studies has been on demonstrating the effects of full gene deletions on the overall functioning of endocytic machinery rather than gaining an understanding of the mechanism underlying the observed changes.

In this study, we demonstrate that AP-2 is present at endocytic sites in both yeast and hyphal cells of *Candida albicans*. Deletion of its putative cargo-binding mu subunit genes (*apm4*Δ/*apm4*Δ) caused disruption of the AP-2 complex and defects in polarized morphogenesis and cell wall organization, though overall fluid-phase endocytosis remained unaffected. We measured marked changes in surface chitin levels, which led to the identification of the cell wall biosynthesis enzyme chitin synthase 3 (Chs3) as a cargo of AP-2 uptake and trafficking. This study also highlights key distinctions between endocytic requirements of growth at yeast buds compared to that at hyphal tips and different requirements of AP-2 in maintaining the polarity of ergosterol and mannosylated proteins at hyphal tips. Together, our findings highlight the importance of correct cell wall deposition in cell shape maintenance and polarized growth and the key regulatory role of endocytic recycling via the AP-2 complex.

## RESULTS

***C. albicans* AP-2 localizes to endocytic sites in yeast and hyphae.** The presence of AP-2 at endocytic sites in *S. cerevisiae* has been demonstrated based on colocalization with endocytic reporters such as Sla1 and Abp1 (11, 12). In this study, the beta-adaptin subunit of AP-2 (Apl1) was tagged on one genomic copy with green fluorescence protein (GFP) in otherwise untagged strains and with red fluorescent protein (RFP) in a strain that also expressed Sla1-GFP. As shown in Fig. 1A, there was clear localization of Apl1-GFP to puncta at the plasma membrane. In yeast cells, there was enrichment to small growing buds and to the bud neck region, especially in medium-to-large budded cells, while in hyphae, there were puncta along the length of the hyphae as well as enrichment near the hyphal tip region. The lifetime of puncta at the plasma membrane was measured for Apl1-GFP in both yeast and hyphae (Fig. 1B). The median lifetime of Apl1-GFP was not significantly different in the yeast or hyphal cells, with a 22.5 s median lifetime in yeast (standard deviation [SD], 45 s; $n = 30$) and 25 s in hyphae (SD, 48 s; $n = 30$). The relatively broad range of lifetimes is frequently seen in proteins present in the early stages of endocytosis in *S. cerevisiae* (14, 15).

Strains coexpressing Apl1-RFP and the endocytic marker Sla1-GFP were then visualized. We observed colocalization at puncta in both yeast and hyphae (Fig. 1C). The recruitment of the two proteins to sites was followed (Fig. 1D shows representative puncta), and we found that the proteins were recruited at approximately the same time and that both signals increased and decreased in intensity over a similar time frame. The similar lifetimes and assembly and disassembly profiles of Apl1 and Sla1 suggest that AP-2 is likely to perform its function in conjunction with recognized endocytic machinery. However, given its possible function as a cargo adapter protein, it may only incorporate into puncta when relevant cargoes are present. Therefore, we next analyzed the extent of colocalization of Apl1-RFP and Sla1-GFP. This was assessed in both *C. albicans* yeast and in hyphae 30 min after induction. As shown in Fig. 1E, in yeast cells, 33% of puncta counted had both Sla1-GFP and Apl1-RFP signals, while 55% contained only Sla1-GFP and 12% contained only Apl1-RFP ($n = 256$ puncta). After 30 min of hyphal induction, 42% of puncta showed colocalization, while 48% had Sla1-GFP alone and 10% contained Apl1-RFP alone. Thus, at least half of the endocytic patches marked with Sla1-GFP did not contain Apl1-RFP, though there was a modest increase in AP-2 association with patches following hyphal induction, possibly indicating a greater need to internalize some specific cargoes.

**AP-2 disruption does not significantly affect endocytic site organization or fluid-phase uptake.** Given that *C. albicans* AP-2 localizes to endocytic sites, we next determined whether deletion of its mu subunit (*apm4*) affected endocytic uptake in yeast. Both genomic copies of *apm4* were deleted, and as expected, loss of this subunit caused disruption of the AP-2 complex such that Apl1-GFP was no longer observed in puncta (see Fig. S1 in the supplemental material). A similar disruption of AP-2 was seen in *S. cerevisiae* when the subunits were deleted (11, 12).The effect of AP-2 disruption on cell growth and uptake of the fluid-phase marker Lucifer yellow were assessed. As shown in Fig. 2A, the growth of *apm4*Δ/*apm4*Δ mutant cells in liquid culture was only slightly reduced compared to that of wild-type cells. This suggests that under conditions used for lab cell growth, the *apm4* deletion does not cause large-scale defects in cell functions. Analysis of bulk fluid-phase endocytosis (Fig. 2B) using the dye Lucifer yellow demonstrated similar levels of uptake in wild-type and mutant cells, signifying no generalized endocytic defect. This is consistent with what others have observed in *S. cerevisiae* (16, 17). The use of rhodamine phalloidin, which binds to F-actin and localizes to endocytic puncta, also confirmed that there was no marked disruption to actin organization in the *apm4*Δ/*apm4*Δ yeast (Fig. 2C) or hyphal cells (Fig. 2D). A very similar pattern of localization of actin patches was observed in both yeast and hyphae of wild-type and mutant cells, suggesting no large-scale defects in the number of endocytic sites nor in their polarized localization.

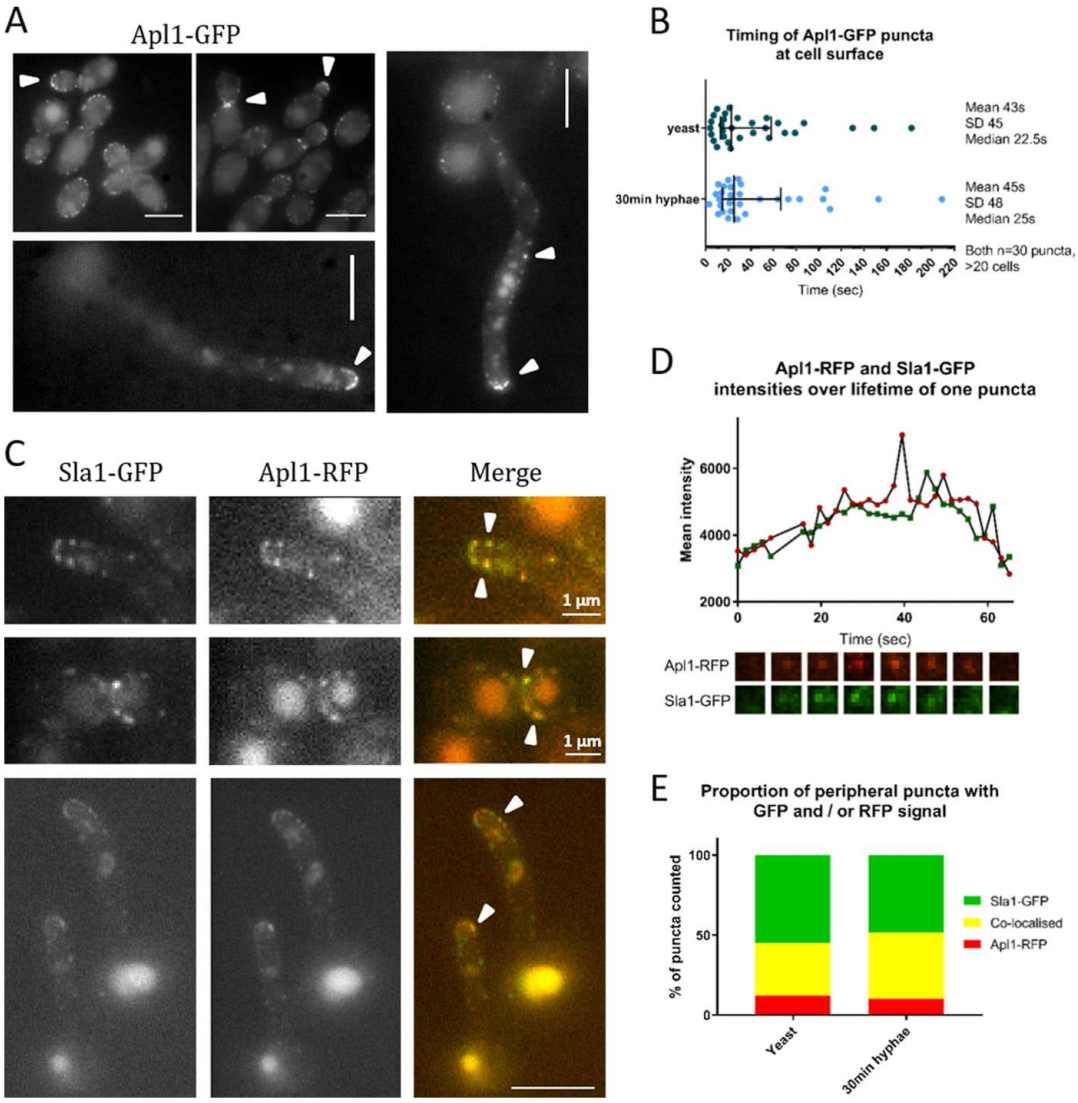


**FIG 1** AP-2 is present at sites of endocytosis in *Candida albicans*. (A) Representative images of yeast and 90-min hyphae showing Apl1-GFP puncta. (B) Analysis of times Apl1-GFP puncta are present at cell surface, in strain with single tag; $n = 30$ puncta measured for each condition. Error bars show means and SDs. (C) Representative images of coexpressed Sla1-GFP and Apl1-RFP. Arrowheads show examples of puncta where signals colocalize. (D) Intensities of Sla1-GFP and Apl1-RFP in a representative surface punctum over time. Images below graph show this punctum every 8 s, corresponding to time axis on graph. (E) More than one hundred peripheral puncta were counted in both yeast and hyphal cells, and whether they contained Apl1-RFP signal, Sla1-GFP signal, or both signals colocalized was recorded. Graph shows percentages of all puncta counted.

**AP-2 disruption affects cell morphology.** While the studies on global organization of endocytic sites did not reveal large differences in numbers or localization, alterations in hyphal morphology were clear. To analyze this in more detail, *C. albicans* cells were grown in yeast form and then reinoculated into medium to induce hyphal formation. While the homozygous mutant *apm4*Δ/*apm4*Δ cells were able to undergo the bud-hyphal transition and initiate hyphae, there were clear differences in hyphal morphol-

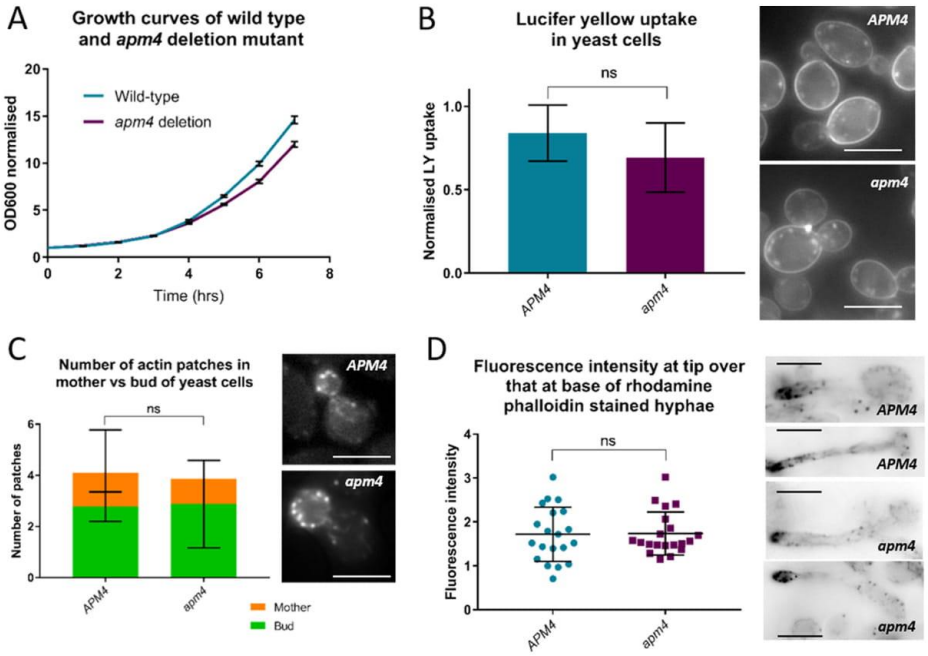


**FIG 2** AP-2 disruption does not significantly affect endocytic site organization or fluid-phase uptake. (A) Growth curves of WT and *apm4* deletion cells over 8 h; 3 biological and 3 technical replicates per strain in 3 separate experiments. (B) Fluid-phase endocytosis assay; cells incubated with Lucifer yellow dye (LY) for 60 min and uptake quantified by fluorimetry. Graph shows uptake normalized to total cell protein. Images are representative of LY uptake in each strain; 3 biological and 3 technical replicates per strain in 3 independent experiments. (C) Representative images of yeast cells stained with rhodamine phalloidin showing actin patches and cables; quantification of number of actin patches in mother and bud of each cell ($n = 20$ cells per strain; 1 representative experiment). (D) Images of hyphal cells stained with rhodamine phalloidin. Quantification of fluorescent signal at hyphal tip divided by that at the "base" of the hypha (closest to mother cell); $n = 20$ cells per strain. Statistics in panels B to D are unpaired *t* tests of data. All error bars represent SD. ns, $P = 0.1234$.

ogy between these cells and the wild-type and heterozygote (*APM4*/*apm4*Δ) cells (Fig. 3A). Mutant cells were able to form septa; although these were sometimes placed at the neck, causing a constriction as in pseudohyphae (1), the majority (75%) of mutant cells containing septa had formed these further down the germ tube, as in true hyphal growth (compared to 93% of wild-type [WT] hyphae; $n > 75$ cells/strain) (representative images in Fig. S2A). Hyphal growth was analyzed after 2 h and a range of parameters was assessed. As shown, both the length of hyphae (Fig. 3B) and width of hyphae (Fig. 3C) were significantly different, with shorter, wider hyphae in the homozygous mutant.

The ability to undergo morphological switching is an important stage in biofilm formation, and the growth of biofilms on catheters and other solid substrates is a major challenge faced in hospital-acquired *C. albicans* infections (18). To determine whether disruption of the AP-2 complex affected the ability to form biofilms, wild-type and *apm4* deletion strains were grown on plastic, and biofilm formation was analyzed. As shown in Fig. 2D and E, the *apm4*Δ/*apm4*Δ mutant was significantly impaired in biofilm formation. (Cell growth in this assay is shown in Fig. S2B.)

**AP-2 disruption affects ability of cells to undergo polarized growth.** The cell morphology defects noted above indicate that while hyphal growth was initiated in AP-2 disrupted cells, there were defects in restricting growth to maintain the normal hyphal form. To analyze the polarity defect further, two markers of polarity were assessed. Ergosterol is the major plasma membrane sterol in *Candida*. It is normally enriched at the tip of the hyphae and has been reported to be important in hyphal

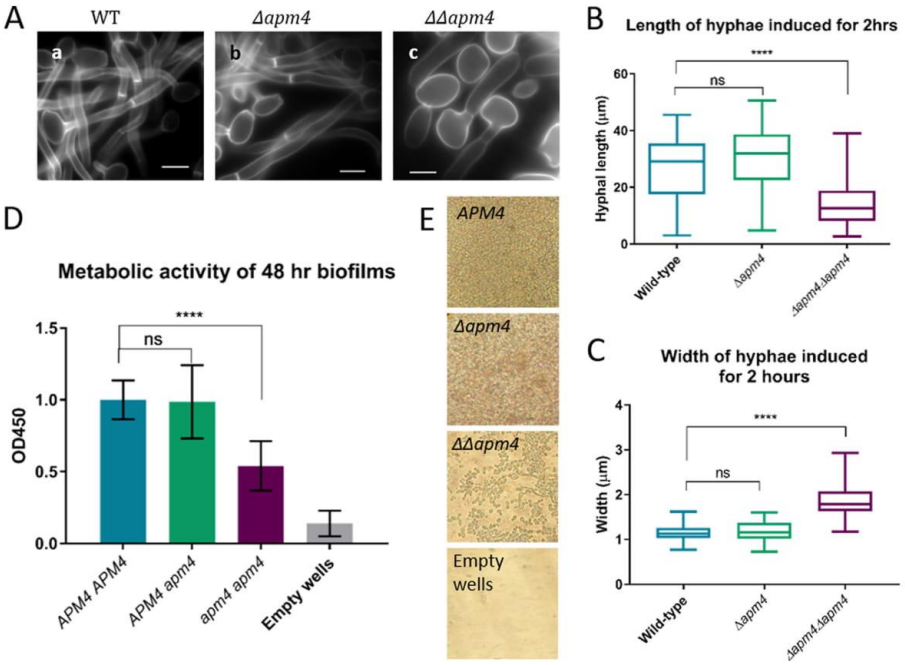


**FIG 3** AP-2 disruption affects cell morphology. (A) Representative images of WT, heterozygous, and homozygous *apm4* deletion strains, grown as hyphae for 2 h and then stained with calcofluor white. Scale bars, 5 μm. Measurements of hyphal length ($n > 100$ cells/strain from 2 independent experiments) (B) and hyphal diameter at the "neck" ($n > 75$ cells/strain; 1 experiment) (C) in WT and *apm4* deletion strains. (D) Metabolic activity as measured by XTT assay of cells grown as biofilms on plastic, after washing. (E) Representative images of biofilms after washing, taken on a light microscope with a 20× objective. All statistics are from one-way ANOVAs with Tukey's *post hoc* tests. (B, C) Central lines at medians; whiskers at minimum and maximum values. (D) Error bars show SDs. ns, $P = 0.1234$; ****, $P < 0.0001$.

growth and virulence (19, 20). Ergosterol localization was analyzed using filipin, a fluorescent molecule that specifically binds to sterol in the plasma membrane (21, 22). As shown in Fig. 4A, wild-type hyphae show clear filipin enrichment to the hyphal tips, whereas the hyphae in *apm4*Δ/*apm4*Δ cells lacked bright hyphal tip ergosterol patches.

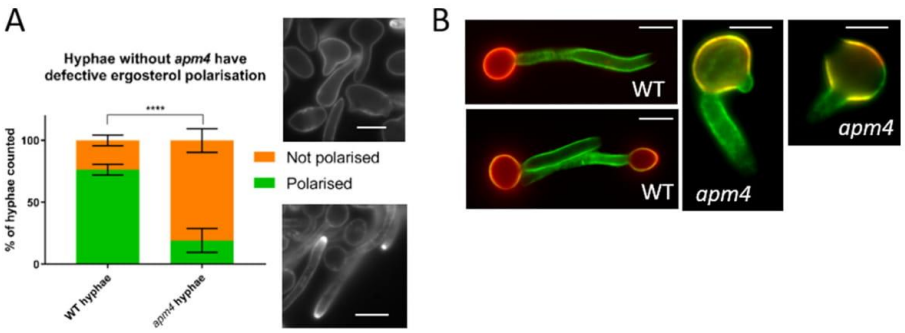


**FIG 4** AP-2 disruption affects ability of cells to undergo polarized growth. (A) Quantification and representative images of hyphal cells stained with filipin ($n > 300$ cells/strain; 4 independent experiments). Statistics are from a two-way ANOVA with Sidak's *post hoc* test. Error bars show SDs. (B) Stationary-phase yeast were stained with concanavalin-A-Alexa 594 (red) and then induced to form hyphae for 90 min and stained with ConA-Alexa 488 (green). Representative images shown. Scale bars, 5 μm. ****, $P < 0.0001$.

A second assay followed the localization of newly secreted mannosylated proteins and lipids. Fluorescently conjugated concanavalin-A (ConA; a lectin which binds mannose residues in the outer cell wall) was applied to cells (23). Stationary-phase yeast were stained with ConA-Alexa 594 (red) to label preexisting mannose. Cells were washed to remove unbound red label before being induced to form hyphae for 90 min and then incubated with ConA-Alexa 488 (green) to stain newly deposited mannose. As shown in Fig. 4B, wild-type cells had a clear distinction between the initial staining of mother cells (red) and the newly grown hyphae (green). In contrast, *apm4*-deleted cells had considerable new mannose deposition in their mother cells, indicating a failure to polarize new mannose deposition to the hyphae during hyphal inducing conditions. The staining also revealed that mutant cells often had more than one site of hyphal initiation. Given that mannose is largely thought to be added to proteins and lipids transiting through the Golgi apparatus which are then secreted in vesicles at the cell surface, the data suggest that the absence of AP-2 leads to the disruption of overall polarized trafficking in cells (24, 25).

**AP-2 disruption affects cell wall distribution.** In fungi, there is a clear link between appropriate deposition of the cell wall and cell morphology (26, 27). The *Candida* cell wall consists mostly of polysaccharides: chitin, glucan (beta 1–3 and beta 1–6 linked), and mannose fibrils, which are linked to integral wall proteins and lipids (28). The inner chitin/glucan layer is important in maintaining cell shape and conferring rigidity, while the outer mannan layer restricts the permeability of the wall (29). *C. albicans* is able to modulate its cell wall composition to adapt to different environments (30), but the underlying mechanisms by which it does this are not well known. Given the changes to hyphal morphology, the *apm4* deletion strain was analyzed to determine whether observed changes correlated with any alterations in organization or composition of cell wall components.

Exposure to different chemicals during growth has been used widely to indicate cell wall defects and was used to highlight possible changes in *apm4*Δ/*apm4*Δ cells. As shown in Fig. 5A, marked growth inhibition was observed in the presence of Congo red and calcofluor white. Calcofluor white specifically binds chitin (31) and Congo red binds glucan chains (32); both are thought to interfere with cross-linking of the polysaccharide network, thereby reducing its stability. Cell wall defects often increase the sensitivity to these two dyes (33). Cells with the *apm4*Δ/*apm4*Δ deletion were also sensitive to the cell membrane detergent SDS and showed slower growth on lactate, a physiologically relevant carbon source (34). However, they showed no altered sensitivity to cytotoxic caffeine levels (see Fig. S3). Wheat germ agglutinin (WGA) is a lectin that can bind exposed chitin in the *Candida* cell wall but is too large to penetrate the inner wall (35). A WGA-fluorescein conjugate was used to visualize the localization of exposed chitin in the wild type and in the *apm4* deletion strain. The polarity of the WGA-fluorescein staining was analyzed using line plots of the hyphal tip (Fig. 5B). In wild-type cells, WGA binding was only observed tightly polarized to the tip region of hyphae. However, in the *apm4* deletion strain, WGA was more broadly distributed along the sides of hyphae, with a significant region around the hyphal tip devoid of exposed chitin (see Fig. 5B and C).

In addition to its use in sensitivity assays, calcofluor white (CFW) is a fluorescent stain which allows localization of chitin in the fungal cell wall to be observed (36). Yeast and hyphal cells were stained with CFW, and the levels and patterns of staining were analyzed (Fig. 5D and E). The overall intensity of CFW staining was higher in the mutant, indicating higher chitin levels (see Fig. 7C for quantification of fluorescence intensity). Furthermore, the polarity of staining was altered, with wild-type hyphae showing the brightest CFW staining immediately adjacent to the tip, while the *apm4* deletion hyphae showed no enrichment at the hyphal tip region but brighter hyphal mother cells.

**AP-2 disruption affects cell wall composition and ultrastructure.** Isolated and hydrolyzed cell wall material was analyzed by high-pressure liquid chromatography

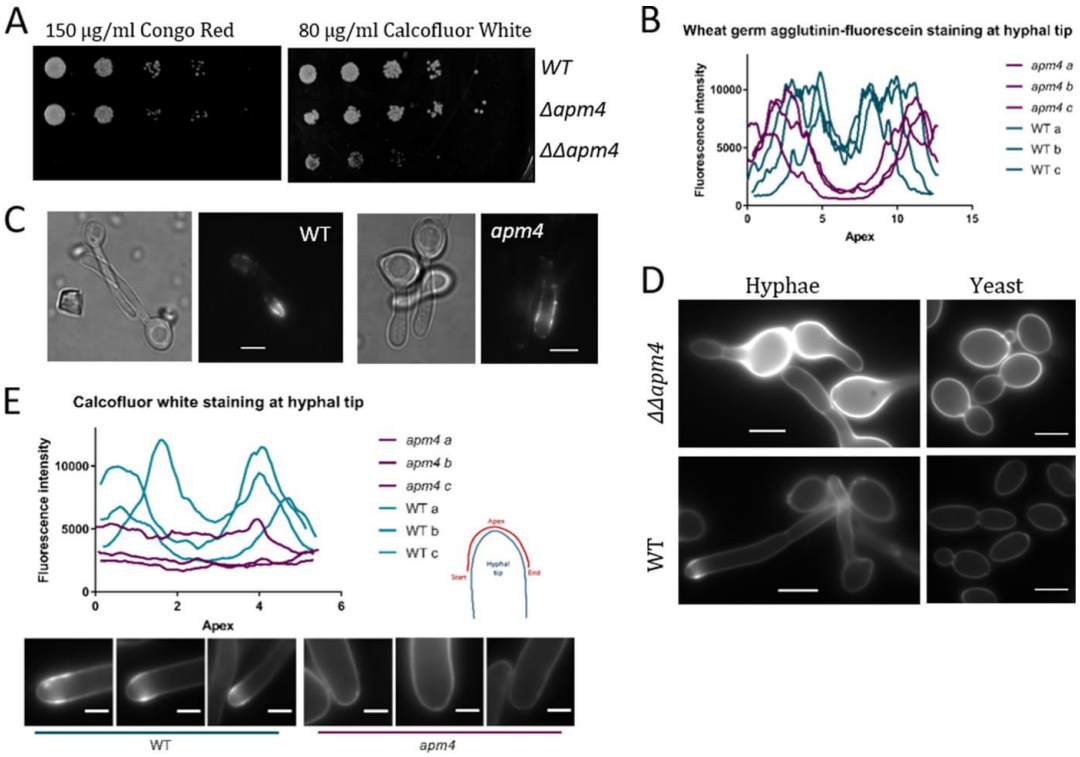


**FIG 5** AP-2 disruption affects cell wall composition. (A) Representative images of plate spotting assay; serial dilutions of each strain plated onto YPD with 150 $\mu$g/ml Congo red (CR) or 80 $\mu$g/ml CFW. (B) Representative line profiles of fluorescence intensity at hyphal tip of cells stained with wheat germ agglutinin (WGA)-fluorescein. See panel E for diagram of how lines were drawn. (C) Representative images of WGA-fluorescein-stained hyphae. (D) Representative images of CFW-stained yeast and hyphal cells. (C, D) Scale bars, 5 $\mu$m. (E) Representative line profiles of fluorescence intensity at hyphal tip of cells stained with CFW. Images below are hyphal tips from which these line profiles were drawn. Scale bars, 1 $\mu$m.

(HPLC) to determine the relative amounts of each sugar component (Fig. 6A). This analysis showed that the mutant (*apm4*Δ/*apm4*Δ) cells had a higher proportion of chitin than wild-type cells, which is consistent with the calcofluor staining and sensitivity assays described above. Cells without AP-2 also had a decreased proportion of glucan and similar proportion of mannan to the wild type, consistent with measurements from transmission electron microscopy (TEM; see below).

As well as analyzing the isolated cell wall components separately, we also looked at the overall ultrastructure of the mutant cell wall, which allowed us to focus on different regions of cells, and found this too was significantly altered (Fig. 6B and C). Freeze substitution transmission electron microscopy (TEM) with high-pressure freezing allowed analysis of high-resolution images of cell wall cross sections (Fig. 6C). Measurements revealed that *apm4* deletion cells had significantly thicker walls than wild-type cells (mean thickness of 255 nm for *apm4* yeast cells, compared to 149 nm in WT cells [$n = 150$]), and this was the case for both yeast and hyphal mother cells (Fig. 6B). Both the inner (chitin/glucan) and outer (mannan) layers were increased in the mutant. The lateral walls of hyphal cells ("hyphal tube") were, however, of a similar thickness to those in wild-type cells. It was also noted that at the hyphal tip, the *apm4* mutant had a significantly thinner wall than wild-type cells, with shorter mannose fibrils.

Taken together, the cell wall analysis data are consistent with a requirement for AP-2 in the recycling of cell wall biosynthesis machinery in order to maintain polarized cell wall deposition focused at the hyphal tip.

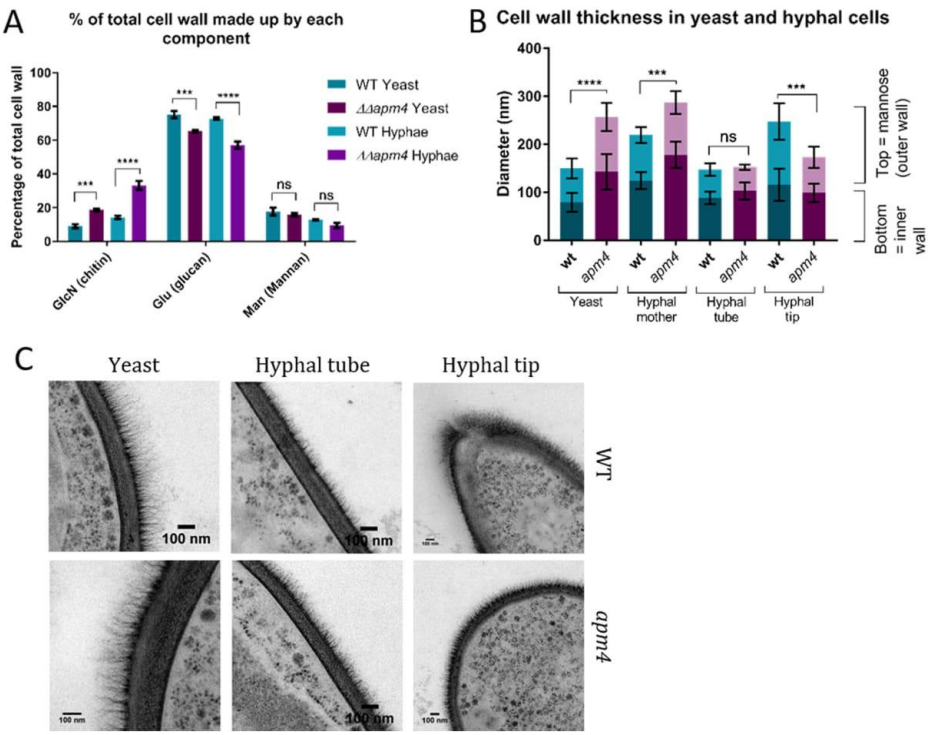


**FIG 6** AP-2 disrupted cells have altered cell wall composition and ultrastructure. (A) HPLC analysis of relative levels of cell wall components in WT and *apm4* deletion cells; 3 biological and 3 technical replicates per strain from 1 experiment. (B) Quantification of cell wall thickness in yeast and different locations on hyphae as measured from TEM images. (C) Representative TEM images. Five measurements per cell for >20 cells per location; 1 experiment. All statistics are from two-way ANOVAs with Tukey's *post hoc* tests. Error bars show SDs. ns, $P = 0.1234$; ***, $P = 0.0002$; ****, $P < 0.0001$.

**Identification of an AP-2 cargo.** Given the significant impact of the *apm4* deletion on chitin distribution and levels, it was reasoned that further analysis might facilitate the identification of potential AP-2 cargoes. Chitin synthesis in *Candida* requires the function of a number of transmembrane chitin synthesis enzymes. Short chitin fibrils or rodlets in the cell wall are generated by the class IV enzyme Chs3. Chs3 is required for ~90% of chitin in the cell wall (37, 38). Because of the defects observed in chitin levels and distribution, and because Chs3 is proposed to be responsible for the majority of chitin synthesis, we tagged Chs3 with GFP and Apl1 ($\beta$ subunit of AP-2) with RFP in the same strain. As shown in Fig. 7A, colocalization of the two proteins was observed in peripheral puncta in yeast cells, indicating that Chs3 localizes to AP-2-containing endocytic patches. Figure 7B shows a line profile analysis of 10 such puncta, showing that the Chs3-GFP and Apl1-RFP signals correlate closely to one another. We then tagged one copy of Chs3 with GFP in wild-type and *apm4*Δ/*apm4*Δ cells. As shown in Fig. 7C, a very dramatic shift in localization was observed. In wild-type cells, Chs3-GFP localized to intracellular puncta, which are polarized toward the tips of hyphae, and to the growing buds and bud necks of yeast cells. These structures are likely to be chitosomes, the organelles proposed to transport Chs3 within cells (39, 40). Chs3-GFP signal observed at the cell periphery was mostly polarized to the tip region. In mutant cells, however, the majority of Chs3-GFP staining was seen at the cell surface and lost the polarization toward hyphal tips and yeast buds. Some signal was also observed in vacuoles.

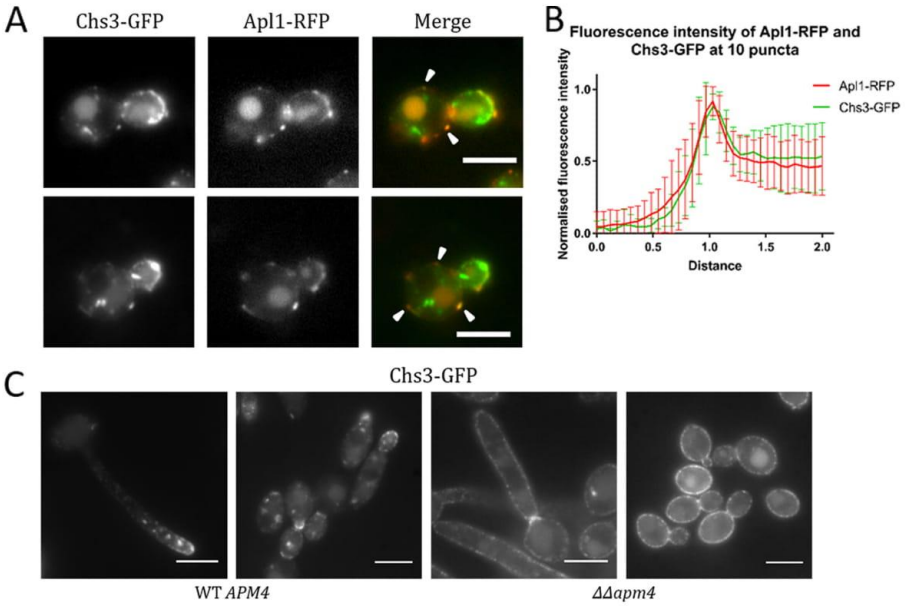


**FIG 7** AP-2 colocalizes with Chs3 and its depletion impairs Chs3 uptake. (A) Representative images of yeast cells in which Chs3 was tagged with GFP and Apl1 with RFP. White arrowheads indicate examples of the two signals colocalizing at peripheral puncta. (B) Intensity profiles of lines drawn across representative puncta from 10 cells. Values shown are normalized to background fluorescence and expressed as a fraction of the peak intensity for each line. Error bars show SDs. (C) Representative images of Chs3-GFP fluorescence in *APM4* WT and *apm4*-deleted cells grown as yeast or 90-min hyphae. Scale bars, 5 $\mu$m.

The data described above suggest that the AP-2 complex is required for the endocytic internalization of Chs3 and that internalization followed by recycling serves to ensure polarized localization of this enzyme. This uptake also prevents the continued addition of chitin to other regions of cells that already have a sufficient cell wall. If this is the case and Chs3 is a physiologically important cargo of AP-2, then some defects observed in the *apm4*Δ/*apm4*Δ mutant might be rescued by reducing Chs3 activity at the cell surface. To test this, a single copy of *chs3* was deleted in the *apm4*Δ/*apm4*Δ cells, and a range of phenotypes was analyzed. Remarkably, in all cases, the combined *chs3*Δ deletion strain demonstrated significant rescue of *apm4*Δ/*apm4*Δ mutant phenotypes, strengthening the evidence for Chs3 as a key cargo of AP-2 (Fig. 8A to E). Heterozygous *chs3* deletion in otherwise wild-type cells did not have a significant effect on yeast or hyphal morphology, indicating that the changes observed in the combined *apm4*Δ/*apm4*Δ *chs3*Δ strain were caused by rescue of AP-2-related defects.

**Chs3 as a bona fide AP-2 cargo in *Candida albicans*.** In mammalian cells, the AP-2 mu subunit has been demonstrated to bind YXXΦ internalization motifs (with Φ representing hydrophobic amino acids) on endocytic cargo, and the key residues in this interaction have been described (41). Despite an absence on the AP-2 beta subunit of the clathrin binding appendage, the *Candida* mu subunit, Apm4, has sequences homologous to those in the mammalian mu2 subunit of AP-2 responsible for YXXΦ motif binding, suggesting that it could function in a similar way (see Fig. S4A). Furthermore, the major predicted cytoplasmic loop of Chs3 has five potential YXXΦ internalization motifs with a further motif in the C-terminal tail region (Fig. S4B). It also has at least one acidic dileucine motif that could potentially bind to the sigma subunit of a functional AP-2 complex, adding additional binding function, possibly to ensure effective uptake by the complex.

To investigate the importance of YXXΦ binding, two approaches were taken: one to mutagenize the YXXΦ binding sites in Apm4, the second to remove YXXΦ motifs

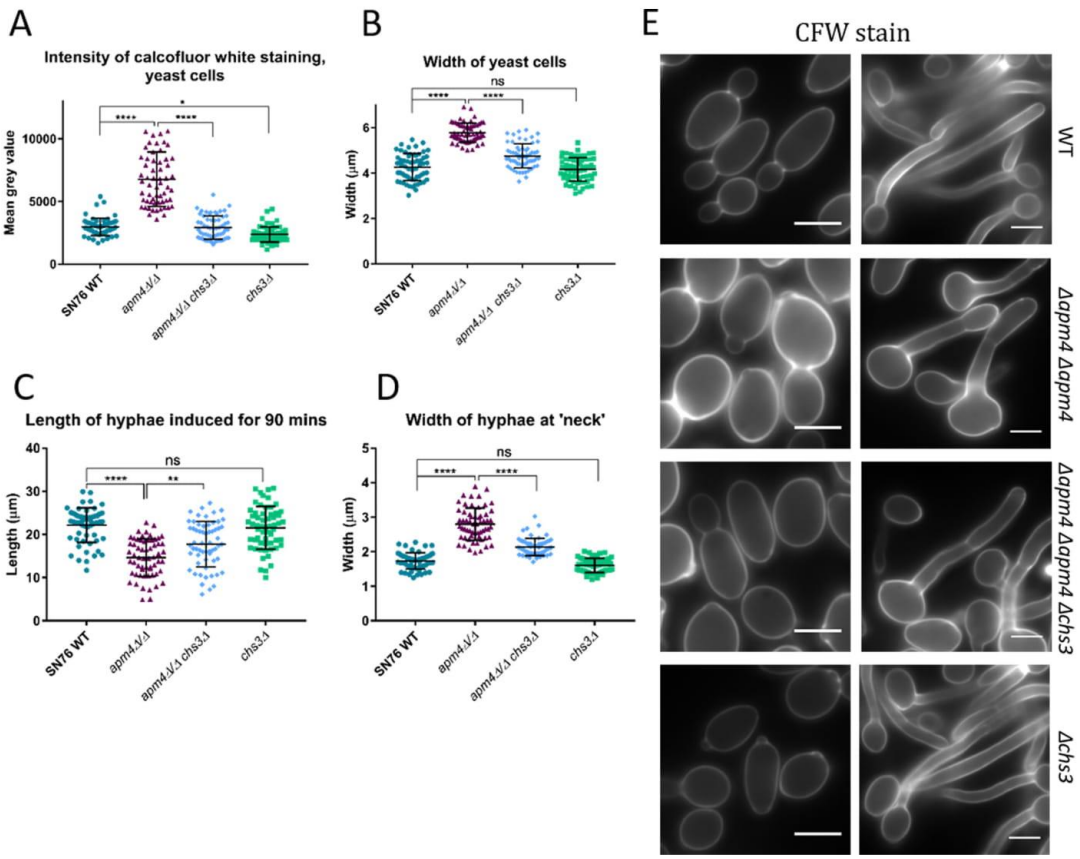


**FIG 8** Deletion of one copy of *chs3* rescues some of the *apm4* mutant phenotypes. (A) Quantification of fluorescence intensity of CFW-stained yeast cells; the mean gray value, minus background, was measured with FIJI for each cell. Widths of yeast cells (B) and lengths (C) and widths (D) of hyphae measured with FIJI after growth for 90 min ($n = 60$ cells per strain for panels A to D, from 2 independent experiments). (E) Representative images of yeast and hyphae stained with CFW. All statistics are from one-way ANOVAs with Tukey's *post hoc* tests. Error bars show SDs. Scale bars, 5 μm. ns, $P = 0.1234$; *, $P = 0.0332$; **, $P = 0.0021$; ****, $P < 0.0001$.

themselves from the Chs3 cargo. The *apm4* subunit of AP-2 was mutated in a strain already carrying a single *apm4* deletion to remove a conserved and predicted critical part of its YXXΦ binding site (Fig. S4A). This *apm4* mutation generated a protein truncated by 16 amino acids to give the strain Δ*apm4 apm4*$^{1-454}$. We hypothesized that this mutation should not compromise the formation of the AP-2 complex but that the resultant complex should not bind YXXΦ motifs. To verify AP-2 complex formation, Apl1-GFP was tagged in this strain and peripheral Apl1-GFP puncta were observed, showing that the AP-2 complex is still able to form with this truncation (Fig. S4C). This is an important distinction from *apm4*Δ/*apm4*Δ deletion, which prevents the formation of an AP-2 complex as judged by the visualization of Apl1-GFP puncta (Fig. S1 and 4C).

If Chs3 is a physiological cargo of AP-2 with binding mediated by the mu subunit via YXXΦ motifs, expression of the *apm4*$^{1-454}$ truncation would not be predicted to alleviate chitin-associated phenotypes of the *apm4*Δ/*apm4*Δ mutant. If, however, YXXΦ motif binding is not relevant in *Candida* or if the acidic-dileucine signal is able to function redundantly, endocytic uptake should be restored. Analysis of the *apm4* truncation strain was undertaken as previously described, though the control strain

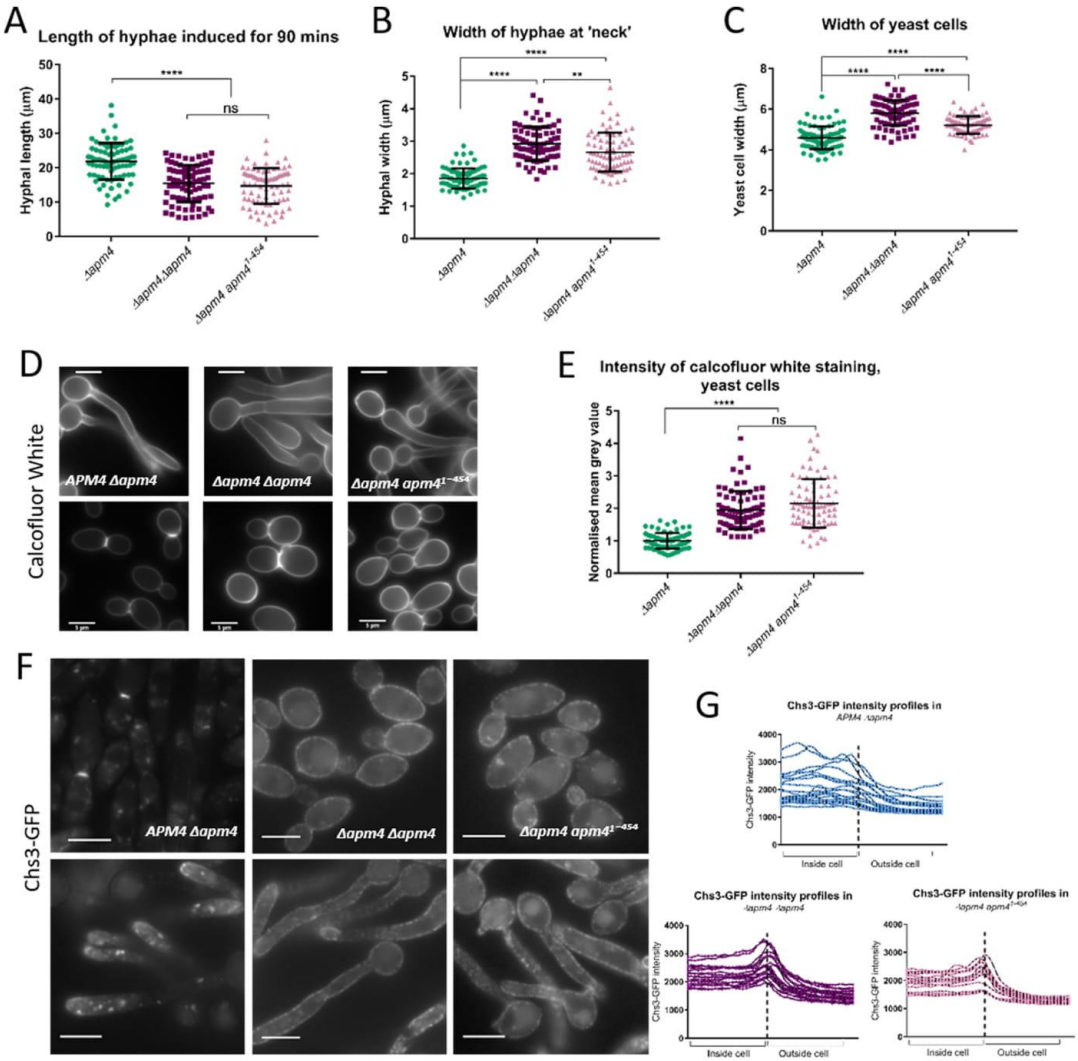


**FIG 9** Apm4 binds Chs3 through its YXXΦ binding domain and truncation of this domain leads to morphological defects. Quantification of hyphal lengths (A), hyphal widths (B), and yeast cell widths (C) in *apm4* cargo-binding mutant compared to those from heterozygous and homozygous *apm4* deletion strains. (D) Representative images of yeast and hyphae stained with CFW. (E) Quantification of CFW staining intensity in these strains (mean gray value minus background for each cell). (F) Chs3 tagged with GFP in each strain. (G) Signals quantified by line profiles drawn from insides to outsides of 20 cells/strain; (A to C and E) $n = 80$ cells/strain from 3 independent experiments. (E) Values are normalized to the mean Δ*apm4* measurement. Statistics are from one-way ANOVAs with Tukey's *post hoc* tests. Error bars show SDs. Scale bars, 5 $\mu$m. ns, $P = 0.1234$; **, $P = 0.0021$; ****, $P < 0.0001$.

used was the heterozygote *apm4* deletion, as the truncation mutant only carried a single copy of the *apm4* truncation. The data shown in Fig. 9A to C reveal that the *apm4* cargo-binding mutant has very similar morphological defects in terms of hyphal length and width and yeast cell size compared to those of the full deletion strain. Furthermore, calcofluor white staining was also significantly elevated compared to that in the control strain (Fig. 9D and E).

Next, Chs3 was tagged with GFP in the strain carrying the *apm4* truncation. As shown in Fig. 9F, the pattern of Chs3 localization was strikingly similar to that for the

full *apm4* deletion, suggesting that Chs3 internalization requires a direct interaction of the AP-2 mu subunit with its YXXΦ sequences. Chs3-GFP localization was quantified by line profiles in Fig. 9G; lines were drawn from the insides to the outsides of cells, centering on the cell periphery, where a peak of intensity was observed in the *apm4* deletion and truncation stains, which was absent in WT cells.

Interestingly, cells expressing the truncated *apm4* cargo-binding mutant showed an increase in the number of intracellular Chs3 puncta compared with that in strains carrying the full *apm4* deletion (quantified in Fig. S4D), suggesting this strain can internalize a small amount of Chs3, perhaps through weaker YXXΦ binding by the remaining elements of the motif binding residues that are not removed in the truncation or possibly through other motifs which the AP-2 sigma subunit may bind (42).

To address whether removal of YXXΦ motifs in the cargo caused a similar defect to that of the Δ*apm4 apm4*$^{1-454}$ strain, truncated versions of Chs3 were also made which carried different numbers of internalization motifs. These were also tagged with GFP (Fig. S5). The shortest mutant (*chs3*Δ*/chs3*$^{1-564}$*-GFP*) contained just one YXXΦ motif and the GFP signal was mostly vacuolar, suggesting the protein could not be folded and/or trafficked properly. Longer versions, containing greater numbers of YXXΦ motifs, showed increasing levels of GFP signal at the plasma membrane, suggesting the enzyme could be trafficked to the cell membrane. However, none of the truncated versions showed a polarized signal resembling full-length *CHS3-GFP*, indicating that none were able to undergo appropriate secretion or recycling.

**Mutant strains reveal distinctions in requirements for ergosterol and mannose polarization.** As described above (Fig. 4), complete *apm4* deletion resulted in defects in ergosterol and mannose polarization following hyphal induction. To determine whether these phenotypes were coupled to the change in chitin itself or if they separately required binding through YXXΦ motifs within proteins other than Chs3, the strains generated in the later parts of these studies were also analyzed for polarity of these two cell components. As shown in Fig. 10A to C, deletion of one copy of *chs3* did not rescue either the observed ergosterol or mannose polarization defects, indicating that elevated chitin synthesis is not the cause of these phenotypes. Interestingly, however, while the YXXΦ-binding mutant did not rescue the mannose polarization defect of the *apm4* deletion (Fig. 10C), it was able to fully rescue polarized filipin staining (Fig. 10A and B). Thus, AP-2 complex function, but not its YXXΦ binding, is required for ergosterol polarization.

## DISCUSSION

The AP-2 endocytic adaptor complex is very well studied in mammalian endocytosis; it enables the endocytic uptake of many important transmembrane cargoes (10, 43). *C. albicans* is known to require endocytosis for its highly polarized hyphal growth phase (44); however, more specific requirements of the process are not well defined. In this study, we show that AP-2 is crucial for the endocytic uptake and recycling of chitin synthase 3 (Chs3), a key cell wall biosynthesis enzyme, and that this recycling is required for correct cell wall composition and cell morphology. We demonstrate that many of the observed morphological defects are caused by elevated chitin synthesis, thus highlighting the role of the cell wall in shape determination and the critical role of endocytosis in its regulation. We also show that the recycling of Chs3 depends on binding of its YXXΦ internalization motif(s) by the AP-2 mu subunit (Apm4).

**AP-2 in fungal endocytosis.** While the endocytic adaptor protein AP-2 complex is clearly present in yeast and fungi, its role, especially with regard to endocytosis, has been unclear. GFP tagging of AP-2 subunits shows localization of the complex to plasma membrane puncta that also contain components of the endocytic machinery in *S. cerevisiae*, such as Sla1 or Abp1 (11, 12) or SlaB and AbpA in *Aspergillus nidulans* (13). While deletion of AP-2 mu or sigma subunits disrupts formation of the tetrameric complex as expected, this does not substantially impact endocytosis as assessed using fluid-phase markers. Instead, polarized growth defects appear to be one of the strongest phenotypes associated with AP-2 loss of function (12, 13). Our analysis of colo-

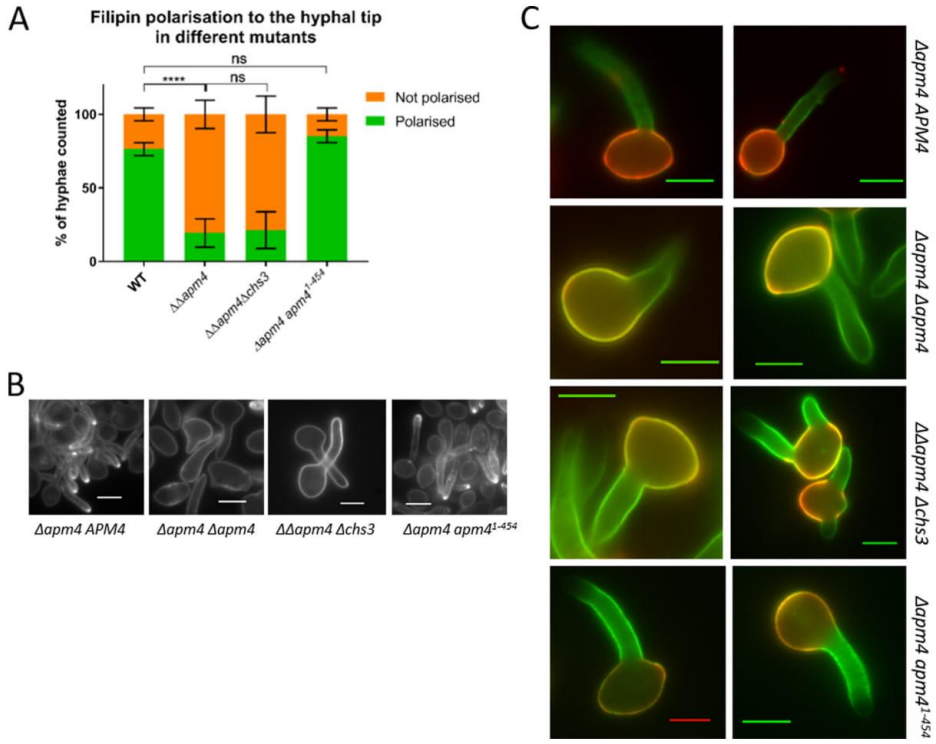


**FIG 10** Distinct requirements for ergosterol and mannose polarization. (A) Hyphae were induced for 60 min and then stained with filipin, which binds ergosterol; the percentages of cells which showed a bright ergosterol-rich domain at the hyphal tip were recorded for each strain ($n > 200$ cells/strain from 3 independent experiments). Statistics are from two-way ANOVAs with Tukey's *post hoc* tests. Error bars show SDs. (B) Representative images of filipin-stained hyphae from each strain. (C) Representative images in which stationary-phase yeast were stained with concanavalin-A-Alexa 594 and then induced to form hyphae for 90 min and stained with ConA-Alexa 488. Scale bars, 5 $\mu$m. ns, $P = 0.1234$; ****, $P < 0.0001$.

calization between the endocytic reporter Sla1 and AP-2 in *C. albicans* suggests they can and do colocalize, and when they are together, the proteins are recruited and disassemble with similar kinetics. However, approximately 50% of patches analyzed did not contain AP-2 at detectable levels. One possible reason for this is that AP-2 is only required for the uptake of a subset of cargoes, and if those cargoes are not present, AP-2 does not associate with other endocytic machinery. Our data would support the idea that fungal AP-2 does not function in the more general invagination process, as suggested also from analyses in *S. cerevisiae* and *A. nidulans* (11, 13, 16). In contrast, the endocytic protein Sla1, which is found in puncta both with and without AP-2 (Fig. 1), binds to a different cargo motif (NPFXD) as well as to actin regulators to support the actin-mediated invagination process. This might suggest that Sla1 plays a more constitutive role linking NPFXD cargoes to endocytic machinery during invagination, while the AP-2 function is possibly more regulated or selective. Martzoukou and colleagues (13) proposed that AP-2 has acquired a specialized clathrin-independent function for fungal polar growth, because while they could see colocalization with AbpA (*S. cerevisiae* Abp1 homologue) and SlaB (*S. cerevisiae* Sla2 homologue), they did not see colocalization with clathrin. They also observed that endocytosis of a number of transporters did not require AP-2. Distinct endocytic routes in *S. cerevisiae* have been reported, including one that involves actin and Abp1, though whether the different endocytic pathways identified are overlapping variants which use a common basic

machinery has not been fully investigated (45, 46). However, it is clear from a number of studies that clathrin function in fungal endocytosis overall is less important than in many mammalian cells. (15, 47, 48). Given the importance of AP-2 in maintaining polarity, one possibility is that cargoes destined to be recycled to the hyphal tip require the AP-2 endocytic adaptor coupled with the generic endocytic machinery, while cargoes destined for degradation, such as nutritional transporters, might use the same general machinery but also require clathrin and possibly distinct adaptors that facilitate trafficking toward vacuolar/lysosomal degradation.

**Chitin synthesis in cell morphology.** Chs3 is responsible for generating short rodlets of chitin that constitute a large proportion of the total chitin in *C. albicans* cells (37, 38, 49). The AP-2 mutants generated in this study have elevated levels of cell wall chitin, indicating that the Chs3 that reaches the plasma membrane is active. Lack of recycling of the enzyme to the tip also means that the synthesis of chitin is less focused. Mutant cell hyphae were shorter and wider than in the wild type, suggesting levels of short-chain chitin fibrils are critical in governing shape. Deletion of one copy of *chs3* in the *apm4*Δ*/apm4*Δ strain resulted in the rescue of phenotypes of hyphal length and width, as well as of chitin levels, judged by calcofluor staining. We propose that in the *apm4* mutant, the excess Chs3 at the membrane means that its partner proteins, such as Chs4 and Chs7, which facilitate its transport and activity, are effectively diluted out and chitin synthase activity is more spread over the cell surface. By reducing the overall pool of Chs3 (*apm4*$^{-/-}$, *chs3*$^{-}$/*CHS3*$^{+}$), there is an increased ratio of the cofactor proteins, which facilitates effective secretion and activity of newly secreted Chs3. This restored tip activity might then be sufficient to reestablish surface constraints that more effectively facilitate polarized growth. Interestingly, heterozygous *chs3* deletion in otherwise wild-type cells resulted in a modest decrease in calcofluor staining but no changes to cell morphology, suggesting that a slight decrease in cellular chitin does not have a major effect on cells: the dramatic changes seen in the combined mutant strain are specific to the rescue of the AP-2 mutant phenotypes. These data demonstrate the importance of short chitin fibrils in governing overall *Candida* cell morphology and the importance of cell wall regulation via AP-2 in maintaining the correct morphology.

In addition to the changes in chitin levels in the *apm4* mutant, changes in mannan secretion were also observed with more depolarized secretion, as well as changes in the length of mannan structures observable by electron microscopy. Despite the increased length of mannose fibrils in the mother cells of *apm4* mutant hypha, the sides of the hyphal tube in the mutant in fact had shorter fibrils than in wild-type cells (Fig. 5B). This depleted outer layer is likely to be the cause of the increased level of chitin exposure along the hyphal tube seen by WGA-fluorescein staining.

**YXXΦ motif binding in Chs3.** In this study, we were able to demonstrate for the first time that the AP-2 mu subunit residues critical for binding YXXΦ motifs are required in fungi for endocytic internalization. We identified at least 5 possible YXXΦ motifs in the cytoplasmic regions of Chs3; however, mutagenesis of YXXΦ motifs in cargoes themselves has not always demonstrated a very marked effect on their uptake (50). Furthermore, in other cell types, it is known that the same YXXΦ motifs can be recognized by other adaptors, such as AP-1, at different stages of trafficking, potentially making outcomes of this approach challenging to interpret (51). However, a number of Chs3 truncations were made removing different numbers of the motifs. As shown in Fig. S5 in the supplemental material, Chs3 truncations expressing between one and four YXXΦ motifs do not appear to be trafficked to the plasma membrane. Truncations with five or six of the seven motifs can reach the plasma membrane but do not show polarized localization. It is not clear whether this defect is due to aberrant exocytosis or endocytosis. Because of the expected weak binding of individual motifs, coupled with the likely perturbation of structure and the trafficking from disrupting the multiple YXXΦ motifs in Chs3 itself, we focused on generating an AP-2 complex that could form and localize but which should be reduced in its capacity to bind YXXΦ motifs. Truncation of the last 16 amino acids in Apm4 removed one of the conserved sites

which was reported to be responsible for YXXΦ binding (41). Strikingly, removal of this small region gave morphological defects almost as severe as in the full *apm4* deletion, showing the importance of YXXΦ-based endocytosis in *Candida*. This mutant was also strongly impaired in Chs3 uptake, though the presence of a low level of intracellular puncta suggests that some Chs3 internalization was still able to occur, perhaps via some residual YXXΦ binding or via acidic dileucine motif binding by the sigma subunit (Chs3 has at least one such motif). It is also interesting to note that the other chitin synthase proteins, Chs1, Chs2, and Chs8, are all predicted to have a similar multiple transmembrane domain structure, and all have several YXXΦ motifs in cytoplasmic loops. An important question going forward then is whether these motifs serve for continual uptake and transport of the various enzymes or whether there is specific regulation triggered by external signals that would facilitate the uptake of individual enzymes at appropriate times. A role for phosphorylation in directing AP-2 binding to certain cargoes has been found in mammalian cells, and there is evidence of phosphorylation of the Apm4 subunit both in *S. cerevisiae* and in *C. albicans*; however, a functional role of mu subunit modifications has yet to be demonstrated in fungi (52–54).

**Ergosterol and mannan polarization.** Intriguingly, while Chs3 uptake and polarized localization required AP-2 mu YXXΦ binding, the analysis of other plasma membrane and cell wall components led to the unexpected finding that YXXΦ binding is required for polarized secretion of mannan but not for polarity of filipin, which marks ergosterol localization. Given that mannan is added to proteins and lipids on transit through the Golgi and that, in the experiments using ConA to identify mannan localization, new material was found in the mother and on hyphae, this suggests that components of the secretory pathway (polarisome or exocyst) also require AP-2 to maintain polarized localization. The capacity of the mutants to initiate and grow hyphae at all does, however, mean that polarized growth is still possible, suggesting a partial mislocalization of these secretory components.

In this study, AP-2 was required for polarized filipin localization to the hyphal tip but not to the yeast bud, highlighting a distinction between mechanisms involved in these forms of polarity. Furthermore, ergosterol polarity required full AP-2 but apparently not YXXΦ binding, indicating a different binding region, potentially involving the sigma subunit known in mammalian cells to also bind separately to cargoes (with acidic and dileucine motifs [42, 55]). The trafficking of ergosterol to the plasma membrane is not fully understood but has been proposed to involve nonvesicular lipid transfer from the endoplasmic reticulum (ER) to the plasma membrane (56, 57). A recent study untethered yeast ER from the plasma membrane, and cells still perform bidirectional lipid exchange, suggesting that stable sites are not required for the transfer (58). Our data add to this and suggest that the polarized addition of ergosterol to the plasma membrane requires an AP-2-dependent endocytic step, possibly allowing the uptake and recycling of a key protein that facilitates the docking of the ER toward the tip region of hyphae.

Overall, this study highlights the importance of AP-2 in integrating the secretory and endocytic pathways required for polarity in fungal hyphal growth. It supports the idea of a distinct endocytic route for polarity maintenance and demonstrates the presence of key interactions to facilitate selection of appropriate cargoes. The work also opens avenues for future studies to elucidate regulatory pathways governing endocytic recycling versus degradation and potentially to determine the importance of specific cell wall changes in host-pathogen interactions.

## MATERIALS AND METHODS

***C. albicans* strains.** *C. albicans* strains used in this study are listed in Table 1. Background strains are SN76 or SN148, and gene tagging or deletion was performed on these strains as described previously (59). Briefly, PCR was used to generate cassettes containing auxotrophic markers, which were transformed using lithium acetate to allow uptake for homologous recombination. Selective medium followed by colony PCR and/or sequencing was used to confirm correct integration.

**TABLE 1** Yeast strains used in this study

| Strain name | Genotype | Reference or source |
|---|---|---|
| SN76 | *ura3Δ::imm$^{434}$/ura3Δ::imm$^{434}$ iro1Δ::imm$^{434}$/iro1Δ::imm$^{434}$ his1Δ/his1Δ arg4Δ/arg4Δ* | 63 |
| SN148 | *ura3Δ::imm$^{434}$/ura3Δ::imm$^{434}$ iro1Δ::imm$^{434}$/iro1Δ::imm$^{434}$ his1Δ/his1Δ arg4Δ/arg4Δ leu2Δ/leu2Δ* | 63 |
| KAF33 | SN76 *APM4/apm4Δ::HIS1* | This study |
| KAF37 | SN76 *apm4Δ::HIS1/apm4Δ::ARG4* | This study |
| KAF44 | SN148 *SLA1/SLA1-GFP::LEU2* | This study |
| KAF45 | SN148 *CHS3/CHS3-GFP::LEU2* | This study |
| KAF47 | SN148 *APL1/APL1-GFP::LEU2* | This study |
| KAF49 | SN148 *CHS3/CHS3-GFP::LEU2 apm4Δ*::HIS1/*apm4Δ*::ARG4 | This study |
| KAF50 | SN148 *APL1/APL1-GFP::LEU2 apm4Δ::HIS1/apm4Δ::ARG4* | This study |
| KAF51 | SN148 *SLA1/SLA1-GFP::LEU2 APL1/APL1-RFP::ARG4* | This study |
| KAF52 | SN76 *apm4Δ::HIS1/apm4Δ::ARG4 CHS3/chs3Δ::SAT1* | This study |
| KAF55 | SN148 *APL1/APL1-GFP::LEU2 apm4Δ::ARG4/apm4$^{1–454}$::HIS1* | This study |
| KAF56 | SN76 *apm4Δ::ARG4/apm4$^{1–454}$::HIS1* | This study |
| KAF57 | SN148 CHS3/*CHS3-GFP::LEU2 apm4Δ::ARG4/apm4$^{1–454}$::HIS1* | This study |
| KAF80 | SN148 *CHS3/CHS3-GFP::LEU2 APL1/APL1-RFP::ARG4* | This study |
| KAF81 | SN148 *chs3Δ::HIS1/chs3$^{1–564}$-GFP::LEU2* | This study |
| KAF82 | SN148 *chs3Δ::HIS1/chs3$^{1–752}$-GFP::LEU2* | This study |
| KAF83 | SN148 *chs3Δ::HIS1/chs3$^{1–820}$-GFP::LEU2* | This study |
| KAF86 | SN148 *chs3Δ::HIS1/CHS3-GFP::LEU2* | This study |
| KAF87 | SN76 *CHS3/chs3Δ::HIS1* | This study |
| KAF90 | SN148 *chs3Δ::HIS1/chs3$^{1–850}$-GFP::LEU2* | This study |

***C. albicans* culture.** *C. albicans* cells were cultured by shaking at 30°C in liquid YPD (1% yeast extract, 2% peptone, 2% glucose plus 40 $\mu$g/ml adenine and 80 $\mu$g/ml uridine unless otherwise stated). Stationary-phase cells were refreshed to an optical density at 600 nm ($OD_{600}$) of 0.2 and grown with shaking at 30°C for yeast cells or at 37°C with 10% fetal bovine serum (FBS) for hyphal induction. Yeast were typically grown for 4 h and hyphae induced for 90 min, unless otherwise stated. For plate spotting assays, 10-fold serial dilutions of each strain were spotted onto YPD agar plates containing either 150 $\mu$g/ml Congo red, 80 $\mu$g/ml calcofluor white, 10 mM caffeine, 0.01% SDS, or 2% lactate (on lactate plates, glucose was omitted). Plates were incubated at 30°C or 37°C.

**Biofilm assays.** For biofilm assays, $1 \times 10^5$ *C. albicans* cells in YPD plus 10% FBS were added per well to 96-well plastic plates. Plates were incubated at 37°C for 48 h, and the $OD_{600}$ was measured to record cell growth. Then, the wells were washed 3 times with phosphate-buffered saline (PBS) to remove nonadhered cells and examined by microscopy. Twenty microliters 2,3-bis-(2-methoxy-4-nitro-5-sulfophenyl)-2H-tetrazolium-5-carboxanilide salt (XTT) reagent (Merck) was added per well and incubated for 2 h at 37°C, the supernatant from each well was removed and its absorbance at 450 nm was measured as an assay of metabolic activity. The background absorbance at 690 nm was subtracted from values.

**Fluorescence microscopy and image analysis.** Images were acquired on either (a) an IX-81 inverted microscope (Olympus) with a Retiga R3 charge-coupled-device (CCD) camera (QImaging) and Micromanager software or (b) a Nikon Ti inverted microscope with TIRF3 on which oblique illumination was used, with an iXon Du-897 EM-CCD camera (Andor) and NIS-elements software. All images were analyzed using FIJI and exported as TIFF files. For endocytic patch timing, actively growing cells were washed briefly in PBS, and then time-lapse movies were taken on the Nikon Ti microscope typically at 1 frame/s for 5 or 10 min. For rhodamine-phalloidin staining, cells were fixed in 3.7% formaldehyde and then incubated with 5% (vol/vol) rhodamine-phalloidin for 30 min at room temperature. They were then washed in PBS and imaged. Filipin complex was used at 27 $\mu$g/ml from a 10-mg/ml stock made fresh each experiment in dimethyl sulfoxide (DMSO). Cells were fixed in 3.7% formaldehyde prior to staining. Calcofluor white was used at 2 $\mu$g/ml and incubated with live cells for 5 min. Concanavalin-A-Alexa used at 25 to 50 $\mu$g/ml and incubated with live cells for 10 min. Wheat germ agglutinin-fluorescein was used at 100 $\mu$g/ml and incubated with live cells for 30 min. All were then washed in PBS and imaged.

**Electron microscopy.** High-pressure freezing (HPF) and freeze substitution sample preparation were performed at the Microscopy and Histology Facility at the University of Aberdeen, as described previously (60). Briefly, cells were washed 3 times in water, and then HPF was performed in a Leica EM PACT 2 (Leica Microsystems, Milton Keynes, UK). Freeze substitution was performed in a Leica AFS 2 in acetone-1% $OsO_4$. Samples were transferred to epoxy resin, and ultrathin sections were cut, stained with uranyl acetate and lead citrate, and imaged with an FEI Tecnai T12 Spirit TEM with Gatan camera. Cell walls were measured via FIJI with 5 measurements averaged per cell ($n > 20$ cells per condition).

**Lucifer yellow uptake assay.** Fluid-phase endocytosis assays were performed on log-phase yeast cells as described previously (61). Briefly, log-phase yeast cells were incubated with Lucifer yellow dye at 4 mg/ml for 1 h with rotation. They were then extensively washed, the cell pellets lysed with lyticase (2,000 U/ml), and fluorescence was measured at 426 nm excitation/550 nm emission. This value was normalized to the total protein concentration of each sample, as determined by Bradford assay.

**HPLC analysis of cell walls.** HPLC analysis of cell walls was performed at the Aberdeen Fungal Group, as described in reference 62. Briefly, cells were disrupted with glass beads using a FastPrep machine (Qbiogene) and washed extensively in 1 M NaCl, and then proteins were removed by boiling for

10 min in 2% SDS, 0.3 M β-mercaptoethanol, 1 mM EDTA. Pellets were freeze-dried and then acid-hydrolyzed in 2 M trifluoroacetic acid for 3 h at 100°C. The acid was evaporated at 65°C, and the samples were resuspended in deionized water. Hydrolyzed samples were analyzed via high-performance anion-exchange chromatography with pulsed amperometric detection (HPAEC-PAD) in a carbohydrate analyzer system (CarboPac PA10 guard and analytical columns) from Thermo Scientific. The concentration of each cell wall component are stated in micrograms per milligram dry cell wall, as calibrated by standard curves of monomeric sugars, and are expressed as a percentage of total wall material.

**Statistical analysis.** Statistical tests unless otherwise stated were one-way analyses of variance (ANOVAs) with Tukey's *post hoc* tests for multiple comparisons performed using GraphPad Prism. Confidence intervals were set to 95%.

## SUPPLEMENTAL MATERIAL

Supplemental material for this article may be found at https://doi.org/10.1128/mBio.02421-18.

**FIG S1**, TIF file, 0.4 MB.
**FIG S2**, TIF file, 0.6 MB.
**FIG S3**, TIF file, 0.8 MB.
**FIG S4**, TIF file, 1.9 MB.
**FIG S5**, TIF file, 1.2 MB.

## ACKNOWLEDGMENTS

We thank Andrew Peden, Simon Johnston, and Josh Parker for critical reading of the manuscript. We also thank Gillian Milne at the Microscopy and Histology Core Facility at the University of Aberdeen for expert assistance with TEM and Craig Murdoch at the School of Clinical Dentistry, University of Sheffield, for training and support in carrying out the biofilm assays.

Imaging was undertaken in part at the Wolfson Light Microscopy Facility at the University of Sheffield, supported by grant number MR/K015753/1. H.C.K. is funded by the BBSRC White Rose DTP to the Universities of Sheffield, Leeds and York (BB/M011151/1); I.I.S.-D.R. is funded by BBSRC grant BB/N007581/1. N.A.R.G. was supported by The Wellcome Trust (101873, 200208, 097377), and L.A.W. and K.K.L. were supported by the MRC Centre for Medical Mycology (MR/N006364/1).

## REFERENCES

1. Sudbery P, Gow N, Berman J. 2004. The distinct morphogenic states of *Candida albicans*. Trends Microbiol 12:317–324. https://doi.org/10.1016/j.tim.2004.05.008.
2. Borth N, Walther A, Reijnst P, Jorde S, Schaub Y, Wendland J. 2010. *Candida albicans* Vrp1 is required for polarized morphogenesis and interacts with Wal1 and Myo5. Microbiology 156:2962–2969. https://doi.org/10.1099/mic.0.041707-0.
3. Douglas LM, Martin SW, Konopka JB. 2009. BAR domain proteins Rvs161 and Rvs167 contribute to *Candida albicans* endocytosis, morphogenesis, and virulence. Infect Immun 77:4150–4160. https://doi.org/10.1128/IAI.00683-09.
4. Epp E, Nazarova E, Regan H, Douglas LM, Konopka JB, Vogel J, Whiteway M. 2013. Clathrin- and Arp2/3-independent endocytosis in the fungal pathogen *Candida albicans*. mBio 4:e00476-13. https://doi.org/10.1128/mBio.00476-13.
5. Oberholzer U, Marcil A, Leberer E, Thomas DY, Whiteway M. 2002. Myosin I is required for hypha formation in *Candida albicans*. Eukaryot Cell 1:213–228. https://doi.org/10.1128/EC.1.2.213-228.2002.
6. Walther A, Wendland J. 2004. Polarized hyphal growth in *Candida albicans* requires the Wiskott-Aldrich syndrome protein homolog Wal1p. Eukaryot Cell 3:471–482. https://doi.org/10.1128/EC.3.2.471-482.2004.
7. Robinson MS. 1987. 100-kD coated vesicle proteins: molecular heterogeneity and intracellular distribution studied with monoclonal antibodies. J Cell Biol 104:887–895. https://doi.org/10.1083/jcb.104.4.887.
8. Gaidarov I, Chen Q, Falck JR, Reddy KK, Keen JH. 1996. A functional phosphatidylinositol 3,4,5-trisphosphate/phosphoinositide binding domain in the clathrin adaptor AP-2 alpha subunit. Implications for the endocytic pathway. J Biol Chem 271:20922–20929. https://doi.org/10.1074/jbc.271.34.20922.
9. Ohno H, Stewart J, Fournier MC, Bosshart H, Rhee I, Miyatake S, Saito T, Gallusser A, Kirchhausen T, Bonifacino JS. 1995. Interaction of tyrosine-based sorting signals with clathrin-associated proteins. Science 269:1872–1875. https://doi.org/10.1126/science.7569928.
10. Collins BM, McCoy AJ, Kent HM, Evans PR, Owen DJ. 2002. Molecular architecture and functional model of the endocytic AP2 complex. Cell 109:523–535. https://doi.org/10.1016/S0092-8674(02)00735-3.
11. Carroll SY, Stirling PC, Stimpson HE, Giesselmann E, Schmitt MJ, Drubin DG. 2009. A yeast killer toxin screen provides insights into a/b toxin entry, trafficking, and killing mechanisms. Dev Cell 17:552–560. https://doi.org/10.1016/j.devcel.2009.08.006.
12. Chapa-y-Lazo B, Allwood EG, Smaczynska-de Rooij II, Snape ML, Ayscough KR. 2014. Yeast endocytic adaptor AP-2 binds the stress sensor Mid2 and functions in polarized cell responses. Traffic 15:546–557. https://doi.org/10.1111/tra.12155.
13. Martzoukou O, Amillis S, Zervakou A, Christoforidis S, Diallinas G. 2017. The AP-2 complex has a specialized clathrin-independent role in apical endocytosis and polar growth in fungi. Elife 6:e20083. https://doi.org/10.7554/eLife.20083.
14. Newpher TM, Smith RP, Lemmon V, Lemmon SK. 2005. *In vivo* dynamics of clathrin and its adaptor-dependent recruitment to the actin-based endocytic machinery in yeast. Dev Cell 9:87–98. https://doi.org/10.1016/j.devcel.2005.04.014.
15. Kaksonen M, Toret CP, Drubin DG. 2005. A modular design for the clathrin- and actin-mediated endocytosis machinery. Cell 123:305–320. https://doi.org/10.1016/j.cell.2005.09.024.
16. Yeung BG, Phan HL, Payne GS. 1999. Adaptor complex-independent clathrin function in yeast. Mol Biol Cell 10:3643–3659. https://doi.org/10.1091/mbc.10.11.3643.
17. Huang KM, D'Hondt K, Riezman H, Lemmon SK. 1999. Clathrin functions in the absence of heterotetrameric adaptors and AP180-related proteins in yeast. EMBO J 18:3897–3908. https://doi.org/10.1093/emboj/18.14.3897.

18. Finkel JS, Mitchell AP. 2011. Genetic control of *Candida albicans* biofilm development. Nat Rev Microbiol 9:109–118. https://doi.org/10.1038/nrmicro2475.
19. Capek A, Simek A, Bruna L, Svab A, Budesinsky Z. 1974. Antimicrobial agents. XX. Ergosterol Content of *Candida albicans* cells during adaptation to antimycotics Folia Microbiol (Praha) 19:79–80. https://doi.org/10.1007/BF02874507.
20. Martin SW, Konopka JB. 2004. Lipid raft polarization contributes to hyphal growth in *Candida albicans*. Eukaryot Cell 3:675–684. https://doi.org/10.1128/EC.3.3.675-684.2004.
21. Kleinschmidt MG, Chough KS. 1972. Effect of filipin on liposomes prepared with different types of steroids. Plant Physiol 49:852–856. https://doi.org/10.1104/pp.49.5.852.
22. Norman AW, Demel RA, de Kruyff B, van Deenen LL. 1972. Studies on the biological properties of polyene antibiotics. Evidence for the direct interaction of filipin with cholesterol. J Biol Chem 247:1918–1929.
23. Derewenda Z, Yariv J, Helliwell JR, Kalb AJ, Dodson EJ, Papiz MZ, Wan T, Campbell J. 1989. The structure of the saccharide-binding site of concanavalin A. EMBO J 8:2189–2193. https://doi.org/10.1002/j.1460-2075.1989.tb08341.x.
24. Stanley P. 2011. Golgi glycosylation. Cold Spring Harb Perspect Biol 3:a005199. https://doi.org/10.1101/cshperspect.a005199.
25. Wang P, Wang H, Gai J, Tian X, Zhang X, Lv Y, Jian Y. 2017. Evolution of protein N-glycosylation process in Golgi apparatus which shapes diversity of protein N-glycan structures in plants, animals and fungi. Sci Rep 7:40301. https://doi.org/10.1038/srep40301.
26. Cabib E, Bowers B, Sburlati A, Silverman SJ. 1988. Fungal cell wall synthesis: the construction of a biological structure. Microbiol Sci 5:370–375.
27. Lesage G, Bussey H. 2006. Cell wall assembly in *Saccharomyces cerevisiae*. Microbiol Mol Biol Rev 70:317–343. https://doi.org/10.1128/MMBR.00038-05.
28. Klis FM, de Groot P, Hellingwerf K. 2001. Molecular organization of the cell wall of *Candida albicans*. Med Mycol 39 Suppl 1:1–8.
29. Gow NA, Hube B. 2012. Importance of the *Candida albicans* cell wall during commensalism and infection. Curr Opin Microbiol 15:406–412. https://doi.org/10.1016/j.mib.2012.04.005.
30. Marakalala MJ, Vautier S, Potrykus J, Walker LA, Shepardson KM, Hopke A, Mora-Montes HM, Kerrigan A, Netea MG, Murray GI, Maccallum DM, Wheeler R, Munro CA, Gow NA, Cramer RA, Brown AJ, Brown GD. 2013. Differential adaptation of *Candida albicans in vivo* modulates immune recognition by dectin-1. PLoS Pathog 9:e1003315. https://doi.org/10.1371/journal.ppat.1003315.
31. Roncero C, Duran A. 1985. Effect of calcofluor white and Congo red on fungal cell wall morphogenesis: *in vivo* activation of chitin polymerization. J Bacteriol 163:1180–1185.
32. Kopecká M, Gabriel M. 1992. The influence of Congo red on the cell wall and (1→3)-beta-D-glucan microfibril biogenesis in *Saccharomyces cerevisiae*. Arch Microbiol 158:115–126. https://doi.org/10.1007/BF00245214.
33. Ram AF, Klis FM. 2006. Identification of fungal cell wall mutants using susceptibility assays based on calcofluor white and Congo red. Nat Protoc 1:2253–2256. https://doi.org/10.1038/nprot.2006.397.
34. Ene IV, Cheng SC, Netea MG, Brown AJ. 2013. Growth of *Candida albicans* cells on the physiologically relevant carbon source lactate affects their recognition and phagocytosis by immune cells. Infect Immun 81:238–248. https://doi.org/10.1128/IAI.01092-12.
35. Nagata Y, Burger MM. 1974. Wheat germ agglutinin. Molecular characteristics and specificity for sugar binding. J Biol Chem 249:3116–3122.
36. Cabib E, Bowers B. 1975. Timing and function of chitin synthesis in yeast. J Bacteriol 124:1586–1593.
37. Bulawa CE, Miller DW, Henry LK, Becker JM. 1995. Attenuated virulence of chitin-deficient mutants of *Candida albicans*. Proc Natl Acad Sci U S A 92:10570–10574. https://doi.org/10.1073/pnas.92.23.10570.
38. Mio T, Yabe T, Sudoh M, Satoh Y, Nakajima T, Arisawa M, Yamada-Okabe H. 1996. Role of three chitin synthase genes in the growth of *Candida albicans*. J Bacteriol 178:2416–2419. https://doi.org/10.1128/jb.178.8.2416-2419.1996.
39. Ziman M, Chuang JS, Schekman RW. 1996. Chs1p and Chs3p, two proteins involved in chitin synthesis, populate a compartment of the *Saccharomyces cerevisiae* endocytic pathway. Mol Biol Cell 7:1909–1919. https://doi.org/10.1091/mbc.7.12.1909.
40. Chuang JS, Schekman RW. 1996. Differential trafficking and timed localization of two chitin synthase proteins, Chs2p and Chs3p. J Cell Biol 135:597–610. https://doi.org/10.1083/jcb.135.3.597.
41. Owen DJ, Evans PR. 1998. A structural explanation for the recognition of tyrosine-based endocytotic signals. Science 282:1327–1332. https://doi.org/10.1126/science.282.5392.1327.
42. Kelly BT, McCoy AJ, Spate K, Miller SE, Evans PR, Honing S, Owen DJ. 2008. A structural explanation for the binding of endocytic dileucine motifs by the AP2 complex. Nature 456:976–979. https://doi.org/10.1038/nature07422.
43. Kirchhausen T. 1999. Adaptors for clathrin-mediated traffic. Annu Rev Cell Dev Biol 15:705–732. https://doi.org/10.1146/annurev.cellbio.15.1.705.
44. Sudbery PE. 2011. Growth of *Candida albicans* hyphae. Nat Rev Microbiol 9:737–748. https://doi.org/10.1038/nrmicro2636.
45. Aghamohammadzadeh S, Smaczynska-de Rooij II, Ayscough KR. 2014. An Abp1-dependent route of endocytosis functions when the classical endocytic pathway in yeast is inhibited. PLoS One 9:e103311. https://doi.org/10.1371/journal.pone.0103311.
46. Prosser DC, Drivas TG, Maldonado-Báez L, Wendland B. 2011. Existence of a novel clathrin-independent endocytic pathway in yeast that depends on Rho1 and formin. J Cell Biol 195:657–671. https://doi.org/10.1083/jcb.201104045.
47. Payne GS, Baker D, van TE, Schekman R. 1988. Protein transport to the vacuole and receptor-mediated endocytosis by clathrin heavy chain-deficient yeast. J Cell Biol 106:1453–1461. https://doi.org/10.1083/jcb.106.5.1453.
48. Sirotkin V, Berro J, Macmillan K, Zhao L, Pollard TD. 2010. Quantitative analysis of the mechanism of endocytic actin patch assembly and disassembly in fission yeast. Mol Biol Cell 21:2894–2904. https://doi.org/10.1091/mbc.E10-02-0157.
49. Lenardon MD, Whitton RK, Munro CA, Marshall D, Gow NA. 2007. Individual chitin synthase enzymes synthesize microfibrils of differing structure at specific locations in the *Candida albicans* cell wall. Mol Microbiol 66:1164–1173. https://doi.org/10.1111/j.1365-2958.2007.05990.x.
50. Ohno H, Fournier MC, Poy G, Bonifacino JS. 1996. Structural determinants of interaction of tyrosine-based sorting signals with the adaptor medium chains. J Biol Chem 271:29009–29015. https://doi.org/10.1074/jbc.271.46.29009.
51. Park SY, Guo X. 2014. Adaptor protein complexes and intracellular transport. Biosci Rep 34:e00123. https://doi.org/10.1042/BSR20140069.
52. Olusanya O, Andrews PD, Swedlow JR, Smythe E. 2001. Phosphorylation of threonine 156 of the mu2 subunit of the AP2 complex is essential for endocytosis *in vitro* and *in vivo*. Curr Biol 11:896–900. https://doi.org/10.1016/S0960-9822(01)00240-8.
53. Ricotta D, Conner SD, Schmid SL, von Figura K, Honing S. 2002. Phosphorylation of the AP2 mu subunit by AAK1 mediates high affinity binding to membrane protein sorting signals. J Cell Biol 156:791–795. https://doi.org/10.1083/jcb.200111068.
54. Chapa-y-Lazo B, Ayscough KR. 2014. Apm4, the mu subunit of yeast AP-2 interacts with Pkc1, and mutation of the Pkc1 consensus phosphorylation site Thr176 inhibits AP-2 recruitment to endocytic sites. Commun Integr Biol 7:e28522. https://doi.org/10.4161/cib.28522.
55. Letourneur F, Klausner RD. 1992. A novel di-leucine motif and a tyrosine-based motif independently mediate lysosomal targeting and endocytosis of CD3 chains. Cell 69:1143–1157. https://doi.org/10.1016/0092-8674(92)90636-Q.
56. Baumann NA, Sullivan DP, Ohvo-Rekila H, Simonot C, Pottekat A, Klaassen Z, Beh CT, Menon AK. 2005. Transport of newly synthesized sterol to the sterol-enriched plasma membrane occurs via nonvesicular equilibration. Biochemistry 44:5816–5826. https://doi.org/10.1021/bi048296z.
57. Schnabl M, Daum G, Pichler H. 2005. Multiple lipid transport pathways to the plasma membrane in yeast. Biochim Biophys Acta 1687:130–140. https://doi.org/10.1016/j.bbalip.2004.11.016.
58. Quon E, Sere YY, Chauhan N, Johansen J, Sullivan DP, Dittman JS, Rice WJ, Chan RB, Di Paolo G, Beh CT, Menon AK. 2018. Endoplasmic reticulum-plasma membrane contact sites integrate sterol and phospholipid regulation. PLoS Biol 16:e2003864. https://doi.org/10.1371/journal.pbio.2003864.
59. Longtine MS, McKenzie A, 3rd, Demarini DJ, Shah NG, Wach A, Brachat A, Philippsen P, Pringle JR. 1998. Additional modules for versatile and economical PCR-based gene deletion and modification in *Saccharomyces cerevisiae*. Yeast 14:953–961. https://doi.org/10.1002/(SICI)1097-0061(199807)14:10<953::AID-YEA293>3.0.CO;2-U.
60. Netea MG, Gow NA, Munro CA, Bates S, Collins C, Ferwerda G, Hobson RP, Bertram G, Hughes HB, Jansen T, Jacobs L, Buurman ET, Gijzen K, Williams DL, Torensma R, McKinnon A, MacCallum DM, Odds FC, Van der Meer JW, Brown AJ, Kullberg BJ. 2006. Immune sensing of *Candida*

*albicans* requires cooperative recognition of mannans and glucans by lectin and Toll-like receptors. J Clin Invest 116:1642–1650. https://doi.org/10.1172/JCI27114.

61. Bar-Yosef H, Vivanco Gonzalez N, Ben-Aroya S, Kron SJ, Kornitzer D. 2017. Chemical inhibitors of *Candida albicans* hyphal morphogenesis target endocytosis. Sci Rep 7:5692. https://doi.org/10.1038/s41598-017-05741-y.
62. Plaine A, Walker L, Da Costa G, Mora-Montes HM, McKinnon A, Gow NA, Gaillardin C, Munro CA, Richard ML. 2008. Functional analysis of *Candida albicans* GPI-anchored proteins: roles in cell wall integrity and caspofungin sensitivity. Fungal Genet Biol 45:1404–1414. https://doi.org/10.1016/j.fgb.2008.08.003.
63. Noble SM, Johnson AD. 2005. Strains and strategies for large-scale gene deletion studies of the diploid human fungal pathogen *Candida albicans*. Eukaryot Cell 4:298–309. https://doi.org/10.1128/EC.4.2.298-309.2005.

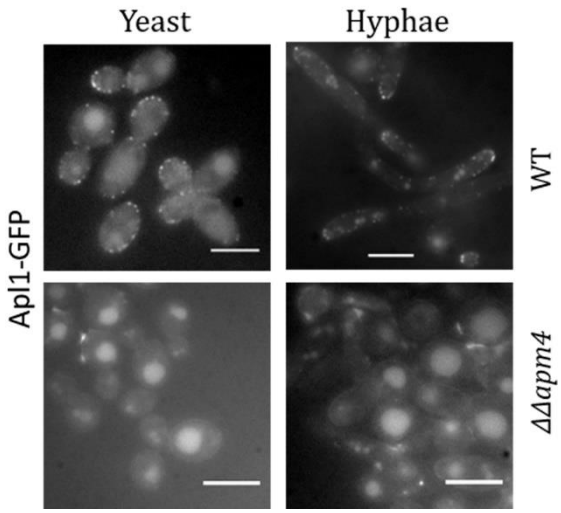


FIG S1

***apm4* deletion disrupts AP-2 complex formation.** Apl1-GFP signal shows peripheral puncta in otherwise WT cells, whereas in *apm4*-deleted cells, there were no puncta and the signal was vacuolar, showing that when *apm4* is deleted, the AP-2 complex cannot form. Scale bars, 5 µm. Download FIG S1, TIF file, 0.4 MB.

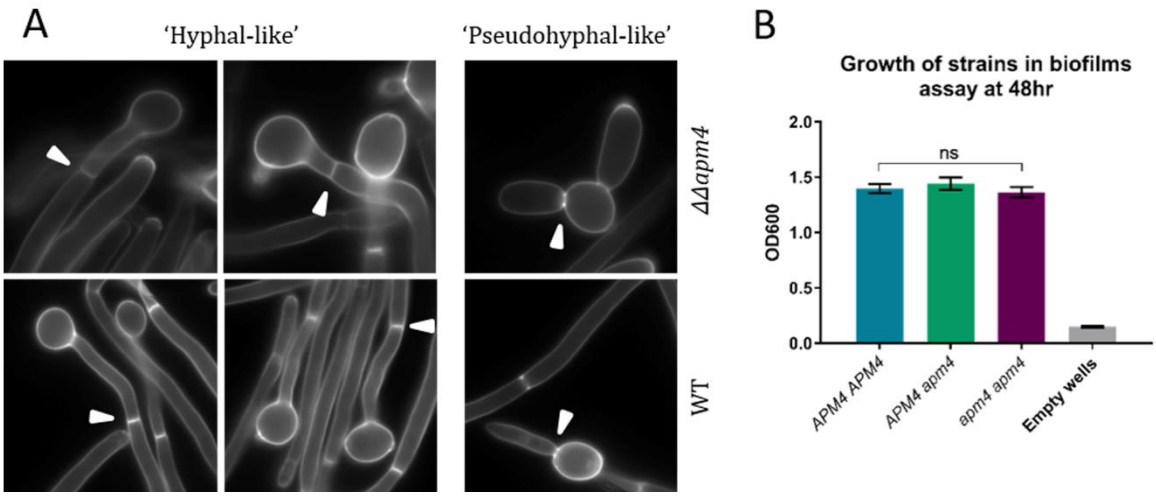


FIG S2

**Septal positioning and biofilm assay control.** (A) Representative images showing calcofluor white-stained hyphal cells with septa either at the neck (right) or further down the hypha (left). (B) Growth of strains in biofilm assay prior to washing. Cells were grown in 96-well plates; the OD measurements here indicate that all strains grew to the same densities. Therefore, the differences seen in **Fig. 3D** (metabolic activity of cells after washing wells) were due to differences in biofilm formation rather than simply growth. Statistics are from one-way ANOVA with Tukey's multiple comparisons. Error bars show SDs. Download FIG S2, TIF file, 0.6 MB.

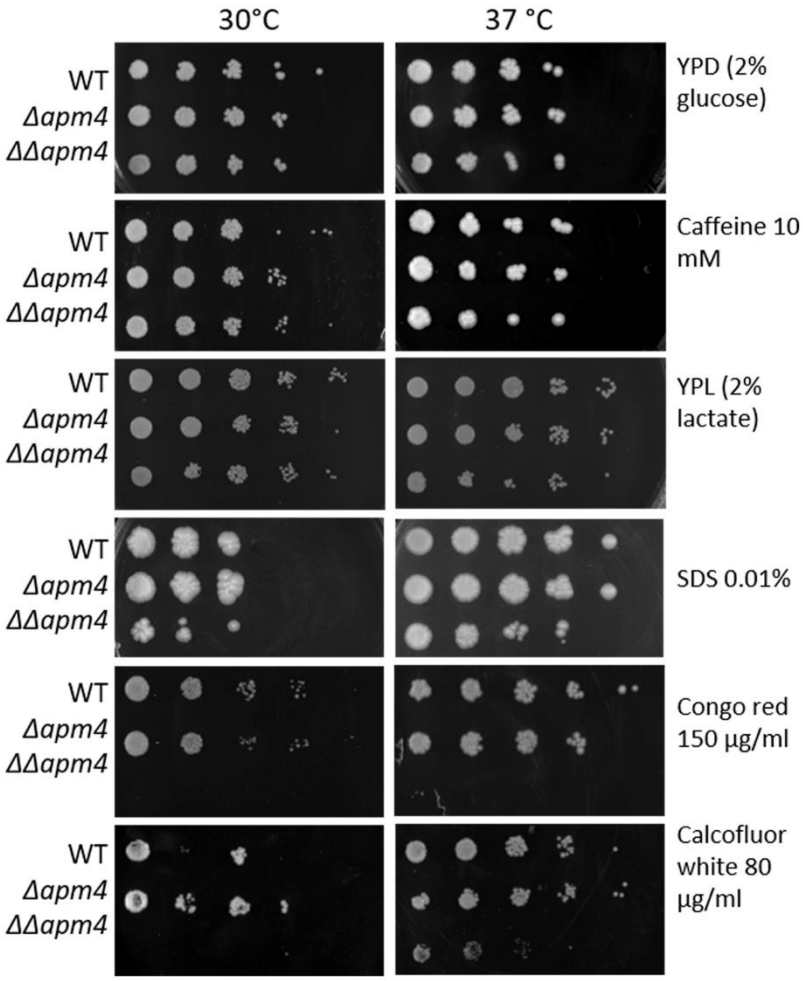


FIG S3

**Plate spotting assays.** Serial dilutions of cells were spotted onto YPD agar plates supplemented with various chemicals. They were incubated at 30°C or 37°C and then photographed to assess growth. Representative images are shown. Download FIG S3, TIF file, 0.8 MB.

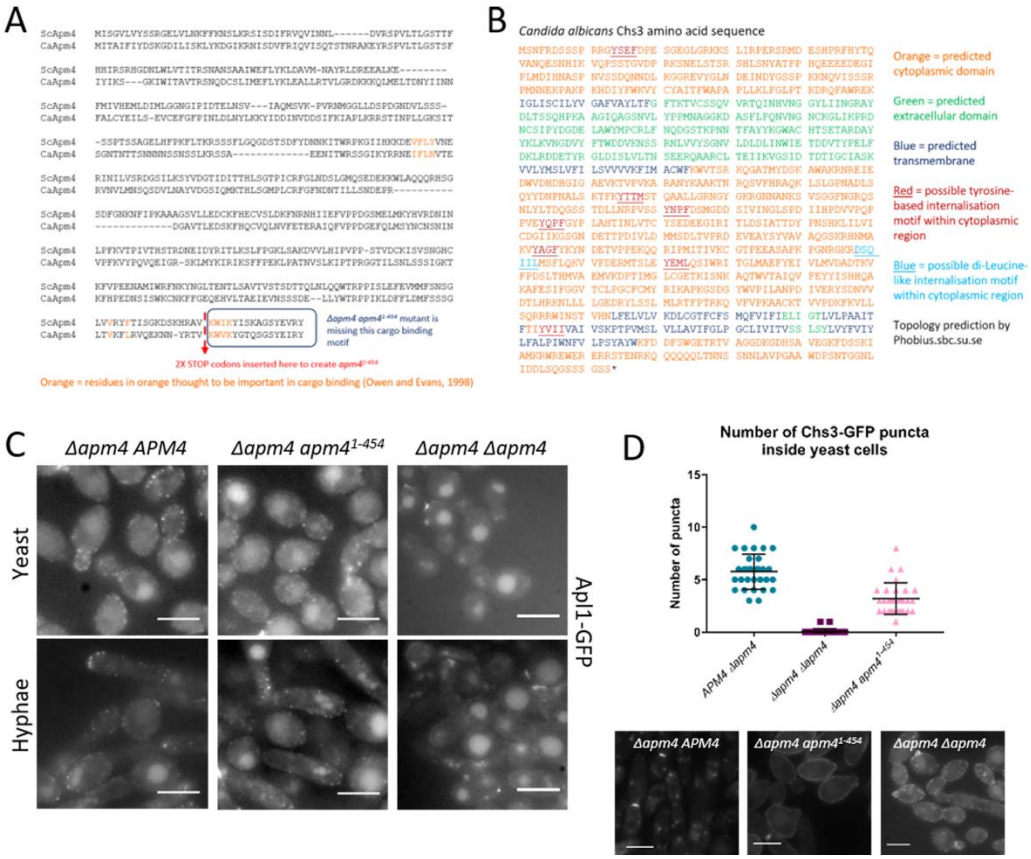


FIG S4

**Identifying *apm4* YXXΦ binding sites and generation of mutants**. (A) Amino acid sequences of *S. cerevisiae* and *C. albicans* Apm4 aligned on BLAST. Highlighted in orange are residues implicated in YXXΦ motif binding by Owen and Evans (**41**). The red arrow indicates where our truncation mutant has two stop codons inserted, and the blue box indicates the amino acids which are missing from the truncated protein encoded by *apm4*$^{1–454}$. (B) Amino acid sequence of *C. albicans* Chs3 with predicted topology and possible YXXΦ and dileucine internalization motifs highlighted. (C) Apl1-GFP peripheral puncta are present in YXXΦ binding mutant, indicating that unlike in full *apm4* deletion, the AP-2 complex is able to form in this strain. (C) Number of Chs3-GFP puncta inside each cell counted in 30 cells/strain; although YXXΦ binding mutant has peripheral Chs3, it also has many more intracellular puncta than the full deletion strain, though not as many as the WT. Error bars show SDs. Scale bars, 5 µm. Download FIG S4, TIF file, 1.9 MB.

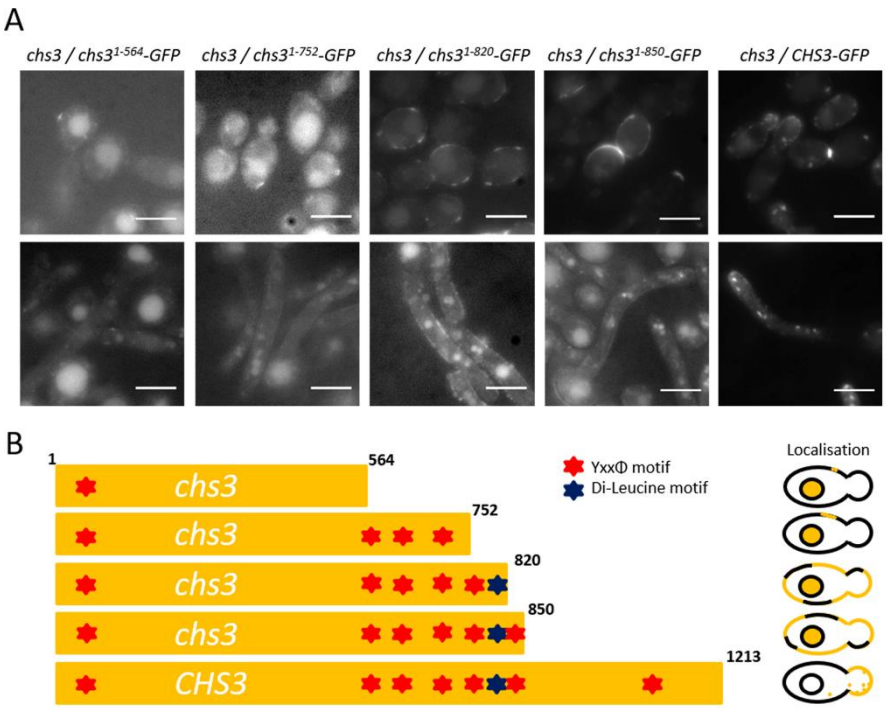


FIG S5

***chs3* truncation strains.** (A) Representative images of strains in which one copy of *chs3* was deleted and the other copy was truncated, such that a shortened version of the protein was expressed with a GFP tag at the C terminus. Scale bars, 5 µm. (B) Cartoon representing putative AP-2 binding motifs present in each of the truncated *chs3* versions and the localization of each truncated version in a cartoon yeast cell. Red star, YXXΦ motif; blue star, dileucine motif; in yeast cartoons: orange, protein localizes here; central circle, vacuole. Download FIG S5, TIF file, 1.2 MB.

# Chapter 5: Further studies on AP-2 dependent cell wall regulation in *Candida albicans*

## 5.1. Introduction to chapter 5

This chapter contains some pieces of data which are related to the role of AP-2 in the regulation of the *C. albicans* cell wall but could not be incorporated into the published paper (Knafler et al, 2019).

### 5.1.1. Glucan in the *C. albicans* cell wall

As mentioned previously, the *C. albicans* cell wall is made up of three major polysaccharides: chitin, glucan, and mannan. The most abundant polysaccharides are the polymers of glucose, β1,3- and β1,6-glucans, comprising 50 – 60% of the dry cell wall weight. The glucans form a highly crosslinked skeleton, conferring strength and shape on the cell (Shepherd 1987). Glucan synthases are restricted to points of active cell growth, where new glucan chains are integrated into the cell wall. Glucan synthases produce long linear glucan chains, which are cross-linked to one another and to other cell wall components outside of the cell. Fks1 is the key catalytic subunit for glucan synthesis, loss of which is lethal in *C. albicans* (Douglas et al. 1997). Glucan biosynthesis is regulated by the small GTPase Rho1 (Kondoh et al. 1997). The echinocandin class of antifungals specifically target β1,3-glucan synthesis, thereby inhibiting wall growth, and mutations in Fks1 can confer echinocandin resistance (Park et al. 2005).

Cell wall glucans also play a major role in the interactions of *C. albicans* with the human host. Glucans are released into the blood of infected patients, where they are toxic (Nakao et al. 1994). Glucans are proposed to suppress monocyte and T-cell function (Nakagawa, Ohno and Murai 2003) and therefore may be key in the establishment of candidiasis. Glucans are also potent activators of immune components such as complement and inflammatory mediators (Czop and Austen 1985). Glucan structures are specifically recognised by various host pattern recognition receptors (PRRs) such as complement receptor 3 (CR3); Toll-like receptor 2 (TLR2) and Dectin-1 (Netea et al. 2008). Dectin-1 binds β1,3-glucan and initiates signalling pathways to induce pro-inflammatory cytokines and phagocytosis (Dennehy and Brown 2007). Anti-β-glucan antibody has also been detected in blood serum of healthy humans and is thought to enhance fungal killing by macrophages (Ishibashi et al. 2005).

To protect itself from host defences, *C. albicans* ensures glucans are 'hidden' from immune receptors by other cell wall components, particularly mannoproteins (Wheeler and Fink 2006). Over the course of infection, and also following treatment with caspofungin, β-glucan is progressively 'unmasked', enabling increased Dectin-1 binding (Wheeler et al. 2008).

### 5.1.2. Mannan in the *C. albicans* cell wall

Mannoproteins; proteins which are modified by mannose-rich polysaccharides, are a major component of the outer cell wall, representing 30 – 40% of the dry cell wall weight (Klis et al. 2001). These proteins are mannosylated inside the cell, then trafficked through the secretory pathway to the extracellular space. Here the mannose residues are crosslinked with sugars in chitin or glucan, anchoring the glycoprotein in the cell wall. Some such proteins have a GPI anchor which localises them in the plasma membrane or cell wall (Bowman and Free 2006).

The oligosaccharide modifications may be *N*-linked, which are usually long and highly branched sugar chains; or *O*-linked, which are shorter linear chains. *N*-glycosylation begins at the endoplasmic reticulum (ER) as the protein is being translated. An oligosaccharide is transferred from a donor lipid to asparagine (N) residues found within specific amino acid motifs (Aebi 2013, Tanner and Lehle 1987). The oligosaccharide itself is built by glycosyltransferases at the ER membrane. As the protein is then trafficked through the ER to the Golgi, the oligosaccharide is extensively modified by various enzymes such as mannosyltransferases, leading to a great diversity of branched sugar structures (Mora-Montes et al. 2010). One such modification is mannosylphosphorylation, which confers negative charge to the *C. albicans* cell wall (Odani et al. 1996). *O*-linked glycosylation also begins at the ER when a single mannose sugar is added to a serine or threonine residue by a protein *O*-mannosyltransferase (PMT; (Prill et al. 2005)). Further sugars are added at the Golgi.

Mannose fibrils are the outermost structures of the *C. albicans* cell wall, and as such they define many of the surface properties of the cell and are a major interface with the host immune system. Alterations in glycosylation and mannose phosphorylation affect the hydrophobicity of the cell surface and this affects virulence (Hazen, Singleton and Masuoka 2007, Antley and Hazen 1988). Mannosylated proteins are thought to induce cytokine production (Vecchiarelli et al. 1991). Host cell receptors such as Toll-like

receptor 4 (TLR4) and mannose receptor (MR) specifically recognise *N*-linked and *O*-linked mannan respectively (Netea et al. 2006). And as mentioned above, mannans play a key role in shielding or masking the highly immunogenic β-glucan from the host immune system.

### 5.1.3. The yeast cell wall stress response

As the primary barrier between the cell and the outside environment, the fungal cell wall protects the cell against osmotic pressure; harsh chemicals; and the host immune system. Rather than being a static barrier, the cell wall is a highly dynamic organelle which the cell can monitor and rapidly remodel in response to changing conditions. The pathways by which yeast cells sense stress and subsequently remodel their cell walls are highly complex and only partially defined. In the classical yeast cell wall integrity pathway (CWI), wall stress is sensed by transmembrane proteins such as Mid2, and signals transduced via activation of the master regulator Rho1; the kinase Pkc1; and a MAP kinase cascade (Popolo, Gualtieri and Ragni 2001). A major output of these pathways is the upregulation of glucan and chitin biosynthesis in order to strengthen and repair the cell wall.

CWI signalling is induced upon treatment with cell wall perturbing agents such as Calcofluor White (CFW), Congo Red (CR) and caffeine; digestion of yeast cell wall; mutations in cell wall biosynthesis genes; and drugs which interfere with cell wall biosynthesis (Boorsma et al. 2004, García et al. 2004). In *S. cerevisiae* Chs3 was shown to be responsible for the elevated chitin levels triggered by this pathway (Valdivieso et al. 2000).

β-glucan and chitin synthases are transcriptionally upregulated under conditions of wall stress in both *S. cerevisiae* and *C. albicans* (Jung and Levin 1999, Munro et al. 2007). However the localisation and activities of these enzymes are also post-transcriptionally regulated. During normal growth in *S. cerevisiae*, 50 – 70% of cellular Chs3 is held in internal reservoirs (Santos and Snyder 1997), which are thought to be rapidly redirected to the plasma membrane when needed. *Sc*Chs3 was shown to be transported from inside the cell to the plasma membrane under conditions of stress, mediated by the master regulators Rho1 and Pkc1 (Valdivia and Schekman 2003).

### 5.1.4. Chitin synthase 8 in the *C. albicans* cell wall

As mentioned previously, *C. albicans* has four chitin biosynthesis enzymes. One of these is chitin synthase 8 (Chs8), a non-essential class I enzyme (the same class as Chs2). *C. albicans* differs from *S. cerevisiae* in this respect, as *S. cerevisiae* has only one class I chitin synthase. In contrast to Chs3, Chs8 generates a very small proportion of cell wall chitin in vivo (Munro et al. 2003). The majority of *C. albicans* cell wall chitin is made up of short microcrystalline rodlets generated by Chs3; interwoven with long microfibrils in bud scars and septa, which are made by Chs8 (Lenardon et al. 2007).

*Ca*Chs8 has been far less well studied than Chs3, and its exact functions have remained elusive, partially due to its mild phenotype upon deletion. Chs8-YFP was shown to localise to hyphal septa and yeast septa just prior to cytokinesis (Lenardon et al. 2007). The class I enzymes Chs8 and Chs2 are up-regulated upon caspofungin and CFW treatment, suggesting they may have a role in protecting cells against cell wall stress (Walker et al. 2008, Munro et al. 2007). After activation with CFW, Chs2 and Chs8 can synthesise a 'salvage septum' in cells lacking the normally essential Chs1 (Walker et al. 2013). Yeast and hyphal cells lacking Chs2 and Chs8 also undergo more cell lysis during early polarised growth (Preechasuth et al. 2015). Taken together, these studies suggest a role for Chs8, partially redundantly with Chs2, in protecting the cell against cell wall stresses, particularly at septa.

### 5.1.5. Mechanical properties of *C. albicans* hyphae

The physical environment in which a *C. albicans* cell resides affects its growth and morphology. When cells are placed within a matrix (for example agar), hyphae are rapidly produced, even under conditions (temperature and chemicals) which would not normally stimulate hyphal growth (Brown et al. 1999). This hyphal induction in response to matrix embedding depends on transcription factors Cph1 and Czf1 and has been hypothesised to simulate invasion of fungal hyphae into a host tissue (Brown et al. 1999).

Invasive growth of fungal hyphae is key to their survival in diverse environments; from nutrient acquisition in soil to tissue invasion during infection. Epithelial invasion by *C. albicans*, a key step in infection, can occur either via induced endocytosis, or via active penetration (Dalle et al. 2010). Invasive growth via active penetration presents mechanical challenges to the cell and requires specific factors, distinct from hyphal

growth in liquid or on a surface. Active penetration requires internal turgor pressure; directed hyphal extension; and cell wall integrity (Wächtler et al. 2011). The mechanical strength of a fungal hypha is largely a product of its internal turgor pressure, balanced with the deformation of its cell wall (Bartnicki-Garcia et al. 2000). The fungal cell wall has been shown to be important for invasive growth (Warenda et al. 2003, Wächtler et al. 2011).

One technique used to measure physical properties of the fungal cell wall is atomic force microscopy (AFM). Briefly, AFM uses a cantilever with a pointed tip to touch the surface of a sample. The deflection of the cantilever after it has deformed the surface, measured via a sensitive laser, gives information on both the topology and the physical properties of the sample's surface. The AFM tip can raster across the surface of a cell, for example, generating hundreds or thousands of force curves which, once fit to mechanical models, can be used to build a map of the physical properties of that cell (see (Kuznetsova et al. 2007, Haase and Pelling 2015). AFM is often used to measure the elasticity of a sample. Young's modulus (or elastic modulus; E) is the ratio of strain (deformation of the material) to stress (force applied to the material). The lower the modulus, the higher the elasticity of the sample (implying a softer or less stiff material).

Various alterations in the fungal cell wall have been shown to lead to changes in elasticity as measured by AFM. For example, loss of chitin has been shown to lead to increased elasticity, and vice versa (Ene et al. 2015), supporting the idea that chitin confers rigidity to the cell wall. Mutants which exhibit glucan 'unmasking' (*kre5 Δ/Δ* and *cho1 Δ/Δ*) had decreased elasticity (Hasim et al. 2017). Treatment of *C. albicans* cells with caspofungin has been shown to decrease elasticity (Formosa et al. 2013, Hasim et al. 2017), perhaps due to elevated chitin content. Different growth conditions can also alter the mechanical properties of the fungal cell wall. For example, *C. albicans* grown on lactate were shown to have a less elastic cell wall compared to cells grown on glucose, which led to increased resistance to osmotic shock (Ene et al. 2015).

# Chapter 5 Results

## 5.2. Cells without AP-2 have similar glucan and mannan levels to WT

As well as measuring total cell wall diameter (see Knafler et al, 2019), transmission electron microscopy (TEM) images were used to measure the length of mannose fibrils

in the outer cell wall. These appear as wispy hair-like structures extending from the darker inner cell wall layer. Mannose fibrils were measured using FIJI, in yeast cells and at different locations on hyphal cells, in both the WT and *apm4* deletion strain. 5 measurements were averaged per cell, and figure 5.1A shows the mean of >20 cells / location. The percentage values are the mean percentage of total cell wall diameter (inner and outer) represented by mannose fibrils. Representative TEM images are shown in figure 5.1B. As shown, cells without AP-2 had longer mannose fibrils in their yeast (114 µm compared to 71 µm for WT) and hyphal mother cells (109 µm compared to 95 µm for WT), but their mannans were shorter at the hyphal tips (74 µm compared to 132 µm for WT). Despite their mannans being longer in yeast and mother cells, they comprised a lower proportion of the overall cell wall than those of WT cells (44% compared to 47% for WT in yeast cells), due to the *apm4* deletion mutant having a much thicker inner cell wall. At the hyphal tips, mannose fibrils made up a smaller proportion of the total cell wall diameter in *apm4* deletion cells (43% compared to 53% for WT). Along the hyphal length, the mannose fibrils were a similar length in both strains.

An Alcian Blue binding assay was used to further analyse cell wall mannose. Alcian Blue is a cationic dye which binds to negatively charged phosphorylated mannose (mannosylphosphate) so can be used to quantify mannosylphosphorylation in yeast cell walls (Ballou, Kern and Raschke 1973, Odani et al. 1996). As shown in figure 5.1C, yeast cells without AP-2 bound 0.27 pg Alcian Blue per cell whilst WT yeast bound 0.24 pg Alcian Blue per cell, indicating the two strains have similar mannosylphosphate levels.

Another dye, Aniline Blue, binds β-(1,3)-glucan in the *C. albicans* cell wall and was used to assess β-(1,3)-glucan levels (Wood and Fulcher 1983). Yeast cells of both strains were stained with Aniline Blue, imaged (see figure 5.1D) and their mean grey value quantified on FIJI (figure 5.1E). As shown, cells without *apm4* did not have significantly different Aniline Blue staining to WT cells, indicating that they have similar levels of cell wall β-(1,3)-glucan.

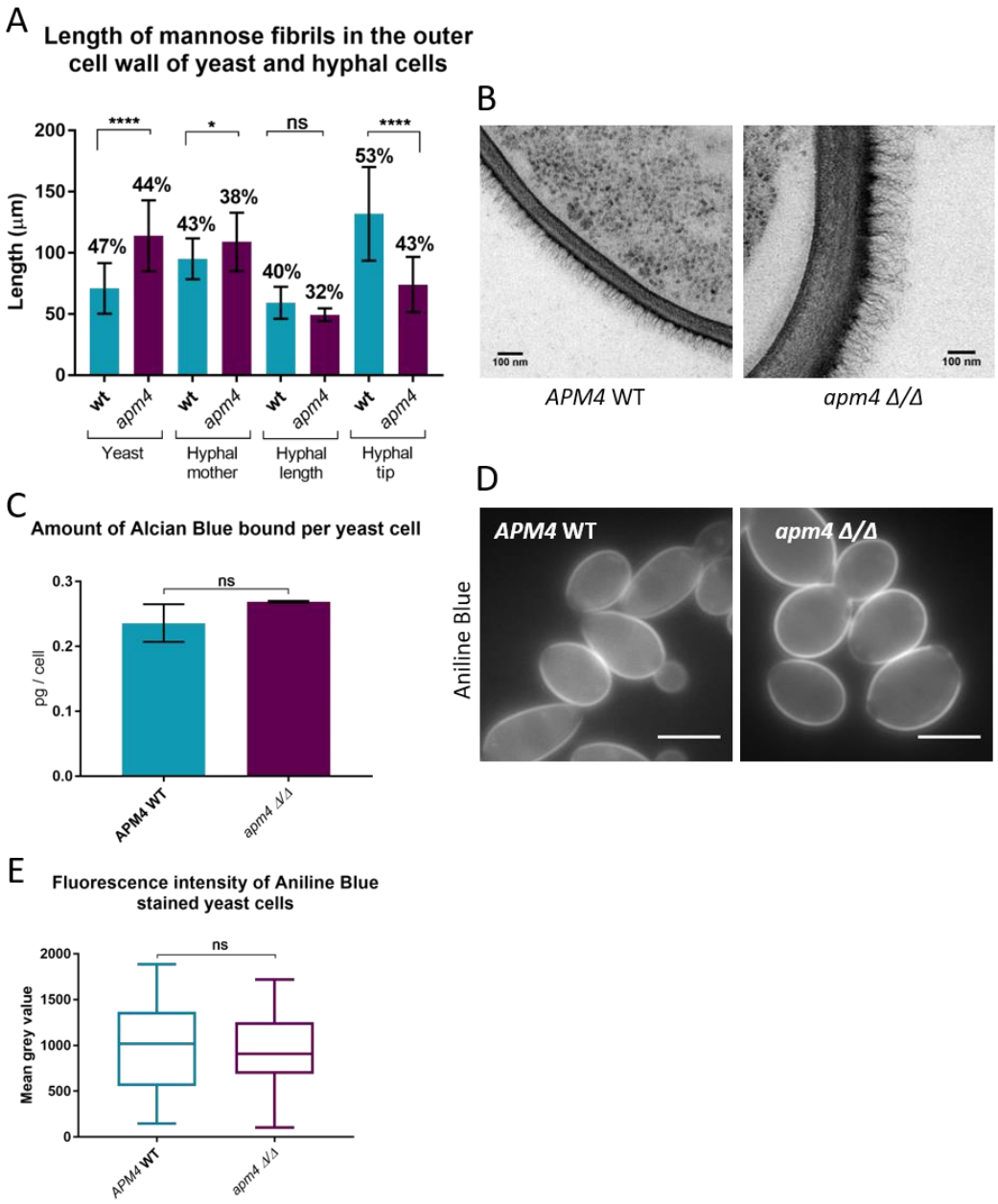


### 5.1. Cells without AP-2 have similar glucan and mannan levels to WT

(A) Mannose fibrils in the outer cell wall were measured from TEM images of WT and *apm4* deletion cells. Bars show mean length of mannose fibrils; numbers show percentage of total cell wall diameter mannose fibrils represent. 5 measurements / cell; >20 cells / location; 1 representative experiment. Stats is a one-way ANOVA with Tukey's multiple comparisons. (B) Representative TEM cross sections of yeast cell walls. (C) Amount of Alcian Blue dye bound by yeast cells of both strains. Stats is an unpaired T-test. (D) Representative images of yeast cells stained with Aniline Blue (scale bars 5 µm); mean grey value quantified in (E). Stats is an unpaired T-test. All error bars show SD.

## 5.3. Chs3 localises to the cell surface in response to wall stress

As shown in Knafler et al (2019), in WT yeast cells growing exponentially in rich media, Chs3-GFP signal is observed in intracellular puncta and at peripheral puncta concentrated to growing buds and larger bud necks. Some further experiments were conducted, to determine whether this Chs3-GFP localisation changes under different growth conditions. As shown in figure 5.2, cells after overnight culture had Chs3-GFP signal in their vacuoles and some intracellular puncta, with very few peripheral puncta. When these cells were refreshed for 30 minutes in fresh YPD, more surface puncta had appeared, though there was still Chs3-GFP signal inside vacuoles. Refreshing in YPL medium (2% lactate instead of glucose) was also tested, as lactate is a physiologically relevant non-fermentable carbon source, growth on which is known to alter cell wall composition (Ene et al. 2012). After 30 minutes in YPL, cells showed a similar pattern of Chs3-GFP localisation to those refreshed in YPD, but with slightly more puncta at the cell surface.

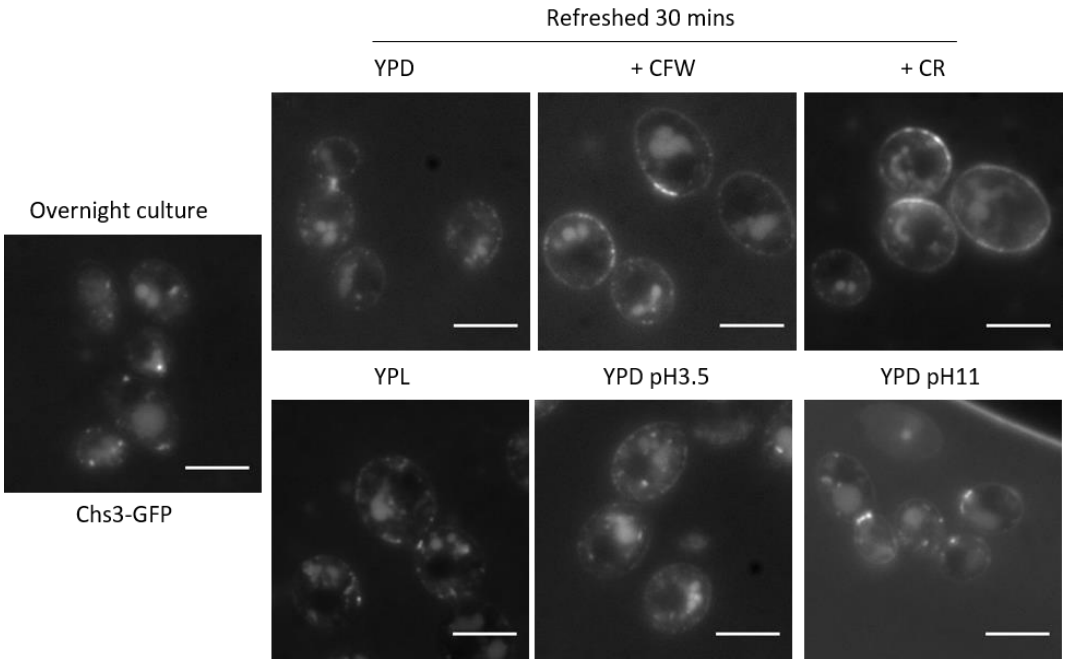


**5.2. Chs3 localises to the cell surface under cell wall stress conditions**
Chs3-GFP was imaged in otherwise WT cells under different conditions. Overnight cultured cells were refreshed into either YPD alone, YPL alone (2% lactate instead of glucose) or YPD containing 40 µg/mL CFW or 100 µg/mL CR or adjusted to pH 3.5 or 11. These cells were grown for 30 minutes at 30°C then imaged.

As shown in figure 5.2, when cell wall stress agents Congo Red or Calcofluor White were added to the media, much more Chs3-GFP signal localised to the cell periphery after 30

minutes. Low and high pH media were also tested (YPD was adjusted to either pH 3.5 or pH 11 with HCl or NaOH respectively). After growth at pH 3.5, the peripheral Chs3-GFP signal was also elevated, however growth at pH 11 did not have an observable effect.

## 5.4. Chs8 localisation is somewhat dependent on AP-2

After showing that AP-2 is required for endocytosis of Chs3 in *C. albicans* (Knafler et al, 2019), we asked whether AP-2 is also required for the recycling of another chitin synthase, Chs8. Chs8 was tagged with GFP in both WT and *apm4* deletion cells. These cells were grown as yeast and Chs8-GFP localisation assessed. As shown in figure 5.3A, Chs8 has a cell cycle-dependent dependent pattern of localisation to yeast septa. Therefore in the analysis, only budding cells were counted, and these were split into categories of cells with small, medium or large buds. Large buds were defined as those of similar size to the mother cell; small buds were defined as no more than an initial protrusion; and medium buds were any in between those categories. Once categorised, cells were assessed for Chs8-GFP signal at their neck region. In small budded cells, there was no recruitment to the neck. As the buds grew larger, more cells had either some Chs8-GFP enrichment to the neck, or bright Chs8-GFP signal at the neck. In cells without AP-2, the localisation was shifted so that more large budding cells had bright Chs8-GFP signal at their necks than in WT. Example images of yeast cells are shown in figure 5.3B, with arrows pointing to examples of bright Chs8-GFP at septa. Line profiles were also drawn across septa of large budding cells, to analyse the Chs8-GFP signal intensity (figure 5.3C). This graph shows line profiles averaged from >10 cells of each strain, and shows that the *apm4* deletion cells had slightly brighter and wider Chs8-GFP signal at their septa than WT.

The tagged strains were also induced to form hyphae for 3 hours (to ensure multiple septa were present), and the pattern of Chs8-GFP staining analysed. Hyphae were stained with Calcofluor White (CFW) to identify septa, then recorded whether each septum had no Chs8-GFP signal; some signal; or bright Chs8-GFP signal (see figure 5.3D). This analysis showed that hyphae without *apm4* had more septa with bright Chs8-GFP signal (43% of septa) than WT hyphae (24% of septa). Images in figure 5.3E show examples of hyphal septa which would be classified as ‘bright septa’ (above) and ‘no visible septa’ (below). Line profiles were also plotted across CFW stained hyphal septa of

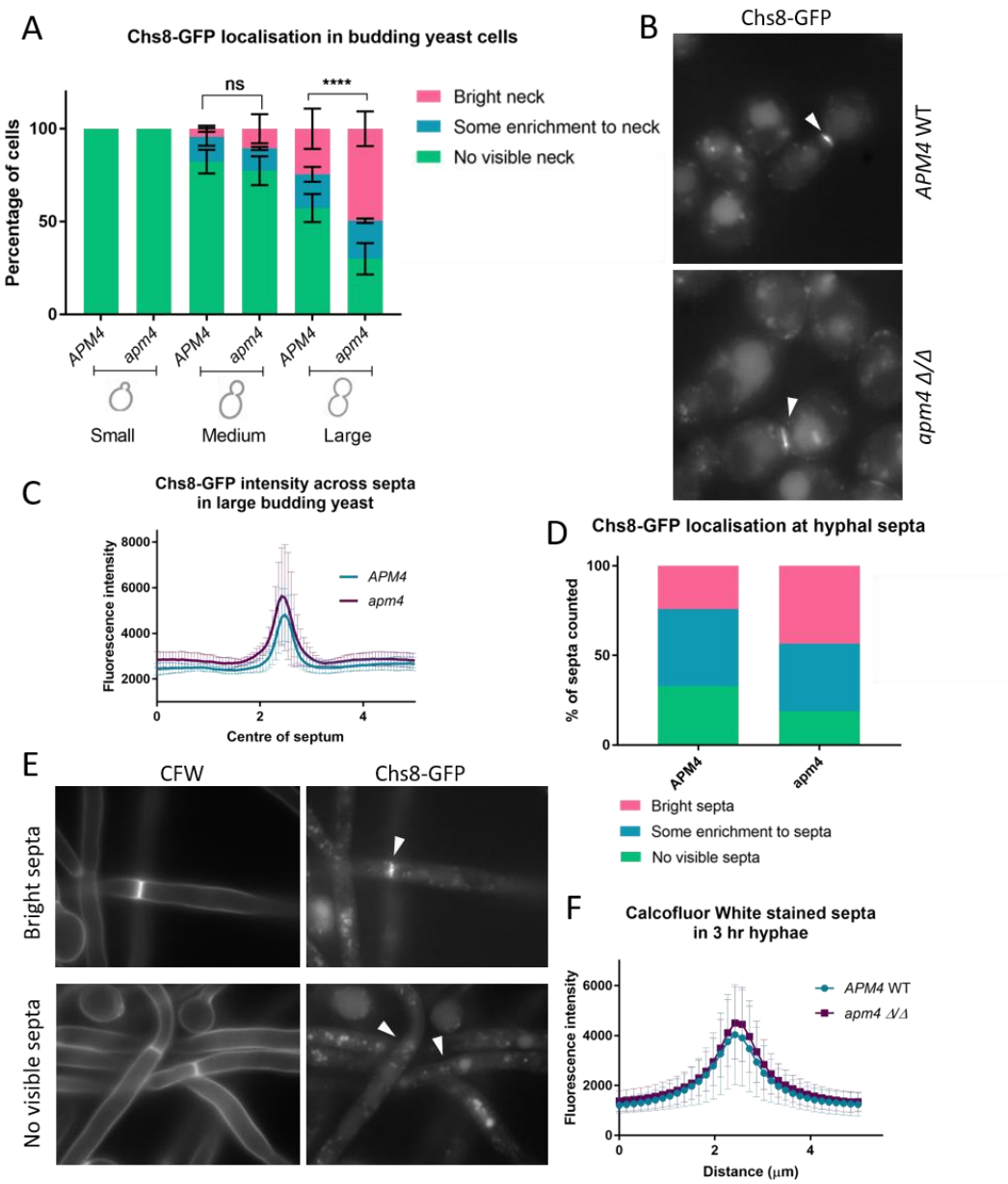


5.3. Cells without AP-2 have altered Chs8-GFP localisation

(A) WT and *apm4* deletion cells expressing Chs8-GFP grown as yeast and the pattern of Chs8-GFP localisation recorded. Data from 100 cells / strain, 3 independent experiments. Stats is a two-way ANOVA. (B) Representative images of yeast cells of each strain, arrows point to Chs8-GFP at septa. (C) Averaged line profiles across Chs8-GFP labelled septa in >10 yeast cells of each strain. (D) Cells grown as hyphae and pattern of Chs8-GFP localisation recorded. (E) Representative images of hyphal cells expressing Chs8-GFP and stained with CFW; example of a septum with bright Chs8 signal, and without Chs8 signal. (F) Averaged line profiles plotting fluorescence intensity across >10 CFW stained septa / strain. All error bars show SD.

both strains (figure 5.3F). As shown, the staining intensity and diameter of CFW stained septa are very similar in WT and *apm4* deletion hyphae.

## 5.5. Growth of hyphae within and on top of solid substrate

Embedding *C. albicans* cells within a solid matrix such as agar can induce them to form hyphae, independent of other temperature or chemical cues (Brown et al. 1999). Yeast cells of both strains were seeded into molten (cooled) agar of different percentages, which was then solidified and incubated at room temperature for 3 days. Colonies which had grown within the agar were then imaged using a light microscope; representative images shown in figure 5.4A. WT cells had formed many dense colonies from which long hyphae extended, often with yeast cells budding from the hyphal sides. WT cells appeared to grow longer hyphae when in 4% agar compared to 1%. Strikingly, cells without AP-2 formed a similar number of colonies but appeared to grow longer hyphae in 1% agar compared to 2 or 4%. In 4% agar, the highest percentage tested, hyphae were rarely observed in the *apm4* deletion strain.

Hyphal growth was also assessed for cells growing on solid medium (on the surface of an agar pad) compared to growth in liquid media. *apm4* deletion cells were grown for 90 minutes either in liquid YPD or solid YPD (2% agar), both at 37°C and with 10% FBS, then imaged and hyphal length and width measured. As shown in figure 5.4B, cells without AP-2 are able to grow significantly longer hyphae on solid medium (mean 18.1 µm) compared with liquid (14.5 µm), though the hyphal width is similar in both conditions.

## 5.6. Hyphae without AP-2 may be stiffer than those of WT

This preliminary data suggesting hyphae without AP-2 may be defective at penetrating stiffer substrate, combined with their known cell wall dysregulation, led us to wonder whether their mechanical properties are altered. To begin to test this, we collaborated with Spyridon Sovatzoglou and Professor Jamie Hobbs (Dept of Physics and Astronomy, University of Sheffield) to perform atomic force microscopy (AFM) on our *C. albicans* strains. Initial Force maps were generated, scanning across individual *C. albicans* cells in acetate buffer to give a map of Young's moduli (a measure of stiffness or elasticity) across the cells, see figure 5.5A, B. Each coloured pixel represents one Force curve, there are 16,384 per image.

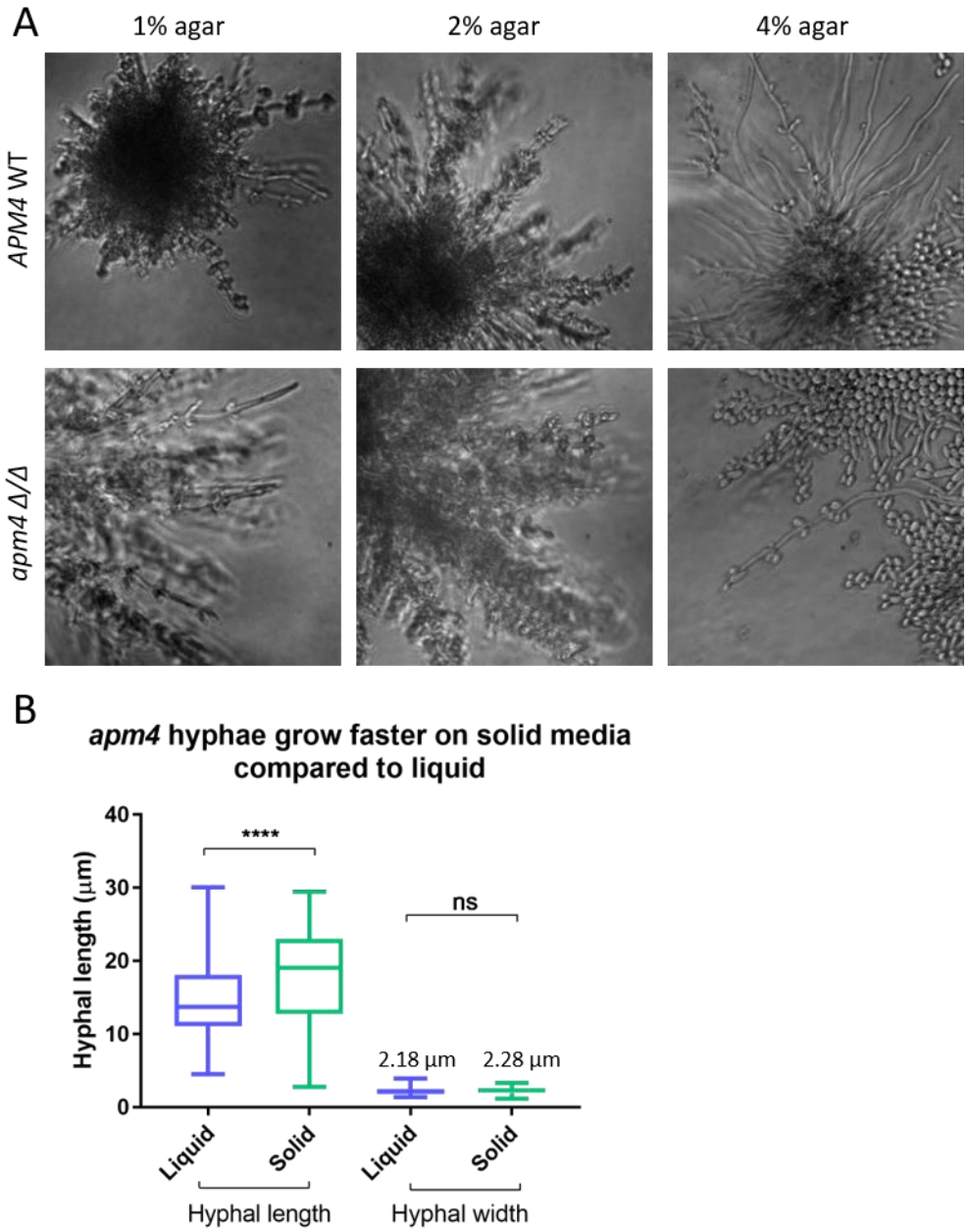


**5.4. Cells without AP-2 are defective at forming hyphae within agar of increasing concentrations but their hyphae grow faster on agar than in liquid**

(A) WT and *apm4* deletion cells were seeded into molten cooled agar of different percentages and grown at room temperature for 3 days, then imaged. Representative images shown. (B) *apm4* deletion cells induced to form hyphae in liquid YPD or on solid YPD agar plates, then imaged and their width and length measured. Data is from 100 cells / condition, 1 representative experiment. Error bars show SD. Stats are unpaired T-tests.

The graphs in figure 5.5C and D show the means of the median Youngs moduli calculated from the mother cells and hyphae separately for both strains. This data is very preliminary but suggests that hyphal cells without AP-2 are stiffer than WT cells (note the scales on the graphs are different, to enable easier comparison within the graphs). Additionally, in WT cells the hyphae were stiffer than the mother cells (mean 0.31 MPa for hyphae; 0.13 MPa for mother cells, n = 5 cells); whereas in *apm4* deletion cells the moduli of hyphae and mother cells were similar (mean 1.5 MPa for hyphae; 1.7 MPa for mother cells, n = 6 cells). These initial results are encouraging but much more work will need to be done to understand whether this difference in elasticity is significant.

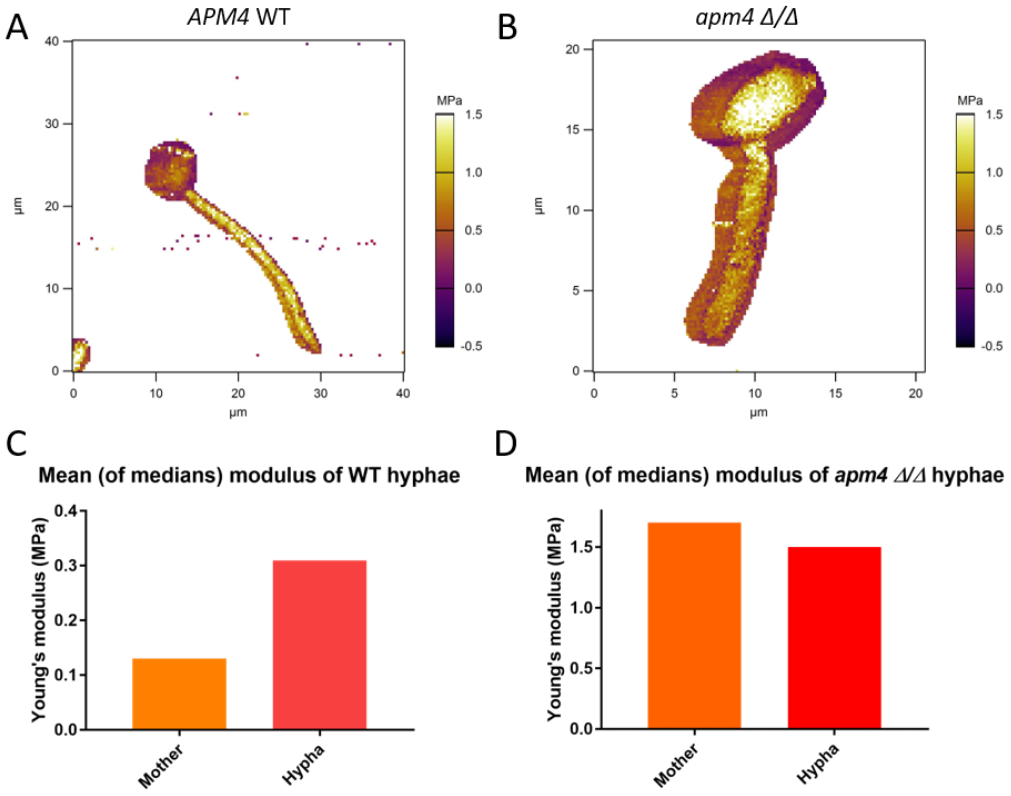


5.5. Hyphae without AP-2 may be stiffer than those of WT cells

(A) Example Force Map of a WT and (B) *apm4* deletion hyphal cell, obtained via AFM. Maps depict Young's Modulus (MPa) at different locations on the hyphae. Note the size scales (µm) are different. 128 x 128 pixels (Force curves) per image. (C) Graph showing the mean of the median Young's Moduli (MPa) from 5 WT hyphae comparing their hypha and their mother cells. (D) As in (C) but the means are from 6 *apm4* deletion hyphae. Note the scales (MPa) are different.

## 5.7. Chapter 5 discussion

### 5.7.1. Discussion of glucan and mannan levels

The HPLC analysis in Knafler et al (2019) is a good measure of the level of each cell wall polysaccharide, as a proportion of total dried cell wall material. This analysis showed that cells without AP-2 had a lower proportion of glucan than WT cells, in both yeast and hyphae. However staining with Aniline Blue did not show a difference between the two strains. A reason for this apparent discrepancy may be that the HPLC analysis shows a decrease in glucan as a proportion of dry cell wall weight; given the greatly elevated chitin content of the *apm4* mutant, this decreased proportion of glucan could represent no difference in the actual amount of glucan between the two strains. This may suggest that the glucan biosynthesis enzyme Fks1, in contrast to Chs3, does not rely on AP-2 for its recycling.

HPLC analysis showed that there was no significant difference in mannose levels between WT and *apm4* deletion cells (yeast and hyphae). In this chapter, measuring the length of mannan fibrils from TEM images showed that these are significantly longer in *apm4* yeast compared to WT yeast. This apparent discrepancy could be due to the *apm4* mutant having longer but less dense fibrils than WT, leading to a similar amount of mannose. Further analysis would be needed to assess whether the mannose fibrils are less dense in the mutant. Alternatively, the *apm4* mutant could have higher mannose levels than WT, but these could represent a similar proportion of the overall cell wall due to its increased chitin content, as mentioned above.

Measuring TEM images also revealed that there are differences in mannose fibril lengths at different locations on the hypha; whilst the HPLC analysis could not distinguish between locations on hyphal cells. Most strikingly, WT hyphae had significantly longer mannose fibrils at their tips, whilst *apm4* deletion hyphae did not. The reason for these differences is not clear. Glycosylation patterns may well change when a cell initiates hyphal growth. Mannose fibrils could also be hydrolysed by enzymes outside the cell, leading to shorter fibrils at the hyphal sides than the most recently secreted ones at the hyphal tip.

Alternatively, it could be that secretion of the mannosylated proteins themselves is disrupted or de-polarised. Staining new mannose using Concanavalin-A (see Knafler et al, 2019) revealed that in hyphae without AP-2 new mannose is added to the yeast mother cell during hyphal growth, when it should be restricted to the growing hypha.

This could be a consequence of de-polarised secretion in the mutant (as show by de-polarisation of exocyst components to hyphal mother cells, see chapter 6). De-polarised secretion of mannosylated proteins could explain the fact that the *apm4* mutant does not have the long fibrils at the hyphal tip seen in WT hyphae.

In yeast cells, we have not distinguished between mother and bud, so could not say whether de-polarised secretion is an issue here. The longer mannose fibrils in *apm4* yeast cells could be explained by impaired hydrolysis or altered glycosylation within the cell. A shift from *O*-linked to *N*-linked glycosylation could perhaps lead to longer but less dense mannose fibrils. Yeast without AP-2 did not show a difference in mannosylphosphate levels, via Alcian Blue binding. Assuming the proportion of phosphorylation is unchanged between WT and mutant, this supports the notion that the mutant has longer but sparser mannose fibrils, leading to a similar overall amount of mannose as WT.

Having longer mannose fibrils at the cell surface may have many implications for virulence. The *apm4* mutant may have altered recognition by the host immune system, due to its different mannan structures. If the longer mannose fibrils mean glucan is more masked in the mutant, we may predict it would be less immunogenic than WT.

### 5.7.2. Discussion of Chs3 in stress

We have previously shown (Knafler et al, 2019) that in the absence of AP-2, Chs3 cannot be effectively internalised and becomes distributed around the cell periphery. We wanted to utilise our Chs3-GFP tagged strain to learn more about Chs3 traffic. Secretion of Chs3 to the cell surface has been much studied in *S. cerevisiae*; and it is known that internal *Sc*Chs3 can be rapidly directed to the plasma membrane under conditions of cell wall stress. Here we show that this is also the case in *C. albicans* (figure 5.2). As expected, upon addition of CFW or CR for 30 minutes, elevated Chs3-GFP signal was observed at the cell periphery.

Interestingly, this increased peripheral Chs3-GFP was observed at pH 3.5 but not at pH 11. Growth at both high and low pH is a considerable stress for *S. cerevisiae* laboratory strains (Ariño 2010) however fungal pathogens such as *C. albicans* must be able to adapt to different host tissues which can vary from pH 2 to 10 (Selvig and Alspaugh 2011). Growth at both low and high pH is known to activate the CWI pathway in *S. cerevisiae*

(de Lucena et al. 2012, Ariño 2010). Our results suggest that stress signalling leading to increased Chs3 at the cell surface occurs at pH 3.5 but not at pH 11 in *C. albicans*, indicating that even the very alkaline pH of 11 is well tolerated by *C. albicans*.

Also interestingly, slightly more Chs3-GFP puncta were seen at the surface of cells utilising the physiologically relevant nonfermentative carbon source lactate, compared with glucose. Growth on lactate is known to significantly reduce the chitin and glucan layer of the cell wall; possibly due to alterations in metabolic flux (Ene et al. 2012). Therefore the slightly increased Chs3-GFP puncta observed with lactate may be required under these conditions, to maintain cell wall strength.

### 5.7.3. Discussion of Chs8 localisation

Chitin synthase 8 is less abundant than Chs3, and less well characterised. Upon deletion of *apm4*, it undergoes a much less dramatic localisation shift than that of Chs3, making it harder to be certain of whether it is an endocytic cargo of AP-2. However in yeast cells it does undergo a shift in localisation pattern, indicating that AP-2 is involved in its traffic.

To study Chs8 in hyphal cells, hyphae were grown for 3 hours to allow time for multiple septa to form. However these very long hyphae were more challenging to image; they were often entangled and not in a single plane of focus, making it hard to distinguish between individual hyphae. For this reason, Chs8 localisation at hyphal septa has not been extensively characterised. For example, it was often observed that the most tip-ward septum (the most recently formed) had the brightest CFW staining and was most likely to have Chs8-GFP signal. This was not quantified though due to frequent difficulties in being certain that two septa were part of the same hypha. As *apm4* mutant hyphae are slower growing they would form fewer septa than WT hyphae in the same amount of time, which could bias the localisation pattern of Chs8.

Many protein components localise to septa of both yeast and hyphae, in order to synthesise the required new cell wall. Many of these components must be internalised via endocytosis once their role at the septum is complete. In *S. cerevisiae*, Chs2 (homologue of *Ca*Chs2 / *Ca*Chs8) is known to be endocytosed dependent on a mitotic exit kinase Dbf2 (Oh et al. 2012), which presumably co-ordinates septum formation with cell cycle progression. Endocytosis of specific cargo such as Chs8 via AP-2 could be another mechanism allowing the cell to temporally regulate septation.

### 5.7.4. Discussion of mechanical properties

Some very preliminary investigation into the physical properties of hyphae without AP-2 is presented here. It was hypothesised that the changes in cell wall composition and organisation observed in this mutant may lead to altered mechanical properties which are important for hyphal penetration and invasion. The first indication of this came from the observation that *apm4* mutant hyphae grew longer when induced on solid medium (on agar) compared to liquid media. This was not the case in WT cells. Hyphal growth on a solid surface is perhaps more representative of a fungi's environmental niche than growth in a shaking flask. A solid surface could act to support the growing hypha, which could aid growth of the *apm4* mutant hyphae which are possibly weakened by their cell wall dysregulation.

As well as growth on an agar surface, growth within agar was tested. Interestingly, cells without *apm4* formed filaments very rapidly within 1% and 2% agar; in 1% agar they formed longer filaments than WT cells. However within 4% agar, although colonies of mutant cells could grow, these were made up mostly of yeast cells with very few hyphae. This contrasts with WT, which formed longer filaments in the higher percentage agar. This difference suggests that perhaps the mutant's defect is in its physical ability to penetrate the agar, rather than a defect in a signalling pathway, as it had no problem forming filaments in lower percentage agar. This is interesting as it suggests cells without AP-2 may have problems invading epithelia for example, which could reduce their virulence.

These observations led us to form a collaboration with Spyridon Sovatzoglou and Professor Jamie Hobbs (Dept of Physics and Astronomy, University of Sheffield) to perform atomic force microscopy (AFM) on our *C. albicans* strains. We measured the Young's moduli of hyphal cells of both strains. We chose an indentation of 100 nm which was predicted to indent the inner cell wall, but no further, so the moduli should reflect the elasticity of the cell wall rather than the turgor pressure of the cell itself. Hyphal growth is thought to depend on a combination of internal turgor pressure driving cytoplasmic expansion, and the extensibility of the cell wall; i.e. how much the cell wall will expand under that pressure (Lew 2011). The extensibility of the cell wall varies with its composition and organisation, for example the extent of crosslinking (Zhao et al. 2005). For simplicity, we have not looked into the turgor pressure of our hyphae. We

hypothesised that the elevated chitin present in the mother cell of hyphae without *apm4* could make this stiffer than WT; but that perhaps the hypha would be more elastic, which could explain its difficulties penetrating 4% agar. Measurements were taken across the whole hyphal cell, so that we could see any differences in elasticity of different areas.

A modulus of 1.6 MPa has been reported for *C. albicans* yeast cells (Ene et al. 2012), which is on a similar scale to our measurements (which ranged from mean 0.13 MPa to 1.7 MPa at different locations, see figure 5.5). The graphs show means of median moduli from just 5 WT hyphae and 6 mutant hyphae, so this is very preliminary and needs further investigation. However this initial experiment has shown an interesting trend. In WT hyphae, the hyphae were stiffer than the mother cells. This may help the hypha penetrate tissue during infection, and 'burst' out of macrophage cells. Hyphae without AP-2 however, had a similar Young's modulus across their hyphal and mother cells, which could be due to the increased chitin in mother cells in the *apm4* mutant (see Knafler et al, figure 5).

To our knowledge, the elastic properties of hyphae compared to their mother cells has not been studied. Ma et al (2005) showed that new cell wall at the tips of *A. nidulans* hyphae was more elastic than that further down the hypha, suggesting that the wall undergoes maturation which stiffens it. We did not observe an obvious gradient from the hyphal tip; more detailed analysis would be needed to determine if this is also the case in *C. albicans*. This would be a very interesting line of research to be continued.

### 5.7.5. Concluding remarks

The results in this chapter have added to work published in Knafler et al (2019). We have shown that cells without AP-2 have similar levels of glucan and mannan to WT, despite their elevated chitin content. We also show Chs8, in addition to Chs3, may be endocytosed via AP-2. Preliminary data also indicates that hyphal cells lacking AP-2 have altered mechanical properties which could impair their ability to penetrate and invade substrate. The link between cell wall changes and defects in invasion raise interesting questions for future investigation.

# Chapter 6: AP-2 is required for polarisation of the secretory pathway and plasma membrane lipids

## 6.1 Introduction to chapter 6: polarity markers and lipids

### 6.1.1. Protein markers of polarised growth

Any cell in which growth is directed to a particular region requires secretion to be polarised towards that region. Secretory vesicles provide both membrane and membrane proteins required for growth. In order to target secretion to the site of growth, there is often a complex hierarchy of proteins which firstly select the site for growth, then, via a series of interactions and positive feedback loops, recruit myriad polarity markers to this site.

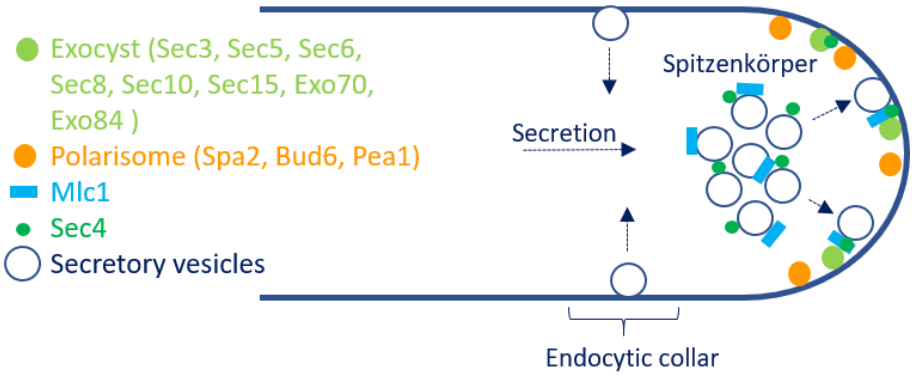


**6.1. Polarity machinery localisation at the hyphal tip**

This cartoon shows where various protein components are localised in an actively growing *Candida albicans* hypha. Exocyst and polarisome protein complexes are localised to a crescent at the hyphal tip. None of the proteins listed are transmembrane proteins, however some bind membrane lipids. Exocyst components Sec3 and Exo70 bind PM PI(4,5)$P_2$. The polarisome is recruited by Cdc42. Secretory vesicles accumulate in a pool in the sub-apical region, termed the Spitzenkörper. Sec4 and Mlc1 (myosin light chain) both associate with secretory vesicles and are residents of both the Spitzenkörper and the hyphal tip.
Diagram based of the following studies:
Jones and Sudbery, 2010 (polarisome and exocyst localisation)
Crampin et al., 2005 (presence of Spitzenkörper in *C. albicans*; Mlc1 localisation)
My own observations (see following results)

A well characterised example of polarised growth is bud growth in *S. cerevisiae*. Here, as in most eukaryotes, a key player is the Rho-type GTPase Cdc42 (Johnson 1999); whose accumulation via positive feedback loops (Butty et al. 2002) in sites selected by

landmark proteins serves to recruit a host of other polarity proteins. Importantly actin nucleator proteins are recruited to generate F-actin cables extending away from the growth site, enabling secretory vesicles to be transported here. The exocyst complex tethers vesicles to the target membrane, where fusion is mediated by SNARE proteins.

Hyphal growth in filamentous fungi relies on many of the same proteins as yeast bud emergence to ensure secretion and growth is continuously targeted to the hyphal tip (see figure 6.1 for summary). In fungal hyphae, vesicles accumulate in a sub-apical region called the Spitzenkörper before they fuse with the hyphal tip, which may be a requirement of the much higher growth rate of hyphae compared to yeast. *C. albicans* hyphae grow twice as fast as yeast cells (Jones and Sudbery 2010), and other filamentous fungi can reach extension rates of up to 40 µm / minute (Meletiadis et al. 2001).

## The exocyst

The exocyst is an octameric protein complex which acts in exocytosis; the process by which intracellular vesicles are transported to and fuse with the plasma membrane. Tethering complexes are required for many aspects of membrane trafficking; they serve as the first connection between a vesicle and its target membrane, preceding fusion (Yu and Hughson 2010). This tethering is thought to enable vesicle targeting to specific locations, and to confer selectivity to vesicle capture. However, the molecular mechanisms of tethering by the exocyst, and the extent to which it regulates membrane fusion remain unclear.

The exocyst is composed of subunits Sec3, Sec5, Sec6, Sec8, Sec10, Sec15, Exo70 and Exo84, with equal stoichiometry (Heider et al. 2016), which are conserved among eukaryotes (Guo, Grant and Novick 1999a, Guo et al. 1999b, TerBush et al. 1996). These subunits form many interactions, enabling both localisation to exocytic sites and interaction with exocytic vesicles. For example, Sec3 has been shown to bind both plasma membrane $PI(4,5)P_2$ and Rho1 and Cdc42 GTPases (Zhang et al. 2008, Yamashita et al. 2010). Exo70 also interacts with $PI(4,5)P_2$; Rho3 and Cdc42 (He et al. 2007, Wu et al. 2010); and the combination of these interactions is thought to target exocyst to the plasma membrane. On secretory vesicles, Sec4 and Myo5 are known to interact with

Sec15 (Guo et al. 1999b, Jin et al. 2011), and Snc (a v-SNARE) interacts with Sec6 (Shen et al. 2013).

One disputed topic is the functional importance of exocyst subcomplexes. For yeast exocyst, the Novick lab proposed that a subcomplex of exocyst (Sec3 and Exo70) is docked at the plasma membrane and the other subunits are carried on secretory vesicles; assembly of these two subcomplexes drives membrane tethering (Boyd et al. 2004). However more recent studies of yeast exocyst found no evidence of subcomplexes and concluded the exocyst functions predominantly as a fully assembled octamer (Donovan and Bretscher 2015, Heider et al. 2016).

In filamentous fungi exocyst components have been shown to localise to the hyphal tip, as one might expect, and there is some evidence for the presence of two subcomplexes. *Ashbya gossypii* exocyst proteins localised to a cortical cap in slow growing hyphae, and to the Spitzenkörper of faster growing hyphae (Köhli et al. 2008). A similar dual localisation was shown in *N. crassa* (Riquelme et al. 2014). In *A. nidulans* exocyst localised to a cortical cap (Taheri-Talesh et al. 2008). Jones and Sudbery (2010) showed that in *C. albicans* the exocyst complex is quite stably located at the cell surface of the hyphal tip, suggesting that in this organism at least the exocyst remains at the PM whilst vesicles are trafficked to it from the Spitzenkörper (figure 6.1).

## The polarisome

The polarisome is another set of polarity proteins, which has been well characterised in budding yeast. In *S. cerevisiae*, the polarisome is associated with cell cycle-dependent polarised growth. Polarisome components include Bud6, Spa2, Pea2 and Bni1 (Evangelista et al. 1997, Sheu et al. 1998). These proteins localise to the tips of growing buds, dependent on the master regulator Cdc42, which interacts with Bud6 (Irazoqui and Lew 2004). Bni1 is a formin, which then nucleates actin cables from the bud tip (Evangelista et al. 1997). Thus the polarisome links actin cables to the site of polarised growth, allowing vesicle transport via myosins to be directed here. As the cell cycle progresses the polarisome is relocated to the bud neck, to direct secretory vesicles to the site of cytokinesis (Lippincott and Li 1998).

Polarisome protein homologues are also present in filamentous fungi and generally localise to the surface of the hyphal tip (Crampin et al. 2005, Meyer et al. 2008, Lichius et al. 2012). Harris et al. (2005) proposed the polarisome to be a subcomponent of the

Spitzenkörper, however Jones and Sudbery (2010) showed that in *C. albicans* hyphae at least, the polarisome is spatially and functionally separate from both the Spitzenkörper and the exocyst (figure 6.1).

## The Spitzenkörper

The Spitzenkörper was first observed via electron microscopy in 1957 (Girbardt) and has since been seen in a wide range of filamentous fungi. It was first described in *C. albicans* by the Sudbery lab (Crampin et al. 2005).

The Spitzenkörper is an accumulation of secretory vesicles just behind, but distinct from, the hyphal tip (Grove and Bracker 1970, Howard 1981). The vesicle supply centre (VSC) model proposes that secretory vesicles are transported along the hypha and accumulate at the Spitzenkörper, before radiating out to fuse with the plasma membrane (Bartnicki-Garcia et al. 1989). The location of the Spitzenkörper means that a greater concentration of vesicles fuse with the tip than at other areas of the hypha. In computer modelling this model closely predicts the shape of hyphal tips (Bartnicki-Garcia et al. 1995).

The Spitzenkörper is thought to be critical and specific to hyphal growth, as yeast and pseudohyphal cells do not have Spitzenkörpers. The much faster extension rate of hyphal cells (0.125 µm/min compared to 0.0625 µm/min in yeast (Jones and Sudbery 2010)) may require a higher volume of secretory vesicles, which could lead to their accumulation in a Spitzenkörper structure. The Spitzenkörper is thought to drive hyphal growth, because changes in growth direction are preceded by re-positioning of the Spitzenkörper (Reynaga-Peña, Gierz and Bartnicki-Garcia 1997).

However, the exact composition and mechanism of the Spitzenkörper are still poorly understood. The lipophilic dye FM4-64, which stains membranes and is used to visualise endocytosis, labels the Spitzenkörper in many fungi (Fischer-Parton et al. 2000, Crampin et al. 2005). This indicates that at least some of the vesicles are of endocytic origin, though the mechanism behind this is not defined. The *C. albicans* Spitzenkörper has been shown to contain Mlc1 (myosin light chain 1, which regulates the class V myosin Myo2); Bni1 (a formin); and Sec4 and Sec2 (a vesicle associated GTPase and its GEF) (Crampin et al. 2005, Jones and Sudbery 2010).

### 6.1.2. Lipid markers of polarised growth

As described above, the network of proteins governing polarised growth and secretion in fungi is quite well characterised. However the lipid composition of the underlying plasma membrane is also key to polarised growth. Many polarity regulating proteins contain lipid binding domains to help localise them to the appropriate position at the plasma membrane. In hyphal growth certain lipids are enriched at the actively growing tip, however less is known about the mechanisms regulating the polarised distribution of these lipids.

#### Plasma membrane ergosterol

Sterols are a major constituent of cell membranes and confer rigidity. The main fungal sterol is ergosterol, making up 30 – 40% of the yeast plasma membrane (Schneiter et al. 1999). Lipid rafts are membrane domains enriched in sterols and sphingolipids (Brown and London 1998), and the asymmetric distribution of these rafts has been implicated in polarisation of a variety of cell types, from yeast to humans (Mañes et al. 2003). In yeast and fungi, lipid rafts cluster together and form µm sized sterol-rich domains (SRDs), which are present at the tips of mating projections in *S. cerevisiae* (Bagnat and Simons 2002) and at the hyphal tips of many fungal species, including *C. albicans* (Martin and Konopka 2004).

This feature seems to be specific to pseudohyphal or hyphal growth; yeast buds do not have polarised SRDs. Martin and Konopka (2004) suggested that SRDs at *C. albicans* hyphal tips arise from clustering of pre-existing lipid rafts, rather than de novo raft formation. It is unclear how SRDs are maintained at hyphal tips, though interactions between proteins within lipid rafts have been shown to promote and maintain raft clustering in T-cells (Janes et al. 2000).

It seems therefore that sterol polarisation is a common cell polarity mechanism, but its precise function remains unclear. Their distinct lipid composition means SRDs can cluster certain proteins; glycosylphosphatidylinositol (GPI)-anchored proteins for example are enriched in lipid raft domains (Brown and Rose 1992). This could be important for *C. albicans* cell growth, as many key cell wall maintenance and virulence proteins are GPI-anchored (Plaine et al. 2008).

## Plasma membrane PI(4,5)$P_2$

PI(4,5)$P_2$ is a minor constituent of cellular membranes, however it plays many important functional roles especially in membrane trafficking and cytoskeleton organisation. It is often critical to polarised growth, and its asymmetric distribution has been observed in several organisms. Vernay et al (2012) showed that PI(4,5)$P_2$ is concentrated towards growing buds and hyphal tips in *C. albicans* and that this is critical for hyphal morphology.

This long-range PI(4,5)$P_2$ gradient observed in *C. albicans* hyphae is relatively rare. Other polarised cells such as neuronal axons and *A. nidulans* do not have a PI(4,5)$P_2$ gradient (Micheva, Holz and Smith 2001, Pantazopoulou and Peñalva 2009). However, apically concentrated PI(4,5)$P_2$ has been observed in plant pollen tubes (Kost et al. 1999). *S. cerevisiae* yeast cells have PI(4,5)$P_2$ enriched at the growing bud and bud neck, and at the tip of mating projections, however it does not form a gradient of concentration, as is observed in *C. albicans* hyphae (Garrenton et al. 2010).

The mechanisms by which this PI(4,5)$P_2$ gradient is induced and maintained in *C. albicans* hyphal growth remain unclear. Vernay et al (2012) showed that Mss4, the PI(4)P-5-kinase, is concentrated at hyphal tips and is required for PI(4,5)$P_2$ polarisation. They also showed that PI(4)P synthesis (via Stt4 PI kinase) is required for PI(4,5)$P_2$ polarisation. They proposed that PI(4,5)$P_2$ clearance at the rear end of the cell, and slow membrane diffusion may also help maintain the gradient.

The function of this PI(4,5)$P_2$ gradient in *C. albicans* is not known, however many possibilities can be imagined. It may help to localise the polarity establishing machinery; in *S. cerevisiae* PI(4,5)$P_2$ binds exocyst subunits and septins (Zhang et al. 2008, Bertin et al. 2010), and is required for correct Cdc42 activation and actin cytoskeleton polarisation (Yakir-Tamang and Gerst 2009). PI(4,5)$P_2$ is involved in many aspects of endocytosis; it is bound by early arriving proteins such as AP-2 and Yap1801/1802 therefore this gradient could serve to concentrate endocytic events to the hyphal apex.

## Plasma membrane PI(4)P

The specific role of PI(4)P is less well studied. For some time, PI(4)P was thought of simply as a precursor to PI(4,5)$P_2$, but although the majority of PI(4,5)$P_2$ is synthesised in this way, depletion of cellular PI(4)P by 4-kinase inhibition has been shown to have only

a very minor effect on the synthesis and functions of $PI(4,5)P_2$ (Hammond et al. 2012), suggesting that PI(4)P may have functions independent of its $PI(4,5)P_2$ precursor role. PI(4)P has a role in establishing membrane negative charge and therefore recruiting transmembrane proteins (Hammond et al. 2012). It has also been suggested to play a role in recruitment of cargo and / or adaptor proteins to endocytic pits (Yamamoto et al. 2018).

The Arkowitz lab also showed that *C. albicans* hyphae have a steep PI(4)P gradient towards the hyphal tip (Ghugtyal et al. 2015). PM PI(4)P is mostly generated by the 4-kinase Stt4 (Yoshida et al. 1994), however this kinase is not polarised towards the hyphal tip (Vernay et al. 2012). By mathematical modelling, Ghugtyal et al (2015) predicted that polarised secretion of PI to the hyphal tip could lead to tip-localised PI(4)P generation, and that this gradient could be maintained by Sac1-dependent PI(4)P hydrolysis in sub-apical regions. Either deletion of *sac1*, or disruption of actin-based secretion via Latrunculin-A, led to loss of the PI(4)P gradient.

### 6.1.3. Regulation of plasma membrane lipids

#### Lipid regulation via ER-PM contact sites

Many proteins and lipids destined for the PM are synthesised or modified in the endoplasmic reticulum (ER). For the cell surface to undergo rapid remodelling in response to stimuli, the PM must feedback to the ER to regulate lipid biosynthesis. ER-PM contact sites are thought to allow rapid crosstalk between these two organelles, bypassing the classic secretory pathway (Stefan, Manford and Emr 2013). Membrane contact sites (MCSs) have been an area of active research in recent years and have been shown to have roles in lipid transport and regulation, cell signalling, and organelle architecture. Since most lipids are synthesised in the ER and transported to the PM in a vesicle-independent manner, it has been proposed that ER-PM contacts act as sites for their incorporation to the PM, and in co-ordinating lipid requirements of the PM with their biosynthesis in the ER (Pichler et al. 2001, Gatta and Levine 2017).

20 - 45% of the yeast PM is associated with cortical ER (cER), held around 30 nm apart (Wei et al. 2012). Three families of ER-PM tethering proteins serve to keep the two membranes in close proximity: VAP proteins Scs2/22; Tbc1/2/3 (tricalbins; orthologs of E-Syt proteins); and Ist2 (related to TMEM16 channels). These proteins are anchored in the ER and bind the PM via lipid or protein binding domains (Manford et al. 2012,

Toulmay and Prinz 2012). *Sc*Ist2 for example has 8 transmembrane domains, and a C-terminal PB (polybasic) domain proposed to bind PIP phospholipids in the PM inner leaflet (Wolf et al. 2012).

Cells lacking tethering proteins have aberrant ER morphology and accumulate excess PI(4)P in their PM (Manford et al. 2012). In a recent paper by Quon et al., (2018), the ER was untethered from the PM via deletion of tethering proteins, and surprisingly sterol transfer between the ER and PM remained robust. However the PM sterols in this strain were perturbed, which was shown to be due to phospholipid disruptions, particularly PI(4)P accumulation in the PM. This finding highlights the importance of ER-PM contacts in the integrated regulation of sterols and phospholipids.

## Lipid regulation via ORP / Osh proteins

As sterols are highly insoluble, their transport is thought to require lipid transport proteins (Mesmin, Antonny and Drin 2013). The ORP family (OSBP (oxysterol binding protein) – related proteins), are thought to be key players, possibly regulating sterol transfer at ER-PM contact sites (Beh et al. 2012, Schulz et al. 2009).

*S. cerevisiae* has seven ORPs, named Osh1 – 7 (see figure 6.13). They are homologues of mammalian OSBP, and part of a large family of lipid-binding proteins. They have roles in many processes including lipid metabolism, trafficking and signalling (Raychaudhuri and Prinz 2010). All ORPs share a conserved ORD (OBSP-related domain) at their C-terminal, which mediates lipid transport and signalling. Combined deletion of all 7 Osh genes is lethal, and a conditional mutant had severe defects in sterol and lipid distribution (Beh and Rine 2004).

*S. cerevisiae* Osh4 binds both sterol and PI(4)P, and exchanges sterol for PI(4)P across membranes (de Saint-Jean et al. 2011). *Sc*Osh3 also binds PI(4)P, however lacks sterol binding ability (Tong et al. 2013).

## Lipid regulation via Sac1

*S. cerevisiae* Sac1 is an integral ER and Golgi protein known to control PI(4)P levels at the ER and Golgi but also at the PM. It is still debated whether Sac1 is able to act 'in trans' and dephosphorylate PM PI(4)P from the ER. The most likely explanation seems to be that it acts via membrane contacts sites (MCSs), where the two membranes are in close

proximity (Manford et al. 2010). Sac1 has been shown to require Osh family proteins for its function.

*Sc*Osh3 – Osh7 have been shown to regulate PM PI(4)P levels via regulation of the Sac1 PI(4)P phosphatase at membrane contact sites (Stefan et al. 2011). Osh3 was shown to localise to ER-PM contact sites, dependent on PM PI(4)P levels (Stefan et al. 2011). Here it activates Sac1 phosphatase activity, which turns over PI(4)P. Thus, *Sc*Osh3 both senses PM PI(4)P levels, and regulates its turnover.

# Chapter 6 Results

## 6.2. Cells without AP-2 have the same number of actin patches at their hyphal tips as WT

Cells of each strain were induced to form hyphae then fixed and stained with rhodamine-conjugated phalloidin, to visualise actin structures. This has been shown in Knafler et al (2019), but here we wanted to count individual actin patches to get a better idea of the number of endocytic events occurring. Actin patches at the hyphal tips were counted, using Z-stacks so that the whole of the tip was assessed. This analysis showed that WT hyphae had an average of 8.85 patches per hyphal tip, and hyphae without *apm4* had an average of 8.7 (n = 40 cells per strain, see figure 6.2A). These are not significantly different, indicating that the absence of AP-2 does not affect endocytic site initiation or progression. Figure 6.2B shows representative images of actin patches at hyphal tips of both strains.

## 6.3. The exocyst component Sec3 is partially mis-localised in the absence of AP-2

In order to gain more of an insight into the status of polarity modules in the *apm4* mutant, several key polarity markers were tagged with GFP in both WT and *apm4* deletion cells, and their localisation analysed. The first of these was Sec3, a component of the exocyst complex. In both WT and *apm4* deletion yeast, Sec3-GFP signal was

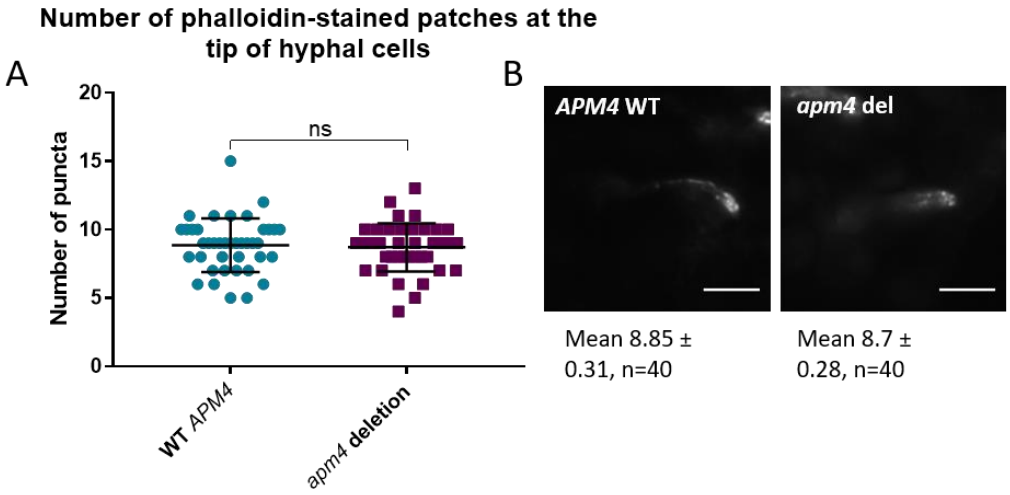


**6.2. Cells without AP-2 have no reduction in actin patches at their hyphal tips**
(A) Cells of each strain were induced to form hyphae for 90 minutes then fixed, stained with 5% rhodamine-phalloidin and imaged. Z-stacks were taken to encompass the whole of the hyphal tip, then the number of puncta present in the 4 $\mu m^2$ tip region were counted. Graph shows data from 40 cells from 2 independent experiments. Stats is a T-test and error bars show SD. (B) Representative images of hyphae from each strain, 1 z-section shown. Scale bars 5 µm.

observed in peripheral puncta, concentrated at growing buds and mother-bud necks (indicated by arrows; figure 6.3A). In WT hyphae, the puncta were highly polarised to hyphal tips, and formed a bright crescent at the surface of each hyphal tip (figure 6.3A). In *apm4* deletion hyphae, the Sec3-GFP was clearly still polarised to hyphal tips, but the crescent appeared to be spread over a larger area than in WT. This is represented by intensity profiles of hyphal tips in figure 6.3B, C. A more pronounced difference was observed in hyphal mother cells: in WT hyphae Sec3-GFP puncta were rarely observed in hyphal mother cells (mean = 1.0 puncta / mother cell; n > 80 cells) however *apm4* deletion cells had many Sec3-GFP puncta in their hyphal mother cells (mean = 3.3 puncta / mother cell; n > 80 cells; representative images figure 6.3D; quantified in figure 6.3E).

These results indicate that the AP-2 complex is not required for Sec3 localisation in yeast, and Sec3 polarisation to the hyphal tip can occur in its absence, however AP-2 is critical to preventing the mis-localisation of Sec3 to other parts of hyphae such as their mother cells.

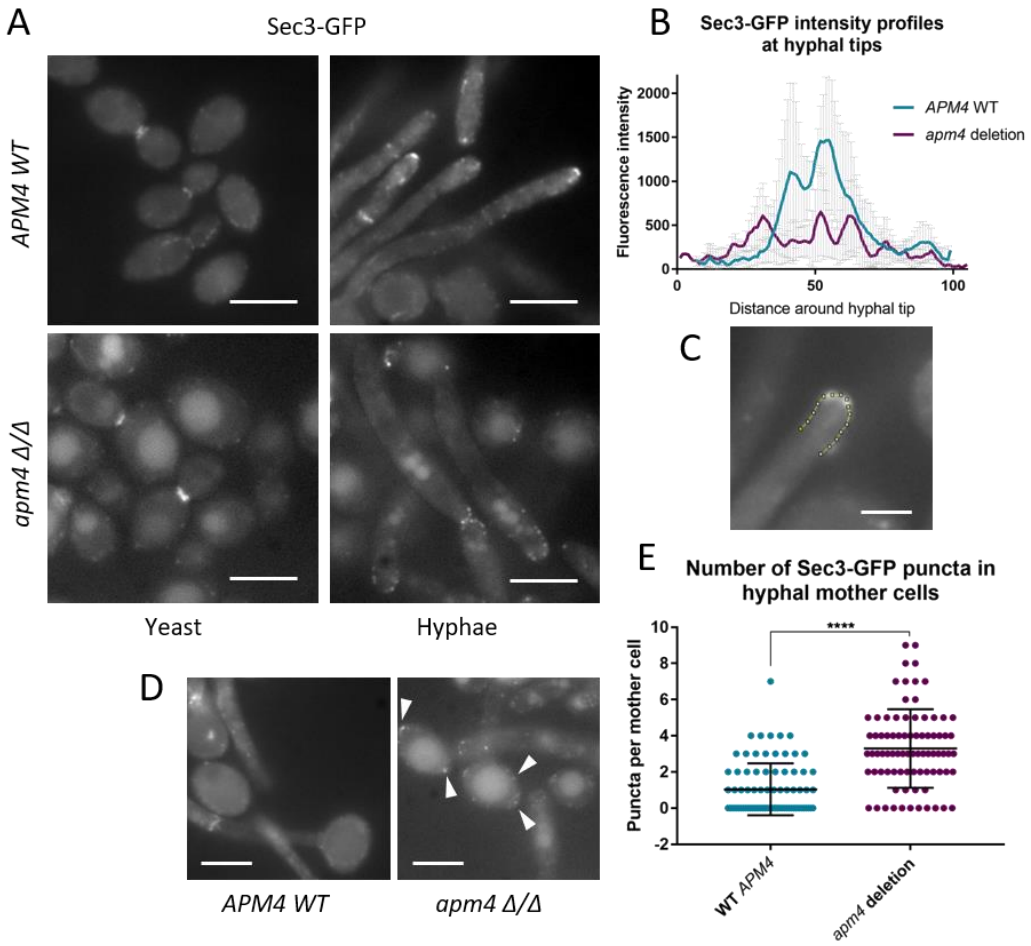


**6.3. The exocyst component Sec3 is partially mis-localised in the absence of AP-2**

(A) Sec3-GFP, tagged in an otherwise WT strain and in a homozygous *apm4* deletion strain. Cells grown as yeast or 90 min hyphae then imaged. Arrows show examples of puncta localised to yeast mother-bud necks and hyphal tips. (B) Line profiles drawn around tips of 3 representative hyphae / strain; graph shows mean Sec3-GFP intensity. (C) Example of how line profiles were drawn on images of hyphal tips using FIJI. (D) Representative images of Sec3-GFP signal in mother cells of both *APM4* WT and *apm4* deletion hyphae. Arrows show examples of peripheral puncta in mother cells. (D) 80 hyphal cells / strain assessed for number of Sec3-GFP puncta visible in their mother cells. Data from 2 experiments; stats is a Mann-Whitney test. All error bars show SD. All scale bars are 5 µm.

## 6.4. The exocyst component Sec8 is partially mis-localised in the absence of AP-2

Another component of the exocyst, Sec8, was also tagged with GFP and its localisation analysed. Its pattern of localisation was very similar to that of Sec3, with peripheral puncta enriched at growing buds, mother-bud necks, and hyphal tips, in both WT and *apm4* deletion cells (figure 6.4A, B, C). However, also like Sec3, Sec8-GFP puncta were

spread over a larger area at the tips of hyphae lacking *apm4* and were also present throughout the length of the hyphae and in mother cells, which was not the case in WT (figure 6.4D, E). Sec8 showed a similar level of mis-localisation as Sec3, with a mean of 3.25 puncta / mother cell (compared to 0.68 in WT; n > 80 cells).

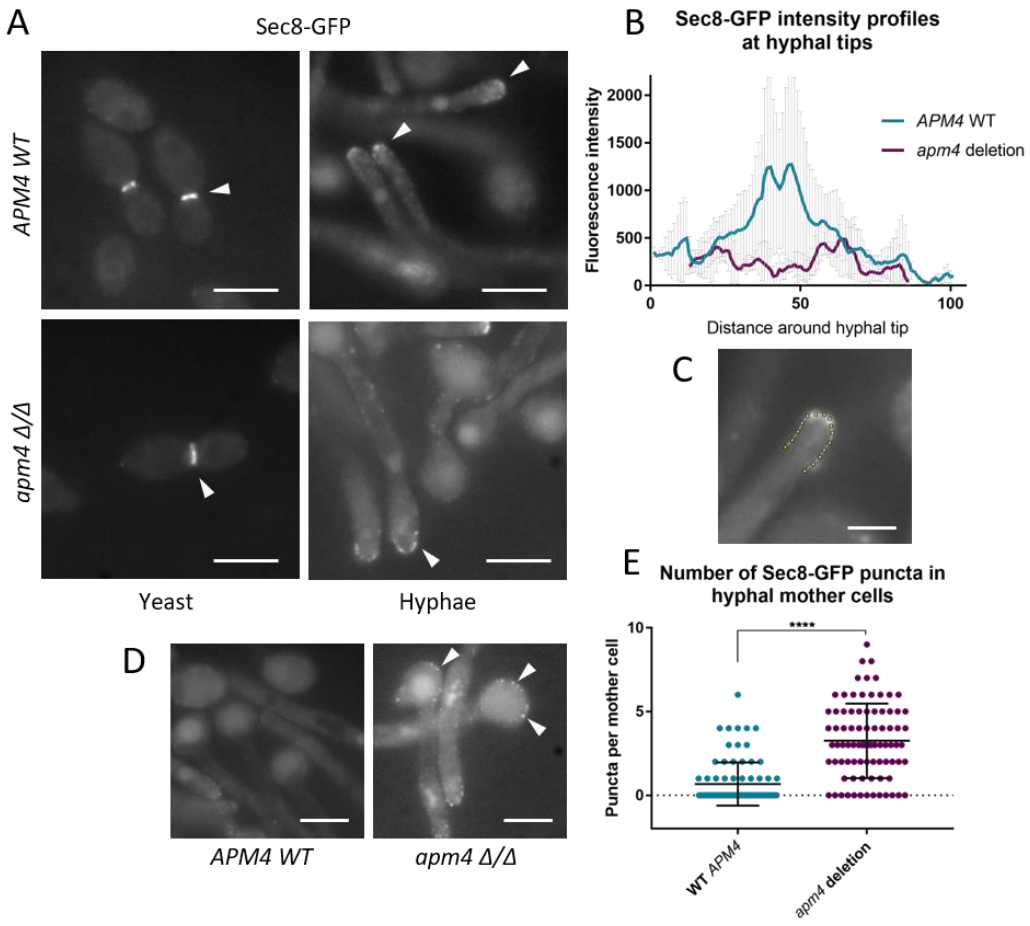


**6.4. The exocyst component Sec8 is partially mis-localised in the absence of AP-2**
(A) Sec8-GFP, tagged in an otherwise WT strain and in a homozygous *apm4* deletion strain. Cells grown as yeast or 90 min hyphae then imaged. Arrows show examples of puncta localised to yeast mother-bud necks and hyphal tips. (B) Line profiles drawn around tips of 3 representative hyphae / strain; graph shows mean Sec8-GFP intensity. (C) Example of how line profiles were placed on images of hyphal tips using FIJI. (D) Representative images of Sec8-GFP signal in hyphal mother cells, of both *APM4* WT and *apm4* deletion cells. Arrows show examples of peripheral puncta in mother cells. (E) 80 hyphal cells / strain assessed for number of Sec8-GFP puncta visible in their mother cells. Data from 2 experiments; stats is a Mann-Whitney test. All error bars show SD. All scale bars are 5 µm.

Taken together, these results suggest that the exocyst, and therefore possibly secretory vesicle targeting are not restricted to the site of active growth in the absence of AP-2. Although some polarisation of secretion to the hyphal tip is clearly taking place, the

presence of exocyst components around the mother cells suggests secretion could be occurring here in the absence of AP-2.

## 6.5. The polarisome component Spa2 is mis-localised in hyphae in the absence of AP-2

Spa2, a component of the polarisome complex, was also tagged with GFP to see whether the polarisome showed a similar partial mis-localisation to the exocyst. Spa2-GFP localisation was similar to that of the exocyst in WT cells, with peripheral puncta enriched to growing buds and mother-bud necks in yeast, and a crescent at the tips of hyphae (figure 6.5A). In *apm4* deletion cells the yeast localisation looked similar to WT (figure 6.5A), however in hyphal cells the Spa2-GFP was highly de-polarised, with enrichment to the hyphal tip only evident in 20% of cells (compared to 88% of WT cells; n = 60 cells; figure 6.5A, quantified in figure 6.5B). 80% of hyphae without AP-2 had Spa2-GFP puncta all around the cell periphery, with no clear polarisation towards the actively growing tip (n = 60 cells). When looking at hyphal mother cells, most WT cells had no Spa2-GFP puncta, whereas *apm4* deleted cells had a mean of 2.8 puncta per mother cell (n > 70 cells; representative images figure 6.5C, quantified in figure 6.5D).

These results suggest that the polarisome has a greater degree of mis-localisation than the exocyst in hyphal cells without AP-2.

## 6.6. The localisation of Mlc1 is shifted in the absence of AP-2

A fourth marker of polarised growth, Mlc1, was tagged with GFP in WT and *apm4* deletion cells. In yeast cells, Mlc1-GFP showed a similar pattern of localisation in WT and *apm4* deletion cells, predominantly at growing buds and mother-bud necks (figure 6.6A). In hyphal cells, two patterns of localisation were observed: either a bright circle within the hyphal tip (termed Spitzenkörper-like) or a crescent of puncta at the surface of the hyphal tip (termed polarisome-like) - these two localisations have been reported in (Crampin et al. 2005). The two different patterns of localisation were observed in both WT and *apm4* deletion hyphae, but in very different proportions (figure 6.6B, C). In WT hyphae, 53% had a Spitzenkörper-like structure at the tip, whereas in *apm4* deletion hyphae just 11% had Spitzenkörper-like Mlc1. Many more hyphae without AP-2 showed no Mlc1-GFP enrichment to the tip (53% compared to 4% of WT hyphae, n > 140). The

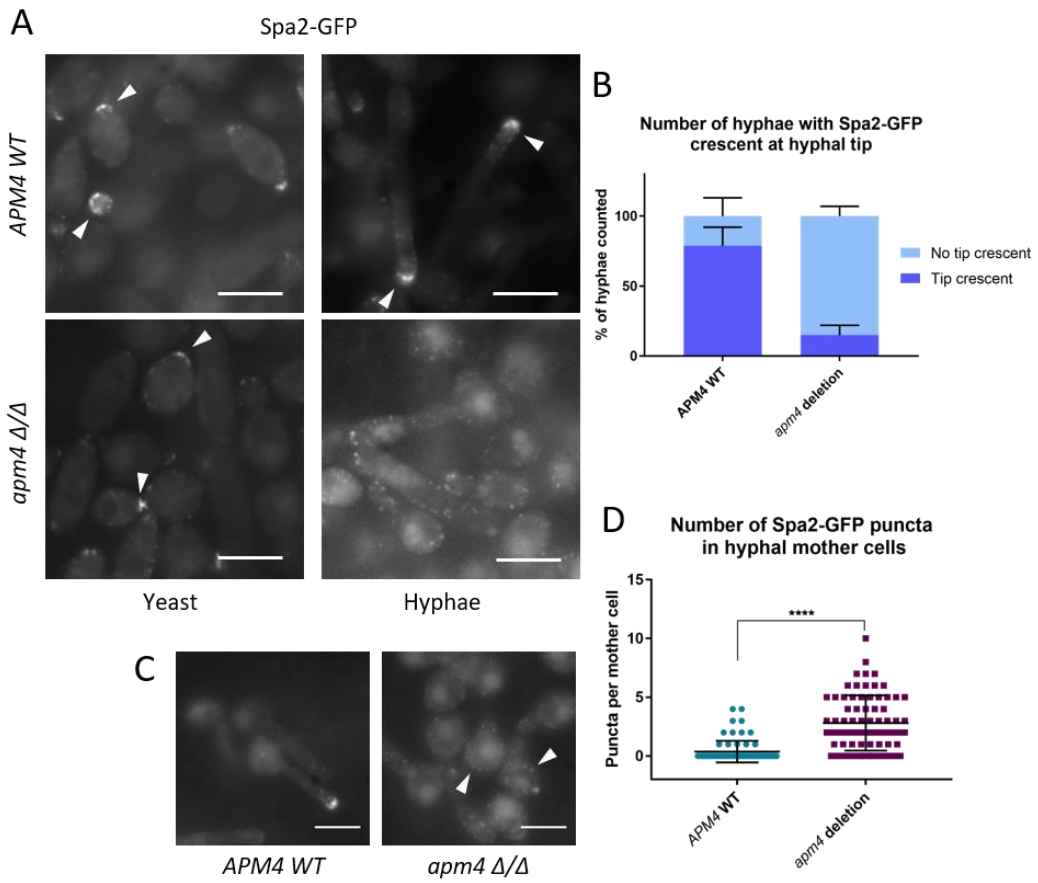


**6.5. The polarisome component Spa2 is mis-localised in hyphae in the absence of AP-2**
(A) Spa2-GFP, tagged in an otherwise WT strain, and in a homozygous *apm4* deletion strain. Cells grown as yeast or 90 min hyphae then imaged. Arrows show examples of puncta localised growing buds and hyphal tips. (B) >70 hyphal cells / strain were analysed and recorded whether a crescent of Spa2-GFP puncta was visible at the hyphal tip. Data from 2 independent experiments. (C) Representative images of Spa2-GFP signal in hyphal mother cells, of both *APM4* WT and *apm4* deletion cells. Arrows show examples of peripheral puncta in mother cells. (D) >70 hyphal cells / strain were analysed and the number of Spa2-GFP puncta visible in their mother cells was recorded. Data from 2 independent experiments. Stats is a Mann-Whitney test. All error bars show SD. All scale bars are 5 µm.

two strains had a similar proportion of hyphae with polarisome-like Mlc1-GFP (see figure 6.6B).

This data suggests that hyphae without AP-2 are much less likely to have Mlc1-GFP at a Spitzenkörper at the hyphal tip compared to WT, though we cannot tell whether it is the Spitzenkörper itself, or just the presence of Mlc1, which is absent in these cells.

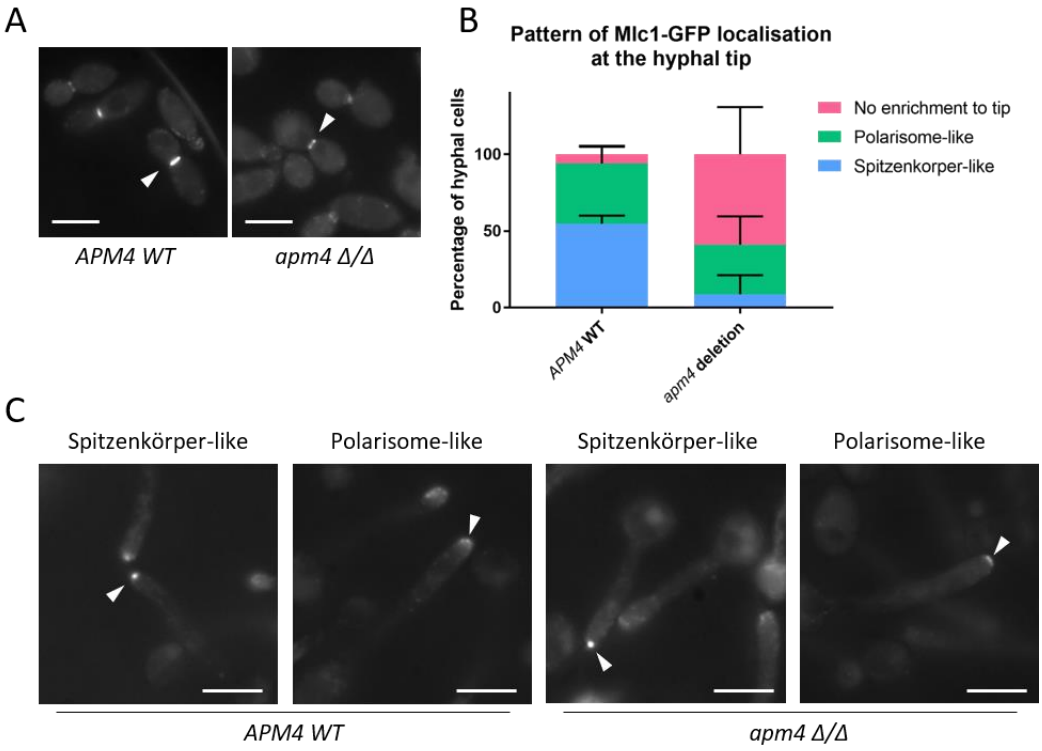


**6.6. The localisation of Mlc1 is shifted away from the Spitzenkörper in the absence of AP-2**
(A) Representative images of Mlc1-GFP tagged yeast cells, arrows show signal localised to mother-bud necks. (B) Mlc1-GFP tagged cells were grown as hyphae then recorded whether the Mlc1-GFP signal at the hyphal tip looked 'polarisome-like' (a surface crescent of puncta); Spitzenkörper-like (a sub-apical circular structure); or showed no enrichment to the hyphal tip. n>140 cells / strain from 2 independent experiments. Error bars show SD. (C) Example images of 'Spitzenkörper-like' and 'polarisome-like' localisations (indicated by arrows) in both *APM4* WT and *apm4* deletion hyphae. All scale bars are 5 µm.

## 6.7. Hyphae without AP-2 are less likely to have a Spitzenkörper

To help us determine whether hyphae without an Mlc1-labelled Spitzenkörper had a Spitzenkörper at all, we used a brief pulse of FM4-64 labelling to visualise the Spitzenkörper independently of any resident proteins. It is not fully understood why the lipophilic dye FM4-64 briefly labels the Spitzenkörper after around 10 minutes incubation with hyphal cells, but it has been known to for some time (Fischer-Parton et al. 2000, Hoffmann and Mendgen 1998, Crampin et al. 2005).

Upon brief incubation with FM4-64, a Spitzenkörper-like structure was observed in around 90% of WT hyphae, and around 40% of *apm4* deletion hyphae (figure 6.7A, representative images in 6.7B). This FM4-64 staining was also performed in the Mlc1-GFP tagged strains, and the two signals co-localised (figure 6.7C). You may note that a higher proportion of hyphae from both strains were observed to have a Spitzenkörper

via FM4-64 staining compared with Mlc1-GFP. It may be harder to see the Mlc1-GFP stained Spitzenkörper due to weaker fluorescence signal, and the 'polarisome-like' Mlc1-GFP localisation may not mean that a Spitzenkörper is not present, but only that more Mlc1 is localised to the hyphal tip at that point.

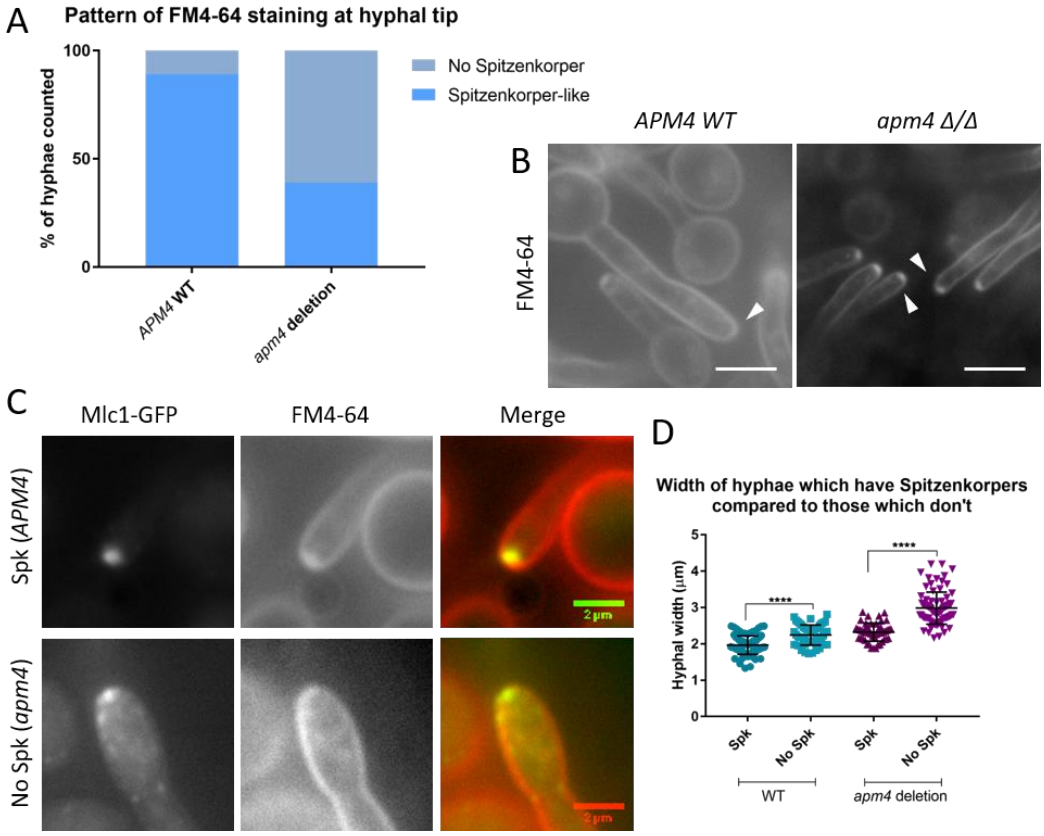


6.7. Hyphae without AP-2 are less likely to have a Spitzenkörper

(A) Cells were grown as hyphae then briefly stained with FM4-64, then recorded whether a Spitzenkörper-like structure (bright circular patch) was visible at the hyphal tip. 100 cells / strain were analysed, from 1 experiment. (B) Representative images of *APM4* WT and *apm4* deletion hyphae stained with FM4-64. Arrows point to presence (WT) or absence (*apm4*) of Spitzenkörper. (C) Representative images of Mlc1-GFP expressing hyphae stained with FM4-64. Top row is example of a WT *APM4* hypha with a Spitzenkörper; bottom row is an example of an *apm4* deletion hypha without a Spitzenkörper. (D) The width of Mlc1-GFP tagged and FM4-64 stained hyphal cells was measured on FIJI (measurement taken at widest point on hypha) and recorded whether that hypha had a Spitzenkörper or not. >100 cells / strain were measured from 3 independent experiments. Error bars show SD; stats are one-way ANOVAs with Tukey's post hoc tests. Scale bars are 5 µm unless otherwise indicated.

It was also observed that, particularly in *apm4* deletion hyphae, those without a Spitzenkörper appeared wider than those with a Spitzenkörper. This is quantified in figure 6.7D, and surprisingly revealed that although hyphae without AP-2 are

significantly wider than WT (see Knafler et al, 2019), the small proportion of *apm4* deletion hyphae which had a Spitzenkörper were similar in width to the small proportion of WT hyphae which did not have a Spitzenkörper. This could indicate the importance of the Spitzenkörper in maintaining polarised growth and tip morphology. For this analysis, hyphae were recorded to have a Spitzenkörper when it was observed both via FM4-64 and Mlc1-GFP fluorescence.

## 6.8. Markers were used to visualise plasma membrane PI(4)P and PI(4,5)$P_2$

The above results show that protein components of the polarisome, exocyst and Spitzenkörper modules are less polarised towards the hyphal tip in the absence of AP-2. However as most of these components are not transmembrane proteins, we thought it unlikely they are direct cargoes of AP-2 themselves. To try to gain more insight into the disruption of multiple polarity modules in *apm4* deleted cells, we looked at plasma membrane phospholipids PI(4)P and PI(4,5)$P_2$ which are thought to be important in localising polarised components.

The Arkowitz lab very kindly shared their two markers for plasma membrane phospholipids which they have optimised for use in *C. albicans*. To visualise PI(4)P, the PH domain of Osh2 fused to two GFPs (pADH1- GFP-$PH^{OSH2}$-$PH^{OSH2}$-GFP) was used (Ghugtyal et al. 2015). To visualise PI(4,5)$P_2$, the PH domain of rat Plexstrin-homology protein was fused to two GFPs (GFP-$PH^{Plc\delta}$-$PH^{Plc\delta}$-GFP; (Vernay et al. 2012)). Both of these GFP fusions have been cloned into the plasmid pExpArg which allows the genes to be integrated into the RPS1 locus of the genome and thus expressed highly in transformed strains.

The pExpArg plasmids described were linearized and transformed into our wild-type and *apm4* deletion strains separately. As shown in figure 6.8, strong GFP signal is observed at the cell periphery of cells grown as either yeast or hyphae. Images of these phospholipid marker strains are presented with the 'Fire' look-up table (LUT; FIJI) to allow easier visual assessment of fluorescence intensity.

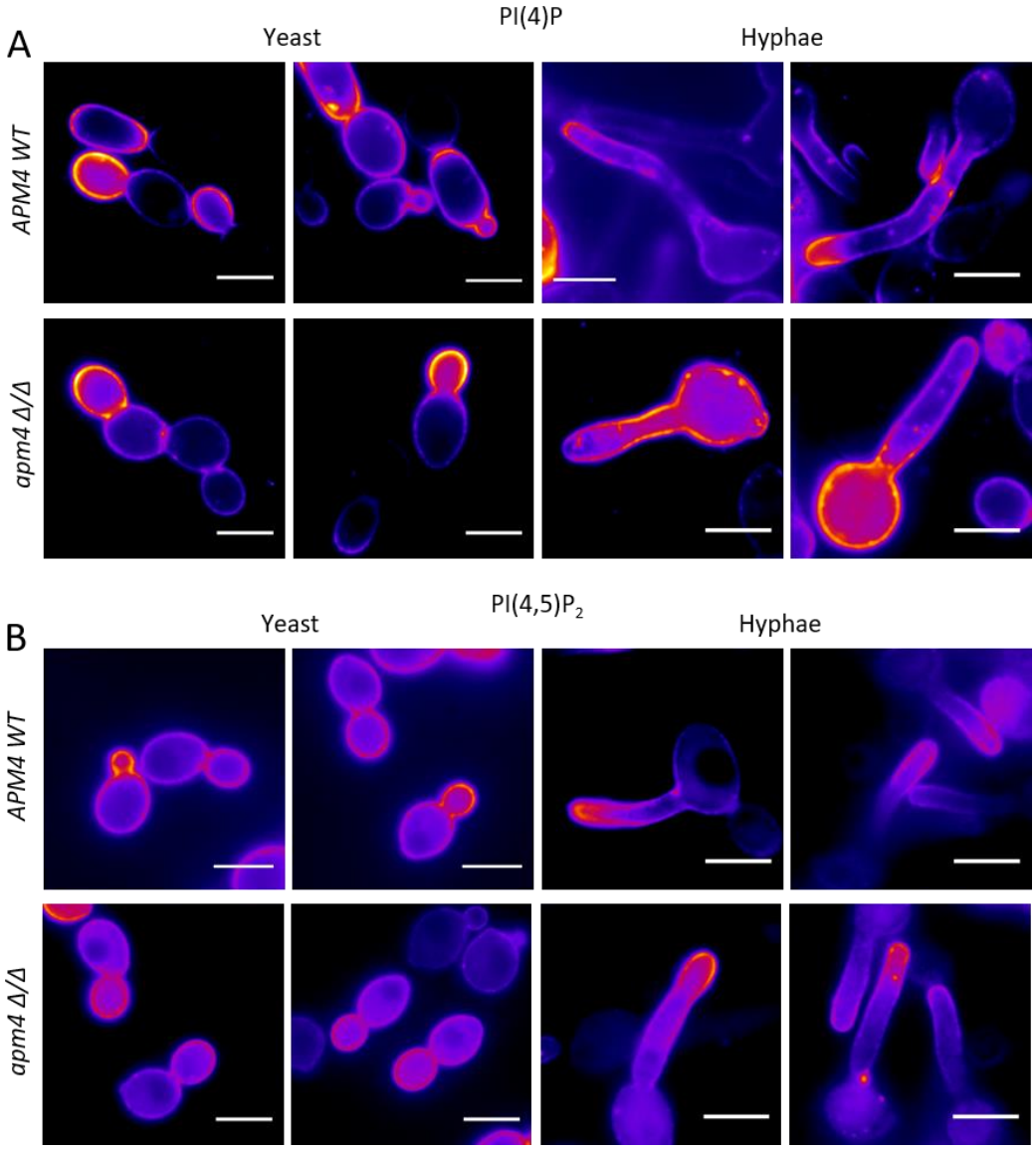


**6.8. Markers were used to visualise plasma membrane PI(4)P and PI(4,5)$P_2$**
(A) pADH1- GFP-$PH^{OSH2}$-$PH^{OSH2}$-GFP was integrated into the RPS1 locus of both WT and *apm4* deletion strains, as a marker of plasma membrane PI(4)P. Representative images of both strains, grown as yeast and hyphae, are shown here. (B) GFP-$PH^{Plc\delta}$-$PH^{Plc\delta}$-GFP was separately integrated into the RP locus of both WT and *apm4* deletion strains, as a marker of plasma membrane PI(4,5)$P_2$. Representative images of both strains grown as yeast and hyphae are shown. All images visualised with 'Fire' LUT on FIJI. All scale bars are 5 µm.

## 6.9. Hyphae without AP-2 have depolarised plasma membrane PI(4)P but not PI(4,5)$P_2$

In yeast cells, the distributions of both phospholipids were polarised towards the growing bud, and this was the case in WT and *apm4* deletion cells (see figure 6.8A, B). In WT hyphae, both phospholipids were polarised towards the hyphal tip, though PI(4)P

formed a steeper gradient or cap at the hyphal tip than PI(4,5)$P_2$ (figure 6.8 and 6.9). In *apm4* deletion hyphae, the PI(4,5)$P_2$ signal remained polarised to the hyphal tip as in WT, however the PI(4)P polarisation was lost, with more PI(4)P in the mother cell than the hypha (images in figure 6.8, quantified in figure 6.9).

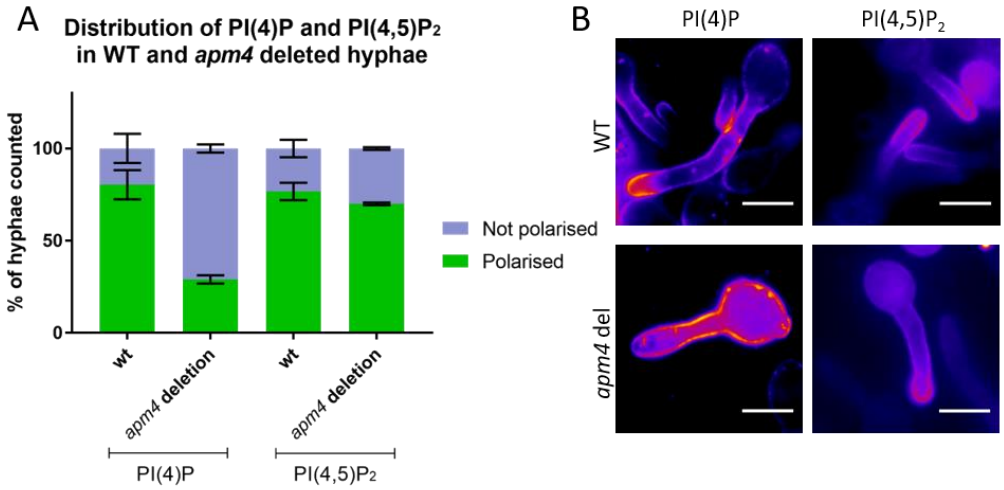


**6.9. Cells without AP-2 are defective in polarising PI(4)P but not PI(4,5)$P_2$.**
(A) Hyphal cells expressing either PI(4)$P^{OSH2\text{-}GFP}$ or PI(4,5)$P_2^{Plc\delta\text{-}GFP}$ were imaged and recorded whether they showed GFP polarisation towards the hyphal tip. n > 100 cells / strain from 2 independent experiments. (B) Representative images of these hyphal cells, visualised using the 'Fire' LUT on FIJI. Scale bars are 5 µm.

## 6.10. Yeast cells without AP-2 have similar PI(4)P and PI(4,5)$P_2$ fluorescence intensity to WT cells

The AP-2 complex appears to play some role in the localisation of plasma membrane phosphoinositides. We next wished to know whether cells without AP-2 had comparable levels of these phosphoinositides to WT. Due to the very different morphologies of hyphal cells of the two strains, and the difference in PI distribution, the fluorescence intensity has only been measured in yeast mother cells.

To get a measure of GFP intensity, cells expressing either PI(4)$P^{OSH2\text{-}GFP}$ or PI(4,5)$P_2^{Plc\delta\text{-}GFP}$ were grown as yeast and imaged. FIJI was used to draw 3 2 µm lines per mother cell, crossing the plasma membrane. From these, the peak fluorescence intensity minus the background intensity was taken. The 3 lines per cell were averaged, and values from 60 cells / strain are shown in figure 6.10A and D. Representative images in figure 6.10B, C. The graphs show that WT and *apm4* deletion yeast cells have similar GFP intensity for

both lipids. The *apm4* deletion cells have a slightly lower mean intensity than WT, perhaps due to a population of cells with very low (near 0) GFP intensities. However there is a high variance in intensity values for both strains, and any difference between them is small.

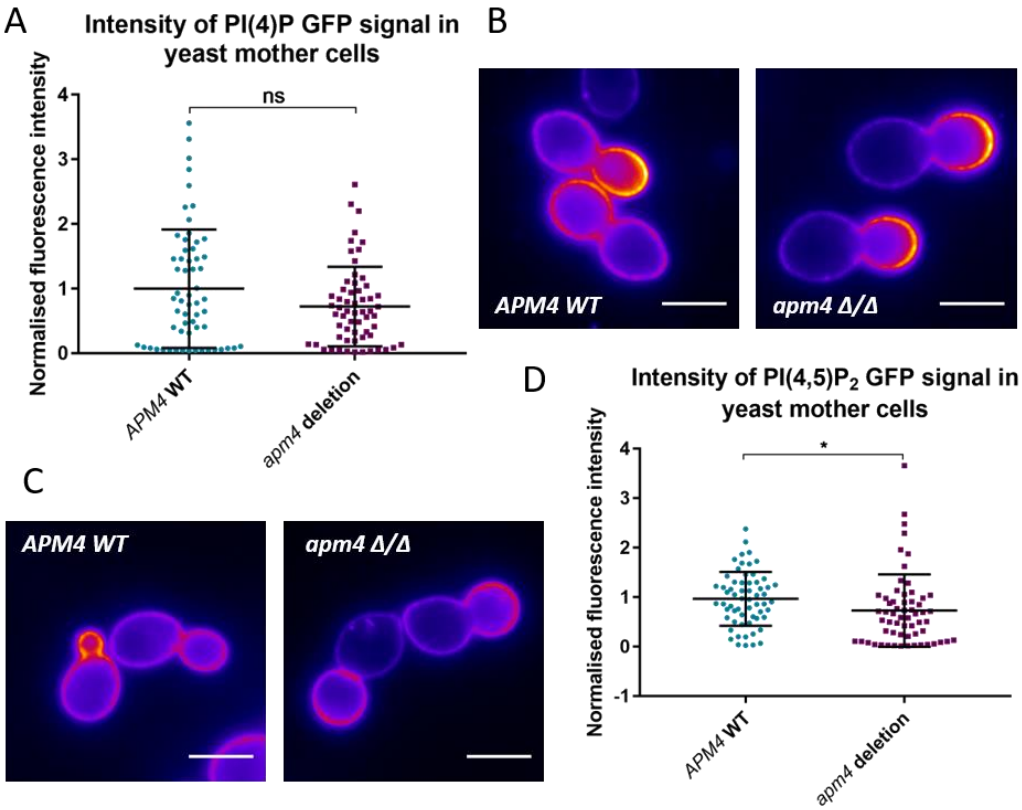


**6.10. Yeast without AP-2 have similar PI(4)P and PI(4,5)$P_2$ fluorescence intensity to WT**
(A, D) Cells expressing either PI(4)$P^{OSH2\text{-}GFP}$ or PI(4,5)$P_2^{Plc\delta\text{-}GFP}$ were grown as yeast and imaged. FIJI was used to draw lines across the plasma membranes of mother cells. From these, the peak intensity of PM staining (minus background) was taken. 3 lines were averaged per cell, and 60 cells were measured per strain (from 3 independent experiments). Values normalised to the mean WT value for each experiment. (B, C) Representative images of these yeast cells, visualised using the 'Fire' LUT on FIJI. All scale bars are 5 µm. In (A) stats is a Mann-Whitney test, P = 0.193. In (D) stats is an unpaired T-test, P = 0.0434.

This analysis indicates that the two strains have similar levels of PI(4)P and PI(4,5)$P_2$ per unit area of membrane. However it cannot tell us the absolute levels of the phospholipids and given that the *apm4* mutant has larger cells than WT, we may expect it to have a higher overall amount of phospholipid simply due to increased membrane area. Accurate analysis of lipid levels could be achieved via lipidomics. In this simple analysis however, we can conclude that cells without AP-2 have similar levels and localisation of PI(4)P and PI(4,5)$P_2$ in their yeast cells as WT. This is in contrast to hyphal

cells, in which PI(4,5)$P_2$ is not affected but PI(4)P is highly depolarised in the absence of AP-2. Taken together this data indicates that *C. albicans* cells have different mechanisms for distributing PM phospholipids in yeast compared to hyphal cells. AP-2 plays a role in the polarised hyphal distribution of PI(4)P but not of PI(4,5)$P_2$.

## 6.11. Cells without AP-2 have defective ergosterol localisation and levels

As AP-2 appears to be required for the distribution of PI(4)P, we also examined another key membrane lipid, ergosterol. Figure 6.11A has already been published in Knafler et al, 2019 (chapter 4) however I have reproduced it here in order to show it alongside the other membrane lipids data. Ergosterol was visualised using filipin complex (from *Streptomyces;* Sigma), a fluorescent molecule which binds ergosterol in the fungal membrane. Hyphal cells were fixed and stained with filipin, then imaged and recorded whether a bright patch was visible at the hyphal tip. Figure 6.11A shows quantification of >200 cells / strain, and 6.11B shows representative images, presented using the 'Green Fire Blue' LUT on FIJI. Hyphae without AP-2 have lost the bright ergosterol-rich domains present in most (76% of) WT hyphae. This loss of SRDs is not rescued by *chs3* deletion, indicating that it is independent of chitin levels; however it is rescued by addition of the *apm4*$^{1-454}$ cargo binding mutant, indicating that this defect is independent of YxxΦ motif binding (figure 6.11A).

Ergosterol shows less obvious polarisation in yeast cells than in hyphae, however it does show some enrichment to small and growing buds, and bud necks at cytokinesis. As with the PM phosphoinositides, yeast cells without AP-2 have polarised ergosterol similar to WT yeast (representative images figure 6.11C). The intensity of fluorescent staining in yeast mother cells was also measured, as described above. Figure 6.11D shows that yeast cells without AP-2 have reduced filipin staining compared to WT. This suggests yeast cells without AP-2 have less ergosterol in their PM than WT. This could indicate a role for AP-2 in ergosterol biosynthesis or delivery to the yeast PM, however it could be simply due to their larger cell size, meaning the same amount of ergosterol would be more spread over a larger area of membrane.

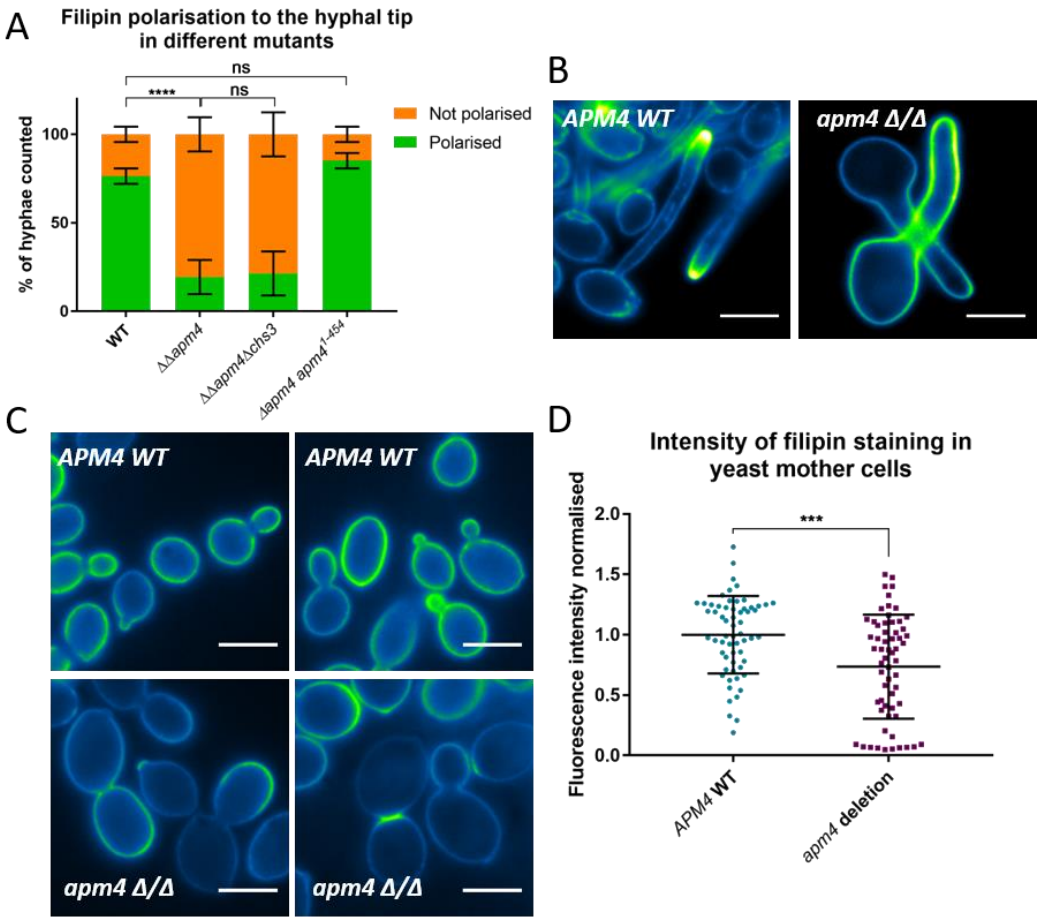


**6.11. Cells without AP-2 have defects in ergosterol localisation and levels**

(A) Cells of different strains were grown as hyphae then fixed and stained with filipin and imaged. >200 cells / strain from 3 independent experiments analysed and recorded whether the filipin was polarised to a patch at the hyphal tip. Stats are two-way ANOVAs with Tukey's multiple comparisons. (B) Representative images of WT hyphae with filipin polarised to tip; and *apm4* hyphae with no filipin polarisation. (C) Representative images of yeast cells of each strain stained with filipin. (D) Filipin stained yeast cells analysed on FIJI by drawing lines across the plasma membranes of mother cells. From these, the peak intensity of PM staining (minus background) was taken. 3 lines averaged per cell, and 60 cells measured per strain (from 3 independent experiments). Values normalised to the mean WT value for each experiment. Stats is a T-test with Welch's correction. All error bars show SD. All scale bars 5 µm. Images visualised with 'Green Fire Blue' LUT on FIJI.

## 6.12. Cells without AP-2 have increased sensitivity to fluconazole and myriocin

To gain further insight into plasma membrane composition and distribution in the *apm4* deletion mutant, growth was assessed in the presence of three drugs which target different aspects of lipid metabolism. A plate spotting assay was used, in which 10-fold serial dilutions of cells were spotted onto agar plates containing each drug. Plates were incubated at 30°C or 37°C for 48 hours, then imaged and the minimum cell

concentration required for growth recorded (ie the smallest dilution at which visible colony growth was observed). Data from the two temperatures were combined, as they all showed the same pattern of growth. Figure 6.12 shows graphs plotted with data from 6 agar plates per condition. To the right of each graph is a photograph of a representative plate of that condition grown at 30°C. For all plates, 4 strains of *C. albicans* were spotted in the same order: top row is WT; second row *apm4 Δ/Δ*; third row *apm4 Δ/Δ , chs3Δ*; fourth row *apm4 Δ / apm4*$^{1-454}$ (the YxxΦ cargo binding mutant).

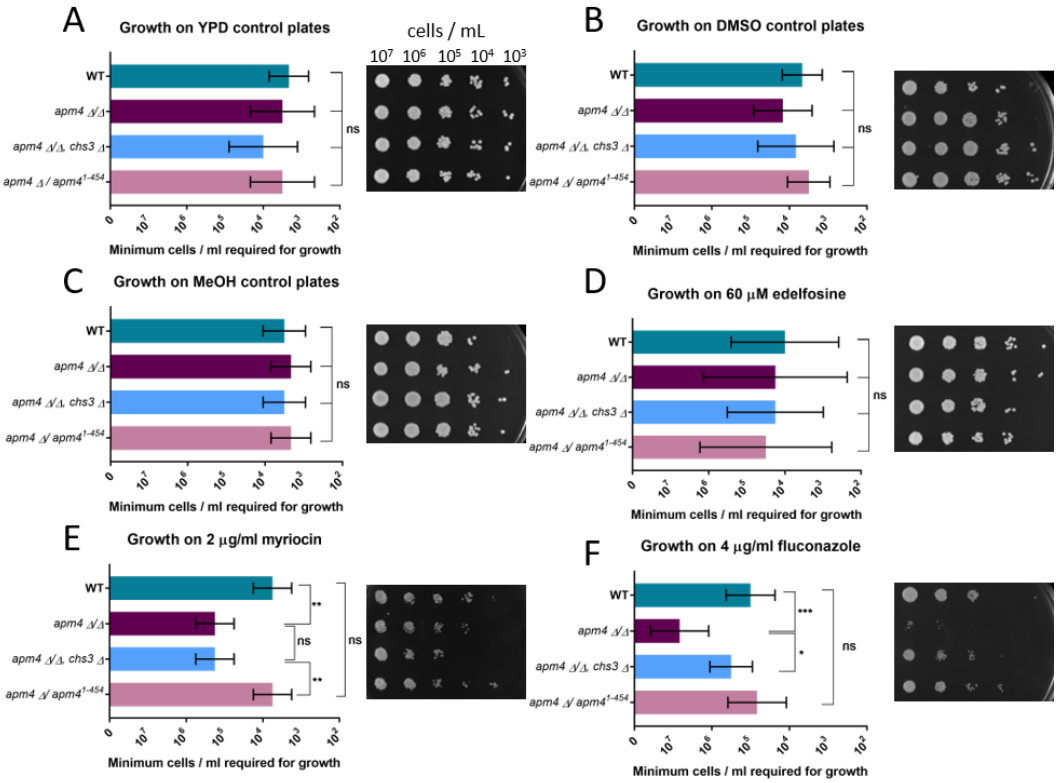


**6.12. Cells without AP-2 have increased sensitivity to fluconazole and myriocin**

(A – F) Ten-fold serial dilutions of cells were spotted onto agar plates containing various chemical additions. Plates were incubated at 30°C or 37°C for 48 hours then imaged. Representative images of 30°C plates shown here (top row is WT; second row *apm4 Δ/Δ*; third row *apm4 Δ/Δ*, *chs3Δ*; fourth row *apm4 Δ / apm4*$^{1-454}$). 6 plates per condition from 3 independent experiments were quantified by recording the minimum cell concentration at which visible cell growth was observed. Half the plates were incubated at 30°C and half at 37°C; these were combined as they showed the same pattern of growth. This is shown in the graphs. Error bars show SD. Stats are one-way ANOVAs with Tukey's multiple comparisons.

Figure 6.12A – C are control plates which show that in the absence of drugs, the four strains grow to the same level. DMSO and MeOH were the solvents for fluconazole and myriocin respectively; both were used at 1:1000 in the drug plates; the control plates

with DMSO or MeOH only (figure 6.12B, C) show that these solvents don't significantly inhibit growth of any of the strains.

Edelfosine is a lysophosphatidylcholine analogue whose cytotoxicity in yeast is mediated by phospholipid flippases. Thus flippase defects can confer edelfosine resistance, whilst other changes in physical properties of the PM can confer edelfosine sensitivity (Hanson et al. 2003). Figure 6.12D shows that the strains don't show significantly different growth on 60 µM edelfosine.

Myriocin is an inhibitor of sphingolipid biosynthesis, and deletion of ER-PM tethers has been shown to confer myriocin sensitivity (Toulmay and Prinz 2012). However yeast cells with complete ER-PM untethering have been shown to be myriocin resistant (Quon et al. 2018). Figure 6.12E shows that cells without AP-2 are sensitive to myriocin, and this is not rescued by *chs3* deletion. The *apm4*$^{1\text{-}454}$ mutant however is not sensitive to myriocin, indicating that the reason for the sensitivity is independent of YxxΦ motif binding via Apm4.

Figure 6.12F shows that cells without AP-2 are sensitive to fluconazole. Fluconazole is an azole antifungal, which inhibits the enzyme lanosterol demethylase, an essential step in ergosterol biosynthesis (Vanden Bossche, Koymans and Moereels 1995, Odds, Brown and Gow 2003). Interestingly, this sensitivity of the *apm4* deletion mutant is rescued by deletion of *chs3*. Again, the *apm4*$^{1\text{-}454}$ cargo binding mutant is not sensitive to fluconazole, indicating that the mechanism causing this sensitivity is independent of YxxΦ motif binding.

Taken together, these results show that AP-2 is required for proper PM lipid organisation, and without it cells have various lipid defects. Unlike Chs3 recycling however, these lipid phenotypes appear to be independent of YxxΦ motif binding by Apm4.

## 6.13. Fluconazole treatment inhibits SRD formation in WT hyphae

Reduced ergosterol biosynthesis has been shown to lead to loss of ergosterol-rich domains (ERDs) at hyphal tips (Quon et al. 2018); and treatment with sub-growth-inhibitory levels of fluconazole has been shown to *increase* expression of genes in the ergosterol biosynthesis pathway (Henry, Nickels and Edlind 2000). Therefore, it was reasoned that treating cells with low concentrations of fluconazole could increase

ergosterol biosynthesis, and thus perhaps rescue the ERD loss in *apm4* deletion hyphae. Cells of each strain were induced to form hyphae in the presence of either 2 or 8 µg/mL fluconazole (DMSO, the solvent for fluconazole, was used as a negative control). Under these conditions, hyphal induction and growth was not inhibited, though hyphae did become more misshapen. Upon fixation and staining with 9 µg/mL filipin, it was clear that low level fluconazole did appear to elevate ergosterol biosynthesis, as shown by the brighter filipin staining in the fluconazole treated cells of both strains (figure 6.13). However, this did not lead to any SRD formation in mutant hyphae; conversely it inhibited SRD formation in WT hyphae (see figure 6.13). With 2 µg/mL fluconazole just a few WT hyphae has ERDs, and with 8 µg/mL fluconazole no ERDs were observed. Hyphae without *apm4* also appeared more misshapen than WT hyphae under increasing fluconazole concentrations, consistent with their elevated sensitivity to fluconazole shown in figure 6.12.

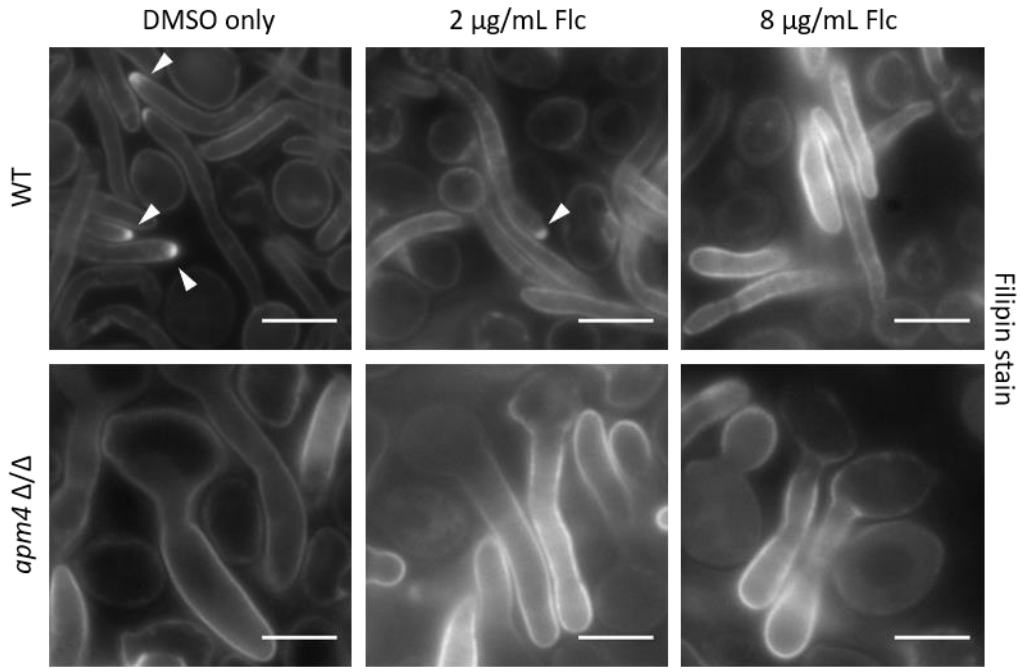


6.13. Treatment with fluconazole inhibits SRD formation in WT hyphae
Images show WT hyphae and *apm4* deleted hyphae, grown for 90 minutes in the presence of varying concentrations of fluconazole. Hyphae were then fixed and stained with filipin, to visualise ergosterol. Arrows point to strong filipin stained regions, indicating the presence of an ERD (ergosterol rich domain).

## 6.14. *C. albicans* has proteins homologous to *S. cerevisiae* Osh family proteins

The results described above clearly indicate that AP-2 is important in the polarised distribution of plasma membrane ergosterol and PI(4)P during hyphal growth. The ORP family (oxysterol-binding protein (OSBP) related proteins) regulate the metabolism and signalling of sterols and phosphoinositide lipids in both yeast and mammalian cells (Raychaudhuri and Prinz 2010, Beh et al. 2012), however they have not been much studied in filamentous fungi. NCBI BLAST (Basic Local Alignment Search Tool) was used to find *C. albicans* homologues to *S. cerevisiae* Osh proteins, and schematic representations of these proteins are shown in figure 6.14. No *C. albicans* homologues to *Sc*Osh1 or *Sc*Osh5 were found.

Three *C. albicans* Osh proteins (*Ca*Osh3, *Ca*Osh6 and *Ca*Osh7) have been previously identified in Hur et al. (2006) and Hull and Johnson (1999). *Ca*Osh6 and *Ca*Osh7 are very similar to their *S. cerevisiae* homologues, which in turn are paralogues of each other, and are both small proteins containing an ORD (OSBP-related domain). *Ca*Osh3 additionally contains a PH domain (Pleckstrin homology domain, which often bind phosphoinositides (Haslam, Koide and Hemmings 1993)) but is lacking the GOLD domain (Golgi-dynamics, often associated with lipid binding domains (Anantharaman and Aravind 2002)) found in *Sc*Osh3.

Two further uncharacterised *C. albicans* proteins: putative *Ca*Osh2 (genome region C1_08180C_A) and putative *Ca*Osh4 (genome region C2_05720cp_a) were identified using BLAST; sharing 36% and 59% sequence homology with the respective *S. cerevisiae* proteins. Both share the same domains as the *S. cerevisiae* proteins, except that *Ca*Osh2 has two Ankyrin repeat domains (mediating protein-protein interactions (Li, Mahajan and Tsai 2006)) rather than three.

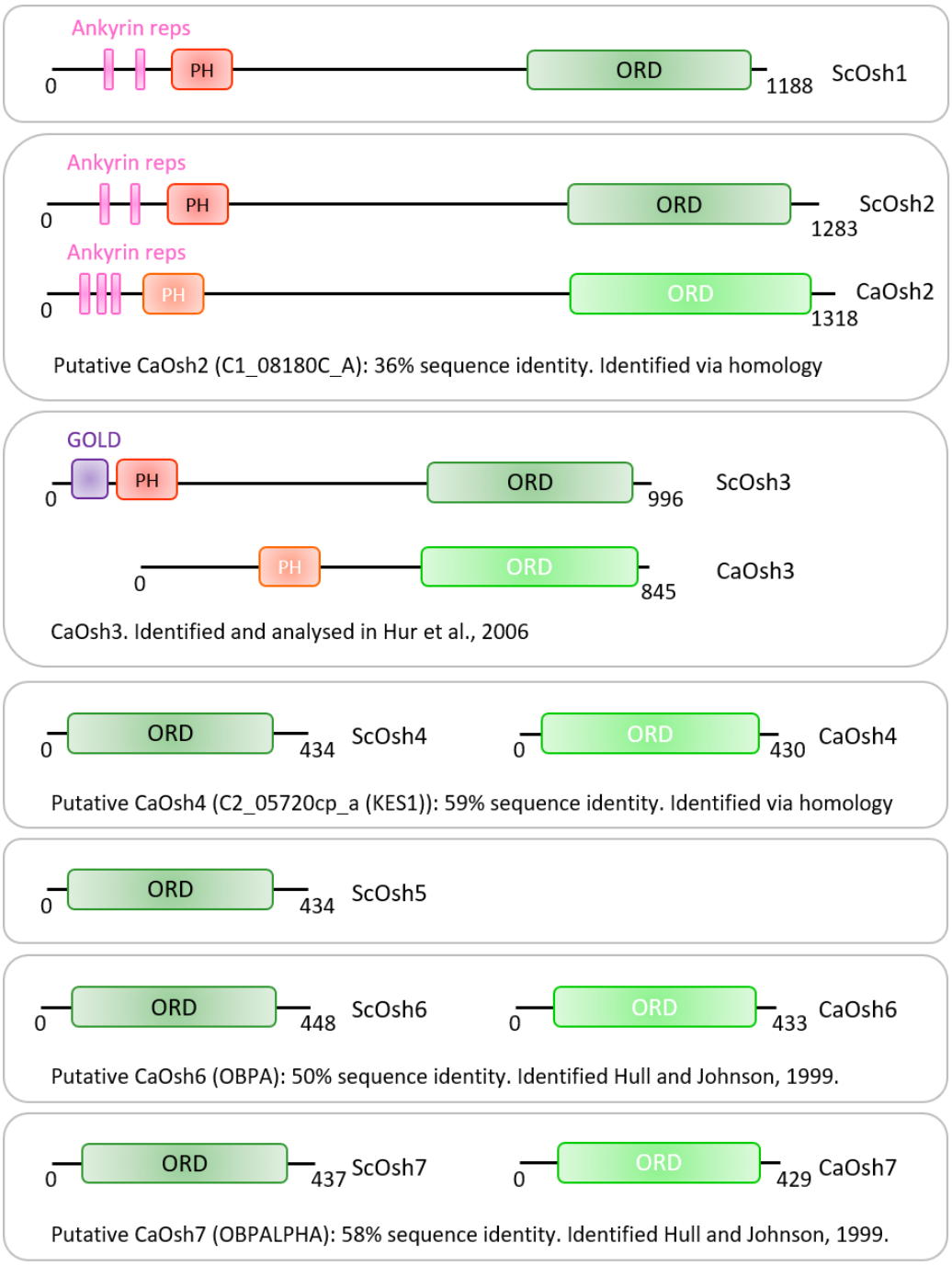


6.14. *Candida albicans* has proteins homologous to *S. cerevisiae* Osh family proteins

Diagrams show representations of the *S. cerevisiae* proteins *Sc*Osh1 – 7, with the homologous *C. albicans* proteins alongside. Three of these: *Ca*Osh3, *Ca*Osh6 and *Ca*Osh7 have been identified in published work. Putative *Ca*Osh2 and *Ca*Osh4 were identified using the NCBI BLAST (basic local alignment search tool). No *C. albicans* homologues to *Sc*Osh1 and *Sc*Osh5 were identified. ORD = OSBP (oxysterol-binding protein)-related domain. PH = Pleckstrin homology domain. GOLD = Golgi dynamics domain.

## 6.15. Cells without AP-2 have more Osh3-GFP puncta

Osh3 was tagged with GFP in both wild-type and *apm4* deletion cells. Osh3 has been shown to localise to ER-PM contact sites in response to PM PI(4)P levels in *S. cerevisiae* (Stefan et al. 2011). The *C. albicans* homologue has been identified and shown to have a role in hyphal growth (Hur et al. 2006). However the extent to which it fulfils the same functions as *Sc*Osh3 is unknown.

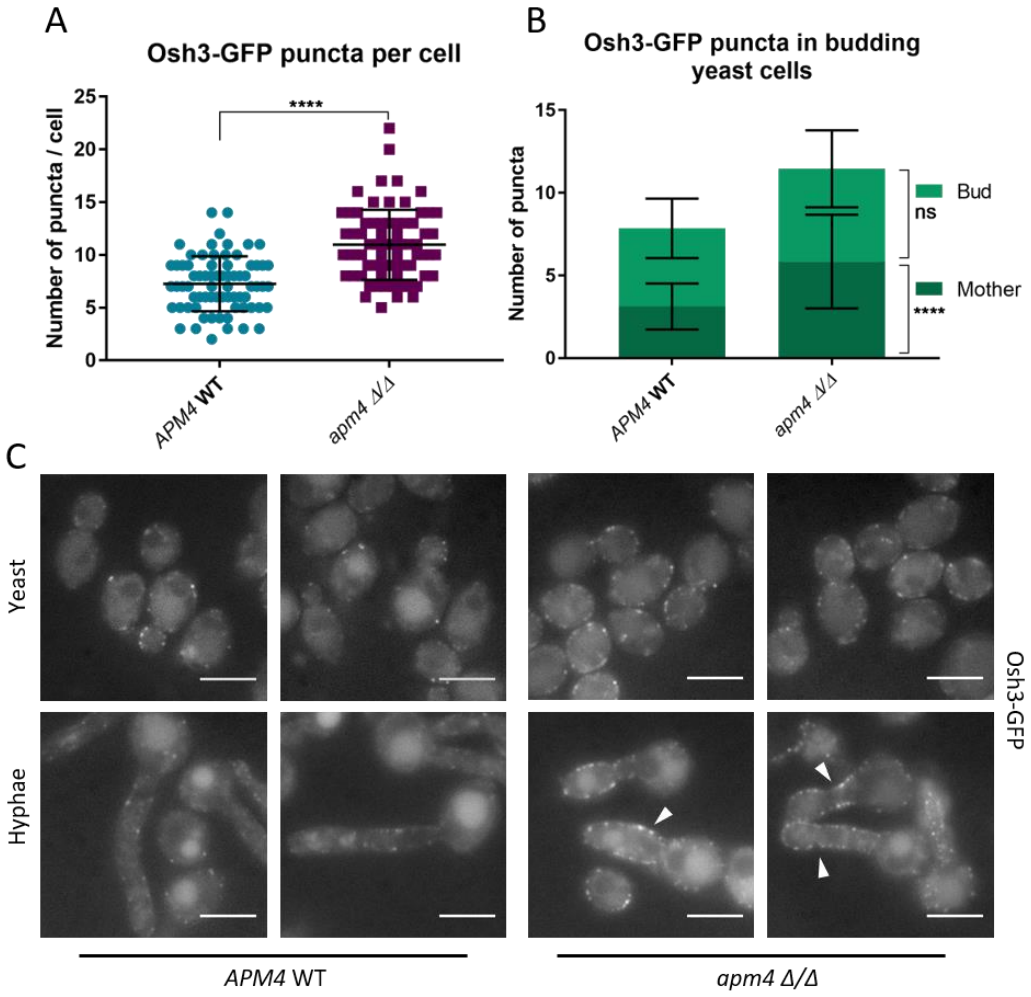


**6.15. Cells without AP-2 had more Osh3-GFP puncta in yeast and hyphal cells.**
(A) Cells expressing Osh3-GFP were grown as yeast and imaged, and the number of fluorescent puncta per cell recorded. Stats is a T-test with Welch's correction. (B) Using the same data as in (A), but this time only including budding yeast cells, and plotting the mean number of puncta in the mother cells vs buds. Stats is a 2-way ANOVA with Sidak's multiple comparisons. (C) Representative images of Osh3-GFP yeast and hyphal cells of both strains. Arrows point to examples of elevated peripheral Osh3-GFP signal in *apm4 Δ/Δ* hyphae. All scale bars 5 µm, all error bars show SD.

In our strains, Osh3-GFP signal was observed in puncta around the cell periphery; characteristic of ER-PM contact site localisation. Cells without *apm4* had increased numbers of Osh3-GFP puncta in yeast cells (figure 6.15A), and this was due to increased puncta in mother yeast cells rather than buds (figure 6.15B). Cells without *apm4* also appeared to have increased Osh3-GFP puncta in hyphae (representative images in figure 6.15C) however this was not quantified due to difficulties counting individual puncta.

## 6.16. Cells without AP-2 have similar Sac1-GFP localisation to WT cells

To try to gain further insight into the lipid depolarisation phenotype, two other proteins were tagged with GFP. Sac1 is an integral ER phosphatase which localises to ER-PM contact sites and dephosphorylates PM PI4P (Manford et al. 2010). Sac1 is activated by ORP proteins in response to high PM PI(4)P (Stefan et al. 2011). It was reasoned that perhaps a loss or mis-localisation of Sac1 could lead to the depolarised PM PI4P seen in *apm4* deletion hyphae, and perhaps also, via loss of ORP family function, to the depolarised ergosterol phenotype.

Sac1 was tagged with GFP in WT and *apm4* deleted cells, which were imaged as both yeast and hyphae (see figure 6.16). In both strains Sac1-GFP signal was observed in

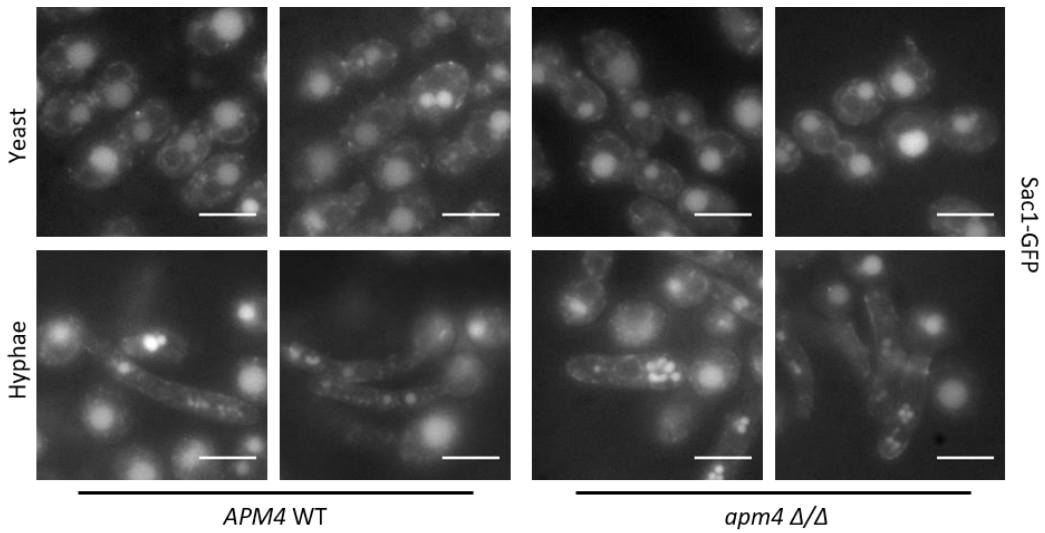


**6.16. Cells without AP-2 appear to have similar Sac1-GFP localisation to WT**

Cells expressing Sac1-GFP were grown as yeast or hyphae then imaged. Representative images of two strains are shown. Scale bars 5 µm.

puncta with an ER-like localisation around the nucleus and cell periphery. There were no obvious differences between the strains.

## 6.17. Cells without AP-2 have more Ist2-GFP puncta in hyphae

Ist2 is an integral ER protein which binds PM phospholipids and thus tethers the ER to the PM at contact sites. As ER-PM contact sites are known to regulate lipid signalling, non-vesicular lipid transfer and membrane trafficking, it was reasoned that disruption or mis-localisation of these contact sites could be causing the lipid defects observed. Ist2 was tagged with GFP as a marker of ER-PM contacts, in WT and *apm4* deletion cells (see figure 6.17). In both strains, Ist2-GFP signal was observed in puncta somewhat around the nucleus but mostly around the cell periphery, consistent with ER-PM contact site localisation. The signal looked similar in the two strains, however hyphae without *apm4* had more Ist2-GFP puncta along their hyphal length, possibly indicating increased ER-PM tethering. This is indicated by white arrows in figure 6.17.

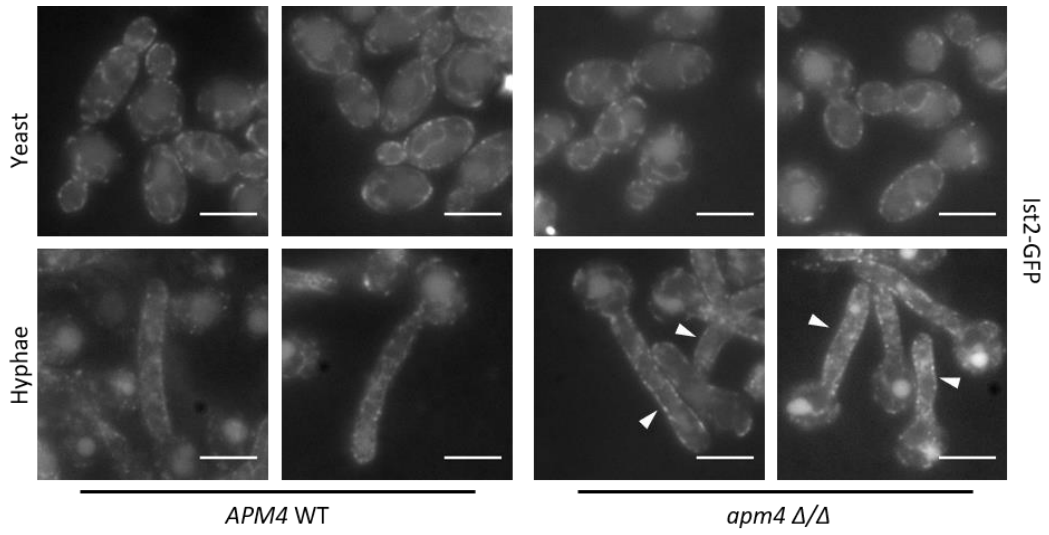


**6.17. Cells without AP-2 appear to have more Ist2-GFP puncta along hyphal length**
Cells expressing Ist2-GFP were grown as yeast or hyphae then imaged. Representative images of two strains are shown. Arrows point to examples of elevated peripheral Ist2-GFP signal in *apm4 Δ/Δ* hyphae. Scale bars 5 µm.

## 6.18. Chapter 3 discussion

### 6.18.1. Discussion of exocyst and polarisome

The results above show that AP-2-depleted cells can still polarise at least some of their exocyst components, as a surface crescent of Sec3 and Sec8 was present in most hyphae. This suggests that secretion can still be directed to the hyphal tip, which is expected, since hyphae can still grow. The crescent of puncta is more spread out than in WT cells, forming a less tight cap. This could be a consequence of the *apm4* mutant's wider hyphal tip geometry.

Although hyphae without AP-2 still had exocyst at the hyphal tip, ~40% of Sec3 and Sec8 puncta were found in other regions of the cell, such as the hyphal mother cell. This mis-localisation of exocyst to the mother cell may cause exocytic vesicles to be targeted to the mother cell as well as the growing hyphal tip. This may be the cause of many of the polarity defects we have observed, such as depolarised mannose deposition (Knafler et al. 2019).

The polarisome component Spa2, which has a similar pattern of localisation to the exocyst in WT hyphae, was even more mis-localised in *apm4* mutant hyphae. Some Spa2-GFP puncta were present at the hyphal tip, but many more were spread around the whole cell periphery including the mother cell. This polarisome mis-localisation could lead to de-polarised actin filaments (via de-polarised formin Bni1) which could in turn impair polarised secretion. Visualisation of actin via rhodamine-phalloidin staining did not reveal a gross defect in its organisation in the absence of AP-2 (Knafler et al, 2019) however this has not been studied in detail.

This exocyst and polarisome mis-localisation could be caused by reduced endocytic recycling at the 'collar region' leading to a failure to maintain these proteins at the hyphal tip. We have shown that AP-2-depleted cells have a similar number of actin patches (ie endocytic events; (Knafler et al. 2019)) at their hyphal tips, so the defect would presumably be an inability to concentrate appropriate cargo into sites of endocytosis, rather than reduced endocytic uptake per se. Mis-localisation then, could be caused by reduced endocytic recycling of exocyst / polarisome components themselves, or of an upstream factor such as a Rho GTPase. However, exocyst / polarisome components and Rho GTPases are membrane associated rather than transmembrane proteins, so would not normally be considered AP-2 cargoes. $PI(4,5)P_2$ is

known to recruit exocyst components, but we found that this lipid maintained its apical polarisation in the absence of AP-2.

From the available data, exocyst and polarisome mis-localisation could be due to impaired recycling of an unknown upstream transmembrane protein; or due to loss of apical PM lipids which may recruit exocyst / polarisome directly or indirectly. There is some evidence that sterol-rich domains may recruit the Cdc42 module (Fischer, Zekert and Takeshita 2008, Takeshita et al. 2008, del Pozo et al. 2000); the loss of SRDs in the absence of AP-2 could be the upstream cause of the exocyst and polarisome de-polarisation. This data emphasises the intimate link between secretion and endocytosis: functional endocytic recycling is required for correctly polarised exocytic machinery (and therefore polarised secretion itself).

### 6.18.2. Discussion of Spitzenkörper

The results above show that hyphae without AP-2 can have a Spitzenkörper, but a much lower proportion of them do compared to WT hyphae. The two methods used to visualise the Spitzenkörper – Mlc1-GFP and FM4-64 staining – gave slightly different results. Fewer hyphae (of both strains) had an Mlc1-GFP marked Spitzenkörper than an FM4-64 stained Spitzenkörper. This could highlight different populations of Spitzenkörper. The fact that Mlc1-GFP signal is not present or is present in a polarisome-like localisation though, does not mean a Spitzenkörper is not present.

Interestingly it was noted that *apm4* deletion hyphae which did have a Spitzenkörper were narrower than those which did not. Indeed, *apm4* mutant hyphae with a Spitzenkörper were a similar width as WT hyphae without a Spitzenkörper (though only a small proportion of cells from each strain fell into these categories). The presence of a Spitzenkörper could be a good readout of correctly polarised growth; if secretion is correctly focussed at the hyphal tip, vesicles will be trafficked here faster than they can be exocytosed therefore will accumulate at a Spitzenkörper. If however secretion is slowed or not correctly polarised (as is indicated by exocyst mis-localisation in *apm4* mutant hyphae) perhaps fewer vesicles will traffic to the hyphal tip therefore a Spitzenkörper will not accumulate. Mathematical modelling has predicted that the Spitzenkörper is responsible for the characteristic shape of a hyphal tip (Bartnicki-Garcia et al. 1989); the absence of Spitzenkörpers in many mutant hyphae could be a cause of their aberrant tip shape.

### 6.18.3. Discussion of SRDs

As shown in Knafler et al (2019); hyphae without AP-2 have a dramatic loss of filipin-stained sterol-rich domains at their hyphal tips. The mechanism behind this is unclear, because little is known about the mechanism of maintaining SRDs at hyphal tips. There is some evidence that lipid rafts may be clustered and held together by the membrane proteins enriched in them (Janes et al. 2000). Septins have also been implicated in limiting the diffusion of membrane lipids in *C. albicans*, and may function to maintain SRDs (Sudbery 2001, Douglas et al. 2005). One can imagine that a loss of recycling of an unknown membrane protein critical in clustering lipid rafts could lead to their dissociation and loss of SRDs. Alternatively, endocytic recycling of the ergosterol itself could be key. Very little is known about pathways for recycling sterol back to the membrane after endocytosis. One model predicts that lipid rafts may cluster endocytic machinery (Munn et al. 1999, Degreif et al. 2019), but other evidence shows that SRDs are inhibitory to endocytosis – their rigidity may prevent membrane invagination (Grossmann et al. 2008, Malinsky, Opekarová and Tanner 2010). It is possible though that recycling of sterols is required to maintain a sterol-rich domain at the hyphal tip in the face of continuous secretory vesicle fusion, and that this recycling may be mediated by AP-2, perhaps independent of protein cargoes.

AP-2-depleted yeast cells also have decreased filipin staining compared to WT, suggesting they have lower PM ergosterol levels. Quon et al., (2018), showed that yeast cells depleted in ergosterol had fewer SRDs, so reduced sterol levels could be the cause of the loss of SRDs. We attempted to upregulate ergosterol biosynthesis using low levels of fluconazole, which we think was successful (as judged by elevated filipin staining) however this did not restore SRDs in *apm4* mutant hyphae. In fact it had the opposite effect, abrogating SRD formation in WT hyphae. This is not too surprising; fluconazole treatment will confer many stresses on the cells, even if they are able to upregulate their ergosterol synthesis pathways in compensation. It would be interesting to measure the ergosterol levels in the PM of both strains via lipidomics; quantification of filipin staining is not a reliable measure and is impractical for hyphal cells due to issues getting the whole hypha in focus and the differential cell sizes and patterns of staining between strains.

One interesting observation is that SRD polarisation and tolerance to myriocin and fluconazole are all dependent on AP-2, but independent of its YxxΦ motif binding function (shown by the *apm4Δ / apm4*$^{1-454}$ mutant). Myriocin sensitivity may be caused by impaired ER-PM contacts (Quon et al. 2018), and fluconazole sensitivity may be caused by defects in ergosterol synthesis (Ghannoum et al. 1994); these phenotypes could be the result of the same thing which causes SRD loss. This could be due to AP-2-mediated recycling of ergosterol itself (perhaps independent of cargo binding); or due to AP-2-mediated recycling of a non-YxxΦ cargo, perhaps bound by the AP-2 δ subunit.

Surprisingly, fluconazole sensitivity in the *apm4* mutant was rescued by deletion of one copy of *chs3*. This indicates that fluconazole sensitivity could be caused by defects in the cell wall organisation of the *apm4* mutant allowing more drug inside the cell, as we know some cell wall defects are rescued by *chs3* deletion. We also know that the combined *apm4 Δ/Δ*, *chs3Δ* mutant rescues several aspects of hyphal polarity (see Knafler et al. (2019), figure 8) so perhaps this rescue of polarised growth allows the strain to compensate for the defective ergosterol regulation in hyphae without AP-2. It should be noted that SRDs are not restored upon *chs3* deletion in the *apm4* null.

Whatever the cause, the loss of SRDs at the hyphal tip could be responsible for many other polarisation defects in the *apm4* deletion mutant. Takeshita et al., (2008) found that intact SRDs were required for the localisation of cell-end markers TeaA and TeaR in *A. nidulans*, but SRDs could still form in the absence of TeaA and TeaR. This suggests that SRDs act upstream of cell end markers. The Cdc42 cascade, possibly via Cdc42 itself which is membrane localised via a geranyl-geranyl modification, could require SRDs for its localisation (Fischer et al. 2008). Interestingly, proteins which have been implicated in the formation of SRDs (class I myosins, septins, Osh proteins) are also members of the Cdc42 cascade; suggesting a positive feedback loop between SRD formation and local Cdc42 activation could function in polarity establishment (Fischer et al. 2008).

### 6.18.4. Discussion of PIs

These results show that hyphae without AP-2 are still able to polarise PM PI(4,5)$P_2$ but not PI(4)P. This was surprising to us at first, for two reasons. Firstly, the mis-localised polarisome and exocyst proteins are recruited by PI(4,5)$P_2$ so we reasoned this lipid may be de-polarised, however this is not the case. These proteins must have other causes for their mis-localisation (see above). Secondly, the majority of PI(4,5)$P_2$ is synthesised from

PI(4)P, so we thought that depolarised PI(4)P would lead to depolarised PI(4,5)$P_2$; this is not the case. It appears that the reduced amount of PI(4)P found at the hyphal tip of *apm4* mutant cells is still enough to make sufficient tip-localised PI(4,5)$P_2$.

The PI(4,5)$P_2$ gradient is thought to be maintained by tip-localised 5-kinase Mss4 (Vernay et al. 2012), meaning that this polarised protein must maintain its polarisation in the absence of AP-2. Perhaps it is recycled via a different endocytic adaptor such as Sla1.

The mechanism behind the PI(4)P gradient is perhaps more complex, as the 4-kinase Stt4 which synthesises PI(4)P from PI is uniformly distributed around the cell (Ghugtyal et al. 2015). These authors proposed the gradient to be maintained by polarised secretion of PI to the hyphal tip, and Sac1-mediated de-phosphorylation. Both of these processes could be dysregulated in hyphae without AP-2. As discussed above, secretion is probably partially mis-localised in the *apm4* mutant, which could mean PI is being delivered to other areas around the hypha, leading to de-polarised PI(4)P generation. Due to time constraints, we were unable to fully analyse the Sac1 activity in this strain, however there is some evidence that ER-PM contact sites are dysregulated (see below), indicating that perhaps impaired Sac1-mediated de-phosphorylation could also be contributing to the PI(4)P phenotype.

Additionally, Quon et al (2018) showed that dysregulated PM phospholipids can lead to dysregulated PM ergosterol, mediated by MCSs, so the PI(4)P defect could be the cause of the loss of SRDs.

### 6.18.5. Discussion of lipid regulation

Cells without AP-2 had increased Osh3 and Ist2 puncta at their cell peripheries, particularly along the length of hyphal cells. As both of these proteins localise to ER-PM contact sites, this could indicate an increase in MCSs. Alternatively, there could be the same number of MCSs, and these proteins could be upregulated or have increased targeting to MCSs. Ideally, we would image the ER using a fluorescently tagged ER-localisation signal.

The PM lipid composition is known to influence ER-PM tethering; PM phospholipids mediate binding of ER tethering proteins such as Ist2. Therefore the altered PM composition in *apm4* deletion hyphae could be causing increased ER-PM tethering.

Quon et al (2018) showed that cells with reduced ergosterol biosynthesis had elevated cortical ER (though the mechanisms behind this are unknown). Our yeast cells without *apm4* had reduced filipin staining, indicating reduced ergosterol levels, so this could be causing increased ER-PM contact, as the cell tries to compensate. Further work is required to determine whether cells without AP-2 do in fact have elevated ER-PM contacts, and whether this has functional significance to the defects observed.

Osh3 has been shown to localise to MCSs in response to PM PI(4)P levels (Stefan et al. 2011). As *apm4* deletion hyphae appear to have increased PI(4)P along their hyphal sides, this could be the cause of the increased Osh3. However when there, Osh3 is thought to activate Sac1 phosphatase, which dephosphorylates PI(4)P. We did not see a change in Sac1 localisation or signal intensity; however we cannot say anything about Sac1 activity. More work should be done to determine whether Sac1-mediated turnover of PI(4)P is disrupted in cells without AP-2.

Osh proteins have also been shown to interact genetically with Cdc42 to promote both the establishment and maintenance of polarity. They were found to be required for the localisation of septins, Cdc42, Rho1 and Sec4, and for polarised secretion (Kozminski et al. 2006). In particular Osh4 is implicated in both sterol and PI(4)P homeostasis. *Sc*Osh4 can bind both PI(4)P and ergosterol, though it is not known if the *C. albicans* homologue has retained these abilities. *S. cerevisiae* Osh4 is thought to regulate polarised secretion, via interactions with both Sac1 and exocyst, and dependent on its sterol binding (Alfaro et al. 2011). We did GFP tag the *C. albicans* homologue of Osh4, but unfortunately the signal was too weak to allow analysis; if more time were available it would be interesting to investigate whether *Ca*Osh4 has a role in the PI(4)P and sterol defects we observe.

### 6.18.6. Concluding remarks

We have shown that AP-2 is required for PM lipid organisation in *C. albicans* hyphae. Although lots is known about the importance of different lipids in membranes, less is known about how lipids are localised and concentrated in certain locations at the cell membrane. The steep lipid gradients observed in *C. albicans* hyphae are proposed to be critical to hyphal growth, but the mechanisms of how they are generated and maintained, and how they mediate polarised growth, have yet to be fully explored. We have shown that AP-2-mediated endocytic recycling is critical for this polarity, but

whether this is via a specific transmembrane cargo(es), or via recycling of the lipids themselves, remains to be seen.

It is tempting to speculate that the loss of PI(4)P and ergosterol gradients is the cause of the mis-localisation of polarisome and exocyst components, and thus a key cause of the myriad polarity defects observed in the *apm4* mutant. However much more work is needed to evaluate this hypothesis. A means to re-instate lipid polarity in the *apm4* deletion mutant, perhaps through addition of exogenous lipid precursors, could be an informative experiment (do any proteins re-gain their polarised localisation?)

This line of research is preliminary and requires further investigation, however has revealed some insights into the key role of AP-2 in maintaining both protein and lipid markers of polarity at the site of active hyphal growth.

# Chapter 7: Discussion

Most results relating to specific data sets are discussed at the end of their related results chapter, and in the discussion section of the paper. This final chapter aims to pull together the key themes of this study, and to ask how these relate to wider questions concerning fungal growth and morphology. The points in this discussion are split into three key themes: points which relate to fungal cell wall regulation; points which relate to polarised growth; and points which relate to the endocytic process.

This thesis has demonstrated that the AP-2 endocytic adaptor complex plays an important role in the fungal pathogen *C. albicans*. This adds to growing evidence showing that, instead of being redundant or of limited importance in yeasts as previously suggested, AP-2 is required for the endocytosis of specific cargoes and this is particularly important during polarised growth. We have shown that AP-2 is required for the endocytosis and subsequent recycling of a key cargo, Chs3, and that this recycling is critical for the composition and organisation of the *C. albicans* cell wall. We show that excess Chs3 at the cell surface is partially responsible for the *apm4* deletion mutant's polarised growth defects. We also show that AP-2 is required for correct localisation of the polarisome and exocyst during hyphal growth, and its depletion leads to loss of the Spitzenkörper in some hyphae. Loss of these polarity markers occurs via an uncharacterised mechanism which could involve plasma membrane lipid polarity. Plasma membrane ergosterol and PI(4)P both rely on AP-2 for their polarised localisation; the detailed mechanism behind this is also unknown. These results leave interesting avenues open for further investigation.

## 7.1. Discussion in relation to fungal cell wall regulation

Firstly, through microscopy and biochemical assays we have shown that cells lacking AP-2 have defects both in levels of cell wall components and in their organisation; see chapter 5 and Knafler et al, 2019. As noted, this is partially due to loss of Chs3 recycling. Elevated Chs3 at the cell surface would not necessarily lead to elevated cell wall chitin, as Chs3 is subject to several other layers of regulation (binding by Chs4; phosphorylation by Pkc1 (Rogg et al. 2012)). However the fact that deletion of one copy of Chs3 led to a decrease in cell wall chitin (as judged by CFW staining) and rescue of morphological

defects strongly suggests that excess chitin caused by elevated surface Chs3 is indeed a major underlying cause of these morphology defects.

### 7.1.1. The role of the cell wall in shape determination

These results very much imply a link between cell wall composition and cellular morphology. The fungal cell wall is known to be important to cell shape, but links between specific cell wall variations and morphological changes have not been unequivocally demonstrated. *C. albicans* hyphal cells have more chitin than yeast cells (Braun and Calderone 1978). As chitin confers rigidity to the cell wall, could increased chitin could be required for maintaining a more complex cell shape? Yeast cells without their cell wall rapidly become spherical, so perhaps the 'further' from spherical a cell is, the more rigid wall is required to maintain its shape. This would not however explain why cells without AP-2, which have elevated chitin therefore presumably stiffer cell walls, have defective hyphal morphology.

Perhaps the location of cell wall deposition is more important than the overall cell wall composition. Yeast cell growth is considered to be a product of internal turgor pressure and the cell wall; new cell wall deposition allows cell expansion (Bartnicki-Garcia et al. 2000). Therefore as long as new cell wall is added, and sufficient membrane is provided by secretion, the cell will grow. Both yeast and hyphal cells maintain their cell wall biosynthesis enzymes at the sites of polarised growth, thereby ensuring that cell growth occurs only at these sites. Targeted exocytosis and endocytosis of glucan synthase was used to develop a mathematical model to predict hyphal shape during growth (Caballero-Lima et al. 2013). Cells without AP-2 have Chs3 depolarised all over their cell surfaces, and chitin deposition is depolarised, as shown by CFW staining in both yeast and hyphal cells (see Knafler et al, 2019). This de-polarised cell wall deposition (all over the cell surface) could then lead to the enlarged yeast cells and wider hyphal cells observed. The reduced length of hyphal cells may also be a consequence of decreased cell wall biosynthesis at the hyphal tip therefore decreased tip growth.

### 7.1.2. The role of chitin in the *C. albicans* cell wall

The results shown here also underscore the importance of chitin specifically in *C. albicans* morphology. Despite being a minor component of the *C. albicans* cell wall, comprising just 1 – 2% of its dry weight, chitin is known to be a very important structural

component due to its high tensile strength (Klis et al. 2001). Although we do not yet know if any other cell wall biosynthetic machinery is dysregulated in cells without AP-2, chitin is the component which shows the most change, and the resulting defects underscore its importance. However depletion of Chs3 levels does not rescue all defects of the *apm4* deletion mutant. These cells still have some morphological defects. They are also still unable to polarise their PM ergosterol nor their mannose deposition (see Knafler et al, 2019). Therefore, Chs3 recycling is clearly not the only critical role of AP-2 in *C. albicans*.

### 7.1.3. The role of AP-2 and the cell wall in K28 killer toxin uptake

One idea arising from the cell wall defects of the *apm4* deletion mutant outlined in chapter 5 and Knafler et al (2019) is that these could help explain the very first phenotype associated with loss of AP-2 in *S. cerevisiae*; resistance to K28 killer toxin (Carroll et al. 2009). This phenotype gave the first hint that the AP-2 complex is in fact involved in endocytosis in yeast, however the pathway by which AP-2 mediates K28 toxin uptake has never been characterised. The K28 toxin is known to interact with a primary receptor in the yeast outer cell wall: the mannose side chains of a GPI-linked protein (Schmitt and Radler 1987). Thus defects in mannosylation, lipid organisation and GPI anchor biosynthesis all affect K28 toxin uptake (Carroll et al. 2009). K28 can then penetrate through the cell wall, and bind its recently identified secondary receptor, the transmembrane Erd2. Interaction with Erd2, mediated by the toxin's K/HDEL motif triggers CME (Becker et al. 2016). AP-2 could directly bind Erd2 and mediate endocytosis of the toxin-receptor complex. Alternatively, loss of AP-2 could indirectly impair K28 uptake through the dysregulation of mannoprotein secretion (see Knafler et al, 2019) or the loss of sterol rich domains which may lead to dysregulation of GPI-anchored proteins (see chapter 6 and Knafler et al, 2019).

## 7.2. Discussion in relation to polarised hyphal growth

### 7.2.1. Comparing yeast and hyphal growth in *C. albicans*

One general observation from the results presented here is that many factors which are de-polarised in the absence of AP-2 in hyphal cells (polarisome, exocyst, PI(4)P), are able to maintain their polarisation in yeast cells of this strain. This highlights a difference in polarity maintenance in yeast compared to hyphal growth. Although yeast and hyphal

cells employ many of the same proteins to regulate polarised growth, it seems that AP-2-mediated endocytic recycling is critical to maintaining their localisation during hyphal but not yeast growth. This observation fits with the fact that AP-2 depletion has a much milder phenotype in *S. cerevisiae* and that many of the observed defects are related to polarised growth. This differential requirement may be due to the smaller size of yeast buds in comparison to hyphae, and the more sustained polarised growth required for hyphal extension. Additionally, yeast cells have been shown to employ septin proteins at the mother-bud neck as a barrier to limit the diffusion of membrane proteins and thus confine them to the growing bud (Takizawa et al. 2000). This compartmentalisation of the cell cortex has been shown to be critical to polarisation during budding (Barral et al. 2000). Although septins are also critical to *C. albicans* hyphal morphogenesis, it is not known whether they function as a diffusion barrier to peripheral proteins here (Warenda and Konopka 2002). Septin barrier function could perhaps also explain why yeast cells have a reduced requirement for AP-2-mediated recycling compared to hyphal cells.

However, yeast cells lacking AP-2 do display depolarised Chs3 (see Knafler et al, 2019), indicating that for this cargo, endocytic recycling is critical for its localisation in yeast cells as well as hyphae. This apparent discrepancy could indicate that although endocytic recycling via AP-2 is required for polarisation of cargoes during yeast and hyphal growth, the smaller size and briefer polarised growth of yeast cells means they are better able to compensate for cargo mis-localisation. As hyphal extension requires sustained polarised growth, de-polarisation of certain cargoes could lead to more pronounced defects.

### 7.2.2. Cdc42 in polarised hyphal growth

Regarding the mis-localisation of polarity markers and lipids shown in chapter 6, it may be challenging to determine the precise role of AP-2, as there are likely to be multiple cargoes each contributing in part to overall polarity. As mentioned previously, many of the depolarised polarity markers are cytoplasmic rather than transmembrane proteins, so may not be candidates for AP-2-mediated recycling themselves. Cdc42 is a master regulator of polarity (Etienne-Manneville 2004), which acts upstream of the exocyst and polarisome (Zhang et al. 2001, Rida and Surana 2005), therefore would be predicted to be at least partially mis-localised in our *apm4* mutant hyphae. Work in *S. cerevisiae* showed Cdc42 accumulation at shmoo tips to be impaired in the absence of AP-2 (Chapa-y-Lazo et al. 2014). An important point here is that polarity is established in cells

without AP-2. Mutant cells almost always produce a germ tube under hyphal inducing conditions, and they quite rarely exhibit more than one bud or hypha. Therefore AP-2 is required for the maintenance rather than the establishment of polarity. Much work and mathematical modelling has focussed on the symmetry breaking required to establish polarity, either to form a bud or germ tube. In the absence of established landmarks, this is thought to depend on positive feedback loops which amplify small differences in local active Cdc42, via actin-based transport; control of lateral diffusion; membrane extraction; and recruitment by Bem1 and Cdc24 (Freisinger et al. 2013, Wedlich-Soldner et al. 2004). Once a polarity axis has been established, it is dynamically maintained by recycling of Cdc42 via two mechanisms (Slaughter et al. 2009). Cdc42 is recycled via actin patches (Slaughter et al. 2013, Marco et al. 2007), and via GDI (guanine nucleotide dissociation inhibitor)-mediated removal from the membrane such that it can be re-polarised (Slaughter et al. 2009, Masuda et al. 1994). AP-2 could theoretically be involved in Cdc42 recycling, either through direct binding to it or to its GDI Rdi1. Alternatively, AP-2 could have an indirect role in Cdc42 recycling via its role in PM lipid organisation. The ratio of PM lipids has been shown to affect GDI-mediated Cdc42 extraction from the membrane (Das et al. 2012), and sterol rich domains may be involved in Cdc42 polarisation (Fischer et al. 2008).

### 7.2.3. Lipid organisation in polarised growth

As discussed previously, the de-polarisation of PM lipids shown in Knafler et al and chapter 6 is likely to be upstream of the mis-localised exocyst and polarisome. Whether this is mediated by endocytic recycling of the lipids themselves, or of a protein intermediate, is unclear. Possible candidates for protein cargoes could be lipid anchoring or tethering proteins; lipid biosynthetic proteins (such as kinases or phosphatases); or proteins mediating lipid transport for example via ER-PM contacts.

Two of the few cargoes show to be polarised via endocytic recycling in filamentous fungi are the phospholipid flippases DnfA and DnfB (Martzoukou et al. 2017, Schultzhaus et al. 2015). Flippases regulate phospholipid asymmetry, moving phospholipids from the external to the cytosolic membrane leaflet, and have roles in membrane bending during vesicle formation (Takeda, Yamagami and Tanaka 2014). They localise to sites of polarised growth in yeast, and are thought to be important to endocytosis and polarised growth (Pomorski et al. 2003). One mechanism by which they may mediate this is

through controlling the GDI-mediated removal of Cdc42 from the plasma membrane, through alterations in bilayer asymmetry, thus controlling polarised growth (Das et al. 2012). If AP-2 is required for the endocytic recycling of these flippases in *C. albicans*, as in *A. nidulans* and *F. graminearum*, this could explain some of the observed PM lipid defects and perhaps some of the polarised growth defects. Cells without AP-2 did not show increased sensitivity to edelfosine (chapter 6), which can indicate flippase defects, however this does not prove that flippases are not affected in our mutant. GFP tagging of the phospholipid flippases in our *apm4* mutant would show us whether their recycling is mediated by AP-2 in *C. albicans*.

### 7.2.4. Mathematical models of hyphal growth

Mathematical modelling by Bartnicki-Garcia and colleagues (1989) demonstrated that a theoretical vesical supply centre (VSC) which is continuously radiating secretory vesicles, supplying both cell membrane and cell wall biosynthetic potential, predicts the shape of fungal hyphae. The VSC model has since been expanded to work in three dimensions rather than two (Gierz and Bartnicki-Garcia 2001) and to include the diffusive movement of vesicles (Tindemans, Kern and Mulder 2006), however it does not include endocytosis. A mathematic model by Arkowitz and colleagues (Weiner et al. 2019) which predicts the minimum number of secretory vesicles required to provide sufficient membrane to sustain apical growth of *C. albicans* also does not incorporate endocytosis. For this reason, the model only gives the minimum number of vesicles required; presumably this number would be higher once endocytic retrieval of membrane is considered. The effect of endocytic internalisation could theoretically be easily added into these models, by measuring the number of endocytic events in hyphal tips. Estimates of the proportion of endocytic vesicles which recycle back to the Spitzenkörper vs the proportion which are sent for lysosomal degradation would be a potentially valuable extension of the model. This could perhaps be achieved through covalently labelling PM lipids and tracking them to their final destination.

The mathematical models developed by Bartnicki-Garcia and Arkowitz however may give us valuable insights into the defective polarised growth observed in the absence of AP-2. As shown in chapter 6, the polarisation machinery is partially mis-localised in *apm4* deleted hyphae, including exocyst components. By counting Sec3 and Sec8 puncta, it was estimated that 60% of puncta were polarised to the tip in hyphae without

AP-2 (compared to almost 100% in WT hyphae). This could mean that roughly 60% of secretory vesicles are targeted to the hyphal tip, with 40% being sent to other regions around the hypha. As well as being a possible cause of the depolarised mannose deposition shown in Knafler et al (2019), this reduced flow of vesicles to the hyphal tip could lead to insufficient membrane supply and slowed apical growth. The loss of Spitzenkörper in some *apm4* deleted hyphae (chapter 6) could be a product of reduced vesicle flow to the hyphal tip. These mathematical models could perhaps be used to make predictions about the effects of reducing secretory flux to the hyphal apex, and whether this would account for the morphological defects observed in hyphae without AP-2.

### 7.2.5. Polarised growth in *C. albicans* compared to other fungi

One thing to note is that many studies on filamentous hyphal growth have looked at model fungi such as *A. nidulans* and *N. crassa*. In many ways *C. albicans* hyphal growth is similar to these fungi; they all involve secretion, endocytosis and a Spitzenkörper. However the Arkowitz lab have suggested that *C. albicans* may have a somewhat different mode of polarised growth compared to these fungi. *C. albicans* has narrower hyphae with a slower extension rate compared to 'true' filamentous fungi, and do not require microtubules (Rida et al. 2006) which are key to growth of other fungal hyphae (Taheri-Talesh et al. 2008). The Arkowitz lab demonstrated that, in contrast to other filamentous fungi, *C. albicans* hyphae do not generally show long-range transport of secretory vesicles along the hyphal length to the tip. Rather in this species, the Golgi is located close to the hyphal apex, and secretory vesicles bud from here and are transported via actin cables the short distance to the Spitzenkörper (Weiner et al. 2019).

This apical Golgi localisation may also be key for endocytic recycling in hyphae. Hernandez-Gonzalez and colleagues (2018) showed that in *A. nidulans*, internalised ChsB is recycled from sorting endosomes to the TGN, from where it is directed back to the apex; and that this recycling is key to its morphology and growth. Recent work from the Glick lab (Day, Casler and Glick 2018) has suggested that in *S. cerevisiae* the endocytic pathway is very simplified, with the TGN acting as an early and recycling endosome through which cargo are recycled back to the secretory pathway. A rapid recycling pathway through the Golgi, either bypassing the endosomes or instead of endosomes, could enable the rapid adaptation to different conditions required for fungal growth.

However more research is needed to characterise this potential pathway. It would be interesting to track our Chs3-GFP strain and try to determine its recycling route in *C. albicans*. Tagging of different markers of membrane compartments, combined with live cell imaging, could provide information about recycling in *C. albicans* hyphal growth.

## 7.3. Discussion in relation to the process of endocytosis

### 7.3.1. The link between endocytosis and exocytosis

It is well known that endocytosis is required in addition to apical exocytosis during hyphal growth, to re-internalise excess membrane and cargo from the cell surface. In yeast, exocytosis has been shown to regulate endocytosis in some ways: compensatory endocytosis is induced by polarised exocytosis in yeast (Johansen, Alfaro and Beh 2016), and many exocytic mutants are also defective in endocytosis (Jose et al. 2015). What is perhaps not so well explored is the impact of endocytosis on polarised exocytosis. This work shows that impaired endocytic recycling leads to de-polarisation of the secretory pathway in *C. albicans* hyphae (as marked by exocyst proteins and mannose deposition, shown in chapter 6 and Knafler et al). This underlines the intimate link between these two pathways and suggests that apical endocytic recycling is required for apical secretion. The de-polarisation of the secretory pathway in hyphae lacking AP-2 is likely to be a cause of many of their morphological defects. The effects of defective endocytosis and defective secretion could be difficult to separate. For example, the loss of Chs3 polarisation could in part be due to its mis-directed secretion rather than a lack of internalisation. However movies of Chs3-GFP in the *apm4* deletion mutant showed the protein was very static at the cell periphery, in contrast to the dynamic vesicles of WT Chs3-GFP, supporting the idea that the primary defect is in internalisation rather than mis-localised secretion.

### 7.3.2. Identifying endocytic cargoes of AP-2

Demonstrating a direct interaction between the AP-2 adaptor and its cargo has been notoriously difficult in mammalian systems due to their weak binding affinities and other requirements for binding (Gaidarov and Keen 2005). For example, purified AP-2 may require phosphorylation and PI(4,5)$P_2$ binding to activate it such that it can bind its cargo. The cargo-binding mutant *apm4*$^{1-454}$ and the fact that cells expressing this mutant have morphology defects almost as severe as the full *apm4* deletion suggests that direct

interactions between AP-2 and YxxΦ containing cargoes are very important in *C. albicans* (to our knowledge, this motif has not been characterised in fungal endocytosis before). Surface proteomics to compare levels of proteins at the cell surface in WT vs. *apm4*$^{1-454}$ cells would be informative in determining how many proteins depend on AP-2 for their localisation. However this would also not prove direct adaptor-cargo relationships, as a change in localisation of one key protein could have an indirect effect on the localisations of many others. This kind of study could however be backed up by pull-downs and in vitro binding assays.

### 7.3.3. The role of clathrin in fungal endocytosis

An interesting question raised by this work and the paper published by Martzoukou and colleagues (2017), is whether AP-2 functions independently of normal clathrin mediated endocytosis in filamentous fungi. There are thought to be two different roles for endocytosis in fungal hyphae: constitutive endocytosis of transporters and receptors which occurs all over the cell; and apical endocytosis which occurs in the hyphal 'collar' region. However these have not been shown to be different pathways with different requirements. The study by Martzoukou and colleagues suggests that these two pathways could be separated by their requirements for AP-2 (critical to apical recycling) and for clathrin (critical to transporter endocytosis). This suggestion could also explain the reduced requirement for AP-2 in *S. cerevisiae* yeast cells under normal growth conditions.

In this study, we have not examined the role of clathrin at all. However although Apl1-GFP signal is concentrated at the hyphal apex, it is certainly present in puncta all around the hypha (images in Knafler et al, 2019), suggesting AP-2 is not exclusively used for apical recycling in *C. albicans* as suggested by Martzoukou et al. We also observed co-localisation of AP-2 with Sla1, a protein involved in CME. The reportedly different roles of AP-2 and clathrin could alternatively be a distinction between recycling and degradative endocytic pathways. It is possible that an AP-2-mediated endocytic pathway could target cargo for recycling, whereas an AP-2-independent clathrin-dependent pathway could target cargo to the lysosome. It is unclear how this would be mediated, as AP-2 is rapidly uncoated from the endocytic vesicle after scission. Targeting could be mediated through different accessory proteins recruited by AP-2 to the endocytic vesicle. It could also be mediated through differential physical properties of the

endocytic vesicle. Differential clustering of cargoes into endocytic pits has been shown to affect the mode of clathrin curvature generation (Maib et al. 2018); implying that endocytic cargo may impact the physical properties of the vesicle generated.

Clathrin is known to function independently of AP-2 in both yeast and mammalian cells (Conner and Schmid 2003a, Motley et al. 2003, Yeung et al. 1999). However the AP-2 adaptor complex had not been shown previously to function independently of clathrin (Martzoukou et al. 2017). When Yeung and colleagues (1999) found AP-2 not to interact physically or genetically with clathrin in *S. cerevisiae* they took this as evidence for its unimportance. Several pathways of clathrin independent endocytosis (CIE) are known in mammalian cells, but until recently these were not thought to exist in yeast. In *S. cerevisiae* however, CIE has been shown to take place when CME is inhibited (Prosser et al. 2011, Aghamohammadzadeh, Smaczynska-de Rooij and Ayscough 2014). Interestingly, a clathrin-independent pathway has also been reported in *C. albicans*, which occurs in the absence of Arp2/3 (Epp et al. 2013). This pathway enables the uptake of lipid and fluid phase markers, but not of the transporters Ste2 and Mup1. Although AP-2 function was not looked at in this paper, this could hypothetically represent the clathrin-independent AP-2-dependent recycling pathway postulated by Martzoukou and colleagues. Also interestingly, CIE has been proposed to function in PM lipid homeostasis in mammalian cells (Shvets et al. 2015) which could be the case in fungi also, considering the lipid dysregulation observed in AP-2-depleted cells. More work is needed to determine whether there are indeed distinct clathrin-dependent and AP-2-dependent endocytic pathways in fungi.

### 7.3.4. Endocytic site localisation

Another interesting observation from this study is that, in the absence of AP-2, the number and location of endocytic sites was not altered (Knafler et al, 2019 and figure 6.2). Cells without *apm4* had the same number of actin patches in their yeast buds and hyphal tips as WT; suggesting that neither endocytic initiation nor progression was altered. This suggests that in *C. albicans* endocytic sites are initiated prior to, or independently of, cargo binding. This is in agreement with imaging studies showing that cargo arrive at endocytic sites after early endocytic proteins (Toshima et al. 2006). It is not known though how endocytic sites are initiated in the correct location at the hyphal tip and yeast buds. Intriguingly, endocytosis was still initiated in yeast even when the

seven earliest arriving endocytic proteins were deleted (Brach et al. 2014). Endocytic patches are found at sites of polarised secretion, and polarised exocytosis has been shown to induce compensatory endocytosis in yeast (Johansen et al. 2016); suggesting that the secretory machinery could determine endocytic site localisation. However our *apm4* mutant showed partially de-polarised secretion but not mis-localised endocytosis. PM lipid signals have also been implicated in endocytic initiation – early proteins Ede1 and Syp1 both bind lipids (Aguilar et al. 2003, Sun and Drubin 2012). Several lipids have been shown to have polarised gradients in *C. albicans* yeast and hyphae, which could serve to polarise sites of endocytosis. In this work the only lipid tested which maintained its polarisation in the absence of AP-2 was PI(4,5)$P_2$, therefore this lipid could be key to localising sites of endocytosis. Many endocytic proteins bind PI(4,5)$P_2$ and this lipid is known to be important to CME initiation and progression in mammalian cells (Antonescu et al. 2011). Further studies on the *apm4* deletion mutant or *apm4*$^{1-454}$ cargo binding mutant could give additional clues on the mechanism of endocytic site selection.

## 7.4. Future directions for this project

This study has raised many questions which would be interesting avenues for future investigation, many of which are outlined in the discussion above. Here is a brief summary of the main things I would like to do to continue the work started here, if time allowed.

- Gain an overview of how many proteins rely of AP-2 for their endocytosis in *C. albicans*, via a cell surface proteomics approach as described previously. This should give an idea as to how many proteins are affected by AP-2 depletion, and whether these fall into a few key categories
- Attempt to define the pathway by which AP-2 mediates PI(4)P and ergosterol distribution. Explore avenues to restore lipid polarisation, such as addition of exogenous ergosterol, or up-regulation of biosynthetic genes, to test whether this could restore polarisation of polarity markers
- Tag Cdc42 in our WT and *apm4* deletion strains, to determine whether Cdc42 requires AP-2 for its polarity maintenance. Explore possible mechanisms by testing whether AP-2 directly binds Cdc42 or any of its regulators

- As sterol rich domains are known to cluster GPI-anchored proteins, use a GFP-linked tag to test whether GPI-linked proteins are dysregulated in cells without AP-2
- Study Apm4 phosphorylation further by mutagenizing phosphorylation sites individually; or identifying the kinase responsible and testing the effect of repression of this kinase or mutagenesis of its recognition site
- Develop an inducible repressed version of Apm4, to study the effects of AP-2 depletion in real time via live cell imaging
- Develop a mathematical model of hyphal growth, incorporating what we now know about the importance of endocytic recycling of specific protein cargoes (irrespective of plasma membrane uptake) in the maintenance of polarised growth
- Continue with atomic force microscopy to determine whether hyphae without AP-2 have altered physical properties such as elasticity, and aim to correlate physical changes with alterations in cell wall composition
- Utilise *in vitro* models of adhesion and invasion to test whether the observed defects of cells without AP-2 correlate with a reduced ability to adhere and invade substrate
- Utilise animal models to test whether the defects of the *apm4* mutant lead to defects in virulence *in vivo*

I hope that the work presented in this thesis will be beneficial for future studies on the human fungal pathogen *C. albicans* and the mechanisms by it dynamically regulates its growth and cell surface organisation in response to changing environmental conditions.

# Chapter 8: References


Adams, A. E. & J. R. Pringle (1984) Relationship of actin and tubulin distribution to bud growth in wild-type and morphogenetic-mutant *Saccharomyces cerevisiae*. *J Cell Biol,* 98**,** 934-45.

Aebi, M. (2013) N-linked protein glycosylation in the ER. *Biochim Biophys Acta,* 1833**,** 2430-7.

Aghamohammadzadeh, S. & K. R. Ayscough (2009) Differential requirements for actin during yeast and mammalian endocytosis. *Nat Cell Biol,* 11**,** 1039-42.

Aghamohammadzadeh, S., I. I. Smaczynska-de Rooij & K. R. Ayscough (2014) An Abp1-dependent route of endocytosis functions when the classical endocytic pathway in yeast is inhibited. *PLoS One,* 9**,** e103311.

Aguilar, R. C., H. A. Watson & B. Wendland (2003) The yeast Epsin Ent1 is recruited to membranes through multiple independent interactions. *J Biol Chem,* 278**,** 10737-43.

Ahle, S., A. Mann, U. Eichelsbacher & E. Ungewickell (1988) Structural relationships between clathrin assembly proteins from the Golgi and the plasma membrane. *EMBO J,* 7**,** 919-29.

Alberti-Segui, C., A. J. Morales, H. Xing, M. M. Kessler, D. A. Willins, K. G. Weinstock, G. Cottarel, K. Fechtel & B. Rogers (2004) Identification of potential cell-surface proteins in *Candida albicans* and investigation of the role of a putative cell-surface glycosidase in adhesion and virulence. *Yeast,* 21**,** 285-302.

Alfaro, G., J. Johansen, S. A. Dighe, G. Duamel, K. G. Kozminski & C. T. Beh (2011) The sterol-binding protein Kes1/Osh4p is a regulator of polarized exocytosis. *Traffic,* 12**,** 1521-36.

Amoutzias, G. D., Y. He, K. S. Lilley, Y. Van de Peer & S. G. Oliver (2012) Evaluation and properties of the budding yeast phosphoproteome. *Mol Cell Proteomics,* 11**,** M111.009555.

Anantharaman, V. & L. Aravind (2002) The GOLD domain, a novel protein module involved in Golgi function and secretion. *Genome Biol,* 3**,** research0023.

Anderson, J. M. & D. R. Soll (1986) Differences in actin localization during bud and hypha formation in the yeast *Candida albicans*. *J Gen Microbiol,* 132**,** 2035-47.

Antley, P. P. & K. C. Hazen (1988) Role of yeast cell growth temperature on *Candida albicans* virulence in mice. *Infect Immun,* 56**,** 2884-90.

Anton, C., J. V. Taubas & C. Roncero (2018) The Functional Specialization of Exomer as a Cargo Adaptor During the Evolution of Fungi. *Genetics,* 208**,** 1483-1498.

Antonescu, C. N., F. Aguet, G. Danuser & S. L. Schmid (2011) Phosphatidylinositol-(4,5)-bisphosphate regulates clathrin-coated pit initiation, stabilization, and size. *Mol Biol Cell,* 22**,** 2588-600.

Araujo-Bazán, L., M. A. Peñalva & E. A. Espeso (2008) Preferential localization of the endocytic internalization machinery to hyphal tips underlies polarization of the actin cytoskeleton in *Aspergillus nidulans*. *Mol Microbiol,* 67**,** 891-905.

Ariño, J. (2010) Integrative responses to high pH stress in *S. cerevisiae*. *OMICS,* 14**,** 517-23.
Asleson, C. M., E. S. Bensen, C. A. Gale, A. S. Melms, C. Kurischko & J. Berman (2001) *Candida albicans* INT1-induced filamentation in *Saccharomyces cerevisiae* depends on Sla2p. *Mol Cell Biol,* 21**,** 1272-84.
Bagnat, M. & K. Simons (2002) Cell surface polarization during yeast mating. *Proc Natl Acad Sci U S A,* 99**,** 14183-8.
Ballou, C. E., K. A. Kern & W. C. Raschke (1973) Genetic control of yeast mannan structure. Complementation studies and properties of mannan mutants. *J Biol Chem,* 248**,** 4667-71.
Bar-Yosef, H., N. Vivanco Gonzalez, S. Ben-Aroya, S. J. Kron & D. Kornitzer (2017) Chemical inhibitors of *Candida albicans* hyphal morphogenesis target endocytosis. *Sci Rep,* 7**,** 5692.
Barlow, L. D., J. B. Dacks & J. G. Wideman (2014) From all to (nearly) none: Tracing adaptin evolution in Fungi. *Cell Logist,* 4**,** e28114.
Barral, Y., V. Mermall, M. S. Mooseker & M. Snyder (2000) Compartmentalization of the cell cortex by septins is required for maintenance of cell polarity in yeast. *Mol Cell,* 5**,** 841-51.
Bartnicki-Garcia, S. (2006) Chitosomes: past, present and future. *FEMS Yeast Res,* 6**,** 957-65.
Bartnicki-Garcia, S., D. D. Bartnicki, G. Gierz, R. López-Franco & C. E. Bracker (1995) Evidence that Spitzenkörper behavior determines the shape of a fungal hypha: a test of the hyphoid model. *Exp Mycol,* 19**,** 153-9.
Bartnicki-Garcia, S., C. E. Bracker, G. Gierz, R. López-Franco & H. Lu (2000) Mapping the growth of fungal hyphae: orthogonal cell wall expansion during tip growth and the role of turgor. *Biophys J,* 79**,** 2382-90.
Bartnicki-Garcia, S., F. Hergert & G. Gierz. 1989. Computer simulation of fungal morphogenesis and the mathematical basis for hyphal (tip) growth. 46 - 57. Protoplasma.
Bartnicki-Garcia, S. & E. Lippman (1969) Fungal morphogenesis: cell wall construction in *Mucor rouxii*. *Science,* 165**,** 302-4.
Beacham, G. M., E. A. Partlow & G. Hollopeter (2019) Conformational regulation of AP1 and AP2 clathrin adaptor complexes. *Traffic*.
Beacham, G. M., E. A. Partlow, J. J. Lange & G. Hollopeter (2018) NECAPs are negative regulators of the AP2 clathrin adaptor complex. *Elife,* 7.
Becker, B., A. Blum, E. Gießelmann, J. Dausend, D. Rammo, N. C. Müller, E. Tschacksch, M. Steimer, J. Spindler, U. Becherer, J. Rettig, F. Breinig & M. J. Schmitt (2016) H/KDEL receptors mediate host cell intoxication by a viral A/B toxin in yeast. *Sci Rep,* 6**,** 31105.
Becker, B. & M. J. Schmitt (2017) Yeast Killer Toxin K28: Biology and Unique Strategy of Host Cell Intoxication and Killing. *Toxins (Basel),* 9.
Beh, C. T., C. R. McMaster, K. G. Kozminski & A. K. Menon (2012) A detour for yeast oxysterol binding proteins. *J Biol Chem,* 287**,** 11481-8.
Beh, C. T. & J. Rine (2004) A role for yeast oxysterol-binding protein homologs in endocytosis and in the maintenance of intracellular sterol-lipid distribution. *J Cell Sci,* 117**,** 2983-96.

Bertin, A., M. A. McMurray, L. Thai, G. Garcia, V. Votin, P. Grob, T. Allyn, J. Thorner & E. Nogales (2010) Phosphatidylinositol-4,5-bisphosphate promotes budding yeast septin filament assembly and organization. *J Mol Biol,* 404**,** 711-31.

Boorsma, A., H. de Nobel, B. ter Riet, B. Bargmann, S. Brul, K. J. Hellingwerf & F. M. Klis (2004) Characterization of the transcriptional response to cell wall stress in *Saccharomyces cerevisiae*. *Yeast,* 21**,** 413-27.

Borth, N., A. Walther, P. Reijnst, S. Jorde, Y. Schaub & J. Wendland (2010) *Candida albicans* Vrp1 is required for polarized morphogenesis and interacts with Wal1 and Myo5. *Microbiology,* 156**,** 2962-9.

Boucrot, E., S. Saffarian, R. Zhang & T. Kirchhausen (2010) Roles of AP-2 in clathrin-mediated endocytosis. *PLoS One,* 5**,** e10597.

Boulant, S., C. Kural, J. C. Zeeh, F. Ubelmann & T. Kirchhausen (2011) Actin dynamics counteract membrane tension during clathrin-mediated endocytosis. *Nat Cell Biol,* 13**,** 1124-31.

Bowman, S. M. & S. J. Free (2006) The structure and synthesis of the fungal cell wall. *Bioessays,* 28**,** 799-808.

Boyd, C., T. Hughes, M. Pypaert & P. Novick (2004) Vesicles carry most exocyst subunits to exocytic sites marked by the remaining two subunits, Sec3p and Exo70p. *J Cell Biol,* 167**,** 889-901.

Brach, T., C. Godlee, I. Moeller-Hansen, D. Boeke & M. Kaksonen (2014) The initiation of clathrin-mediated endocytosis is mechanistically highly flexible. *Curr Biol,* 24**,** 548-54.

Bracker, C. E., J. Ruiz-Herrera & S. Bartnicki-Garcia (1976) Structure and transformation of chitin synthetase particles (chitosomes) during microfibril synthesis in vitro. *Proc Natl Acad Sci U S A,* 73**,** 4570-4.

Brand, A., D. M. MacCallum, A. J. Brown, N. A. Gow & F. C. Odds (2004) Ectopic expression of URA3 can influence the virulence phenotypes and proteome of *Candida albicans* but can be overcome by targeted reintegration of URA3 at the RPS10 locus. *Eukaryot Cell,* 3**,** 900-9.

Braun, P. C. & R. A. Calderone (1978) Chitin synthesis in *Candida albicans*: comparison of yeast and hyphal forms. *J Bacteriol,* 133**,** 1472-7.

Brown, D. A. & E. London (1998) Functions of lipid rafts in biological membranes. *Annu Rev Cell Dev Biol,* 14**,** 111-36.

Brown, D. A. & J. K. Rose (1992) Sorting of GPI-anchored proteins to glycolipid-enriched membrane subdomains during transport to the apical cell surface. *Cell,* 68**,** 533-44.

Brown, D. H., A. D. Giusani, X. Chen & C. A. Kumamoto (1999) Filamentous growth of *Candida albicans* in response to physical environmental cues and its regulation by the unique CZF1 gene. *Mol Microbiol,* 34**,** 651-62.

Brown, G. D., D. W. Denning, N. A. Gow, S. M. Levitz, M. G. Netea & T. C. White (2012) Hidden killers: human fungal infections. *Sci Transl Med,* 4**,** 165rv13.

Butty, A. C., N. Perrinjaquet, A. Petit, M. Jaquenoud, J. E. Segall, K. Hofmann, C. Zwahlen & M. Peter (2002) A positive feedback loop stabilizes the guanine-nucleotide exchange factor Cdc24 at sites of polarization. *EMBO J,* 21**,** 1565-76.

Caballero-Lima, D., I. N. Kaneva, S. P. Watton, P. E. Sudbery & C. J. Craven (2013) The spatial distribution of the exocyst and actin cortical patches is sufficient to organize hyphal tip growth. *Eukaryot Cell,* 12**,** 998-1008.

Cabib, E., B. Bowers, A. Sburlati & S. J. Silverman (1988) Fungal cell wall synthesis: the construction of a biological structure. *Microbiol Sci,* 5**,** 370-5.

Cabib, E., S. J. Silverman & J. A. Shaw (1992) Chitinase and chitin synthase 1: counterbalancing activities in cell separation of *Saccharomyces cerevisiae*. *J Gen Microbiol,* 138**,** 97-102.

Calderone, R. A. & W. A. Fonzi (2001) Virulence factors of *Candida albicans*. *Trends Microbiol,* 9**,** 327-35.

Carroll, S. Y., P. C. Stirling, H. E. Stimpson, E. Giesselmann, M. J. Schmitt & D. G. Drubin (2009) A yeast killer toxin screen provides insights into a/b toxin entry, trafficking, and killing mechanisms. *Dev Cell,* 17**,** 552-60.

Chaffin, W. L. (2008) *Candida albicans* cell wall proteins. *Microbiol Mol Biol Rev,* 72**,** 495-544.

Chapa-y-Lazo, B., E. G. Allwood, I. I. Smaczynska-de Rooij, M. L. Snape & K. R. Ayscough (2014) Yeast endocytic adaptor AP-2 binds the stress sensor Mid2 and functions in polarized cell responses. *Traffic,* 15**,** 546-57.

Chapa-Y-Lazo, B. & K. R. Ayscough (2014) Apm4, the mu subunit of yeast AP-2 interacts with Pkc1, and mutation of the Pkc1 consensus phosphorylation site Thr176 inhibits AP-2 recruitment to endocytic sites. *Commun Integr Biol,* 7**,** e28522.

Cleveland, A. A., L. H. Harrison, M. M. Farley, R. Hollick, B. Stein, T. M. Chiller, S. R. Lockhart & B. J. Park (2015) Declining incidence of candidemia and the shifting epidemiology of *Candida* resistance in two US metropolitan areas, 2008-2013: results from population-based surveillance. *PLoS One,* 10**,** e0120452.

Cocucci, E., F. Aguet, S. Boulant & T. Kirchhausen (2012) The first five seconds in the life of a clathrin-coated pit. *Cell,* 150**,** 495-507.

Cohen, R., F. J. Roth, E. Delgado, D. G. Ahearn & M. H. Kalser (1969) Fungal flora of the normal human small and large intestine. *N Engl J Med,* 280**,** 638-41.

Collins, B. M., A. J. McCoy, H. M. Kent, P. R. Evans & D. J. Owen (2002) Molecular architecture and functional model of the endocytic AP2 complex. *Cell,* 109**,** 523-35.

Colombo, A. L., T. Guimarães, L. R. Silva, L. P. de Almeida Monfardini, A. K. Cunha, P. Rady, T. Alves & R. C. Rosas (2007) Prospective observational study of candidemia in São Paulo, Brazil: incidence rate, epidemiology, and predictors of mortality. *Infect Control Hosp Epidemiol,* 28**,** 570-6.

Conner, S. D. & S. L. Schmid (2002) Identification of an adaptor-associated kinase, AAK1, as a regulator of clathrin-mediated endocytosis. *J Cell Biol,* 156**,** 921-9.

--- (2003a) Differential requirements for AP-2 in clathrin-mediated endocytosis. *J Cell Biol,* 162**,** 773-9.

--- (2003b) Regulated portals of entry into the cell. *Nature,* 422**,** 37-44.

Conner, S. D., T. Schröter & S. L. Schmid (2003) AAK1-mediated micro2 phosphorylation is stimulated by assembled clathrin. *Traffic,* 4**,** 885-90.

Crampin, H., K. Finley, M. Gerami-Nejad, H. Court, C. Gale, J. Berman & P. Sudbery (2005) *Candida albicans* hyphae have a Spitzenkörper that is distinct from the polarisome found in yeast and pseudohyphae. *J Cell Sci,* 118**,** 2935-47.

Czop, J. K. & K. F. Austen (1985) Generation of leukotrienes by human monocytes upon stimulation of their beta-glucan receptor during phagocytosis. *Proc Natl Acad Sci U S A,* 82**,** 2751-5.

Dalle, F., B. Wächtler, C. L'Ollivier, G. Holland, N. Bannert, D. Wilson, C. Labruère, A. Bonnin & B. Hube (2010) Cellular interactions of *Candida albicans* with human oral epithelial cells and enterocytes. *Cell Microbiol,* 12**,** 248-71.

Daran, J. M., N. Dallies, D. Thines-Sempoux, V. Paquet & J. François (1995) Genetic and biochemical characterization of the UGP1 gene encoding the UDP-glucose pyrophosphorylase from *Saccharomyces cerevisiae*. *Eur J Biochem,* 233**,** 520-30.

Das, A., B. D. Slaughter, J. R. Unruh, W. D. Bradford, R. Alexander, B. Rubinstein & R. Li (2012) Flippase-mediated phospholipid asymmetry promotes fast Cdc42 recycling in dynamic maintenance of cell polarity. *Nat Cell Biol,* 14**,** 304-10.

David, L. A., C. F. Maurice, R. N. Carmody, D. B. Gootenberg, J. E. Button, B. E. Wolfe, A. V. Ling, A. S. Devlin, Y. Varma, M. A. Fischbach, S. B. Biddinger, R. J. Dutton & P. J. Turnbaugh (2014) Diet rapidly and reproducibly alters the human gut microbiome. *Nature,* 505**,** 559-63.

Day, K. J., J. C. Casler & B. S. Glick (2018) Budding Yeast Has a Minimal Endomembrane System. *Dev Cell,* 44**,** 56-72.e4.

de Lucena, R. M., C. Elsztein, D. A. Simões & M. A. de Morais (2012) Participation of CWI, HOG and Calcineurin pathways in the tolerance of *Saccharomyces cerevisiae* to low pH by inorganic acid. *J Appl Microbiol,* 113**,** 629-40.

de Saint-Jean, M., V. Delfosse, D. Douguet, G. Chicanne, B. Payrastre, W. Bourguet, B. Antonny & G. Drin (2011) Osh4p exchanges sterols for phosphatidylinositol 4-phosphate between lipid bilayers. *J Cell Biol,* 195**,** 965-78.

Degreif, D., B. Cucu, I. Budin, G. Thiel & A. Bertl (2019) Lipid determinants of endocytosis and exocytosis in budding yeast. *Biochim Biophys Acta Mol Cell Biol Lipids,* 1864**,** 1005-1016.

del Pozo, M. A., L. S. Price, N. B. Alderson, X. D. Ren & M. A. Schwartz (2000) Adhesion to the extracellular matrix regulates the coupling of the small GTPase Rac to its effector PAK. *EMBO J,* 19**,** 2008-14.

Dell'Angelica, E. C. (2001) Clathrin-binding proteins: got a motif? Join the network! *Trends Cell Biol,* 11**,** 315-8.

Dennehy, K. M. & G. D. Brown (2007) The role of the beta-glucan receptor Dectin-1 in control of fungal infection. *J Leukoc Biol,* 82**,** 253-8.

Donovan, K. W. & A. Bretscher (2015) Tracking individual secretory vesicles during exocytosis reveals an ordered and regulated process. *J Cell Biol,* 210**,** 181-9.

Doray, B., I. Lee, J. Knisely, G. Bu & S. Kornfeld (2007) The gamma/sigma1 and alpha/sigma2 hemicomplexes of clathrin adaptors AP-1 and AP-2 harbor the dileucine recognition site. *Mol Biol Cell,* 18**,** 1887-96.

Douglas, C. M., J. A. D'Ippolito, G. J. Shei, M. Meinz, J. Onishi, J. A. Marrinan, W. Li, G. K. Abruzzo, A. Flattery, K. Bartizal, A. Mitchell & M. B. Kurtz (1997) Identification of the FKS1 gene of *Candida albicans* as the essential target of 1,3-beta-D-glucan synthase inhibitors. *Antimicrob Agents Chemother,* 41**,** 2471-9.

Douglas, L. M., F. J. Alvarez, C. McCreary & J. B. Konopka (2005) Septin function in yeast model systems and pathogenic fungi. *Eukaryot Cell,* 4**,** 1503-12.

Ehrlich, M., W. Boll, A. Van Oijen, R. Hariharan, K. Chandran, M. L. Nibert & T. Kirchhausen (2004) Endocytosis by random initiation and stabilization of clathrin-coated pits. *Cell,* 118**,** 591-605.

Ene, I. V., A. K. Adya, S. Wehmeier, A. C. Brand, D. M. MacCallum, N. A. Gow & A. J. Brown (2012) Host carbon sources modulate cell wall architecture, drug resistance and virulence in a fungal pathogen. *Cell Microbiol,* 14**,** 1319-35.

Ene, I. V., S. C. Cheng, M. G. Netea & A. J. Brown (2013) Growth of *Candida albicans* cells on the physiologically relevant carbon source lactate affects their recognition and phagocytosis by immune cells. *Infect Immun,* 81**,** 238-48.

Ene, I. V., L. A. Walker, M. Schiavone, K. K. Lee, H. Martin-Yken, E. Dague, N. A. Gow, C. A. Munro & A. J. Brown (2015) Cell Wall Remodeling Enzymes Modulate Fungal Cell Wall Elasticity and Osmotic Stress Resistance. *MBio,* 6**,** e00986.

Engqvist-Goldstein, A. E., C. X. Zhang, S. Carreno, C. Barroso, J. E. Heuser & D. G. Drubin (2004) RNAi-mediated Hip1R silencing results in stable association between the endocytic machinery and the actin assembly machinery. *Mol Biol Cell,* 15**,** 1666-79.

Epp, E., E. Nazarova, H. Regan, L. M. Douglas, J. B. Konopka, J. Vogel & M. Whiteway (2013) Clathrin- and Arp2/3-independent endocytosis in the fungal pathogen *Candida albicans*. *MBio,* 4**,** e00476-13.

Erb Downward, J. R., N. R. Falkowski, K. L. Mason, R. Muraglia & G. B. Huffnagle (2013) Modulation of post-antibiotic bacterial community reassembly and host response by *Candida albicans*. *Sci Rep,* 3**,** 2191.

Erwig, L. P. & N. A. Gow (2016) Interactions of fungal pathogens with phagocytes. *Nat Rev Microbiol,* 14**,** 163-76.

Etienne-Manneville, S. (2004) Cdc42--the centre of polarity. *J Cell Sci,* 117**,** 1291-300.

Evangelista, M., K. Blundell, M. S. Longtine, C. J. Chow, N. Adames, J. R. Pringle, M. Peter & C. Boone (1997) Bni1p, a yeast formin linking cdc42p and the actin cytoskeleton during polarized morphogenesis. *Science,* 276**,** 118-22.

Falagas, M. E., N. Roussos & K. Z. Vardakas (2010) Relative frequency of *albicans* and the various non-*albicans Candida* spp among candidemia isolates from inpatients in various parts of the world: a systematic review. *Int J Infect Dis,* 14**,** e954-66.

Fidel, P. L., J. A. Vazquez & J. D. Sobel (1999) *Candida glabrata*: review of epidemiology, pathogenesis, and clinical disease with comparison to *C. albicans*. *Clin Microbiol Rev,* 12**,** 80-96.

Fingerhut, A., K. von Figura & S. Honing (2001) Binding of AP2 to sorting signals is modulated by AP2 phosphorylation. *J Biol Chem,* 276**,** 5476-82.

Fischer, R., N. Zekert & N. Takeshita (2008) Polarized growth in fungi--interplay between the cytoskeleton, positional markers and membrane domains. *Mol Microbiol,* 68**,** 813-26.

Fischer-Parton, S., R. M. Parton, P. C. Hickey, J. Dijksterhuis, H. A. Atkinson & N. D. Read (2000) Confocal microscopy of FM4-64 as a tool for analysing endocytosis and vesicle trafficking in living fungal hyphae. *J Microsc,* 198**,** 246-59.

Fonzi, W. A. & M. Y. Irwin (1993) Isogenic strain construction and gene mapping in Candida albicans. *Genetics,* 134**,** 717-28.

Forche, A., P. T. Magee, B. B. Magee & G. May (2004) Genome-wide single-nucleotide polymorphism map for *Candida albicans*. *Eukaryot Cell,* 3**,** 705-14.

Formosa, C., M. Schiavone, H. Martin-Yken, J. M. François, R. E. Duval & E. Dague (2013) Nanoscale effects of caspofungin against two yeast species, *Saccharomyces cerevisiae* and *Candida albicans*. *Antimicrob Agents Chemother,* 57**,** 3498-506.

Fradin, C., P. De Groot, D. MacCallum, M. Schaller, F. Klis, F. C. Odds & B. Hube (2005) Granulocytes govern the transcriptional response, morphology and proliferation of *Candida albicans* in human blood. *Mol Microbiol,* 56**,** 397-415.

Freisinger, T., B. Klünder, J. Johnson, N. Müller, G. Pichler, G. Beck, M. Costanzo, C. Boone, R. A. Cerione, E. Frey & R. Wedlich-Söldner (2013) Establishment of a robust single axis of cell polarity by coupling multiple positive feedback loops. *Nat Commun,* 4**,** 1807.

Fujiwara, M., H. Horiuchi, A. Ohta & M. Takagi (1997) A novel fungal gene encoding chitin synthase with a myosin motor-like domain. *Biochem Biophys Res Commun,* 236**,** 75-8.

Gaidarov, I., Q. Chen, J. R. Falck, K. K. Reddy & J. H. Keen (1996) A functional phosphatidylinositol 3,4,5-trisphosphate/phosphoinositide binding domain in the clathrin adaptor AP-2 alpha subunit. Implications for the endocytic pathway. *J Biol Chem,* 271**,** 20922-9.

Gaidarov, I. & J. H. Keen (1999) Phosphoinositide-AP-2 interactions required for targeting to plasma membrane clathrin-coated pits. *J Cell Biol,* 146**,** 755-64.

--- (2005) Membrane targeting of endocytic adaptors: cargo and lipid do it together. *Dev Cell,* 8**,** 801-2.

Gantner, B. N., R. M. Simmons & D. M. Underhill (2005) Dectin-1 mediates macrophage recognition of *Candida albicans* yeast but not filaments. *EMBO J,* 24**,** 1277-86.

García, R., C. Bermejo, C. Grau, R. Pérez, J. M. Rodríguez-Peña, J. Francois, C. Nombela & J. Arroyo (2004) The global transcriptional response to

transient cell wall damage in *Saccharomyces cerevisiae* and its regulation by the cell integrity signaling pathway. *J Biol Chem,* 279**,** 15183-95.
Garrenton, L. S., C. J. Stefan, M. A. McMurray, S. D. Emr & J. Thorner (2010) Pheromone-induced anisotropy in yeast plasma membrane phosphatidylinositol-4,5-bisphosphate distribution is required for MAPK signaling. *Proc Natl Acad Sci U S A,* 107**,** 11805-10.
Gatta, A. T. & T. P. Levine (2017) Piecing Together the Patchwork of Contact Sites. *Trends Cell Biol,* 27**,** 214-229.
Ghannoum, M. A., B. J. Spellberg, A. S. Ibrahim, J. A. Ritchie, B. Currie, E. D. Spitzer, J. E. Edwards & A. Casadevall (1994) Sterol composition of *Cryptococcus neoformans* in the presence and absence of fluconazole. *Antimicrob Agents Chemother,* 38**,** 2029-33.
Ghugtyal, V., R. Garcia-Rodas, A. Seminara, S. Schaub, M. Bassilana & R. A. Arkowitz (2015) Phosphatidylinositol-4-phosphate-dependent membrane traffic is critical for fungal filamentous growth. *Proc Natl Acad Sci U S A,* 112**,** 8644-9.
Gierz, G. & S. Bartnicki-Garcia (2001) A three-dimensional model of fungal morphogenesis based on the vesicle supply center concept. *J Theor Biol,* 208**,** 151-64.
Girbardt, M. 1957. Der Spitzenkörper von Polystictus versicolor (L.). 47 - 59. Planta.
Goode, B. L., J. A. Eskin & B. Wendland (2015) Actin and endocytosis in budding yeast. *Genetics,* 199**,** 315-58.
Gow, N. A. (1997) Germ tube growth of *Candida albicans*. *Curr Top Med Mycol,* 8**,** 43-55.
Gow, N. A. & G. W. Gooday (1982) Vacuolation, branch production and linear growth of germ tubes in Candida albicans. *J Gen Microbiol,* 128**,** 2195-8.
Gow, N. A. R., J. P. Latge & C. A. Munro (2017) The Fungal Cell Wall: Structure, Biosynthesis, and Function. *Microbiol Spectr,* 5.
Grossmann, G., J. Malinsky, W. Stahlschmidt, M. Loibl, I. Weig-Meckl, W. B. Frommer, M. Opekarová & W. Tanner (2008) Plasma membrane microdomains regulate turnover of transport proteins in yeast. *J Cell Biol,* 183**,** 1075-88.
Grove, S. N. & C. E. Bracker (1970) Protoplasmic organization of hyphal tips among fungi: vesicles and Spitzenkörper. *J Bacteriol,* 104**,** 989-1009.
Guo, W., A. Grant & P. Novick (1999a) Exo84p is an exocyst protein essential for secretion. *J Biol Chem,* 274**,** 23558-64.
Guo, W., D. Roth, C. Walch-Solimena & P. Novick (1999b) The exocyst is an effector for Sec4p, targeting secretory vesicles to sites of exocytosis. *EMBO J,* 18**,** 1071-80.
Haase, K. & A. E. Pelling (2015) Investigating cell mechanics with atomic force microscopy. *J R Soc Interface,* 12**,** 20140970.
Hall, R. A., F. Cottier & F. A. Mühlschlegel (2009) Molecular networks in the fungal pathogen *Candida albicans*. *Adv Appl Microbiol,* 67**,** 191-212.
Hall, R. A. & N. A. Gow (2013) Mannosylation in *Candida albicans*: role in cell wall function and immune recognition. *Mol Microbiol,* 90**,** 1147-61.

Hammond, G. R., M. J. Fischer, K. E. Anderson, J. Holdich, A. Koteci, T. Balla & R. F. Irvine (2012) PI4P and PI(4,5)P2 are essential but independent lipid determinants of membrane identity. *Science,* 337**,** 727-30.

Hanson, P. K., L. Malone, J. L. Birchmore & J. W. Nichols (2003) Lem3p is essential for the uptake and potency of alkylphosphocholine drugs, edelfosine and miltefosine. *J Biol Chem,* 278**,** 36041-50.

Harpaz, R., R. M. Dahl & K. L. Dooling (2016) Prevalence of Immunosuppression Among US Adults, 2013. *JAMA,* 316**,** 2547-2548.

Harris, S. D., N. D. Read, R. W. Roberson, B. Shaw, S. Seiler, M. Plamann & M. Momany (2005) Polarisome meets spitzenkörper: microscopy, genetics, and genomics converge. *Eukaryot Cell,* 4**,** 225-9.

Hasim, S., D. P. Allison, S. T. Retterer, A. Hopke, R. T. Wheeler, M. J. Doktycz & T. B. Reynolds (2017) β-(1,3)-Glucan Unmasking in Some *Candida albicans* Mutants Correlates with Increases in Cell Wall Surface Roughness and Decreases in Cell Wall Elasticity. *Infect Immun,* 85.

Haslam, R. J., H. B. Koide & B. A. Hemmings (1993) Pleckstrin domain homology. *Nature,* 363**,** 309-10.

Hazan, I. & H. Liu (2002) Hyphal tip-associated localization of Cdc42 is F-actin dependent in *Candida albicans*. *Eukaryot Cell,* 1**,** 856-64.

Hazan, I., M. Sepulveda-Becerra & H. Liu (2002) Hyphal elongation is regulated independently of cell cycle in *Candida albicans*. *Mol Biol Cell,* 13**,** 134-45.

Hazen, K. C., D. R. Singleton & J. Masuoka (2007) Influence of outer region mannosylphosphorylation on N-glycan formation by *Candida albicans*: normal acid-stable N-glycan formation requires acid-labile mannosylphosphate addition. *Glycobiology,* 17**,** 1052-60.

He, B., F. Xi, X. Zhang, J. Zhang & W. Guo (2007) Exo70 interacts with phospholipids and mediates the targeting of the exocyst to the plasma membrane. *EMBO J,* 26**,** 4053-65.

Heider, M. R., M. Gu, C. M. Duffy, A. M. Mirza, L. L. Marcotte, A. C. Walls, N. Farrall, Z. Hakhverdyan, M. C. Field, M. P. Rout, A. Frost & M. Munson (2016) Subunit connectivity, assembly determinants and architecture of the yeast exocyst complex. *Nat Struct Mol Biol,* 23**,** 59-66.

Heilmann, C. J., A. G. Sorgo, S. Mohammadi, G. J. Sosinska, C. G. de Koster, S. Brul, L. J. de Koning & F. M. Klis (2013) Surface stress induces a conserved cell wall stress response in the pathogenic fungus *Candida albicans*. *Eukaryot Cell,* 12**,** 254-64.

Henne, W. M., E. Boucrot, M. Meinecke, E. Evergren, Y. Vallis, R. Mittal & H. T. McMahon (2010) FCHo proteins are nucleators of clathrin-mediated endocytosis. *Science,* 328**,** 1281-4.

Henry, K. W., J. T. Nickels & T. D. Edlind (2000) Upregulation of ERG genes in *Candida* species by azoles and other sterol biosynthesis inhibitors. *Antimicrob Agents Chemother,* 44**,** 2693-700.

Hernández-González, M., I. Bravo-Plaza, M. Pinar, V. de Los Ríos, H. N. Arst & M. A. Peñalva (2018) Endocytic recycling via the TGN underlies the polarized hyphal mode of life. *PLoS Genet,* 14**,** e1007291.

Hinrichsen, L., J. Harborth, L. Andrees, K. Weber & E. J. Ungewickell (2003) Effect of clathrin heavy chain- and alpha-adaptin-specific small inhibitory RNAs

on endocytic accessory proteins and receptor trafficking in HeLa cells. *J Biol Chem,* 278**,** 45160-70.
Hoffmann, J. & K. Mendgen (1998) Endocytosis and membrane turnover in the germ tube of uromyces fabae. *Fungal Genet Biol,* 24**,** 77-85.
Hollopeter, G., J. J. Lange, Y. Zhang, T. N. Vu, M. Gu, M. Ailion, E. J. Lambie, B. D. Slaughter, J. R. Unruh, L. Florens & E. M. Jorgensen (2014) The membrane-associated proteins FCHo and SGIP are allosteric activators of the AP2 clathrin adaptor complex. *Elife,* 3.
Howard, R. J. (1981) Ultrastructural analysis of hyphal tip cell growth in fungi: Spitzenkörper, cytoskeleton and endomembranes after freeze-substitution. *J Cell Sci,* 48**,** 89-103.
Hube, B. (2004) From commensal to pathogen: stage- and tissue-specific gene expression of *Candida albicans*. *Curr Opin Microbiol,* 7**,** 336-41.
Hull, C. M. & A. D. Johnson (1999) Identification of a mating type-like locus in the asexual pathogenic yeast *Candida albicans*. *Science,* 285**,** 1271-5.
Hur, H. S., J. H. Ryu, K. H. Kim & J. Kim (2006) Characterization of Osh3, an oxysterol-binding protein, in filamentous growth of *Saccharomyces cerevisiae* and *Candida albicans*. *J Microbiol,* 44**,** 523-9.
Höning, S., D. Ricotta, M. Krauss, K. Späte, B. Spolaore, A. Motley, M. Robinson, C. Robinson, V. Haucke & D. J. Owen (2005) Phosphatidylinositol-(4,5)-bisphosphate regulates sorting signal recognition by the clathrin-associated adaptor complex AP2. *Mol Cell,* 18**,** 519-31.
Irazoqui, J. E. & D. J. Lew (2004) Polarity establishment in yeast. *J Cell Sci,* 117**,** 2169-71.
Ishibashi, K., M. Yoshida, I. Nakabayashi, H. Shinohara, N. N. Miura, Y. Adachi & N. Ohno (2005) Role of anti-beta-glucan antibody in host defense against fungi. *FEMS Immunol Med Microbiol,* 44**,** 99-109.
Jackson, L. P., B. T. Kelly, A. J. McCoy, T. Gaffry, L. C. James, B. M. Collins, S. Höning, P. R. Evans & D. J. Owen (2010) A large-scale conformational change couples membrane recruitment to cargo binding in the AP2 clathrin adaptor complex. *Cell,* 141**,** 1220-9.
Janes, P. W., S. C. Ley, A. I. Magee & P. S. Kabouridis (2000) The role of lipid rafts in T cell antigen receptor (TCR) signalling. *Semin Immunol,* 12**,** 23-34.
Jin, Y., A. Sultana, P. Gandhi, E. Franklin, S. Hamamoto, A. R. Khan, M. Munson, R. Schekman & L. S. Weisman (2011) Myosin V transports secretory vesicles via a Rab GTPase cascade and interaction with the exocyst complex. *Dev Cell,* 21**,** 1156-70.
Johansen, J., G. Alfaro & C. T. Beh (2016) Polarized Exocytosis Induces Compensatory Endocytosis by Sec4p-Regulated Cortical Actin Polymerization. *PLoS Biol,* 14**,** e1002534.
Johnson, D. I. (1999) Cdc42: An essential Rho-type GTPase controlling eukaryotic cell polarity. *Microbiol Mol Biol Rev,* 63**,** 54-105.
Jones, L. A. & P. E. Sudbery (2010) Spitzenkorper, exocyst, and polarisome components in *Candida albicans* hyphae show different patterns of localization and have distinct dynamic properties. *Eukaryot Cell,* 9**,** 1455-65.

Jose, M., S. Tollis, D. Nair, R. Mitteau, C. Velours, A. Massoni-Laporte, A. Royou, J. B. Sibarita & D. McCusker (2015) A quantitative imaging-based screen reveals the exocyst as a network hub connecting endocytosis and exocytosis. *Mol Biol Cell,* 26**,** 2519-34.

Jung, U. S. & D. E. Levin (1999) Genome-wide analysis of gene expression regulated by the yeast cell wall integrity signalling pathway. *Mol Microbiol,* 34**,** 1049-57.

Kadlecova, Z., S. J. Spielman, D. Loerke, A. Mohanakrishnan, D. K. Reed & S. L. Schmid (2017) Regulation of clathrin-mediated endocytosis by hierarchical allosteric activation of AP2. *J Cell Biol,* 216**,** 167-179.

Kaksonen, M. (2008) Taking apart the endocytic machinery. *J Cell Biol,* 180**,** 1059-60.

Kaksonen, M., Y. Sun & D. G. Drubin (2003) A pathway for association of receptors, adaptors, and actin during endocytic internalization. *Cell,* 115**,** 475-87.

Kaksonen, M., C. P. Toret & D. G. Drubin (2005) A modular design for the clathrin- and actin-mediated endocytosis machinery. *Cell,* 123**,** 305-20.

Kapteyn, J. C., L. L. Hoyer, J. E. Hecht, W. H. Müller, A. Andel, A. J. Verkleij, M. Makarow, H. Van Den Ende & F. M. Klis (2000) The cell wall architecture of *Candida albicans* wild-type cells and cell wall-defective mutants. *Mol Microbiol,* 35**,** 601-11.

Kirchhausen, T. (1999) Adaptors for clathrin-mediated traffic. *Annu Rev Cell Dev Biol,* 15**,** 705-32.

Klis, F. M., A. Boorsma & P. W. De Groot (2006) Cell wall construction in *Saccharomyces cerevisiae*. *Yeast,* 23**,** 185-202.

Klis, F. M., P. de Groot & K. Hellingwerf (2001) Molecular organization of the cell wall of *Candida albicans*. *Med Mycol,* 39 Suppl 1**,** 1-8.

Knafler, H. C., I. I. Smaczynska-de Rooij, L. A. Walker, K. K. Lee, N. A. R. Gow & K. R. Ayscough (2019) AP-2-Dependent Endocytic Recycling of the Chitin Synthase Chs3 Regulates Polarized Growth in *Candida albicans*. *MBio,* 10.

Kondoh, O., Y. Tachibana, Y. Ohya, M. Arisawa & T. Watanabe (1997) Cloning of the RHO1 gene from *Candida albicans* and its regulation of beta-1,3-glucan synthesis. *J Bacteriol,* 179**,** 7734-41.

Kornitzer, D. (2019) Regulation of. *J Fungi (Basel),* 5.

Korolchuk, V. I. & G. Banting (2002) CK2 and GAK/auxilin2 are major protein kinases in clathrin-coated vesicles. *Traffic,* 3**,** 428-39.

Kost, B., E. Lemichez, P. Spielhofer, Y. Hong, K. Tolias, C. Carpenter & N. H. Chua (1999) Rac homologues and compartmentalized phosphatidylinositol 4, 5-bisphosphate act in a common pathway to regulate polar pollen tube growth. *J Cell Biol,* 145**,** 317-30.

Kozminski, K. G., G. Alfaro, S. Dighe & C. T. Beh (2006) Homologues of oxysterol-binding proteins affect Cdc42p- and Rho1p-mediated cell polarization in *Saccharomyces cerevisiae*. *Traffic,* 7**,** 1224-42.

Kullberg, B. J. & M. C. Arendrup (2015) Invasive Candidiasis. *N Engl J Med,* 373**,** 1445-56.

Kuznetsova, T. G., M. N. Starodubtseva, N. I. Yegorenkov, S. A. Chizhik & R. I. Zhdanov (2007) Atomic force microscopy probing of cell elasticity. *Micron,* 38**,** 824-33.
Köhli, M., V. Galati, K. Boudier, R. W. Roberson & P. Philippsen (2008) Growth-speed-correlated localization of exocyst and polarisome components in growth zones of *Ashbya gossypii* hyphal tips. *J Cell Sci,* 121**,** 3878-89.
Kübler, E. & H. Riezman (1993) Actin and fimbrin are required for the internalization step of endocytosis in yeast. *EMBO J,* 12**,** 2855-62.
Lackey, E., G. Vipulanandan, D. S. Childers & D. Kadosh (2013) Comparative evolution of morphological regulatory functions in *Candida species*. *Eukaryot Cell,* 12**,** 1356-68.
Latgé, J. P. (2007) The cell wall: a carbohydrate armour for the fungal cell. *Mol Microbiol,* 66**,** 279-90.
Lenardon, M. D., C. A. Munro & N. A. Gow (2010) Chitin synthesis and fungal pathogenesis. *Curr Opin Microbiol,* 13**,** 416-23.
Lenardon, M. D., R. K. Whitton, C. A. Munro, D. Marshall & N. A. Gow (2007) Individual chitin synthase enzymes synthesize microfibrils of differing structure at specific locations in the *Candida albicans* cell wall. *Mol Microbiol,* 66**,** 1164-73.
Lew, R. R. (2011) How does a hypha grow? The biophysics of pressurized growth in fungi. *Nat Rev Microbiol,* 9**,** 509-18.
Li, J., A. Mahajan & M. D. Tsai (2006) Ankyrin repeat: a unique motif mediating protein-protein interactions. *Biochemistry,* 45**,** 15168-78.
Lichius, A., M. E. Yáñez-Gutiérrez, N. D. Read & E. Castro-Longoria (2012) Comparative live-cell imaging analyses of SPA-2, BUD-6 and BNI-1 in *Neurospora crassa* reveal novel features of the filamentous fungal polarisome. *PLoS One,* 7**,** e30372.
Lim, C. S., R. Rosli, H. F. Seow & P. P. Chong (2012) *Candida* and invasive candidiasis: back to basics. *Eur J Clin Microbiol Infect Dis,* 31**,** 21-31.
Lionakis, M. S., J. K. Lim, C. C. Lee & P. M. Murphy (2011) Organ-specific innate immune responses in a mouse model of invasive candidiasis. *J Innate Immun,* 3**,** 180-99.
Lippincott, J. & R. Li (1998) Sequential assembly of myosin II, an IQGAP-like protein, and filamentous actin to a ring structure involved in budding yeast cytokinesis. *J Cell Biol,* 140**,** 355-66.
Liu, J., M. Kaksonen, D. G. Drubin & G. Oster (2006) Endocytic vesicle scission by lipid phase boundary forces. *Proc Natl Acad Sci U S A,* 103**,** 10277-10282.
Lo, H. J., J. R. Köhler, B. DiDomenico, D. Loebenberg, A. Cacciapuoti & G. R. Fink (1997) Nonfilamentous *C. albicans* mutants are avirulent. *Cell,* 90**,** 939-49.
Loerke, D., M. Mettlen, D. Yarar, K. Jaqaman, H. Jaqaman, G. Danuser & S. L. Schmid (2009) Cargo and dynamin regulate clathrin-coated pit maturation. *PLoS Biol,* 7**,** e57.
Longtine, M. S., A. McKenzie, D. J. Demarini, N. G. Shah, A. Wach, A. Brachat, P. Philippsen & J. R. Pringle (1998) Additional modules for versatile and economical PCR-based gene deletion and modification in *Saccharomyces cerevisiae*. *Yeast,* 14**,** 953-61.

Lorenz, M. C., J. A. Bender & G. R. Fink (2004) Transcriptional response of *Candida albicans upon internalization by macrophages. Eukaryot Cell, 3*, *1076-87.*

Ma, H., L. A. Snook, S. G. Kaminskyj & T. E. Dahms (2005) Surface ultrastructure and elasticity in growing tips and mature regions of *Aspergillus hyphae* describe wall maturation. *Microbiology,* 151**,** 3679-88.

Maib, H., F. Ferreira, S. Vassilopoulos & E. Smythe (2018) Cargo regulates clathrin-coated pit invagination via clathrin light chain phosphorylation. *J Cell Biol,* 217**,** 4253-4266.

Malinsky, J., M. Opekarová & W. Tanner (2010) The lateral compartmentation of the yeast plasma membrane. *Yeast,* 27**,** 473-8.

Manford, A., T. Xia, A. K. Saxena, C. Stefan, F. Hu, S. D. Emr & Y. Mao (2010) Crystal structure of the yeast Sac1: implications for its phosphoinositide phosphatase function. *EMBO J,* 29**,** 1489-98.

Manford, A. G., C. J. Stefan, H. L. Yuan, J. A. Macgurn & S. D. Emr (2012) ER-to-plasma membrane tethering proteins regulate cell signaling and ER morphology. *Dev Cell,* 23**,** 1129-40.

Marco, E., R. Wedlich-Soldner, R. Li, S. J. Altschuler & L. F. Wu (2007) Endocytosis optimizes the dynamic localization of membrane proteins that regulate cortical polarity. *Cell,* 129**,** 411-22.

Martin, R., D. Hellwig, Y. Schaub, J. Bauer, A. Walther & J. Wendland (2007) Functional analysis of *Candida albicans* genes whose *Saccharomyces cerevisiae* homologues are involved in endocytosis. *Yeast,* 24**,** 511-22.

Martin, S. W. & J. B. Konopka (2004) Lipid raft polarization contributes to hyphal growth in *Candida albicans*. *Eukaryot Cell,* 3**,** 675-84.

Martzoukou, O., S. Amillis, A. Zervakou, S. Christoforidis & G. Diallinas (2017) The AP-2 complex has a specialized clathrin-independent role in apical endocytosis and polar growth in fungi. *Elife,* 6.

Martín-Cuadrado, A. B., E. Dueñas, M. Sipiczki, C. R. Vázquez de Aldana & F. del Rey (2003) The endo-beta-1,3-glucanase eng1p is required for dissolution of the primary septum during cell separation in *Schizosaccharomyces pombe*. *J Cell Sci,* 116**,** 1689-98.

Masuda, T., K. Tanaka, H. Nonaka, W. Yamochi, A. Maeda & Y. Takai (1994) Molecular cloning and characterization of yeast rho GDP dissociation inhibitor. *J Biol Chem,* 269**,** 19713-8.

Mavor, A. L., S. Thewes & B. Hube (2005) Systemic fungal infections caused by Candida species: epidemiology, infection process and virulence attributes. *Curr Drug Targets,* 6**,** 863-74.

Mayer, F. L., D. Wilson & B. Hube (2013) *Candida albicans* pathogenicity mechanisms. *Virulence,* 4**,** 119-28.

Mayer, K., S. Albrecht & A. Schaller (2015) Targeted Analysis of Protein Phosphorylation by 2D Electrophoresis. *Methods Mol Biol,* 1306**,** 167-76.

Mañes, S., R. Ana Lacalle, C. Gómez-Moutón & C. Martínez-A (2003) From rafts to crafts: membrane asymmetry in moving cells. *Trends Immunol,* 24**,** 320-6.

Meletiadis, J., J. F. Meis, J. W. Mouton & P. E. Verweij (2001) Analysis of growth characteristics of filamentous fungi in different nutrient media. *J Clin Microbiol,* 39**,** 478-84.

Mesmin, B., B. Antonny & G. Drin (2013) Insights into the mechanisms of sterol transport between organelles. *Cell Mol Life Sci,* 70**,** 3405-21.
Meyer, V., M. Arentshorst, C. A. van den Hondel & A. F. Ram (2008) The polarisome component SpaA localises to hyphal tips of *Aspergillus niger* and is important for polar growth. *Fungal Genet Biol,* 45**,** 152-64.
Micheva, K. D., R. W. Holz & S. J. Smith (2001) Regulation of presynaptic phosphatidylinositol 4,5-biphosphate by neuronal activity. *J Cell Biol,* 154**,** 355-68.
Monteoliva, L., M. L. Matas, C. Gil, C. Nombela & J. Pla (2002) Large-scale identification of putative exported proteins in *Candida albicans* by genetic selection. *Eukaryot Cell,* 1**,** 514-25.
Mora-Montes, H. M., S. Bates, M. G. Netea, L. Castillo, A. Brand, E. T. Buurman, D. F. Díaz-Jiménez, B. Jan Kullberg, A. J. Brown, F. C. Odds & N. A. Gow (2010) A multifunctional mannosyltransferase family in *Candida albicans* determines cell wall mannan structure and host-fungus interactions. *J Biol Chem,* 285**,** 12087-95.
Motley, A., N. A. Bright, M. N. Seaman & M. S. Robinson (2003) Clathrin-mediated endocytosis in AP-2-depleted cells. *J Cell Biol,* 162**,** 909-18.
Mouyna, I., T. Fontaine, M. Vai, M. Monod, W. A. Fonzi, M. Diaquin, L. Popolo, R. P. Hartland & J. P. Latgé (2000) Glycosylphosphatidylinositol-anchored glucanosyltransferases play an active role in the biosynthesis of the fungal cell wall. *J Biol Chem,* 275**,** 14882-9.
Moyes, D. L., M. Runglall, C. Murciano, C. Shen, D. Nayar, S. Thavaraj, A. Kohli, A. Islam, H. Mora-Montes, S. J. Challacombe & J. R. Naglik (2010) A biphasic innate immune MAPK response discriminates between the yeast and hyphal forms of *Candida albicans* in epithelial cells. *Cell Host Microbe,* 8**,** 225-35.
Moyes, D. L., D. Wilson, J. P. Richardson, S. Mogavero, S. X. Tang, J. Wernecke, S. Höfs, R. L. Gratacap, J. Robbins, M. Runglall, C. Murciano, M. Blagojevic, S. Thavaraj, T. M. Förster, B. Hebecker, L. Kasper, G. Vizcay, S. I. Iancu, N. Kichik, A. Häder, O. Kurzai, T. Luo, T. Krüger, O. Kniemeyer, E. Cota, O. Bader, R. T. Wheeler, T. Gutsmann, B. Hube & J. R. Naglik (2016) Candidalysin is a fungal peptide toxin critical for mucosal infection. *Nature,* 532**,** 64-8.
Munn, A. L., A. Heese-Peck, B. J. Stevenson, H. Pichler & H. Riezman (1999) Specific sterols required for the internalization step of endocytosis in yeast. *Mol Biol Cell,* 10**,** 3943-57.
Munro, C. A., S. Selvaggini, I. de Bruijn, L. Walker, M. D. Lenardon, B. Gerssen, S. Milne, A. J. Brown & N. A. Gow (2007) The PKC, HOG and Ca2+ signalling pathways co-ordinately regulate chitin synthesis in *Candida albicans*. *Mol Microbiol,* 63**,** 1399-413.
Munro, C. A., R. K. Whitton, H. B. Hughes, M. Rella, S. Selvaggini & N. A. Gow (2003) CHS8-a fourth chitin synthase gene of *Candida albicans* contributes to in vitro chitin synthase activity, but is dispensable for growth. *Fungal Genet Biol,* 40**,** 146-58.
Murad, A. M., P. Leng, M. Straffon, J. Wishart, S. Macaskill, D. MacCallum, N. Schnell, D. Talibi, D. Marechal, F. Tekaia, C. d'Enfert, C. Gaillardin, F. C.

Odds & A. J. Brown (2001) NRG1 represses yeast-hypha morphogenesis and hypha-specific gene expression in *Candida albicans*. *EMBO J,* 20**,** 4742-52.

Naglik, J. R., F. Fostira, J. Ruprai, J. F. Staab, S. J. Challacombe & P. Sundstrom (2006) *Candida albicans* HWP1 gene expression and host antibody responses in colonization and disease. *J Med Microbiol,* 55**,** 1323-7.

Nakagawa, Y., N. Ohno & T. Murai (2003) Suppression by *Candida albicans* beta-glucan of cytokine release from activated human monocytes and from T cells in the presence of monocytes. *J Infect Dis,* 187**,** 710-3.

Nakao, A., H. Kato, T. Kanbe, K. Tanaka, H. Tamura, S. Tanaka & H. Takagi (1994) Quantitative assay of (1-3)-beta-D-glucan in culture media of *Candida albicans* using the G-test. *Eur Surg Res,* 26**,** 194-200.

Netea, M. G., G. D. Brown, B. J. Kullberg & N. A. Gow (2008) An integrated model of the recognition of *Candida albicans* by the innate immune system. *Nat Rev Microbiol,* 6**,** 67-78.

Netea, M. G., N. A. Gow, C. A. Munro, S. Bates, C. Collins, G. Ferwerda, R. P. Hobson, G. Bertram, H. B. Hughes, T. Jansen, L. Jacobs, E. T. Buurman, K. Gijzen, D. L. Williams, R. Torensma, A. McKinnon, D. M. MacCallum, F. C. Odds, J. W. Van der Meer, A. J. Brown & B. J. Kullberg (2006) Immune sensing of *Candida albicans* requires cooperative recognition of mannans and glucans by lectin and Toll-like receptors. *J Clin Invest,* 116**,** 1642-50.

Noble, S. M. & A. D. Johnson (2005) Strains and strategies for large-scale gene deletion studies of the diploid human fungal pathogen *Candida albicans*. *Eukaryot Cell,* 4**,** 298-309.

Oberholzer, U., A. Marcil, E. Leberer, D. Y. Thomas & M. Whiteway (2002) Myosin I is required for hypha formation in *Candida albicans*. *Eukaryot Cell,* 1**,** 213-28.

Odani, T., Y. Shimma, A. Tanaka & Y. Jigami (1996) Cloning and analysis of the MNN4 gene required for phosphorylation of N-linked oligosaccharides in *Saccharomyces cerevisiae*. *Glycobiology,* 6**,** 805-10.

Odds, F. C., A. J. Brown & N. A. Gow (2003) Antifungal agents: mechanisms of action. *Trends Microbiol,* 11**,** 272-9.

Oh, Y., K. J. Chang, P. Orlean, C. Wloka, R. Deshaies & E. Bi (2012) Mitotic exit kinase Dbf2 directly phosphorylates chitin synthase Chs2 to regulate cytokinesis in budding yeast. *Mol Biol Cell,* 23**,** 2445-56.

Ohno, H., J. Stewart, M. C. Fournier, H. Bosshart, I. Rhee, S. Miyatake, T. Saito, A. Gallusser, T. Kirchhausen & J. S. Bonifacino (1995) Interaction of tyrosine-based sorting signals with clathrin-associated proteins. *Science,* 269**,** 1872-5.

Olusanya, O., P. D. Andrews, J. R. Swedlow & E. Smythe (2001) Phosphorylation of threonine 156 of the mu2 subunit of the AP2 complex is essential for endocytosis in vitro and in vivo. *Curr Biol,* 11**,** 896-900.

Owen, D. J. & P. R. Evans (1998) A structural explanation for the recognition of tyrosine-based endocytotic signals. *Science,* 282**,** 1327-32.

Owen, D. J., Y. Vallis, B. M. Pearse, H. T. McMahon & P. R. Evans (2000) The structure and function of the beta 2-adaptin appendage domain. *EMBO J,* 19**,** 4216-27.

Pantazopoulou, A. & M. A. Peñalva (2009) Organization and dynamics of the *Aspergillus nidulans* Golgi during apical extension and mitosis. *Mol Biol Cell,* 20**,** 4335-47.

Park, S., R. Kelly, J. N. Kahn, J. Robles, M. J. Hsu, E. Register, W. Li, V. Vyas, H. Fan, G. Abruzzo, A. Flattery, C. Gill, G. Chrebet, S. A. Parent, M. Kurtz, H. Teppler, C. M. Douglas & D. S. Perlin (2005) Specific substitutions in the echinocandin target Fks1p account for reduced susceptibility of rare laboratory and clinical *Candida* sp. isolates. *Antimicrob Agents Chemother,* 49**,** 3264-73.

Pawson, T. & J. D. Scott (1997) Signaling through scaffold, anchoring, and adaptor proteins. *Science,* 278**,** 2075-80.

Payne, G. S., D. Baker, E. van Tuinen & R. Schekman (1988) Protein transport to the vacuole and receptor-mediated endocytosis by clathrin heavy chain-deficient yeast. *J Cell Biol,* 106**,** 1453-61.

Pearse, B. M. (1985) Assembly of the mannose-6-phosphate receptor into reconstituted clathrin coats. *EMBO J,* 4**,** 2457-60.

Pearse, B. M. & M. S. Robinson (1984) Purification and properties of 100-kd proteins from coated vesicles and their reconstitution with clathrin. *EMBO J,* 3**,** 1951-7.

Peñalva, M. (2010) Endocytosis in filamentous fungi: Cinderella gets her reward. *Curr Opin Microbiol,* 13**,** 684-92.

Pfaller, M. A. (2012) Antifungal drug resistance: mechanisms, epidemiology, and consequences for treatment. *Am J Med,* 125**,** S3-13.

Pichler, H., B. Gaigg, C. Hrastnik, G. Achleitner, S. D. Kohlwein, G. Zellnig, A. Perktold & G. Daum (2001) A subfraction of the yeast endoplasmic reticulum associates with the plasma membrane and has a high capacity to synthesize lipids. *Eur J Biochem,* 268**,** 2351-61.

Plaine, A., L. Walker, G. Da Costa, H. M. Mora-Montes, A. McKinnon, N. A. Gow, C. Gaillardin, C. A. Munro & M. L. Richard (2008) Functional analysis of *Candida albicans* GPI-anchored proteins: roles in cell wall integrity and caspofungin sensitivity. *Fungal Genet Biol,* 45**,** 1404-14.

Pomorski, T., R. Lombardi, H. Riezman, P. F. Devaux, G. van Meer & J. C. Holthuis (2003) Drs2p-related P-type ATPases Dnf1p and Dnf2p are required for phospholipid translocation across the yeast plasma membrane and serve a role in endocytosis. *Mol Biol Cell,* 14**,** 1240-54.

Pope, L. M. & G. T. Cole (1982) Comparative studies of gastrointestinal colonization and systemic spread by *Candida albicans* and nonlethal yeast in the infant mouse. *Scan Electron Microsc***,** 1667-76.

Popolo, L., T. Gualtieri & E. Ragni (2001) The yeast cell-wall salvage pathway. *Med Mycol,* 39 Suppl 1**,** 111-21.

Preechasuth, K., J. C. Anderson, S. C. Peck, A. J. Brown, N. A. Gow & M. D. Lenardon (2015) Cell wall protection by the *Candida albicans* class I chitin synthases. *Fungal Genet Biol,* 82**,** 264-76.

Prill, S. K., B. Klinkert, C. Timpel, C. A. Gale, K. Schröppel & J. F. Ernst (2005) PMT family of *Candida albicans*: five protein mannosyltransferase isoforms affect growth, morphogenesis and antifungal resistance. *Mol Microbiol,* 55**,** 546-60.

Prosser, D. C., T. G. Drivas, L. Maldonado-Báez & B. Wendland (2011) Existence of a novel clathrin-independent endocytic pathway in yeast that depends on Rho1 and formin. *J Cell Biol,* 195**,** 657-71.

Quon, E., Y. Y. Sere, N. Chauhan, J. Johansen, D. P. Sullivan, J. S. Dittman, W. J. Rice, R. B. Chan, G. Di Paolo, C. T. Beh & A. K. Menon (2018) Endoplasmic reticulum-plasma membrane contact sites integrate sterol and phospholipid regulation. *PLoS Biol,* 16**,** e2003864.

Ray, T. L. & C. D. Payne (1988) Scanning electron microscopy of epidermal adherence and cavitation in murine candidiasis: a role for *Candida* acid proteinase. *Infect Immun,* 56**,** 1942-9.

Raychaudhuri, S. & W. A. Prinz (2010) The diverse functions of oxysterol-binding proteins. *Annu Rev Cell Dev Biol,* 26**,** 157-77.

Read, N. D. & E. R. Kalkman (2003) Does endocytosis occur in fungal hyphae? *Fungal Genet Biol,* 39**,** 199-203.

Reider, A. & B. Wendland (2011) Endocytic adaptors--social networking at the plasma membrane. *J Cell Sci,* 124**,** 1613-22.

Reijnst, P., A. Walther & J. Wendland (2010) Functional analysis of *Candida albicans* genes encoding SH3-domain-containing proteins. *FEMS Yeast Res,* 10**,** 452-61.

Reynaga-Peña, C. G., G. Gierz & S. Bartnicki-Garcia (1997) Analysis of the role of the Spitzenkörper in fungal morphogenesis by computer simulation of apical branching in *Aspergillus niger*. *Proc Natl Acad Sci U S A,* 94**,** 9096-101.

REYNOLDS, E. S. (1963) The use of lead citrate at high pH as an electron-opaque stain in electron microscopy. *J Cell Biol,* 17**,** 208-12.

Richard, M. L. & A. Plaine (2007) Comprehensive analysis of glycosylphosphatidylinositol-anchored proteins in *Candida albicans*. *Eukaryot Cell,* 6**,** 119-33.

Ricotta, D., S. D. Conner, S. L. Schmid, K. von Figura & S. Honing (2002) Phosphorylation of the AP2 mu subunit by AAK1 mediates high affinity binding to membrane protein sorting signals. *J Cell Biol,* 156**,** 791-5.

Rida, P. C., A. Nishikawa, G. Y. Won & N. Dean (2006) Yeast-to-hyphal transition triggers formin-dependent Golgi localization to the growing tip in *Candida albicans*. *Mol Biol Cell,* 17**,** 4364-78.

Rida, P. C. & U. Surana (2005) Cdc42-dependent localization of polarisome component Spa2 to the incipient bud site is independent of the GDP/GTP exchange factor Cdc24. *Eur J Cell Biol,* 84**,** 939-49.

Riezman, H., P. G. Woodman, G. van Meer & M. Marsh (1997) Molecular mechanisms of endocytosis. *Cell,* 91**,** 731-8.

Riquelme, M., E. L. Bredeweg, O. Callejas-Negrete, R. W. Roberson, S. Ludwig, A. Beltrán-Aguilar, S. Seiler, P. Novick & M. Freitag (2014) The *Neurospora crassa* exocyst complex tethers Spitzenkörper vesicles to the apical plasma membrane during polarized growth. *Mol Biol Cell,* 25**,** 1312-26.

Robinson, M. S. (1987) 100-kD coated vesicle proteins: molecular heterogeneity and intracellular distribution studied with monoclonal antibodies. *J Cell Biol,* 104**,** 887-95.

--- (2004) Adaptable adaptors for coated vesicles. *Trends Cell Biol,* 14**,** 167-74.

Robinson, M. S. & J. S. Bonifacino (2001) Adaptor-related proteins. *Curr Opin Cell Biol,* 13**,** 444-53.
Rogg, L. E., J. R. Fortwendel, P. R. Juvvadi & W. J. Steinbach (2012) Regulation of expression, activity and localization of fungal chitin synthases. *Med Mycol,* 50**,** 2-17.
Romani, L. (2011) Immunity to fungal infections. *Nat Rev Immunol,* 11**,** 275-88.
Royle, S. J. (2006) The cellular functions of clathrin. *Cell Mol Life Sci,* 63**,** 1823-32.
Ruiz-Herrera, J. & S. Bartnicki-Garcia (1974) Synthesis of cell wall microfibrils in vitro by a "soluble" chitin synthetase from *Mucor rouxii*. *Science,* 186**,** 357-9.
Sanchatjate, S. & R. Schekman (2006) Chs5/6 complex: a multiprotein complex that interacts with and conveys chitin synthase III from the trans-Golgi network to the cell surface. *Mol Biol Cell,* 17**,** 4157-66.
Santos, B. & M. Snyder (1997) Targeting of chitin synthase 3 to polarized growth sites in yeast requires Chs5p and Myo2p. *J Cell Biol,* 136**,** 95-110.
Sardi, J. C., L. Scorzoni, T. Bernardi, A. M. Fusco-Almeida & M. J. Mendes Giannini (2013) *Candida* species: current epidemiology, pathogenicity, biofilm formation, natural antifungal products and new therapeutic options. *J Med Microbiol,* 62**,** 10-24.
Schmitt, M. & F. Radler (1987) Mannoprotein of the yeast cell wall as primary receptor for the killer toxin of *Saccharomyces cerevisiae* strain 28. *J Gen Microbiol,* 133**,** 3347-54.
Schneiter, R., B. Brügger, R. Sandhoff, G. Zellnig, A. Leber, M. Lampl, K. Athenstaedt, C. Hrastnik, S. Eder, G. Daum, F. Paltauf, F. T. Wieland & S. D. Kohlwein (1999) Electrospray ionization tandem mass spectrometry (ESI-MS/MS) analysis of the lipid molecular species composition of yeast subcellular membranes reveals acyl chain-based sorting/remodeling of distinct molecular species en route to the plasma membrane. *J Cell Biol,* 146**,** 741-54.
Schultzhaus, Z., H. Yan & B. D. Shaw (2015) *Aspergillus nidulans* flippase DnfA is cargo of the endocytic collar and plays complementary roles in growth and phosphatidylserine asymmetry with another flippase, DnfB. *Mol Microbiol,* 97**,** 18-32.
Schulz, T. A., M. G. Choi, S. Raychaudhuri, J. A. Mears, R. Ghirlando, J. E. Hinshaw & W. A. Prinz (2009) Lipid-regulated sterol transfer between closely apposed membranes by oxysterol-binding protein homologues. *J Cell Biol,* 187**,** 889-903.
Sekiya-Kawasaki, M., A. C. Groen, M. J. Cope, M. Kaksonen, H. A. Watson, C. Zhang, K. M. Shokat, B. Wendland, K. L. McDonald, J. M. McCaffery & D. G. Drubin (2003) Dynamic phosphoregulation of the cortical actin cytoskeleton and endocytic machinery revealed by real-time chemical genetic analysis. *J Cell Biol,* 162**,** 765-72.
Selvig, K. & J. A. Alspaugh (2011) pH Response Pathways in Fungi: Adapting to Host-derived and Environmental Signals. *Mycobiology,* 39**,** 249-56.
Shaw, B. D., D. W. Chung, C. L. Wang, L. A. Quintanilla & S. Upadhyay (2011) A role for endocytic recycling in hyphal growth. *Fungal Biol,* 115**,** 541-6.

Shen, D., H. Yuan, A. Hutagalung, A. Verma, D. Kümmel, X. Wu, K. Reinisch, J. A. McNew & P. Novick (2013) The synaptobrevin homologue Snc2p recruits the exocyst to secretory vesicles by binding to Sec6p. *J Cell Biol,* 202**,** 509-26.

Shepherd, M. G. (1987) Cell envelope of *Candida albicans*. *Crit Rev Microbiol,* 15**,** 7-25.

Sheu, Y. J., B. Santos, N. Fortin, C. Costigan & M. Snyder (1998) Spa2p interacts with cell polarity proteins and signaling components involved in yeast cell morphogenesis. *Mol Cell Biol,* 18**,** 4053-69.

Shibata, N., K. Ikuta, T. Imai, Y. Satoh, R. Satoh, A. Suzuki, C. Kojima, H. Kobayashi, K. Hisamichi & S. Suzuki (1995) Existence of branched side chains in the cell wall mannan of pathogenic yeast, *Candida albicans*. Structure-antigenicity relationship between the cell wall mannans of *Candida albicans* and *Candida parapsilosis*. *J Biol Chem,* 270**,** 1113-22.

Shvets, E., V. Bitsikas, G. Howard, C. G. Hansen & B. J. Nichols (2015) Dynamic caveolae exclude bulk membrane proteins and are required for sorting of excess glycosphingolipids. *Nat Commun,* 6**,** 6867.

Sirotkin, V., J. Berro, K. Macmillan, L. Zhao & T. D. Pollard (2010) Quantitative analysis of the mechanism of endocytic actin patch assembly and disassembly in fission yeast. *Mol Biol Cell,* 21**,** 2894-904.

Slaughter, B. D., A. Das, J. W. Schwartz, B. Rubinstein & R. Li (2009) Dual modes of cdc42 recycling fine-tune polarized morphogenesis. *Dev Cell,* 17**,** 823-35.

Slaughter, B. D., J. R. Unruh, A. Das, S. E. Smith, B. Rubinstein & R. Li (2013) Non-uniform membrane diffusion enables steady-state cell polarization via vesicular trafficking. *Nat Commun,* 4**,** 1380.

Slepnev, V. I. & P. De Camilli (2000) Accessory factors in clathrin-dependent synaptic vesicle endocytosis. *Nat Rev Neurosci,* 1**,** 161-72.

Smaczynska-de Rooij, I. I., E. G. Allwood, S. Aghamohammadzadeh, E. H. Hettema, M. W. Goldberg & K. R. Ayscough (2010) A role for the dynamin-like protein Vps1 during endocytosis in yeast. *J Cell Sci,* 123**,** 3496-506.

Smits, G. J., H. van den Ende & F. M. Klis (2001) Differential regulation of cell wall biogenesis during growth and development in yeast. *Microbiology,* 147**,** 781-94.

Smythe, E. & K. R. Ayscough (2006) Actin regulation in endocytosis. *J Cell Sci,* 119**,** 4589-98.

Sobel, J. D. (2007) Vulvovaginal candidosis. *Lancet,* 369**,** 1961-71.

Starr, T. L., S. Pagant, C. W. Wang & R. Schekman (2012) Sorting signals that mediate traffic of chitin synthase III between the TGN/endosomes and to the plasma membrane in yeast. *PLoS One,* 7**,** e46386.

Stefan, C. J., A. G. Manford, D. Baird, J. Yamada-Hanff, Y. Mao & S. D. Emr (2011) Osh proteins regulate phosphoinositide metabolism at ER-plasma membrane contact sites. *Cell,* 144**,** 389-401.

Stefan, C. J., A. G. Manford & S. D. Emr (2013) ER-PM connections: sites of information transfer and inter-organelle communication. *Curr Opin Cell Biol,* 25**,** 434-42.

Steinberg, G. (2007) Hyphal growth: a tale of motors, lipids, and the Spitzenkörper. *Eukaryot Cell,* 6**,** 351-60.
--- (2011) Motors in fungal morphogenesis: cooperation versus competition. *Curr Opin Microbiol,* 14**,** 660-7.
Stimpson, H. E., C. P. Toret, A. T. Cheng, B. S. Pauly & D. G. Drubin (2009) Early-arriving Syp1p and Ede1p function in endocytic site placement and formation in budding yeast. *Mol Biol Cell,* 20**,** 4640-51.
Sudbery, P., N. Gow & J. Berman (2004) The distinct morphogenic states of *Candida albicans*. *Trends Microbiol,* 12**,** 317-24.
Sudbery, P. E. (2001) The germ tubes of *Candida albicans* hyphae and pseudohyphae show different patterns of septin ring localization. *Mol Microbiol,* 41**,** 19-31.
--- (2011) Growth of *Candida albicans* hyphae. *Nat Rev Microbiol,* 9**,** 737-48.
Sun, Y. & D. G. Drubin (2012) The functions of anionic phospholipids during clathrin-mediated endocytosis site initiation and vesicle formation. *J Cell Sci,* 125**,** 6157-65.
Sun, Y., A. C. Martin & D. G. Drubin (2006) Endocytic internalization in budding yeast requires coordinated actin nucleation and myosin motor activity. *Dev Cell,* 11**,** 33-46.
Sundstrom, P. (2002) Adhesion in *Candida* spp. *Cell Microbiol,* 4**,** 461-9.
Swidergall, M., M. Khalaji, N. V. Solis, D. L. Moyes, R. A. Drummond, B. Hube, M. S. Lionakis, C. Murdoch, S. G. Filler & J. R. Naglik (2019) Candidalysin Is Required for Neutrophil Recruitment and Virulence During Systemic *Candida albicans* Infection. *J Infect Dis,* 220**,** 1477-1488.
Taheri-Talesh, N., T. Horio, L. Araujo-Bazán, X. Dou, E. A. Espeso, M. A. Peñalva, S. A. Osmani & B. R. Oakley (2008) The tip growth apparatus of *Aspergillus nidulans*. *Mol Biol Cell,* 19**,** 1439-49.
Takeda, M., K. Yamagami & K. Tanaka (2014) Role of phosphatidylserine in phospholipid flippase-mediated vesicle transport in *Saccharomyces cerevisiae*. *Eukaryot Cell,* 13**,** 363-75.
Takeshita, N., Y. Higashitsuji, S. Konzack & R. Fischer (2008) Apical sterol-rich membranes are essential for localizing cell end markers that determine growth directionality in the filamentous fungus *Aspergillus nidulans*. *Mol Biol Cell,* 19**,** 339-51.
Takizawa, P. A., J. L. DeRisi, J. E. Wilhelm & R. D. Vale (2000) Plasma membrane compartmentalization in yeast by messenger RNA transport and a septin diffusion barrier. *Science,* 290**,** 341-4.
Tanner, W. & L. Lehle (1987) Protein glycosylation in yeast. *Biochim Biophys Acta,* 906**,** 81-99.
Taylor, M. J., D. Perrais & C. J. Merrifield (2011) A high precision survey of the molecular dynamics of mammalian clathrin-mediated endocytosis. *PLoS Biol,* 9**,** e1000604.
ter Haar, E., S. C. Harrison & T. Kirchhausen (2000) Peptide-in-groove interactions link target proteins to the beta-propeller of clathrin. *Proc Natl Acad Sci U S A,* 97**,** 1096-100.

TerBush, D. R., T. Maurice, D. Roth & P. Novick (1996) The Exocyst is a multiprotein complex required for exocytosis in *Saccharomyces cerevisiae*. *EMBO J,* 15**,** 6483-94.

Tindemans, S. H., N. Kern & B. M. Mulder (2006) The diffusive vesicle supply center model for tip growth in fungal hyphae. *J Theor Biol,* 238**,** 937-48.

Toenjes, K. A., S. M. Munsee, A. S. Ibrahim, R. Jeffrey, J. E. Edwards & D. I. Johnson (2005) Small-molecule inhibitors of the budded-to-hyphal-form transition in the pathogenic yeast *Candida albicans*. *Antimicrob Agents Chemother,* 49**,** 963-72.

Tong, J., H. Yang, S. H. Eom & Y. J. Im (2013) Structure of Osh3 reveals a conserved mode of phosphoinositide binding in oxysterol-binding proteins. *Structure,* 21**,** 1203-13.

Torralba, S. & I. B. Heath (2002) Analysis of three separate probes suggests the absence of endocytosis in *Neurospora crassa* hyphae. *Fungal Genet Biol,* 37**,** 221-32.

Tortorano, A. M., C. Kibbler, J. Peman, H. Bernhardt, L. Klingspor & R. Grillot (2006) Candidaemia in Europe: epidemiology and resistance. *Int J Antimicrob Agents,* 27**,** 359-66.

Toshima, J. Y., J. Toshima, M. Kaksonen, A. C. Martin, D. S. King & D. G. Drubin (2006) Spatial dynamics of receptor-mediated endocytic trafficking in budding yeast revealed by using fluorescent alpha-factor derivatives. *Proc Natl Acad Sci U S A,* 103**,** 5793-8.

Toulmay, A. & W. A. Prinz (2012) A conserved membrane-binding domain targets proteins to organelle contact sites. *J Cell Sci,* 125**,** 49-58.

Traub, L. M., M. A. Downs, J. L. Westrich & D. H. Fremont (1999) Crystal structure of the alpha appendage of AP-2 reveals a recruitment platform for clathrin-coat assembly. *Proc Natl Acad Sci U S A,* 96**,** 8907-12.

Unanue, E. R., E. Ungewickell & D. Branton (1981) The binding of clathrin triskelions to membranes from coated vesicles. *Cell,* 26**,** 439-46.

Underhill, D. M. & I. D. Iliev (2014) The mycobiota: interactions between commensal fungi and the host immune system. *Nat Rev Immunol,* 14**,** 405-16.

Ushinsky, S. C., D. Harcus, J. Ash, D. Dignard, A. Marcil, J. Morchhauser, D. Y. Thomas, M. Whiteway & E. Leberer (2002) CDC42 is required for polarized growth in human pathogen *Candida albicans*. *Eukaryot Cell,* 1**,** 95-104.

Valdez-Taubas, J. & H. R. Pelham (2003) Slow diffusion of proteins in the yeast plasma membrane allows polarity to be maintained by endocytic cycling. *Curr Biol,* 13**,** 1636-40.

Valdivia, R. H., D. Baggott, J. S. Chuang & R. W. Schekman (2002) The yeast clathrin adaptor protein complex 1 is required for the efficient retention of a subset of late Golgi membrane proteins. *Dev Cell,* 2**,** 283-94.

Valdivia, R. H. & R. Schekman (2003) The yeasts Rho1p and Pkc1p regulate the transport of chitin synthase III (Chs3p) from internal stores to the plasma membrane. *Proc Natl Acad Sci U S A,* 100**,** 10287-92.

Valdivieso, M. H., L. Ferrario, M. Vai, A. Duran & L. Popolo (2000) Chitin synthesis in a gas1 mutant of *Saccharomyces cerevisiae*. *J Bacteriol,* 182**,** 4752-7.

van de Veerdonk, F. L., B. J. Kullberg, J. W. van der Meer, N. A. Gow & M. G. Netea (2008) Host-microbe interactions: innate pattern recognition of fungal pathogens. *Curr Opin Microbiol,* 11**,** 305-12.

van der Graaf, C. A., M. G. Netea, I. Verschueren, J. W. van der Meer & B. J. Kullberg (2005) Differential cytokine production and Toll-like receptor signaling pathways by *Candida albicans* blastoconidia and hyphae. *Infect Immun,* 73**,** 7458-64.

Vanden Bossche, H., L. Koymans & H. Moereels (1995) P450 inhibitors of use in medical treatment: focus on mechanisms of action. *Pharmacol Ther,* 67**,** 79-100.

Vecchiarelli, A., M. Puliti, A. Torosantucci, A. Cassone & F. Bistoni (1991) In vitro production of tumor necrosis factor by murine splenic macrophages stimulated with mannoprotein constituents of *Candida albicans* cell wall. *Cell Immunol,* 134**,** 65-76.

Vernay, A., S. Schaub, I. Guillas, M. Bassilana & R. A. Arkowitz (2012) A steep phosphoinositide bis-phosphate gradient forms during fungal filamentous growth. *J Cell Biol,* 198**,** 711-30.

Vigers, G. P., R. A. Crowther & B. M. Pearse (1986) Location of the 100 kd-50 kd accessory proteins in clathrin coats. *EMBO J,* 5**,** 2079-85.

Walker, L. A., M. D. Lenardon, K. Preechasuth, C. A. Munro & N. A. Gow (2013) Cell wall stress induces alternative fungal cytokinesis and septation strategies. *J Cell Sci,* 126**,** 2668-77.

Walker, L. A., C. A. Munro, I. de Bruijn, M. D. Lenardon, A. McKinnon & N. A. Gow (2008) Stimulation of chitin synthesis rescues *Candida albicans* from echinocandins. *PLoS Pathog,* 4**,** e1000040.

Walther, A. & J. Wendland (2004) Polarized hyphal growth in *Candida albicans* requires the Wiskott-Aldrich Syndrome protein homolog Wal1p. *Eukaryot Cell,* 3**,** 471-82.

Wang, C. W., S. Hamamoto, L. Orci & R. Schekman (2006) Exomer: A coat complex for transport of select membrane proteins from the trans-Golgi network to the plasma membrane in yeast. *J Cell Biol,* 174**,** 973-83.

Warenda, A. J., S. Kauffman, T. P. Sherrill, J. M. Becker & J. B. Konopka (2003) *Candida albicans* septin mutants are defective for invasive growth and virulence. *Infect Immun,* 71**,** 4045-51.

Warenda, A. J. & J. B. Konopka (2002) Septin function in *Candida albicans* morphogenesis. *Mol Biol Cell,* 13**,** 2732-46.

Wedlich-Soldner, R., S. Altschuler, L. Wu & R. Li (2003) Spontaneous cell polarization through actomyosin-based delivery of the Cdc42 GTPase. *Science,* 299**,** 1231-5.

Wedlich-Soldner, R., S. C. Wai, T. Schmidt & R. Li (2004) Robust cell polarity is a dynamic state established by coupling transport and GTPase signaling. *J Cell Biol,* 166**,** 889-900.

Wei, D., S. Jacobs, S. Modla, S. Zhang, C. L. Young, R. Cirino, J. Caplan & K. Czymmek (2012) High-resolution three-dimensional reconstruction of a whole yeast cell using focused-ion beam scanning electron microscopy. *Biotechniques,* 53**,** 41-8.

Weinberg, J. & D. G. Drubin (2012) Clathrin-mediated endocytosis in budding yeast. *Trends Cell Biol,* 22**,** 1-13.
Weiner, A., F. Orange, S. Lacas-Gervais, K. Rechav, V. Ghugtyal, M. Bassilana & R. A. Arkowitz (2019) On-site secretory vesicle delivery drives filamentous growth in the fungal pathogen *Candida albicans*. *Cell Microbiol,* 21**,** e12963.
Wheeler, R. T. & G. R. Fink (2006) A drug-sensitive genetic network masks fungi from the immune system. *PLoS Pathog,* 2**,** e35.
Wheeler, R. T., D. Kombe, S. D. Agarwala & G. R. Fink (2008) Dynamic, morphotype-specific *Candida albicans* beta-glucan exposure during infection and drug treatment. *PLoS Pathog,* 4**,** e1000227.
Wilde, A. & F. M. Brodsky (1996) In vivo phosphorylation of adaptors regulates their interaction with clathrin. *J Cell Biol,* 135**,** 635-45.
Willger, S. D., Z. Liu, R. A. Olarte, M. E. Adamo, J. E. Stajich, L. C. Myers, A. N. Kettenbach & D. A. Hogan (2015) Analysis of the *Candida albicans* Phosphoproteome. *Eukaryot Cell,* 14**,** 474-85.
Wisplinghoff, H., T. Bischoff, S. M. Tallent, H. Seifert, R. P. Wenzel & M. B. Edmond (2004) Nosocomial bloodstream infections in US hospitals: analysis of 24,179 cases from a prospective nationwide surveillance study. *Clin Infect Dis,* 39**,** 309-17.
Wolf, W., A. Kilic, B. Schrul, H. Lorenz, B. Schwappach & M. Seedorf (2012) Yeast Ist2 recruits the endoplasmic reticulum to the plasma membrane and creates a ribosome-free membrane microcompartment. *PLoS One,* 7**,** e39703.
Wood, P. J. & R. G. Fulcher (1983) Dye interactions. A basis for specific detection and histochemistry of polysaccharides. *J Histochem Cytochem,* 31**,** 823-6.
Wrobel, A. G., Z. Kadlecova, J. Kamenicky, J. C. Yang, T. Herrmann, B. T. Kelly, A. J. McCoy, P. R. Evans, S. Martin, S. Müller, F. Sroubek, D. Neuhaus, S. Honing & D. J. Owen (2019) Temporal Ordering in Endocytic Clathrin-Coated Vesicle Formation via AP2 Phosphorylation. *Dev Cell,* 50**,** 494-508.e11.
Wu, H., C. Turner, J. Gardner, B. Temple & P. Brennwald (2010) The Exo70 subunit of the exocyst is an effector for both Cdc42 and Rho3 function in polarized exocytosis. *Mol Biol Cell,* 21**,** 430-42.
Wächtler, B., D. Wilson, K. Haedicke, F. Dalle & B. Hube (2011) From attachment to damage: defined genes of *Candida albicans* mediate adhesion, invasion and damage during interaction with oral epithelial cells. *PLoS One,* 6**,** e17046.
Xu, L., M. Wang, G. Tang, Z. Ma & W. Shao (2019) The endocytic cargo adaptor complex is required for cell-wall integrity via interacting with the sensor FgWsc2B in *Fusarium graminearum*. *Curr Genet,* 65**,** 1071-1080.
Yakir-Tamang, L. & J. E. Gerst (2009) A phosphatidylinositol-transfer protein and phosphatidylinositol-4-phosphate 5-kinase control Cdc42 to regulate the actin cytoskeleton and secretory pathway in yeast. *Mol Biol Cell,* 20**,** 3583-97.

Yamamoto, W., S. Wada, M. Nagano, K. Aoshima, D. E. Siekhaus, J. Y. Toshima & J. Toshima (2018) Distinct roles for plasma membrane PtdIns(4)P and PtdIns(4,5)P. *J Cell Sci,* 131.

Yamashita, M., K. Kurokawa, Y. Sato, A. Yamagata, H. Mimura, A. Yoshikawa, K. Sato, A. Nakano & S. Fukai (2010) Structural basis for the Rho- and phosphoinositide-dependent localization of the exocyst subunit Sec3. *Nat Struct Mol Biol,* 17**,** 180-6.

Yeung, B. G., H. L. Phan & G. S. Payne (1999) Adaptor complex-independent clathrin function in yeast. *Mol Biol Cell,* 10**,** 3643-59.

Yoshida, S., Y. Ohya, M. Goebl, A. Nakano & Y. Anraku (1994) A novel gene, STT4, encodes a phosphatidylinositol 4-kinase in the PKC1 protein kinase pathway of *Saccharomyces cerevisiae*. *J Biol Chem,* 269**,** 1166-72.

Yu, I. M. & F. M. Hughson (2010) Tethering factors as organizers of intracellular vesicular traffic. *Annu Rev Cell Dev Biol,* 26**,** 137-56.

Yue, H., J. Bing, Q. Zheng, Y. Zhang, T. Hu, H. Du, H. Wang & G. Huang (2018) Filamentation in *Candida auris*, an emerging fungal pathogen of humans: passage through the mammalian body induces a heritable phenotypic switch. *Emerg Microbes Infect,* 7**,** 188.

Zhang, J., Y. Yun, Y. Lou, Y. S. Abubakar, P. Guo, S. Wang, C. Li, Y. Feng, M. Adnan, J. Zhou, G. D. Lu & W. Zheng (2019) *Fg*AP-2 complex is essential for pathogenicity and polarised growth and regulates the apical localisation of membrane lipid flippases in *Fusarium graminearum*. *Cell Microbiol,* 21**,** e13041.

Zhang, X., E. Bi, P. Novick, L. Du, K. G. Kozminski, J. H. Lipschutz & W. Guo (2001) Cdc42 interacts with the exocyst and regulates polarized secretion. *J Biol Chem,* 276**,** 46745-50.

Zhang, X., K. Orlando, B. He, F. Xi, J. Zhang, A. Zajac & W. Guo (2008) Membrane association and functional regulation of Sec3 by phospholipids and Cdc42. *J Cell Biol,* 180**,** 145-58.

Zhao, L., D. Schaefer, H. Xu, S. J. Modi, W. R. LaCourse & M. R. Marten (2005) Elastic properties of the cell wall of *Aspergillus nidulans* studied with atomic force microscopy. *Biotechnol Prog,* 21**,** 292-9.

Zhu, K., J. Zhao, D. M. Lubman, F. R. Miller & T. J. Barder (2005) Protein pI shifts due to posttranslational modifications in the separation and characterization of proteins. *Anal Chem,* 77**,** 2745-55.

Ziman, M., J. S. Chuang & R. W. Schekman (1996) Chs1p and Chs3p, two proteins involved in chitin synthesis, populate a compartment of the *Saccharomyces cerevisiae* endocytic pathway. *Mol Biol Cell,* 7**,** 1909-19.